

## Energetics, robustness and product formation in slow- and non-growing yeast cultures

Vos, Tim

**DOI**

[10.4233/uuid:6c66df88-b72d-4604-b1b6-f7141e251775](https://doi.org/10.4233/uuid:6c66df88-b72d-4604-b1b6-f7141e251775)

**Publication date**

2016

**Document Version**

Final published version

**Citation (APA)**

Vos, T. (2016). *Energetics, robustness and product formation in slow- and non-growing yeast cultures*. [Dissertation (TU Delft), Delft University of Technology]. <https://doi.org/10.4233/uuid:6c66df88-b72d-4604-b1b6-f7141e251775>

**Important note**

To cite this publication, please use the final published version (if applicable). Please check the document version above.

**Copyright**

Other than for strictly personal use, it is not permitted to download, forward or distribute the text or part of it, without the consent of the author(s) and/or copyright holder(s), unless the work is under an open content license such as Creative Commons.

**Takedown policy**

Please contact us and provide details if you believe this document breaches copyrights. We will remove access to the work immediately and investigate your claim.

Energetics, robustness and product formation in  
slow- and non-growing yeast cultures

Tim Vos



# **Energetics, robustness and product formation in slow- and non-growing yeast cultures**

## **Proefschrift**

ter verkrijging van de graag van doctor

aan de Technische Universiteit Delft,

op gezag van de Rector Magnificus prof. ir. K.Ch.A.M. Luyben,

voorzitter van het College voor Promoties,

in het openbaar te verdedigen op woensdag 26 oktober 2016 om 10:00 uur

door

**Tim Vos**

Ingenieur in Life Science and Technology,

Geboren te Bobeldijk.

This dissertation has been approved by the

Promoter: Prof. dr. J.T. Pronk

Copromotor: Dr. ir. P. Daran-Lapujade

Composition of the doctoral committee:

Rector Magnificus	chairperson
Prof. dr. J.T. Pronk	Technische Universiteit Delft, promotor
Dr. ir. P. Daran-Lapujade	Technische Universiteit Delft, copromotor
Prof. Dipl.-Ing. dr. D. Mattanovich	Universität für Bodenkultur Wien

Independent members:

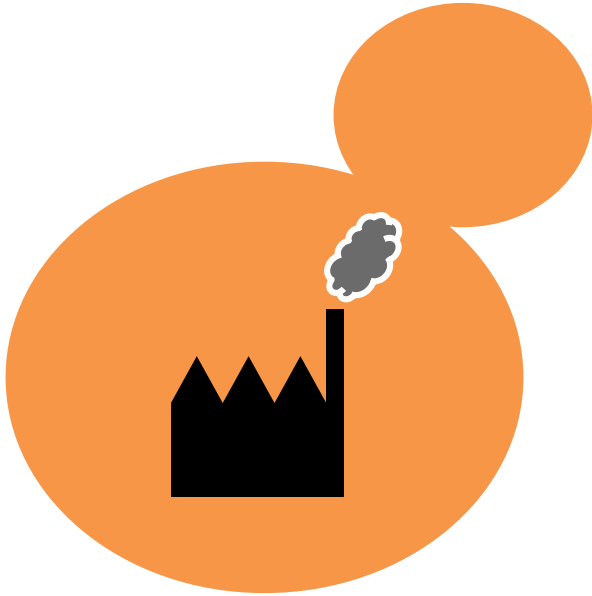
Prof. Dr.-Ing. R. Takors	Universität Stuttgart
Dr. ir. M.L. Jansen	Koninklijke DSM N.V.
Prof. dr. J.H. de Winde	Universiteit Leiden
Prof. dr. J.G. Kuenen (emeritus)	Technische Universiteit Delft
Prof. dr. W.R. Hagen	Technische Universiteit Delft, reservelid

The studies represented in this thesis were performed at the Industrial Microbiology section, Department of Biotechnology, Delft University of Technology, the Netherlands and financed by the European Union via the FP7 grant and the Netherlands Organisation for Scientific Research (NWO) via the B-Basic programme.

Cover: Impression of 'cells as factories' and 'cells in factories'.

# Contents

1	General introduction	<b>1</b>
2	Growth-rate dependency of <i>de novo</i> resveratrol production in chemostat cultures of an engineered <i>Saccharomyces cerevisiae</i> strain	<b>25</b>
3	Oxygen availability strongly affects chronological lifespan and thermotolerance in batch cultures of <i>Saccharomyces cerevisiae</i>	<b>49</b>
4	Maintenance-energy requirements and robustness of <i>Saccharomyces cerevisiae</i> at aerobic near-zero specific growth rates	<b>73</b>
5	<i>Pichia pastoris</i> exhibits high viability and low maintenance-energy requirement at near-zero specific growth rates	<b>101</b>
	Bibliography	<b>131</b>
	Summary & samenvatting	<b>151</b>
	Acknowledgements	<b>165</b>
	<i>Curriculum Vitae</i>	<b>168</b>
	List of publications	<b>169</b>



# *1*

General introduction



## The potential for industrial biotechnology to address global challenges

Humanity is up against many challenges. The global population is expected to have increased by 38% in the year 2050 and, in particular developed countries, will be confronted with an aging society [57]. At the same time, the world faces a declining reserve of fossil fuels, increasing demands for nutrition, scarcity of clean drinking water, anthropogenic climate change, and continually progressing threats to public health and aptitude of current medicine [2, 94, 233, 297]. As a result, there is an urgent need to establish a socially, economically and environmentally sustainable society that is not dependent on finite natural resources and that focuses on long-term solutions to global challenges.

Industrial biotechnology, the application of microorganisms for the production of added-value compounds, could contribute to sustainable solutions for energy, nutrition and medicine related issues. Compared to many (petro)chemical processes, biotechnology offers more environmentally friendly processes due to less harsh operational conditions and lower greenhouse gas emissions. In addition, the raw materials come from renewable feedstock and waste streams. Industrial biotechnology has a modest, but steadily increasing market share in the commercial production of renewable fuels, chemicals, food ingredients, and medicine [254]. Examples of bio-based chemicals include bioethanol, vitamins, amino acids, and antibiotics [254]. Ongoing scientific and technological developments create opportunities to synthesize such added-value compounds even more sustainably and to further expand the product range of industrial biotechnology.

**Domestication and application of microorganisms** | The use of microorganisms has a rich history and a large impact on human society. Although microbes were only to be discovered by Antonie van Leeuwenhoek using his hand-made microscopic lenses around the year 1676 [280], these “tiny animalcules” were already unknowingly applied in bread baking and wine making for millennia [164]. The microbial conversion of sugars into e.g. ethanol (by yeasts) or lactic acid (by lactic acid bacteria) in food products, commonly known as fermentation, has been essential to produce and preserve cheese, yoghurt, bread, salami, beer, wine and kimchi for many millennia [134]. Over these long time periods, the use of microbial cultures in these processes led to their “domestication” [11]. Only much later, mankind started to knowingly employ their natural capability in the dairy and alcoholic beverage industries. Microorganisms also played a historic role beyond food applications. The industrial conversion of starch to acetone, an essential ingredient for British explosives used during World War I, is an example of the first industrial application of a pure microbial culture. Chaim Weizmann, then a scientist in the United Kingdom, used the natural capacity of *Clostridium acetobutylicum* to anaerobically digest sugars into acetone, butanol and ethanol, a process now known as

the 'Weizmann process' [300]. The discovery of microorganisms, and early developments in their industrial application have paved the way for modern biotechnology.

Today, a distinction can be made between microorganisms that naturally produce compounds of interest and microbes that have been genetically engineered to produce non-native chemicals. Before the introduction of genetic engineering in the second half of the 20<sup>th</sup> century, improving the natural production characteristics of microorganisms relied mostly on classical strain improvement; a process involving random mutagenesis or classical breeding, followed by screening to identify and isolate mutants with desirable traits [205]. As an example, the productivity and yield of penicillin, produced by the mold *Penicillium*, has been increased tremendously since its first discovery by Alexander Fleming in 1928, with repeated mutagenesis and screening as the most important approach for strain improvement [273]. Classical strain improvement of *Corynebacterium glutamicum* has similarly benefited the bulk production of glutamate and lysine [130]. Since the 1970s, the discovery of recombinant DNA technologies allowed researchers to engineer the genetic makeup of organisms by removing parts of their genetic code, or by introducing recombinant DNA into their genomes [58]. This major breakthrough introduced genetic engineering possibilities in industrial biotechnology. For example, ten years later, recombinant DNA technologies enabled the industrial application of a genetically engineered bacterium that produced 'human' insulin at a commercial scale, which replaced purification of insulin from animal pancreases [137]. During the same period, the groundbreaking technology of DNA sequencing emerged and, after automation in the 1990s [238], led to the ability to 'read' the complete genetic code of an organism. The first eukaryotic genome was published in 1996, making available the 12 million base pairs covering the 16 chromosomes and over 6000 genes of the yeast *Saccharomyces cerevisiae* [105]. Back then, this was achieved through a global cooperation between numerous laboratories over a period of years and at the expense of many millions of dollars. Nowadays, whole genome sequencing of the same organism has become a routine procedure that can be performed in a few days for much less than a thousand dollars (Figure 1.1).

Techniques for reading and writing the genetic code and for engineering cells have been subject to continuous developments. The past few years, heralded by some as the beginning of the 'synthetic biology era' have been particularly rich in novel methods that enable faster and more efficient engineering of popular microorganisms [6]. The most recent breakthrough is the application of the prokaryotic immune system CRISPR/Cas for DNA editing in a wide range of organisms [237]. This fast, cheap and efficient technique allows for precise addition, removal or modification of multiple nucleotides and/or genes at any desired location in the genome. This and other discoveries have led, in only two decades, to a revolution in genetic engineering. From a situation in which making a single gene knock-out was a laborious process, entire biosynthetic pathways (often

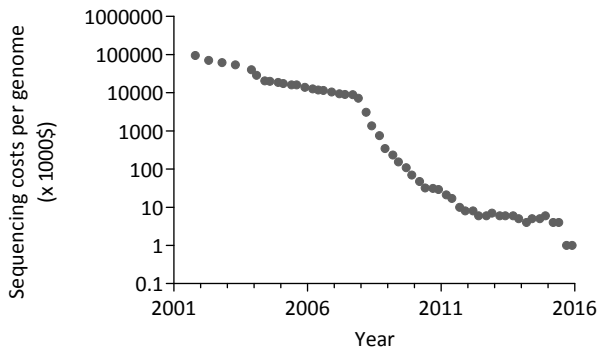


**Figure 1.1:** Development of cost price for sequencing a single human-sized genome, since 2001. Adapted from data publicly available on the website of the National Human Genome Research Institute. *Wetterstrand KA. DNA Sequencing Costs: Data from the NHGRI Genome Sequencing Program (GSP) Available at: [www.genome.gov/sequencingcosts](http://www.genome.gov/sequencingcosts). Accessed on January 15, 2016.*

foreign to the host organism) can be overexpressed in a few days and engineering of whole chromosomes is technically feasible [114, 142, 204].

Ever since the expression of a short gene encoding the human insulin peptide in a bacterium, industrial biotechnology realized its potential to improve existing microbial production strains, and to employ microorganisms for production of compounds based on complex metabolic routes, catalysed by combinations of native and heterologous enzymes. Nowadays, traditional and novel engineering strategies are intensively explored to extend the use of microorganisms for optimized conversion of renewable feedstocks into new sustainable products. For example, filamentous fungi often found on (rotting) plants in nature, are mined for enzymes responsible for the conversion of cellulosic plant material [23]. Other efforts focus on increasing the substrate range of *S. cerevisiae* to include plant waste streams from e.g. corn production, which is particularly interesting for the production of bulk chemicals such as bioethanol [160, 305]. In terms of product range, microbes are engineered for the synthesis of high-value compounds, such as the food ingredients stevia and resveratrol, and the anti-cancer drug taxol, which are otherwise extracted from crops that grow slowly and suffer from low product yields [20, 83, 166]. These ongoing research efforts in biotechnology reflect the crucial role that microbes play in developing a Biobased or Circular Economy and their potential in solving global challenges resulting from an expanding population and declining natural reserves.

## Microbial energetics and the challenges of large-scale bioprocessing

**Anabolism vs catabolism** | Cells grow by converting simple substrates into cellular constituents through a complex network of metabolic pathways. Microbial production of economically interesting compounds largely relies on the same network of metabolic

routes that is involved in the synthesis of microbial cells. Metabolic networks can be classified in two major types of reactions: anabolic and catabolic reactions. Anabolic reactions convert small simple molecules to larger and more complex molecules, such as the conversion of ammonia and sugars into amino acids, which can subsequently be polymerized into peptides and proteins. Thermodynamically, building up such macromolecules results in a decrease in entropy, and is therefore typically characterized by a positive Gibbs free energy change. The required input of energy is provided by catabolism, which covers the biochemical reactions that conserve Gibbs free energy in biologically accessible forms such as adenosine triphosphate (ATP). In catabolic reactions, substrate molecules such as sugars are typically dissimilated to smaller molecules, as is the case when glucose is respired to carbon dioxide and water. These processes are accompanied by an increase in entropy, and the free energy conserved from these catabolic reactions can be used in anabolism. Biochemical precursors required for anabolism are often intermediates of catabolic pathways, which make anabolism and catabolism heavily interdependent. According to the set of reactions leading to their synthesis, products can likewise be categorized into catabolic products and anabolic products. For instance, ethanol, a classical catabolic, industrially-relevant product of *S. cerevisiae* results from the anaerobic dissimilation of sugars. Characteristic anabolic products of interest formed by this organism include yeast biomass itself, proteins such as the peptide hormone insulin, but also secondary metabolites such as isoprenoids, fatty acids and resveratrol [20, 51, 146, 277].

**Division of substrate into growth, product formation and maintenance** | Catabolism and anabolism both depend on substrate availability, which therefore is a key parameter in microbial growth kinetics. In most biotechnological processes microbial growth is controlled by a limiting concentration of a single essential nutrient in the growth medium. In 1949, Jacques Monod proposed that the specific growth rate ( $\mu$ ) depends on the concentration of the growth-limiting substrate (S) according to [194]:

$$\mu = \mu_{max} \frac{C_S}{C_S + K_S} \quad (1.1)$$

Where  $\mu_{max}$  is the maximum specific growth rate in a given environment when all nutrients are present in excess,  $C_S$  is the substrate concentration of the limiting nutrient, and  $K_S$  is the concentration of the limiting nutrient at which  $\mu = \frac{1}{2} \mu_{max}$ . In classical batch cultivation, all nutrients are initially present in excess ( $C_S \gg K_S$ ), and microbes can grow at their  $\mu_{max}$ . When one of the essential substrates (most often the carbon and energy source) is depleted ( $C_S = 0$ ), growth stops. In industrial applications and applied research, microbial growth is typically controlled by feeding a medium containing a single growth-limiting nutrient, which is often the carbon and energy source (e.g. glucose). Once this nutrient is taken up by the cell, it is partly metabolized in anabolic processes and partly

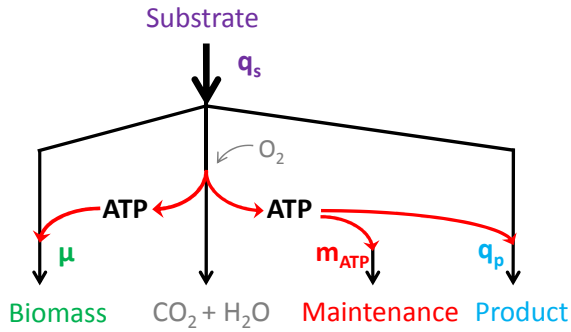


**Figure 1.2:** Schematic representation of the substrate and energy (ATP) distribution according to the modified Pirt equation (Equation 1.3).  $q_s$  represents the biomass-specific glucose consumption rate and  $q_p$  represents the biomass-specific product formation rate. In this example, the energy substrate (e.g. glucose) is catabolized to carbon dioxide ( $\text{CO}_2$ ) and water ( $\text{H}_2\text{O}$ ), using oxygen ( $\text{O}_2$ ) as the electron acceptor. The combination of substrate-level and oxidative phosphorylation results in a net generation of ATP, required for cellular maintenance ( $m_{\text{ATP}}$ ) and to fuel energy-demanding anabolic pathways leading to biomass and product formation.

combusted in catabolic pathways to provide the energy for anabolism (Figure 1.2). Energy is also invested in activities such as ion homeostasis, preservation of electrochemical gradients, macromolecules turnover, cellular damage repair, defense against stresses, or cell motility. These processes, which are necessary for cellular survival but do not directly contribute to growth, are grouped under the general term ‘maintenance’ [272]. Futile cycles can also represent a substantial drain of energy-rich moieties irrespective of the presence of growth [272]. The amount of ATP required for maintenance depends on the environment (e.g. temperature and presence of organic acids), and varies between microorganisms [271, 85].

For cells that solely invest their carbon and energy source in growth and maintenance, an empirical linear relationship between the culture specific substrate uptake ( $q_s$ ) and specific growth rate ( $\mu$ ) was proposed by Pirt (Equation 1.2, Figure 1.2) [217]. The model holds for energy-limited conditions and assumes a growth-rate independent substrate requirement for maintenance and a theoretical maximum growth yield on substrate ( $Y_{X/S}^{\text{max}}$ ).

$$q_s = \frac{\mu}{Y_{X/S}^{\text{max}}} + m_s \quad (1.2)$$

Equation 1.2 implies that, when the specific uptake rate of the energy substrate equals the maintenance requirement ( $m_s$ ), growth is absent (zero-growth), and substrate is exclusively used in catabolic reactions. Microbes that produce and excrete compounds derived from anabolism have an additional drain of substrate and energy, and describing their growth kinetics in energy-limited cultures requires an extension of the Pirt equation (Equation 1.3) [120].

$$q_s = \frac{\mu}{Y_{X/S}^{\text{max}}} + m_s + \frac{q_p}{Y_{P/S}^{\text{max}}} \quad (1.3)$$

The theoretical maximum product yield ( $Y_{P/S}^{\max}$ ) is determined by the stoichiometry of the metabolic pathway from substrate to product in which redox cofactors are balanced and ATP requirements are accounted for by dissimilation of additional substrate. This theoretical value cannot be achieved in practice with living microorganisms, which, even in the absence of growth, need to dissipate part of their energy source for cellular maintenance. The maintenance requirement thereby represents a continuous drain of substrate necessary to keep microbial 'cell factories' active.

From an industrial perspective, the yield of product on substrate is an important economic driver and should be as high as possible for a process to become cost effective. This holds in particular for bulk chemicals and fuels. Additional commercial drivers are the overall production rate and the final product titer, which affect the operational expenses by influencing e.g. total operation time or downstream processing efficiency. The highest product yields can theoretically be achieved when cells are in a state in which they do not grow, but invest all energy substrate in product formation and maintenance. However, because anabolic reactions for product formation and growth are often metabolically intertwined and their respective specific rates are therefore likely correlated, the production of anabolic compounds at zero-growth remains a challenge.

From a theoretical viewpoint, many microbial production processes would function optimally in an uninterrupted bioprocess in which cells are continuously fed with nutrient-limited feed to control substrate uptake and growth, and are engineered to spend most of the substrate on product formation with a high yield and high specific production rates [61]. Compared to batch bioprocessing, continuous bioprocessing would therefore be the preferred alternative. An example of industrial application of continuous cultures is the commercial production of insulin by an engineered *S. cerevisiae* strain [146]. However, practical challenges that are inherent to continuous cultures, such as heterogeneity of biomass and nutrient concentrations in reactor vessels, nutrient shortage, infection risks, inflexible and long term operation, metabolic burden, and genetic instability of cells are the reason why fed-batch bioprocessing is often the preferred cultivation mode at industrial scale [61]. In a fed-batch culture, cells first go through a batch phase with nutrients excess and grow exponentially until a limiting nutrient, usually the carbon and energy source, is depleted. The produced biomass is then fed with a nutrient-limited feed to control growth, at a rate that is often constrained by the oxygen transfer capacity of the reactor, which determines how fast oxygen can be transferred from the air sparged into the bioreactor (gas phase), to the liquid phase, thereby making it available for metabolism [277]. To moderate capital and operational expenses, industrial bioprocesses are generally performed at large scale ( $> 50 \text{ m}^3$ ) with high biomass concentrations, which increases the demand for oxygen and heat-transfer capacity. Oxygen and heat-transfer limitations require operators to restrict microbial growth, usually by controlling the sugar feed, to rates that are at least an order of magnitude below the organism's  $\mu_{\max}$  [98]. However,

restriction of growth can lead to suboptimal fluxes in the production pathways that make use of the microbial anabolic machinery [136, 151, 224]. Furthermore, under these calorie-restricted and slow-growth regimes, a relatively large fraction of the sugar is combusted for cellular maintenance energy requirements, while specific anabolic (production) rates are relatively low, affecting the product yields [120, 265]. While the high biomass concentrations that can be reached in fed-batch processes partly compensate for suboptimal product yields and specific productivities, uncoupling product formation from growth and minimizing the maintenance energy requirements are pivotal for the development of economically viable microbial production of anabolic compounds.

## **Budding yeasts as cell factory and industrial workhorse**

Budding yeasts have a long track record in industrial biotechnology. *Saccharomyces cerevisiae*, also known as bakers' yeast, was already sold by Dutch tradesmen in 1780 [149]. Nowadays this yeast is still widely applied in the food and beverage industry, mostly for its fermentative capacity in the preparation of alcoholic beverages and bread doughs, but also as an ingredient itself for flavoring soups and sauces. Furthermore, industrial production of bioethanol by *S. cerevisiae* is currently the largest-volume microbial fermentation product and represents a sustainable alternative to oil-based liquid fuels [201]. *S. cerevisiae* has a robust phenotype that can withstand relatively harsh conditions present in bioprocesses, and it is most probably the second best studied eukaryote after humans [10, 33]. The early access to its genome sequence combined with the arsenal of genetics tools developed for this yeast make it a popular model organism for both fundamental and applied research [33]. Developments in molecular biology tools for this organism still continue today, exemplified by the identification of new recyclable deletion markers [257], and the effective exploitation of homologous recombination for *in vivo* assembly and targeted integration of large DNA parts [49, 158, 102]. In parallel, the CRISPR-Cas system was successfully implemented in *S. cerevisiae* [77, 180], further extending the molecular possibilities in this organism and arguably making it an even better microbial platform for molecular genetics construction work than the laboratory model bacterium *Escherichia coli* [64]. The extensive knowledge and tools available for *S. cerevisiae*, together with its beneficial characteristics for industrial application, continue to attract scientists to further explore and expand the scope of applications of this versatile organism. Introduction of heterologous genes and pathways into this yeast, combined with directed evolution strategies, has increased the range of consumable sugar substrates, allowing for example the utilization of C5 sugars present in polymers of plant waste streams [160, 305]. Furthermore, its product spectrum has been expanded and includes non-native anabolic products, such as heterologous proteins, isoprenoids, flavonoids and fatty acids [51, 122]. Examples of compounds readily commercialized by biotechnological companies include yeast-based production of the anti-malarial drug-

precursor artemisinin (Amyris, San Francisco), human insulin (Novo Nordisk, Denmark), the versatile chemical building block succinic acid (Reverdia, Netherlands/France) and high-value plant secondary metabolites resveratrol and vanillin (Evolva, Switzerland).

*Saccharomyces cerevisiae* is a facultative anaerobe which ferments sugars to ethanol under anaerobic conditions, and can respire sugars to carbon dioxide and water in the presence of oxygen when external sugar concentrations are sufficiently low [276]. High external sugar concentrations favor fermentative metabolism in this yeast even under aerobic conditions, which is a phenomenon called the Crabtree effect [70]. Fully respiratory metabolism can be achieved by controlling the sugar feed in a bioreactor setup, thereby limiting sugar uptake and keeping residual sugar concentrations low.

The energetic cost of enzyme-catalysed reactions in biochemical production pathways affects the maximum yield of product on substrate. Therefore, optimal product yields of anabolic products requires metabolism to be energetically efficient. Fermentation of glucose into ethanol results in the production of net 2 ATP per mol of glucose through substrate-level phosphorylation (SLP) in glycolysis. The 2 moles of NADH produced in this pathway are re-oxidized by reducing pyruvate, the final product of glycolysis, through concerted enzymatic conversions by pyruvate decarboxylase and alcohol dehydrogenase to ethanol and carbon dioxide. Alternatively, when glucose is fully respired in the presence of sufficient oxygen, the pyruvate originating from glycolysis enters the mitochondrial tri-carboxylic acid cycle (TCA cycle) through the mitochondrial pyruvate-dehydrogenase complex, leading to oxidation of pyruvate to carbon dioxide and water. This process yields 2 ATP per mol of oxidized glucose through SLP, while 8 mol NAD and 2 mol FAD are reduced to 10 NADH equivalents. Re-oxidation of the 12 NADH equivalents from glycolysis and the TCA cycle is then initiated by external and internal mitochondrial NADH dehydrogenases, which transfer the electrons from NADH to ubiquinone in the respiratory chain situated in the mitochondrial inner membrane (Figure 1.3). Subsequently, the electrons are transferred through a set of membrane-associated redox reactions to the final external electron acceptor  $O_2$ , which is reduced to  $H_2O$ . These redox reactions are coupled to the transfer of protons from the mitochondrial matrix to the intermembrane space. The resulting electrochemical gradient drives protons back through the mitochondrial cross-membrane ATPase, which, in *S. cerevisiae*, phosphorylates an estimated 1 mol of ADP to ATP per oxidized NADH (or, in other words, a P/O ratio of 1) [287, 291]. In total, complete respiration of glucose then results in 4 ATP from SLP and 12 ATP from oxidative phosphorylation. The ATP yield on sugars between fermentative and respiratory metabolism thereby differs roughly 8-fold, which is why respiratory metabolism is preferred in yeast-based production of ATP-demanding compounds.

Bakers' yeast is not the only budding yeast that is used for academic and industrial purposes. While *S. cerevisiae* has beneficial traits for industrial applications and is widely



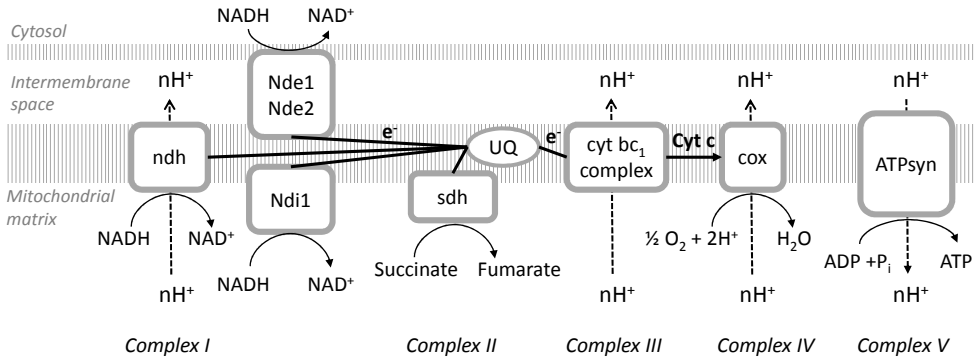


**Figure 1.3:** Important constituents of the respiratory chain. In *S. cerevisiae*, oxidation of cytosolic and mitochondrial NADH is catalysed by internal and external mitochondrial NADH dehydrogenases (Ndi1 and Nde1/2 respectively). *Pichia pastoris* couples NADH oxidation to proton translocation over the mitochondrial innermembrane, catalysed by Complex I. Electrons from NADH dehydrogenases and succinate dehydrogenase (sdh) are transported to ubiquinone (UQ), which passes the electrons to the cytochrome *bc1* complex. Complex III in turn, transfers the electrons to cytochrome *c*, coupled to proton transport from the mitochondrial matrix to the intermembrane space. In Complex IV, cytochrome *c* is oxidized, coupled to the reduction of molecular oxygen and translocation of more protons. The resulting electro-chemical gradient over the mitochondrial inner membrane is used to phosphorylate ADP to ATP, catalysed by the ATP synthase (ATPsyn) which uses the free energy released from the reflux of protons to the mitochondrial matrix [13, 234].

studied, it is not always the organism of choice. For example, the *in vivo* P/O ratio of *S. cerevisiae* for oxidation of mitochondrial NADH equivalents, estimated around 1 [291], is lower than in many other eukaryotes. *S. cerevisiae* lacks a respiratory complex I [200], which in e.g. the budding yeast *Pichia pastoris* (syn. to *Komagataella sp.*) couples oxidation of mitochondrial NADH to the transfer of protons over the mitochondrial membrane [39] (Figure 1.3). The electron transport chain in *P. pastoris* therefore has a higher capacity for proton translocation, which benefits the overall ATP yield on glucose compared to *S. cerevisiae*. The methylotrophic yeast *P. pastoris* has historically been developed as an industrial microorganism to provide protein rich animal-feed, using methanol as cheap carbon and energy source when oil prices were low. The rise in oil prices during 1973 prevented the exploitation of *P. pastoris* for this particular application, but certain physiological traits identified later qualified this yeast as an excellent expression system for the production and secretion of (heterologous) proteins, including therapeutics [4]. Microbial-based protein therapeutics often suffer from post-translational modifications foreign to humans, thereby compromising their efficacy in the human body. Recent ‘humanization’ of the glycosylation machinery in *P. pastoris* showed significant promise for the production of humanized therapeutic glycoproteins such as monoclonal antibodies [294]. Expression of proteins of interest in *P. pastoris* is typically driven by the strong, methanol-inducible *AOX1* promoter, providing an efficient method for initiation of production during the feed-phase of a fed-batch process [60]. Furthermore, *P. pastoris* is a Crabtree-negative budding yeast that does not aerobically ferment sugars, a characteristic that has been linked to the absence of low-affinity high-

velocity hexose transporters [185], thereby favoring high ATP yields necessary to fuel anabolic reactions (biomass or product formation) even during growth in aerobic batch cultures. Although the maximum sugar uptake rate measured in aerobic batch cultures of *P. pastoris* is ca. 7 fold lower than that of *S. cerevisiae* [125, 255], its maximum specific growth rate on glucose is only 30 % lower [126, 25]. These properties make *P. pastoris* an interesting ‘cell factory’ that, moreover, has already proven its applicability in industrial settings [4].

The examples above illustrate the applicability of budding yeasts in industrial biotechnology. Therefore, both *S. cerevisiae* and *P. pastoris* are used as model microorganisms in the research chapters of this thesis.

## Specific growth rate vs. microbial product formation

**Cultivation tools to study yeast physiology** | Batch cultures are the most traditional and straightforward systems to study microbial physiology. Because all nutrients, including the carbon and energy source, are available in excess in the growth medium, substrate uptake is not restricted and cultures can grow at their maximum growth rate under the chosen environmental conditions (see Equation 1.1). In this dynamic cultivation system, sugars are rapidly depleted and products accumulate. Upon exhaustion of carbon sources, the culture promptly transitions into a zero-growth state most commonly known as stationary phase. In aerobic batch cultures of *S. cerevisiae*, high glucose concentrations repress the synthesis of respiratory enzymes, leading to respiro-fermentative metabolism during which most of the sugars are fermented to ethanol at high rates [96]. This so-called carbon-catabolite repression is relieved when sugars are (nearly) depleted, allowing cells to enter a fully respiratory, diauxic growth phase on ethanol (and other compounds such as acetate or glycerol) produced in the exponential growth phase. When all fermentable and non-fermentable carbon sources are depleted growth stops and the culture enters stationary phase (Figure 1.4).

Chemostat cultivation is an alternative, valuable tool to study microbial physiology, which enables growth under strictly controlled conditions [198]. Cell growth can be kept constant in time by supplying the culture with a constant feed medium restricted in a single nutrient, while the volume in the bioreactor is kept constant by continuous removal of broth. The rate at which the broth is removed ( $F_{\text{out}}$ , in  $\text{L h}^{-1}$ ) divided by the constant volume in the bioreactor ( $V$ , in L) is known as the dilution rate ( $D$ , in  $\text{h}^{-1}$ ) of the culture. Assuming all biomass participates in growth and neglecting evaporation ( $F_{\text{in}} = F_{\text{out}}$ ) the biomass balance can be solved as follows:

$$\frac{dC_X}{dt} = -D \cdot C_X + \mu \cdot C_X \quad (1.4)$$

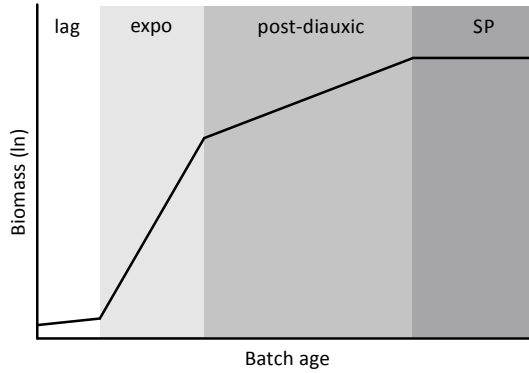


**Figure 1.4:** Growth phases of *S. cerevisiae* in aerobic batch cultures with all nutrients in excess relative to carbon and energy source glucose. After a short lag phase to adapt to the environment, cells display fast exponential growth on glucose and exhibit a predominantly fermentative glucose metabolism. When glucose is depleted from the medium, metabolism is rearranged during the so-called 'diauxic shift', thereby preparing cells for growth on non-fermentable carbon sources (ethanol, glycerol and organic acids) produced during the preceding exponential growth phase on glucose. The following post-diauxic growth phase is characterized by a fully respiratory metabolism and by a lower specific growth rate. Once all carbon and energy sources are depleted, growth ceases and the culture enters stationary phase. It should be noted that environmental conditions can affect growth significantly. For example, culture acidification could lead to growth cessation before carbon sources are depleted.

Because growth is strictly controlled by nutrient limitation, biomass and metabolite concentrations will reach steady state values as their respective specific rates become constant. At this point,  $\frac{dC_X}{dt} = 0$ , and  $D \cdot C_X = \mu \cdot C_X$ , or  $D = \mu$ . Since, in chemostats, the growth-limiting nutrient is almost completely consumed, its residual concentration in the bioreactor is very low. By choosing sugar as the limiting substrate, carbon-catabolite repression can be released, allowing for complete respiratory growth under fully aerobic conditions. In steady-state conditions, the rate of sugar consumption ( $q_S$ ) is constant, and becomes a function of the dilution rate (assuming a completely viable culture) resulting in a modified Pirt equation:

$$q_S = \frac{D}{Y_{X/S}^{max}} + m_S + \frac{q_P}{Y_{P/S}^{max}} \quad (1.5)$$

In chemostats, the dilution rate can be easily varied to study microbial physiology at different specific growth rates under steady-state conditions [90, 225, 279]. This cultivation system has also been used to study and compare steady-state growth kinetics and microbial physiology between different strains or environmental conditions [119, 264, 275, 309]. In addition, chemostats operated at different dilution rates have been used to assess the correlation between  $q_S$  and  $\mu$ , and obtain values for  $m_S$  and  $Y_{X/S}^{max}$  (See Figure 1.5) [28, 186, 265]. Developments in the different 'omics' fields have popularized chemostat studies because of their reproducibility and ease of comparative studies on multiple levels of cell biology including transcriptomics, proteomics, and metabolomics

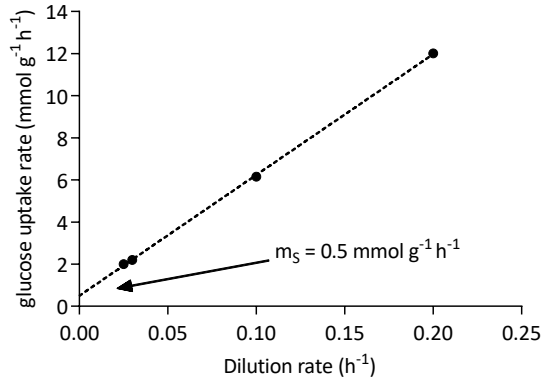


**Figure 1.5:** Relationship between the biomass-specific glucose uptake rate and specific growth rate for *S. cerevisiae*, measured in anaerobic chemostat cultures at different dilution rates (where the dilution rate equals the specific growth rate). The maintenance requirements can be derived by extrapolating the linear correlation between  $q_S$  and  $\mu$  to a dilution rate of zero, where the y-axis intercept represents the energy flux required for maintenance processes independent of growth ( $m_S$ ) [28].

[65, 129, 157, 249, 153, 67] . This cultivation tool thereby contributed to ‘systems biology’ approaches for integration of multi-layered biological data into mathematical models of biological systems [47].

Prolonged cultivation in chemostats imposes a selective pressure for cells with an increased affinity for the growth-limiting nutrient and for cells with higher biomass yields ( $\mu/q_S$ ) [41, 132]. Because anabolic product formation competes with growth (Figure 1.2) and can lead to a substantial cellular burden, studying the steady-state physiology of microbes that produce such compounds requires genetically stable (engineered) strains.

**Growth-rate dependency of product formation** | The relationship between specific growth rate and specific product formation rate depends on the product of interest. A common relationship with growth found for catabolic products, in organisms that do not have branched fermentation pathways, is described by a linear positive correlation [72]. Such a relationship holds true for example for anaerobic ethanol production by *S. cerevisiae* [28], and has been validated using glucose-limited chemostat cultures at different dilution rates. The production of this catabolic product is stoichiometrically coupled to the production of ATP and consumption of glucose, and the y-axis intercept represents the catabolic (energy) flux required for maintenance processes (See Figure 1.5). For anabolic products, the relationship between growth and product formation is more difficult to predict [72, 186]. Because anabolic product formation typically competes for substrate and metabolites with biomass formation, the distribution of nutrients, ATP, and redox-cofactors depends on the competition between enzymes involved in anabolic routes. How the kinetic properties of the competing enzymes relate to growth rate

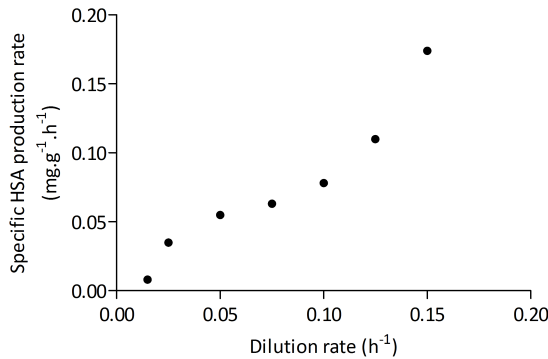


**Figure 1.6:** Correlation between the specific rate of heterologous protein production and specific growth rate measured in aerobic, glucose-limited chemostat cultures of an engineered *P. pastoris* strain producing human serum albumin (HSA), grown at different dilution rates [224].

depends on enzymes abundance, products and metabolic pathways of interest, and *in vivo* concentration of key metabolites. There are only few examples of studies in which yeast-based production of anabolic compounds has been investigated in relation to specific growth rate, and the majority of these relate to protein production [116, 122, 136, 151, 170, 186].

The low growth rates typically observed during fed-batch processes imply the necessity to predict the performance of (engineered) strains under industrial conditions, and requires quantitative data on the growth-rate dependency of anabolic product formation. For example, the production of heterologous protein by an engineered *P. pastoris* strain has been shown to positively correlate with growth rate (Figure 1.6) [224]. This correlation was proposed to be a result of the impact of growth rate on endoplasmic reticulum functioning, and translation. A study in aerobic glucose-limited chemostats at two different dilution rates indicated a positive correlation between  $q_p$  and  $\mu$  for  $\alpha$ -santalene production by an engineered *S. cerevisiae* [239]. The specific production rate of ethylene by an engineered *S. cerevisiae* strain was also shown to positively correlate to specific growth rate [136]. However, ethylene yields on glucose decreased at higher specific growth rates. Likewise, an engineered polyhydroxybutyrate-producing *S. cerevisiae* strain displayed a decrease in product yield at increasing specific growth rate [151], underlining the importance of specific growth rate in the definition of optimal production conditions. Chapter 2 of this thesis explores the impact of specific growth rate on microbial production of resveratrol, a commercially attractive, energy-intensive compound, by an engineered *S. cerevisiae* strain.

## Energetics, robustness and product formation at near-zero growth

**Relevance of microbial zero-growth** | In their natural habitat, microbes can encounter changing environments, including variations in the availability of basic nutrients required for growth. Because essential substrates in such environments can become extremely scarce [91], many microorganisms grow at rates far below their  $\mu_{\max}$  or remain in a non-proliferating/dormant state during most of their life [40]. It has been postulated that 60% of all microbes in nature exist in such a quiescent state, in which cells do not replicate but remain metabolically active [229]. Conversely, most academic studies on microbial physiology are performed in settings in which nutrients are abundant (batch cultures) and microbes grow fast and to relatively high cell densities. These high growth rates are beneficial for applications in which biomass is the target product (as is the case for production of bakers' yeast).

As outlined in the previous section, low growth rates are relevant for industrial applications of microbes. Slow growth is inherent to operational limitations in aerobic fed-batch bioprocesses. Moreover, slow-growing or even non-growing cultures can theoretically lead to high product yields when biomass is a byproduct, provided that specific production rates are high and cellular integrity is maintained. In addition, periods of non-growth are common for *S. cerevisiae* in large-scale processes such as beer and wine production, where growth stops when the essential nutrients from wort or must become limited, but cells are required to stay metabolically active to contribute to essential developments in the flavor profile of the final products [34]. Moreover, zero-growth is encountered by yeast during cold storage of bread doughs [127] and during storage in tanks in between fermentation cycles for e.g. bioethanol production or beer brewing. In the latter processes, biomass is harvested at the end of a production process and used to 're-pitch' a second fermentation run [18]. In industrial bioethanol production, up to 95% of yeast cells are recycled as inoculum in high cell density cultures. During a fermentation cycle with a duration of ca. 6-10 hours, the total biomass hardly grows and is estimated to increase by only 5 to 10% [18]. In addition to nutrient limitation and slow or zero-growth, microbes face many stresses in industrial processes, such as heterogeneity of the reaction mixture, unfavorably high or low and fluctuating temperatures, osmotic stress due to high salt or sugar concentrations, fluctuating and sometimes low pH, strongly acidic environments, and the presence of toxic metabolites [135, 10]. Maintaining the vitality and metabolic activity of the microbial catalysts under such stressful conditions is crucial to the economics of any bioprocess, which make the robustness of microorganisms a key parameter of their performance. Several studies show that a relationship exists between stress resistance and growth rate in *S. cerevisiae*, exemplified by slow-growth induced heat-shock tolerance in nutrient-limited cultures [174, 307]. Also, compared to rapidly growing cultures that are in the exponential growth phase, non-growing stationary-phase cultures of *S. cerevisiae* display increased heat-

shock tolerance as well [5, 301]. Considering the frequent occurrence of zero-growth in both nature and industry, a better definition and, ultimately, understanding of its connection with stress tolerance and its potential in uncoupling product formation from growth, studies on zero-growth yeast physiology could benefit industrial biotechnology. Chapter 3, 4 and 5 of this thesis focus specifically on this topic.

**Stationary-phase cultures in zero-growth studies** | The most common cultivation system employed to study non-growing *S. cerevisiae* is the final stage of an aerobic batch culture, during which the culture enters stationary phase (SP, Figure 1.4). The definite cause of growth arrest can be ambiguous, but critically influences experiments and should therefore be carefully assessed [44]. Most *S. cerevisiae* SP studies are characterized by depletion of the carbon and energy source (Figure 1.4), and focus on understanding the cellular mechanisms involved in aging [301]. For example, the chronological lifespan (CLS) of yeast cells is measured by their survival in non-growing SP cultures in the absence of extracellular energy sources [87]. Oxygen and respiration have been described to both positively and negatively impact the CLS of *S. cerevisiae* via ROS-mediated stress [14, 175, 212], and increased survival was observed when the culture faced calorie restriction prior to SP [248, 251]. The identification of similar aging-related responses in higher eukaryotes, combined with the abundant experimental techniques available for *S. cerevisiae*, have made this yeast a popular model for chronologically aging metazoan cells [141]. Characteristics that distinguish non-growing SP cultures from fast-growing exponential cultures include a mostly non-budded morphology, increased tolerance to environmental cues such as heat-shock and oxidative stress, increased levels of the storage polymers glycogen and trehalose, increased cell wall thickness, and altered membrane composition [301]. In addition, transcription and translation rates are reduced upon cell arrest, and SP cultures display differences in mRNA (and corresponding protein) levels of e.g. *SNZ1* and stress-response genes *UBI4*, *HSP12*, *HSP26*, *HSP104* and *SSA3* [69, 181]. The CLS and associated characteristics of SP cultures are heavily dependent on the organism and the growth environment. For example, the increase in CLS observed in calorie restricted *S. cerevisiae* cultures was not observed for cultures of the Crabtree-negative yeast *Hansenula polymorpha*, which rather showed a positive correlation of CLS with the concentration of different carbon substrates [145]. Acidification due to e.g. acetate excretion by *S. cerevisiae* was shown to negatively impact CLS, a factor that can be attenuated by dietary restriction [172].

Studies in *S. cerevisiae* have shown that nutrient signaling pathways play an important role in proper entry into SP and CLS extension [95]. Absence of glucose in the culture medium upon SP activates the transcription factor Snf1, resulting in transcription of genes necessary for respiratory growth on alternative (non-fermentable) carbon sources [96]. Furthermore, a drastic drop in nutrient availability deactivates the PKA and TOR pathways, allowing a transcriptional reprogramming that is required for SP survival to

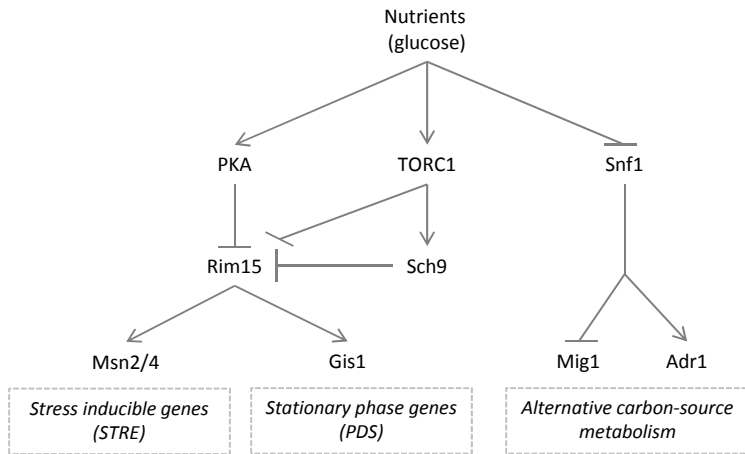


**Figure 1.7:** *S. cerevisiae* nutrient signalling pathways that regulate transcription in response to nutrient availability, for example during the transition from exponential growth on glucose to post-diauxic growth and stationary phase [95]. TOR and PKA signalling cascades are active in the presence of nutrients, resulting in an inactive Rim15 kinase. Rim15 is activated in response to nutrient limitation, and activates transcription factors Msn2/4 and Gis1, which in turn are responsible for the transcriptional induction of genes associated to stress and stationary phase. Snf1 is a protein kinase inactivated in the presence of glucose, required for transcription of glucose repressed genes via Mig1 and ADR1. Glucose limitation (and associated low extracellular glucose concentrations and low glucose consumption rates) induces Snf1, resulting in the expression of genes involved in alternative carbon-source utilization, such as catabolism of non-fermentable carbon sources during the post-diauxic growth phase (Figure 1.4).

take place, [250]. The PKA and TOR pathways act on the central kinase Rim15 which in turn activates transcription factors Msn2/4, Gis1 and Hsf1, responsible for the expression of genes related to the increased stress resistance of cultures in SP (Figure 1.7) [162, 308].

*S. cerevisiae* SP cultures are not just interesting experimental models for post-mitotic eukaryotic cells. In addition, the increased robustness observed in energy-starved cultures is highly relevant for industrial applications of *S. cerevisiae*. However, the use of SP cultures as model systems to study these phenomena has several drawbacks. For example, the recently identified sub-populations of quiescent and non-quiescent cells in SP cultures starved for carbon impede the dissection of molecular mechanisms of interest at whole-culture level [5, 7]. Compared to the non-quiescent fraction, quiescent cells (mostly virgin daughter cells) have been shown to be more robust, live longer and display reprogrammed transcriptomes and proteomes that reflect these phenotypic traits [7, 69]. Perhaps even more importantly, SP is a state that is preferably avoided in many industrial applications. The loss of metabolic activity and vitality of SP cultures, which is accelerated when extracellular energy sources and intracellular reserves such as trehalose, glycogen and lipids are depleted [165, 304], is detrimental to microbial product formation and limits their applicability for studies on the development of highly productive, non-dividing yeast strains. An alternative experimental system is therefore



directly needed to explore the physiology of highly metabolically active but non- or slowly-dividing cells.

**Retentostat to study metabolically active non dividing microbes** | To prevent cell death and deterioration, the cultivation of non-growing but metabolically active yeast populations requires a continuous supply of energy substrate, such as glucose. Fed-batch cultures offer such a constant energy supply. However, in fed-batch cultures, accumulation of metabolites may affect culture integrity and, moreover, restrictions in working volume limit operation time. Chemostat cultures do not suffer from these drawbacks and have been widely applied to study microbial growth under strictly controlled conditions. As described above, the specific growth rate in chemostat cultures is determined by the dilution rate, which can be set by the operator. Chemostat studies have been performed to study yeast physiology down to specific growth-rates of  $0.015 \text{ h}^{-1}$  [224]. However, under these conditions a large fraction of substrate is still invested in growth. For instance, *S. cerevisiae* cultures grown at  $30 \text{ }^\circ\text{C}$  under aerobic conditions using glucose as limiting substrate, exhibit a maximum biomass yield ( $Y_{X/S}^{\text{max}}$ ) of ca.  $0.5 \text{ g g}^{-1}$  [78, 279]. A theoretical calculation of the substrate requirements for maintenance based on thermodynamic principles showed that under these conditions, the expected  $m_S$  equals  $0.018 \text{ g}_{\text{glucose}} \text{ g}_{\text{biomass}}^{-1} \text{ h}^{-1}$  [121]. Solving Equation 1.2 for a non-producing strain then shows that under these conditions, the specific substrate-uptake rate ( $q_S$ ) should equal  $\frac{0.015}{0.5} + 0.018 = 0.038 \text{ g g}^{-1} \text{ h}^{-1}$ . Then, the fraction of substrate invested in growth ( $\frac{0.015}{0.5} \div 0.038 = 0.63$ ) still represents almost two-thirds of all consumed substrate. Because technical limits of chemostat cultures prevent accurate operation of specific growth-rates below  $0.015 \text{ h}^{-1}$ , alternative cultivation systems are required to quantitatively study microorganisms at near-zero growth.

In 1979, Chesbro and co-workers introduced the recycling fermenter, a modified version of a chemostat in which biomass is completely retained in the bioreactor, while spent medium is continuously removed to maintain a constant working volume [53]. In this system, which has later also become known as the retentostat, a constant supply of a growth-limiting energy substrate, combined with progressive accumulation of biomass in the bioreactor, results in a gradual decrease of the substrate availability per cell per unit of time. Consequently, specific-substrate uptake and specific growth rate smoothly decrease to extremely low values. When, ultimately, the cells receive just enough substrate to provide the energy to maintain their cellular integrity and viability ( $q_S = m_S$ ), growth ceases ( $\mu = 0$ , see Equation 1.2). Retentostat cultivation therefore offers the possibility to study metabolically active, non-dividing microorganisms [85]. Assuming that a Pirt-like relationship between energy distribution and growth applies, hypothetical growth kinetics of microbial retentostat cultures would follow the trends depicted in Figure 1.8. Because retentostat cultivation allows for a much better approximation of zero-growth

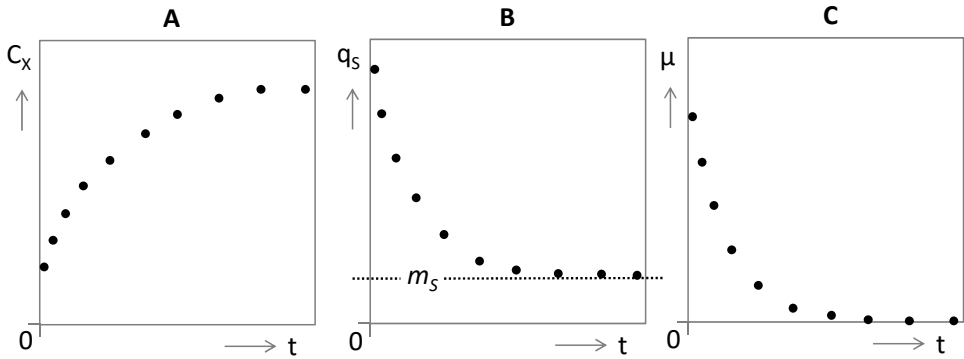


**Figure 1.8:** Theoretical microbial growth kinetics in retentostat cultures supplied with a constant, growth limiting feed of the energy source. Biomass retention in the retentostat leads to a progressive increase of the biomass concentration ( $C_x$ , panel A). Consequently, supply of growth-limiting energy source is divided over an increasing amount of biomass, leading to a decrease of the specific consumption rate ( $q_s$ , panel B) and a concomitant decrease in the specific growth rate ( $\mu$ , panel C). Ultimately,  $q_s$  reaches levels that approach or even equal the energetic demands for cellular maintenance ( $m_s$ ), and growth stops (see Equation 1.2).

than chemostat cultivation, it can be used to accurately determine and compare  $m_s$  values for different microorganisms and culture conditions [85].

Before the introduction of genomics tools, the retentostat system has been applied by environmental biotechnologists to study diverse bacterial species at extremely slow specific growth rates. The bacteria studied in retentostat, including the model prokaryote *Escherichia coli*, reacted to extreme calorie restriction by changing their metabolism to an ‘energy-saving’ mode, via a transcriptional reprogramming process known as the stringent response [8, 53]. In practice, the growth rates and yields obtained in these retentostat studies did not reach zero, which was explained by a decrease in cellular maintenance energy requirements at extremely slow growth rates [53]. The stringent response, which is conserved among different bacterial species, is typically initiated at low specific growth rates and characterized by increased levels of the alarmone molecules guanosine 5'-diphosphate,3'-diphosphate (ppGpp) and guanosine 5'-triphosphate,3'-diphosphate (pppGpp) and down-regulation of energy-intensive processes such as protein turnover [8].

In a more recent project, performed at the Delft University of Technology, glucose-limited retentostat cultures were set up and used to characterize the physiology and genome-wide transcriptional responses of the laboratory reference *S. cerevisiae* strain CEN.PK113-7D to near-zero growth under anaerobic conditions [28, 29, 27]. In the absence of oxygen, *S. cerevisiae* conserves energy required for growth by catabolising sugar to ethanol. Theoretically there is no use of carbon substrate for biomass formation in anaerobic zero-growth retentostat cultures. Sugars should therefore solely be fermented to provide the energy for maintenance and ethanol yields should be near the theoretical maximum, which is an industrially appealing concept. Furthermore, the stoichiometric

coupling between ATP formation and ethanol production in the fermentative metabolism of *S. cerevisiae* allows for straightforward calculations on the energetics of maintenance metabolism at near-zero growth based on specific ethanol formation rates. Indeed, research on anaerobic retentostat cultures showed that, at near-zero specific growth rates (below  $0.001 \text{ h}^{-1}$ ), near-theoretical ethanol yields were achieved. Maintenance requirements for the resulting non-dividing anaerobic *S. cerevisiae* were estimated at  $0.5 \text{ mmol g}_X^{-1} \text{ h}^{-1}$ , or  $1.0 \text{ mmol}_{\text{ATP}} \text{ g}_X^{-1} \text{ h}^{-1}$  [28]. This value corresponded well with an  $m_S$  value extrapolated from a  $q_S - \mu$  correlation from a set of anaerobic chemostat experiments at growth rates between  $0.025 \text{ h}^{-1} - 0.2 \text{ h}^{-1}$  (Figure 1.5). This observation indicated that, contrary to many prokaryotes, *S. cerevisiae* displays a growth-independent maintenance energy requirement. The severe calorie restriction in the retentostats did, however, affect viability, which decreased from ca. 90% to ca. 80% after ca. 20 days of cultivation. The retentostat cultures exhibited characteristics previously associated with the fraction of quiescent cells from stationary phase cultures, such as increased heat-shock resistance, accumulation of storage carbohydrates (i.e. glycogen), down-regulation of genes involved in biosynthetic processes, increased expression of genes involved in autophagy, and differential expression of genes downstream of the regulator Rim15 that were previously associated with quiescence [29, 27]. This transcriptional response was not specific to near-zero growth but already occurred at specific growth rates above  $0.025 \text{ h}^{-1}$ , indicating that the observed phenotype is not specific to energy-starved SP cultures [27]. An increase in abundance of heat-shock related proteins identified in a proteome study of anaerobic *S. cerevisiae* retentostat cultures confirmed the stress-tolerance associated transcriptional response at slow growth, while other identified transcriptional changes were only partially observed at the proteome level [24]. Contrary to SP cultures, anaerobic retentostat cultures remained viable and metabolically active at near-zero growth rates. This research was extended by studying the response of prolonged calorie-restricted retentostat cultures to a sudden, complete glucose starvation [27]. The onset of starvation resulted in immediate mobilization of glycogen, and reduction of ATP turnover rates by at least two orders of magnitude, further down-tuning of biosynthetic processes such protein synthesis and, ultimately, loss of culture viability. The importance of the central nutrient signalling protein Rim15 was illustrated by the phenotype in retentostat cultures of a mutant *S. cerevisiae* strain in which *RIM15* was deleted [26]. This strain showed a failure to enter a robust non-growing state, as indicated by an increase in  $m_S$ , a decrease in glycogen accumulation and heat-shock tolerance, an attenuated transcriptional response to nutrient restriction and a decreased viability compared to a reference strain. The characteristic phenotype of non-dividing *S. cerevisiae* and the role of Rim15 observed in anaerobic retentostats, was confirmed in a study by American colleagues, in which non-growing yeast cultures were obtained by growth in calcium alginate beads, packed in a bioreactor under anaerobic calorie-unrestricted conditions [195].

The physiological and genome-wide transcriptional responses at near-zero growth rates of several other industrial microbes have recently also been characterized in retentostats. In particular, these studies focused on *Bacillus subtilis*, *Lactobacillus plantarum*, *Lactococcus lactis* and *Aspergillus niger* [86, 106, 139, 202]. With the exception of *Aspergillus niger*, specific growth rates below  $0.001 \text{ h}^{-1}$  were achieved for all these organisms, corresponding to the use of over 98% of the energy substrate for maintenance energy requirements. As previously observed for *S. cerevisiae*, the bacteria studied in retentostats were quite tolerant to calorie restriction and maintained a culture viability above 90% during prolonged retentostat cultivation. Their transcriptional responses to calorie restriction and near-zero growth resembled those of *S. cerevisiae*, including an important role for nutrient sensing pathways, down regulation of anabolic processes, and increased expression of stress responsive genes. Furthermore, retentostat cultures of *L. plantarum* showed near theoretical product yields for the industrially relevant catabolic product lactic acid.

The examples given in this section illustrate the impact of uncoupling microbial growth from product formation on the yield of catabolic products. Even more challenging is uncoupling growth from microbial production of anabolic compounds, such as proteins, peptides, pharmaceuticals, or food ingredients. The synthesis of these energy-intensive compounds not only requires ATP but also relies on the anabolic machinery for precursor supply. Maintaining high specific production rates in non-growing microbes therefore requires the cells to overcome the general down-tuning of protein synthesis and anabolic routes, while activating specific metabolic pathways and maintaining ATP supply, required for product formation. These targets present a scientifically interesting and industrially relevant challenge for synthetic biologists and metabolic engineers. However, before engineering of cells can be contemplated, it is essential to first gain insights into the physiology of metabolically active non-dividing microbial cultures to develop them as non-growing cell factories. The research described in this thesis builds further on the anaerobic retentostat work performed in the section of Industrial Microbiology at the Delft University of Technology, and focusses on the energetics, robustness and production characteristics of slow- and non-growing budding yeasts under aerobic conditions that enable a fully respiratory sugar metabolism.

## **Scope: towards uncoupling metabolism from growth**

The PhD project described in this thesis was part of a EU funded initiative entitled: “Robustness of yeast strains and bioprocesses for industrial production of novel compounds”, a collaboration between the Institute of Biochemical Engineering at the University of Stuttgart, Fluxome Sciences A/S in Denmark, and the Industrial Microbiology Section of the Delft University of Technology. The initial aim of this public-private partnership was to enable rational design and construction of microbes

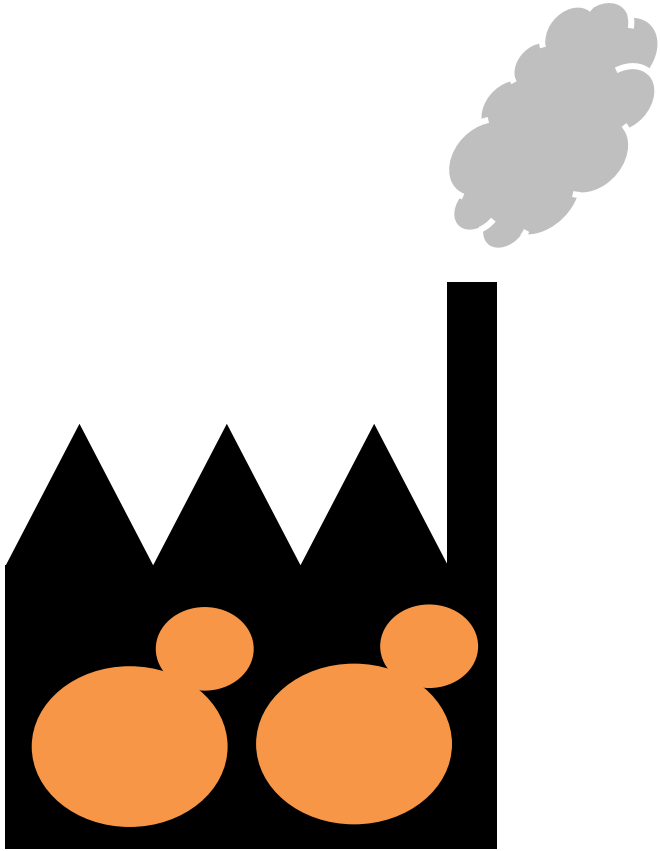
producing novel energy-demanding compounds that maintain high productivity under the dynamic, low specific-growth rate conditions in large-scale industrial fed-batch bioreactors. This goal follows from the crucial need to consider the impact of the final process conditions on the robustness and production characteristics of microorganisms to ensure the realization of a commercially successful bioprocess. Within this initiative, this PhD project focused on the impact of slow-growth conditions commonly faced by engineered *S. cerevisiae* strains producing novel compounds on large scale, and aims at identifying engineering targets to improve the host's robustness and production characteristics towards these conditions.

Chapter 2 of this thesis presents a model case in which the impact of specific growth rate on the production of resveratrol by an engineered *S. cerevisiae* strain was characterized in a range of glucose-limited chemostats at different dilution rates. The high ATP requirements for the synthesis of this compound were reflected by the oxygen demands in the stoichiometry of the metabolic production pathway. The high maintenance energy requirements observed for this strain were a result of the process conditions, and caused a substantial loss of carbon substrates at low growth rates. Together with the observed strong correlation between specific product formation and specific growth rates, these results emphasized the need to uncouple anabolic product formation from growth.

Many scientific studies and publications have explored the physiology of *S. cerevisiae* in stationary phase. The literature on this subject is extremely valuable as it gives a reference for non-growing, non or poorly-metabolically active yeast cultures. Unfortunately, the vast majority, if not all of these studies are performed in shake flasks, without any control of important culture parameters such as pH and dissolved oxygen concentration. In contrast, the research described in this thesis relies on cultures performed in tightly controlled bioreactors. To disentangle SP-specific responses from responses due to poorly-controlled growth conditions, Chapter 3 reports an in-depth multi-level analysis of SP in *S. cerevisiae* grown in bioreactors. Although oxygen availability may strongly influence the physiology of *S. cerevisiae*, for example due to differences in glucose metabolism or ROS-induced stress, the responses of non-growing *S. cerevisiae* cultures to oxygen availability have received little attention. In Chapter 3, the ability of *S. cerevisiae*, rare among yeasts, to grow in the presence as well as in the complete absence of oxygen was employed to evaluate the impact of oxygen on the robustness of SP-cultures at a physiological and transcriptome level.

Optimal yeast-based production of anabolic compounds demands high ATP yields on substrate and presents an inherent requirement for respiratory metabolism. To study non-dividing, metabolically active respiring yeast cultures, aerobic retentostats were set up. Chapter 4 describes the model-aided design of retentostat feeding regimes, and reports a first physiological and transcriptional characterization of fully respiring *S. cerevisiae* under near-zero growth conditions. This study focused in particular on

the energetics, robustness and metabolic capacity of *S. cerevisiae* at near-zero growth, because of their relevance for industrial applications. The successful implementation of aerobic retentostats with *S. cerevisiae* led to an exploration of the industrially relevant, Crabtree-negative yeast *P. pastoris*. In a joint project with the University of Natural Resources and Life Sciences in Vienna, the physiological changes and transcriptional response of this yeast at near zero-growth rates were explored and described in chapter 5. This study enabled a first comparative analysis of the physiology of yeasts grown in the 'twilight zone' between exponential growth and starvation for two industrially relevant yeast species.



Growth-rate dependency of *de novo* resveratrol production in chemostat cultures of an engineered *Saccharomyces cerevisiae* strain

Tim Vos, Pilar de la Torre Cortés, Walter M. van Gulik, Jack T. Pronk, Pascale Daran-Lapujade

Published in *Microbial Cell Factories* 2015, 14:131



### Abstract

*Saccharomyces cerevisiae* has become a popular host for production of non-native compounds. The metabolic pathways involved generally require a net input of energy. To maximize the ATP yield on sugar in *S. cerevisiae*, industrial cultivation is typically performed in aerobic, sugar-limited fed-batch reactors which, due to constraints in oxygen transfer and cooling capacities, have to be operated at low specific growth rates. Because intracellular levels of key metabolites are growth-rate dependent, slow growth can significantly affect biomass-specific productivity. Using an engineered *Saccharomyces cerevisiae* strain expressing a heterologous pathway for resveratrol production as a model energy-requiring product, the impact of specific growth rate on yeast physiology and productivity was investigated in aerobic, glucose-limited chemostat cultures.

Stoichiometric analysis revealed that *de novo* resveratrol production from glucose requires 13 moles of ATP per mole of produced resveratrol. The biomass-specific production rate of resveratrol showed a strong positive correlation with the specific growth rate. At low growth rates a substantial fraction of the carbon source was invested in cellular maintenance-energy requirements (e.g. 27% at 0.03 h<sup>-1</sup>). This distribution of resources was unaffected by resveratrol production. Formation of the by-products coumaric, phloretic and cinnamic acid had no detectable effect on maintenance energy requirement and yeast physiology in chemostat. Expression of the heterologous pathway led to marked differences in transcript levels in the resveratrol-producing strain, including increased expression levels of genes involved in pathways for precursor supply (e.g. *ARO7* and *ARO9* involved in phenylalanine biosynthesis). The observed strong differential expression of many glucose-responsive genes in the resveratrol producer as compared to a congeneric reference strain could be explained from higher residual glucose concentrations and higher relative growth rates in cultures of the resveratrol producer.

*De novo* resveratrol production by engineered *S. cerevisiae* is an energy demanding process. Resveratrol production by an engineered strain exhibited a strong correlation with specific growth rate. Since industrial production in fed-batch reactors typically involves low specific growth rates, this study emphasizes the need for uncoupling growth and product formation via energy-requiring pathways.

## Introduction

The budding yeast *Saccharomyces cerevisiae* is intensively used for metabolic engineering studies aimed at the production of non-native low-molecular compounds. In such research, the rapidly expanding toolbox for yeast synthetic biology is used for functional expression of heterologous product pathways, optimization of precursor supply from central carbon metabolism, minimization of by-product formation and efficient product export [128]. For successful implementation of engineered yeast strains in large-scale processes, energetics of product formation and conditions in industrial bioreactors need to be taken into consideration.

Virtually all non-native compounds produced by engineered strains require a net input of ATP for their formation from glucose [122, 19, 51]. In such scenarios, product formation competes for precursors and ATP with growth and maintenance processes [217]. In *S. cerevisiae*, the ATP yield from alcoholic fermentation is  $2 \text{ mol mol}_{\text{glucose}}^{-1}$ . The ATP yield from oxidative phosphorylation is determined by the P/O ratio: the number of ATP molecules synthesized for each electron pair transferred to oxygen via the mitochondrial respiratory chain [291]. Although the *in vivo* P/O ratio for oxidation of NADH and FADH in *S. cerevisiae* (ca. 1.0 [291]) is lower than in many other eukaryotes, respiratory glucose dissimilation still yields approximately 8-fold more ATP per mole of glucose than alcoholic fermentation. For yeast-based production of compounds whose synthesis requires a net input of ATP, it is therefore crucial that glucose dissimilation occurs exclusively via respiration. Even under fully aerobic conditions, *S. cerevisiae* exhibits a predominantly fermentative metabolism when grown at high sugar concentrations [70]. Only at low to intermediate specific growth rates in aerobic, sugar-limited cultures, sugar dissimilation occurs exclusively via respiration.

In industry, aerobic, sugar-limited yeast cultivation is typically performed in fed-batch reactors [190], in which the sugar feed rate controls the specific growth rate. However, the limited oxygen-transfer capacity and cooling capacity of large-scale (50 – 200 m<sup>3</sup>) bioreactors forces operators to decrease the specific growth rate when the dissolved oxygen concentration in bioreactors decreases to a critical value to prevent glucose dissimilation through alcoholic fermentation. Especially towards the end of high-biomass density fed-batch processes, this measure can result in specific growth rates that are below 5% of the maximum specific growth rate observed in batch cultures grown on excess sugar [98, 277]. Therefore, prediction of the performance of strains in industrial processes requires quantitative data on growth-rate-dependent product formation. Ideally, performance under industrial conditions should already be taken into account in strain design and construction.

The relationship between specific growth rate ( $\mu$ , h<sup>-1</sup>) and the biomass-specific rate of product formation ( $q_p$ , mmol<sub>product</sub> g<sub>biomass</sub><sup>-1</sup> h<sup>-1</sup>) can be investigated in steady-state

chemostat cultures, in which the specific growth rate equals the dilution rate [198]. Using this approach, a positive correlation between growth and product formation was found for several heterologous proteins [116, 170]. In the case of heterologous proteins, such a positive correlation of  $q_p$  and  $\mu$  may be caused by several factors, including the capacity of the ribosomal machinery, size of amino-acyl-tRNA pools, activity of excretion pathways and cellular energy status. Unlike catabolic products, the formation of ATP-requiring products is not stoichiometrically coupled to growth. Instead, the distribution of carbon to either biomass or product formation depends on the competition between enzymes involved in anabolic routes and in the product synthetic pathway for precursors, ATP and co-factors. The sensitivity of such kinetics to changes in growth rate depends on a multitude of factors, in particular the nature of the synthetic route of the product of interest, the cellular concentration of key metabolites and the abundance and kinetic properties of the competing enzymes. The impact of growth on formation of an “anabolic” product is therefore extremely arduous to predict. So far, very few published studies describe the growth-rate dependency of physiological and production characteristics of non-native, ATP-requiring products in *S. cerevisiae* [151, 136].

Resveratrol (trans-3,5,4'-trihydroxystilbene) is a polyphenolic stilbenoid sold as nutraceutical and food ingredient. Reported health benefits include anti-oxidant effects, life span extension, inhibiting obesity and cancer prevention [252]. Commercial production of resveratrol from plant sources such as *Polygonum cuspidatum* is complicated by slow growth, low product yield, inconsistent performance, and difficult purification procedures [152]. Hence, the use of microbial production hosts has gained attention as a promising industrially relevant alternative. Formation of resveratrol from L-phenylalanine by engineered *S. cerevisiae* involves four heterologous reactions, catalysed by phenylalanine ammonia lyase (*PAL*) [231], cinnamate 4-hydroxylyase (*C4H*) [21] which associates with a heterologous cytochrome p450 reductase (*ATR2*) [193] and a native cytochrome *b5* electron carrier (*CYB5*), 4-coumarate-CoA ligase (*4CL*) [82], and stilbene synthase (*VST* or *STS*) [19]. The latter enzyme reaction requires three malonyl-CoA molecules to form one molecule of resveratrol. Pathway stoichiometry predicts that *de novo* synthesis of resveratrol by the engineered yeast strain costs 12 mol ATP per mol resveratrol, not taking into account possible ATP costs for product export or regeneration of co-factors, thereby making resveratrol a relevant model for an ATP-required, heterologous product of engineered *S. cerevisiae*.

Hitherto, studies on microbial production of resveratrol have focussed on metabolic pathway engineering in *Escherichia coli* and *Saccharomyces cerevisiae*, and physiological tests have only been reported for uncontrolled shake flask or batch fermentations on rich media or media supplemented with the resveratrol precursors p-coumaric acid, phenylalanine or tyrosine (reviewed in [188]). Such cultures, however, do not provide

data on strain physiology and kinetics of product formation under industrially relevant process conditions.

The goal of the present study was to investigate the impact of specific growth rate on biomass-specific productivity, product yield, by-product formation and host strain physiology of a *S. cerevisiae* strain that was previously engineered for *de novo* production of resveratrol from glucose. To this end, (by)product formation, physiology and transcriptome were analysed in steady-state, glucose-limited chemostat cultures grown at different dilution rates.

## Results

***De novo* production in an engineered *Saccharomyces cerevisiae* strain: pathway and stoichiometry** | To facilitate interpretation of results from chemostat cultures, a metabolic model covering *S. cerevisiae* central carbon metabolism was expanded to include the resveratrol synthesis pathway present in *S. cerevisiae* strain FS09322 [67]. This strain expresses 5 heterologous plant enzymes that, together, catalyse the conversion of L-phenylalanine and malonyl-CoA to resveratrol (Figure 2.1). *PAL2* encodes a phenylalanine ammonia-lyase that converts L-phenylalanine to cinnamate. Subsequently, cinnamate-4-hydroxylase (encoded by *C4H*) in conjunction with the electron carrier cytochrome *b5* (*CYB5*) and a cytochrome p450 reductase (*ATR2*), oxidizes cinnamate to coumarate. A coumarate co-A-ligase (*4CL2*) covalently binds a coenzyme-A group to coumarate, forming coumaroyl-CoA. Finally, trihydroxystilbene synthases encoded by *VST1* and *STS* catalyse the reaction of coumaroyl-CoA with three molecules of the precursor malonyl-CoA, thereby forming resveratrol. The *SNQ2* gene, which encodes an ATP dependent plasma membrane transporter, was overexpressed to optimize resveratrol export. *ARO10*, which encodes a phenylpyruvate decarboxylase was deleted to reduce catabolism of phenylpyruvate via the Ehrlich pathway [232]. Three molecules of malonyl-CoA are required per molecule of resveratrol, which are produced from cytosolic acetyl-CoA.

In *S. cerevisiae*, cytosolic acetyl-CoA is formed by the concerted action of glycolysis, pyruvate decarboxylase, acetaldehyde dehydrogenase and acetyl-CoA synthetase. Further, *S. cerevisiae* produces L-phenylalanine via the shikimate pathway from erythrose 4-phosphate and phosphoenolpyruvate. Erythrose-4P formation can occur via the oxidative and the non-oxidative pentose phosphate pathway, depending on the overall pathway balance of redox-cofactor NADPH. Because *S. cerevisiae* has both NADH and NADPH dependent acetaldehyde dehydrogenases and glutamate dehydrogenases, 4 different scenarios were incorporated in the stoichiometric model to determine the theoretical maximum yield of resveratrol on glucose (Table 2.1). In total, 13 moles ATP need to be invested for the production and export of one mole resveratrol, with

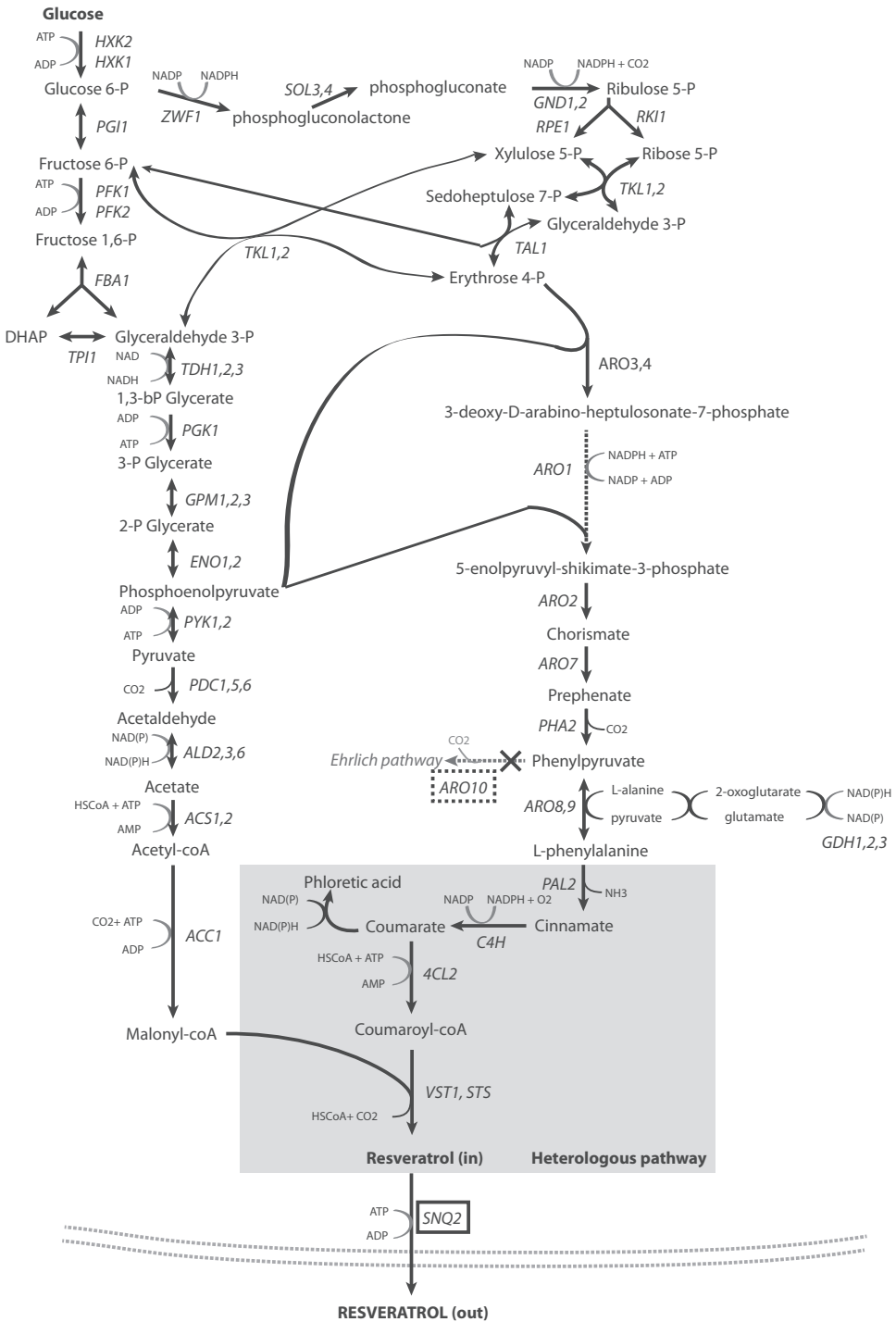


**Figure 2.1:** Schematic representation of the engineered *de novo* resveratrol production pathway in a *S. cerevisiae* strain. Dotted framed boxes indicate deleted genes and grey boxes indicate heterologous genes encoding enzymes in the resveratrol biosynthesis pathway. Phloretic acid is hypothetically formed from coumaric acid from an unidentified reduction reaction [27].

**Table 2.1:** Maximum theoretical yield of resveratrol on glucose, depending on co-factor specificity of specific enzymes. A stoichiometric model was used to determine the maximum theoretical yield of resveratrol on glucose, and to calculate the ATP demand per mol of product by summing the ATP produced in glycolysis (Glyc), the citric acid cycle (TCA) and by oxidative phosphorylation (OxPh).

Active proteins (co-factor specificity)	$Y_{P/S}^{\max}$ $mol.mol^{-1}$	ATP			
		Glyc (mol)	TCA (mol)	OxPh (mol)	Total (mol)
Ald6 (NADP) & Gdh2 (NAD)	0.284	2.875	0.875	9.25	13
Ald6 (NADP) & Gdh1/3 (NADP)	0.282	2.750	0.750	9.50	13
Ald2/3 (NAD) & Gdh2(NAD)	0.279	2.500	0.500	10.00	13
Ald2/3 (NAD) & Gdh1/3 (NADP)	0.277	2.375	0.375	10.25	13

an estimated *in vivo* P/O ratio in *S. cerevisiae* of 1.0 [291] and assuming no growth or maintenance requirements. This ATP requirement can be fulfilled by reoxidizing the cytosolic NADH that is formed during resveratrol production by mitochondrial respiration, combined with combustion of up to 0.44 moles of glucose, depending on co-factor specificity of the pathway. For *S. cerevisiae* grown on glucose, Ald6 has been described as the major acetaldehyde dehydrogenase and Gdh1 as the major glutamate dehydrogenase, which both use NADP as a co-factor [187, 75]. Assuming these reactions occur in the pathway yields the overall reaction:



As a result, the maximum theoretical yield of resveratrol on glucose produced in recombinant *S. cerevisiae* equals  $0.28 \text{ mol mol}^{-1}$ .

**Resveratrol production affects yeast physiology** | Growth and product formation by the resveratrol-producing strain *S. cerevisiae* FS09322 were compared to that of the congeneric reference strain CEN.PK113-7D in batch and chemostat cultures. The maximum specific growth rate of strain FS09322, estimated from duplicate shake-flask batch cultures on glucose synthetic medium, was  $0.25 \text{ h}^{-1}$ . This growth rate was 38 % lower than that of the reference strain. In steady-state chemostat cultures grown at a dilution rate of  $0.10 \text{ h}^{-1}$ , not only resveratrol, but also the intermediates coumaric acid, cinnamic acid and phloretic acid were produced by strain FS09322 (see Table 2.2). In these chemostat cultures, the biomass yield on glucose of strain FS09322 was lower and respiration rates were consistently higher than that of the reference strain. For both strains, viability of these chemostat cultures, as assessed by staining with fluorescent dyes and flow cytometry, was above 90% (Figure 2.2A). The formation rates of the by-products coumaric acid, phloretic acid and cinnamic acid are relatively low (Figure 2.2C). Still, it was conceivable that their formation contributed to the reduced biomass yield of strain FS09322 in the chemostat cultures, e.g. via weak-acid uncoupling. To investigate this possibility, glucose-limited chemostat cultures of the reference strain CEN.PK113-7D were supplemented with the products of the resveratrol pathway at concentrations close to their solubility in water.

**Table 2.2:** Physiological characteristics of FS09322 and congenic strain CEN.PK113-7D in aerobic glucose-limited chemostats. A dilution rate of  $0.10 \text{ h}^{-1}$  was applied. Data represent the average  $\pm$  standard deviation of measurements on three independent chemostats for resveratrol producing strain FS09322 and two independent chemostats for congenic reference strain CEN.PK113-7D.

	FS09322	CEN.PK113-7D
<i>Concentrations (<math>\mu\text{M}</math>)</i>		
Resveratrol	$437 \pm 39$	n.d. <sup>1</sup>
Coumaric acid	$86 \pm 11$	n.d.
Phloretic acid	$120 \pm 20$	n.d.
Cinnamic acid	$20 \pm 10$	n.d.
<i>Biomass specific uptake and production rates (<math>\text{mmol.gX}^{-1}.\text{h}^{-1}</math>)</i>		
Glucose	$-1.22 \pm 0.03$	$-1.11 \pm 0.01$
CO <sub>2</sub>	$3.18 \pm 0.05$	$2.65 \pm 0.05$
O <sub>2</sub>	$-3.09 \pm 0.03$	$-2.61 \pm 0.02$
Pooled products	$0.02 \pm 0.00$	n.d.
<i>Yields on glucose</i>		
Biomass ( $\text{g g}^{-1}$ )	$0.44 \pm 0.00$	$0.50 \pm 0.00$
Resveratrol ( $\text{mol mol}^{-1}$ )	$0.011 \pm 0.001$	
Pooled products ( $\text{mol mol}^{-1}$ )	$0.016 \pm 0.002$	

<sup>1</sup>n.d. = not detected

**Table 2.3:** Impact of resveratrol pathway products on physiology of CEN.PK113-7D. The prototrophic reference strain CEN.PK113-7D was grown in aerobic, glucose-limited chemostat cultures in the absence or presence of phloretic acid, cinnamic acid, coumaric acid or resveratrol. Data represent the average  $\pm$  standard deviation of measurements on two independent chemostat cultures. Phloretic acid, cinnamic acid, coumaric acid or resveratrol were not consumed by CEN.PK113-7D in chemostat cultures.

	Concentration $\text{mg L}^{-1}$	Biomass yield $\text{g g}^{-1}$	q <sub>S</sub> $\text{g gX}^{-1} \text{h}^{-1}$	q <sub>CO2</sub> $\text{g gX}^{-1} \text{h}^{-1}$	Viability %
Reference	-	$0.49 \pm 0.00$	$-1.13 \pm 0.00$	$2.62 \pm 0.01$	$92 \pm 1$
Phloretic acid	$253 \pm 1$	$0.50 \pm 0.00$	$-1.12 \pm 0.01$	$2.58 \pm 0.06$	$91 \pm 3$
Cinnamic acid <sup>1</sup>	$154 \pm 18$	$0.47 \pm 0.00$	$-1.18 \pm 0.02$	-	$94 \pm 1$
Coumaric acid	$91 \pm 5$	$0.49 \pm 0.00$	$-1.14 \pm 0.00$	$2.67 \pm 0.00$	$93 \pm 1$
Resveratrol	$6.3 \pm 0.8$	$0.49 \pm 0.00$	$-1.15 \pm 0.00$	$2.68 \pm 0.02$	$95 \pm 0$

<sup>1</sup> Repeated efforts to obtain a steady state with cultures grown in the presence of cinnamic acid consistently resulted in periodic variations in the oxygen uptake and carbon dioxide production.

None of these compounds were consumed and they affected neither the biomass yield on glucose nor the culture viability (above 90% in all cultures, Table 2.3).

**Specific growth rate affects product formation** | The effect of specific growth rate on resveratrol production by *S. cerevisiae* was analyzed in steady-state glucose-limited chemostat cultures of the resveratrol-producing strain FS09322 and the reference strain CEN.PK113-7D. Independent replicate cultures of each strain were grown at  $0.025 \text{ h}^{-1}$ ,  $0.05 \text{ h}^{-1}$ ,  $0.075 \text{ h}^{-1}$  (FS09322 only),  $0.10 \text{ h}^{-1}$  and  $0.15 \text{ h}^{-1}$ . At these dilution rates, sugar dissimilation in the chemostat cultures was completely respiratory, as evident from the

absence of ethanol in culture supernatants and a respiratory quotient ( $q_{\text{CO}_2}/q_{\text{O}_2}$ ) that was close to unity. Culture viability remained above 90% for both strains at dilution rates above  $0.075 \text{ h}^{-1}$ . However, below this dilution rate, viability of strain FS09322 decreased, reaching a value of ca. 76% at a dilution rate of  $0.025 \text{ h}^{-1}$  (Figure 2.2A). This implied that, especially at low dilution rates, the specific growth rate no longer exactly matched the dilution rate. For the sake of clarity, we will refer to the value of the dilution rate throughout this paper.

Residual glucose concentrations in culture supernatants remarkably differed between the two strains. While the residual glucose concentration in cultures of the reference strain remained between 0.1 and 0.17 mM over this range of dilution rates, it strongly increased with increasing dilution rate in cultures of the resveratrol producer, reaching  $0.37 \pm 0.02 \text{ mM}$  at the highest dilution rate tested (Figure 2.2B). The biomass-specific resveratrol production rate exhibited a strong positive correlation with the specific growth rate in strain FS09322 (Figure 2.2C, linear regression  $R^2 > 0.9$ ). A similar positive correlation was found for the specific coumaric acid production rate (Figure 2.2C) and for the pooled phenylpropanoid-pathway-derived products (resveratrol, coumaric acid, cinnamic acid and phloretic acid, Figure 2.2D). This biomass-specific pooled product formation rate reached  $0.024 \pm 0.002 \text{ mmol g}_{\text{biomass}}^{-1} \text{ h}^{-1}$  at the highest tested dilution rate ( $0.15 \text{ h}^{-1}$ ). Conversely, the biomass-specific production of phloretic acid, presumably formed from coumaric acid via an unidentified reduction reaction [17], was not correlated to the specific growth rate. The yield of total products on glucose was stable around  $0.018 \text{ g g}^{-1}$  at dilution rates ranging from  $0.025$  to  $0.10 \text{ h}^{-1}$ , but decreased to  $0.014 \pm 0.001 \text{ g g}^{-1}$  at a dilution rate of  $0.15 \text{ h}^{-1}$  (Figure 2.2E). The maximum resveratrol yield was obtained at a dilution rate of  $0.10 \text{ h}^{-1}$  and equaled  $0.011 \pm 0.001 \text{ mol mol}^{-1}$  (Table 2.2), representing 4.1% of the maximum theoretical yield of  $0.28 \text{ mol mol}^{-1}$  (see above). The difference in biomass yield between the resveratrol-producing strain FS09322 and the reference strain CEN.PK113-7D that was observed at a dilution rate of  $0.10 \text{ h}^{-1}$  (Table 2.2) was also found at the other dilution rates (Figure 2.2F). The average difference in biomass yield between the two strains was 12%, while  $q_{\text{CO}_2}$  and  $q_{\text{O}_2}$  increased on average by 21% and 22%, respectively (Supplementary Figure 2.4). These differences were significant ( $p$ -value  $< 0.05$ ) for all dilution rates above  $0.025 \text{ h}^{-1}$ .

**Expression of the resveratrol production pathway does not impact cellular maintenance energy requirements** | Growth-rate-independent maintenance energy requirements ( $m_s$ ) of the resveratrol producing strain FS09322 and the reference strain CEN.PK113-7D were estimated by plotting biomass-specific glucose consumption rates as a function of specific growth rate [28, 218]. This yielded similar values for  $m_s$  of  $0.12 \pm 0.02 \text{ mmol (g biomass)}^{-1} \text{ h}^{-1}$  for strain FS09322 and  $0.10 \pm 0.01 \text{ mmol g}_{\text{biomass}}^{-1} \text{ h}^{-1}$  for strain CEN.PK113-7D (Figure 2.2G). When assuming a P/O ratio of 1.0 [291] in fully respiratory metabolism, the maintenance energy requirements can be translated to



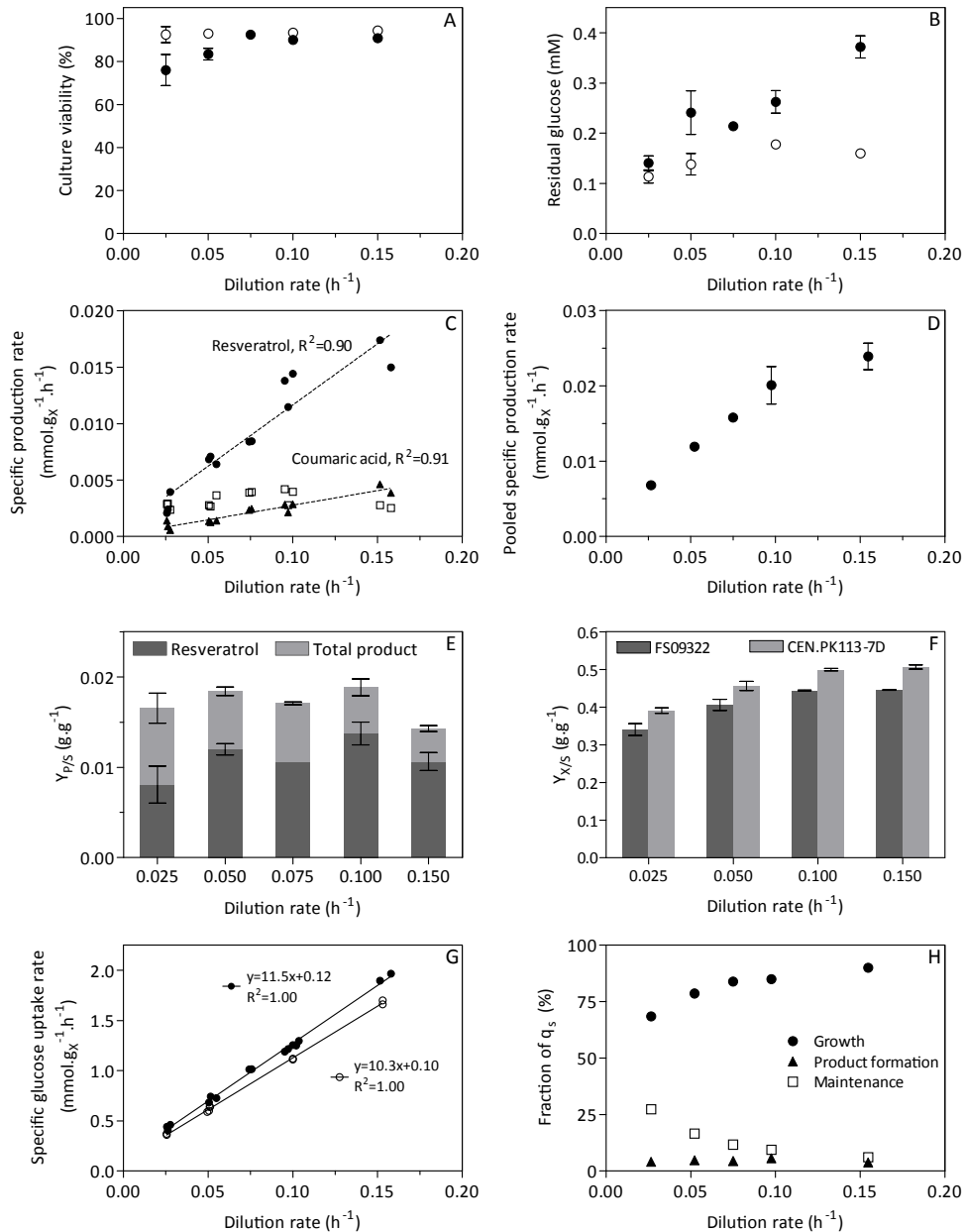


**Figure 2.2:** Physiological characteristics of the resveratrol producer FS09322 and of the congeneric prototrophic strain CEN.PK113-7D. The data were obtained from aerobic glucose-limited chemostat cultures at various growth rates. A. Culture viability measured by flow cytometry analysis of PI and CFDA staining (see Material and Methods section). Open symbols indicate CEN.PK113-7D, closed symbols indicate FS09322. B. Residual glucose concentration, closed symbols FS09322, empty circles CEN.PK113-7D. C. Biomass specific production rate of resveratrol (circles) coumaric acid (triangles) and phloretic acid (squares) in FS09322. D. Biomass specific production rate of the pooled products (resveratrol + coumaric acid + phloretic acid + cinnamic acid) for FS09322. E. Resveratrol and total product yield on glucose. F. Biomass yield on glucose. G. Biomass specific glucose uptake rate, FS09322 in closed symbols and CEN.PK113-7D in open symbols. H. Distribution of the specific substrate uptake ( $q_s$ ) in FS09322 as calculated from the Herbert-Pirt equation (Equation 2.2) for independent chemostats. In panels A, B, D, E, F and H, the shown data represent the average and standard deviation of at least two independent culture replicates for each dilution rate and each strain.

values of  $1.92 \pm 0.32$  and  $1.52 \pm 0.15$  mmol g<sup>-1</sup> h<sup>-1</sup> ATP for FS09322 and CEN.PK113-7D, respectively.

The Herbert-Pirt equation [218] specifies that, in energy-source-limited chemostat cultures, the biomass-specific substrate uptake rate ( $q_S$ ) is distributed over growth, expressed as  $\left(\mu \cdot (Y_{X/S}^{max})^{-1}\right)$ , maintenance ( $m_S$ ) and product formation, expressed as  $\left(\sum_i (q_{P_i} \cdot (Y_{P_i/S}^{max})^{-1})\right)$ , which is the sum of all anabolic products excreted by the organism. The reference strain CEN.PK113-7D invests all glucose in growth and maintenance and does not make product, which simplifies the Herbert-Pirt relation to Equation 2.1:

$$q_S = \frac{\mu}{Y_{X/S}^{max}} + m_S \quad (2.1)$$

Because strain FS09322 also invests part of the consumed glucose in product formation and excretion, the production term has to be added in the equation, resulting in Equation 2.2:

$$q_S = \frac{\mu}{Y_{X/S}^{max}} + m_S + \left(\sum_i \frac{q_{P_i}}{Y_{P_i/S}^{max}}\right) \quad (2.2)$$

For both the reference strain and the producing strain, the substrate uptake rate ( $q_S$ ) was experimentally determined at each dilution rate (Figure 2.2G). Furthermore, the substrate requirements for maintenance purposes ( $m_S$ ) were estimated for both strains as described above. For the production strain, the maximum theoretical product yield was calculated using the stoichiometric model, and the specific production rates were determined experimentally for all products (Figure 2.2C). Subsequently, Equation 2.2 was used to calculate the substrate fractions distributed between product formation ( $q_S$  divided by the production term), maintenance energy requirements ( $q_S$  divided by  $m_S$ ), and growth (remaining fraction), for strain FS09322 at each tested dilution rate (Figure 2.2H). Accordingly, in the resveratrol producer the fraction of substrate invested in maintenance processes increased at low growth rates, reaching  $27 \pm 2$  % of the total specific substrate consumption at the lowest dilution rate. Conversely, the fraction of the glucose channeled towards (pooled) product formation was remarkably growth-rate independent at  $4.5 \pm 0.5$  % (Figure 2.2H).

**Specific growth rate differentially affects gene expression in a resveratrol producer and a reference strain** | To assess the impact of expressing a resveratrol pathway on the transcriptome of *S. cerevisiae*, genome-wide transcript levels of the resveratrol producer and the reference strain were compared over the whole range of dilution rates. Growth rate is known to strongly affect gene expression [225]. As expected, in both strains this typical transcriptome response was observed with an overrepresentation of genes involved in biosynthetic processes and protein synthesis among the genes

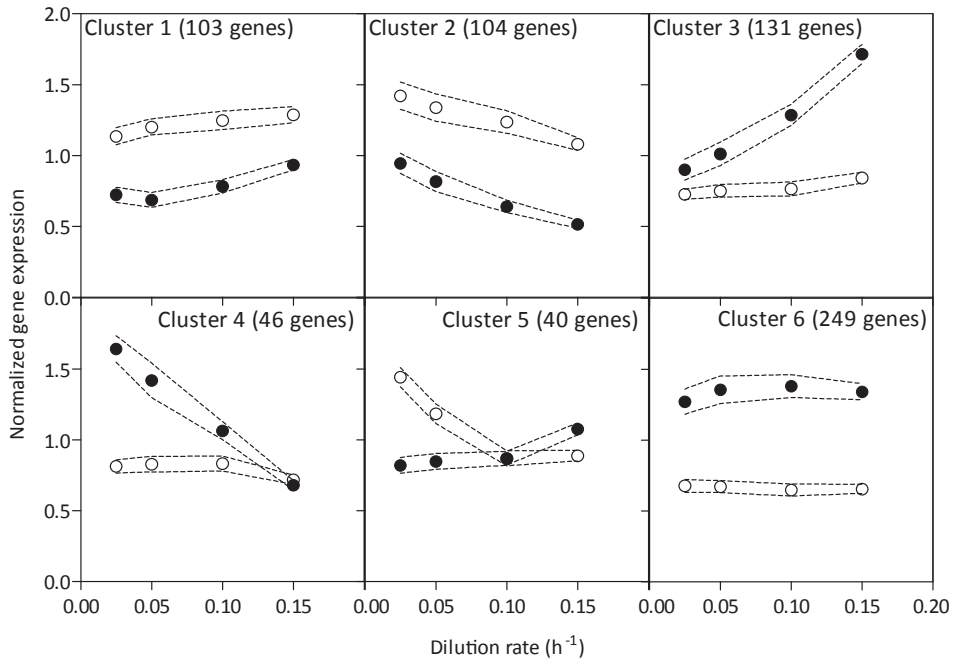


**Figure 2.3:** K-mean clustering of the 673 genes with differential expression profiles between FS09322 and CEN.PK113-7D. The data results from a dilution range of independent chemostat cultures (q-value for differential expression profiles below 0.005, see Material and Methods section). For each cluster, the averaged normalized expression values are depicted for the resveratrol producing *S. cerevisiae* FS09322 (black circles) and for its congenic reference strain CEN.PK113-7D (open symbols) for the different dilution rates. The grey dotted lines exhibit the average standard error of these values.

which expression was negatively correlated to growth rate, and an enrichment for stress-responsive genes among the genes which expression was positively correlated to growth rate. More interesting was the set of genes that were specifically differentially expressed in the resveratrol producer as compared to the reference strain. 673 genes with significantly divergent expression profiles (q-value < 0.005, see Material and Method section) in the resveratrol-producing and reference strain were identified and classified in 6 clusters according to their expression profile (Figure 2.3).

Only gene expression profiles in clusters 1 and 6 showed no obvious correlation with dilution rate, but revealed a strong, consistent difference in expression between the two strains. Remarkably, a strong overrepresentation of genes whose transcript levels were previously identified as being glucose-responsive were found in cluster 2 (34 out of 104 genes, p-value of  $5.7 \cdot 10^{-11}$ ), cluster 3 (44 out of 131 genes, p-value of  $5.5 \cdot 10^{-14}$ ) and cluster 6 (44 out of 249 genes, p-value  $1.8 \cdot 10^{-4}$ ) (Table 2.4) [157]. Genes known to be down-regulated in response to high glucose levels were overall more down-regulated in the resveratrol producing strain with increasing growth rate (Cluster 2). Several structural genes that encode enzymes involved in *de novo* production of resveratrol and

**Table 2.4:** Overrepresentation of MIPS categories among the clusters of differentially expressed genes (see Figure 3). A statistical Bonferroni-corrected p-value threshold for overrepresentation of 0.05 was applied.

Cluster	Functional category	# genes in cluster	# genes in category	Bonf.-corrected p-value <sup>1</sup>
1	Ribosome biogenesis	18	343	$1.68 \cdot 10^{-2}$
2	Glucose responsive DOWN [157]	34	565	$5.73 \cdot 10^{-11}$
	Lipid, fatty acid and isoprenoid metabolism	20	291	$7.10 \cdot 10^{-05}$
	ENERGY	18	360	$3.77 \cdot 10^{-02}$
3	Glucose responsive UP [157]	44	589	$5.48 \cdot 10^{-14}$
4	No significant terms			
5	No significant terms			
6	Glucose responsive UP [157]	44	589	$5.48 \cdot 10^{-14}$

<sup>1</sup> A statistical Bonferroni-corrected p-value threshold for overrepresentation of 0.05 was applied.

its precursors from glucose were differentially expressed in the resveratrol-producing and reference strain. *PDC1*, which is involved in cytosolic acetyl-CoA synthesis and, thereby, in malonyl-CoA supply (cluster 3), as well as *ARO7* and *ARO9* (clusters 3 and 6 respectively), which are involved in phenylalanine biosynthesis, displayed higher expression levels in strain FS09322 than in the reference strain. *TKL1* (cluster 3) and *RKII* (cluster 1) encoding a transketolase and ribose-5-phosphate ketol-isomerase respectively, two key enzymes in the pentose phosphate pathway, were also differentially expressed in the two strains. *SNQ2* (multi-drug transporter) and *CYB5* (cytochrome *b5*), of which additional copies were integrated in the genome of the resveratrol producing strain, were unexpectedly not significantly differentially expressed. *PDR12*, which encodes for another multidrug ABC transporter displayed higher expression levels in the resveratrol production strain than in the reference strain (cluster 3). Furthermore, cluster 1 was enriched for genes encoding ribosomal proteins (18 out of 343 genes, p-value of  $1.7 \cdot 10^{-2}$ ), suggesting a constitutively lower expression of these genes in FS09322 as compared to CEN.PK113-7D. However, measurement of whole cell protein content did not show differences between the two strains (Supplementary Figure 2.5). Finally, gene expression levels indicated that *ALD6* (100-fold higher expression than *ALD2* and *ALD3*) and *GDH1* (6-fold higher expression than *GDH2* and *GDH3*) encoded the main acetaldehyde and glutamate dehydrogenases respectively in our cultivation conditions, as hypothesized earlier.

## Discussion

**Resveratrol yield in chemostat cultures** | Earlier studies on resveratrol production by yeast did not allow for a quantitative analysis of product yields on glucose, as the strains used lacked a complete biosynthetic pathway and were fed with coumaric acid or aromatic amino acids as precursors [188]. The present study describes a first quantitative

analysis of a *S. cerevisiae* strain that was engineered for *de novo* production of resveratrol from glucose. In glucose-limited, aerobic chemostat cultures of *S. cerevisiae* FS09322, the resveratrol yield on glucose was approximately  $0.011 \pm 0.002 \text{ g g}^{-1}$  (Figure 2.2E), irrespective of the specific growth rate.

The resveratrol yield on glucose found in this study is ca. three-fold higher than the product yield in batch cultures of a *S. cerevisiae* strain engineered for production of naringenin, a product that is also derived from the phenylpropanoid pathway [154]. However, the experimental resveratrol yield is only ca. 4 % of the maximum theoretical yield of  $0.28 \text{ mol mol}^{-1}$ , indicating that there is substantial room for further improvement of resveratrol yields. One aspect that should be addressed in this context is formation of by-products derived from the phenylpropanoid pathway. Excretion of coumaric acid and phloretic acid by the resveratrol-producing strain (Figure 2.2C) represents a loss of approximately one third of the carbon entering the phenylpropanoid pathway. These by-products were also found in cultures of a *S. cerevisiae* strain engineered for naringenin production [154], indicating that their formation is a generic challenge in engineering of the phenylpropanoid pathway. Addressing this carbon loss by further metabolic engineering is complicated by the fact that the enzyme(s) responsible for phloretic acid synthesis in *S. cerevisiae*, possibly through a NAD(P)H-dependent reduction of coumaric acid, is (are) as yet unknown [17, 154]. Other metabolic engineering strategies that may contribute to improved resveratrol production include deregulation of aromatic amino acid metabolism [176], engineering flux and energy coupling of cytosolic acetyl-CoA synthesis [196, 155], and expression of a deregulated allele of *ACC1* [246].

**Resveratrol productivity is growth-rate dependent |** The relationship between specific growth rate ( $\mu$ ) and biomass-specific productivity ( $q_p$ ) is a key parameter in the design of aerobic fed-batch processes for microbial product formation. We observed a strong positive correlation between  $q_p$  and  $\mu$  in aerobic, glucose-limited cultures of an engineered, resveratrol-producing strain of *S. cerevisiae*. Well documented  $q_p$ - $\mu$  relationships for engineered yeast strains are scarce. Similar positive correlations between  $q_p$  and  $\mu$  relations as identified in this study were found for heterologous production of proteins by engineered yeasts [224, 170] and for production of ethylene by a *S. cerevisiae* strain expressing a heterologous ethylene-forming enzyme [136]. Measurements at two dilution rates in aerobic, glucose-limited chemostat cultures of an *S. cerevisiae* strain engineered for production of  $\alpha$ -santalene, a product derived from the isoprenoid pathway, also indicated a positive correlation of these parameters [151]. These processes share an ATP requirement for product formation, as well as the use of precursors that also play a key role in biomass synthesis (in the case of resveratrol production, phenylalanine and malonyl-CoA).

The same mechanisms that tune down anabolic routes as the growth rate decreases most probably also tune down product formation. In glucose-limited cultures of *S. cerevisiae*, the strong correlation of specific growth rate with the intracellular concentrations of key metabolic intermediates [30], provides a plausible explanation for the observed positive correlation of  $q_P$  and  $\mu$ . In view of the central role of many of the involved precursors in central metabolism, breaking this correlation represents a major challenge for metabolic engineers and synthetic biologists [28]. Conversely to  $q_P$ , the fraction of substrate invested in product formation is rather insensitive to growth rate. It is remarkable that, while yeast cells have to carefully allocate their limited carbon and energy resources between biomass formation and maintenance, the fraction of resources channelled towards product formation remains unchanged over the tested growth rate range.

**High maintenance-energy requirements are caused by process conditions rather than by resveratrol production** | Large-scale aerobic fed-batch processes invariably involve a decreasing specific growth rate. Maintenance-energy requirements ( $m_S$ ,  $\text{mmol}_{\text{glucose}} \text{g}_{\text{biomass}}^{-1} \text{h}^{-1}$ ) can therefore have a strong impact on the performance of microbial strains in such processes. This was also observed in chemostat cultures of the resveratrol-producing strain. At a dilution rate of  $0.025 \text{ h}^{-1}$  which, with a culture viability of 76 %, corresponded to a specific growth rate of ca.  $0.03 \text{ h}^{-1}$ , 27 % of the glucose fed to the cultures was respired to meet cellular maintenance energy requirement, rather than channelled towards growth or resveratrol production (Figure 2.1H). Reducing this loss of substrate carbon, for example by choice of a microbial host with a lower maintenance-energy requirement, can have a significant impact on product yields in industrial fed-batch processes.

When analysed under the conditions employed in this study,  $m_S$  values for a resveratrol-producing strain and a congeneric reference strain were not significantly different. Moreover, control experiments confirmed that products originating from the phenylpropanoid pathway that were excreted by the resveratrol-producing strain did not affect biomass yields of the reference strain at pH 6.5 (Table 2.3). Although formation of by-products should ultimately be prevented by further engineering, our data indicate that *S. cerevisiae* is remarkably tolerant towards these by-products. Coumaric acid, cinnamic acid and phloretic acid have previously been reported to suppress bacterial growth (e.g. *Lactobacillus plantarum* at pH 6.5, [17]). Tolerance of *S. cerevisiae* is, however, likely to be strongly pH dependent. At a pH of 4.0, growth of a wine strain of *S. cerevisiae* was strongly inhibited by  $35 \text{ mg L}^{-1}$  cinnamic acid [48], suggesting that cinnamic acid induces toxicity by diffusion of the undissociated form across the yeast membrane, as has been described for benzoic acid and other weak acids [215].

Although the  $m_S$  values estimated for the resveratrol-producing strain and the reference strain were not significantly different (Figure 2.2G), they were 40-50 % higher than found in earlier studies with *S. cerevisiae*. An ATP requirement for maintenance ( $m_{ATP}$ ) of  $1.5 \pm 0.15 \text{ mmol g}_{\text{biomass}}^{-1} \text{ h}^{-1}$  ATP was estimated for *S. cerevisiae* strain CEN.PK113-7D in this work. Rogers and Stewart [230] estimated an  $m_{ATP}$  of  $1.12 \text{ mmol g}_{\text{biomass}}^{-1} \text{ h}^{-1}$  ATP from aerobic, glucose-limited chemostat cultures of a diploid wild-type *S. cerevisiae* strain. Using anaerobic chemostat and retentostat cultures of *S. cerevisiae* CEN.PK113-7D, Boender *et al.* [28] calculated an  $m_{ATP}$  of  $1.0 \text{ mmol g}_{\text{biomass}}^{-1} \text{ h}^{-1}$  for this strain. The higher maintenance energy requirement observed in our experiments may be related to the elevated concentrations of copper in the medium, which were needed to induce the *PAL2* gene in the resveratrol-producing strain. Because copper is toxic at higher concentrations [109], the use of copper-dependent induction systems should preferably be avoided in bioprocesses.

### **Resveratrol production pathway impacts expression levels of upstream genes |**

Among the genes encoding enzymes directly involved in phenylalanine biosynthesis *TKL1*, *ARO7*, and *ARO9* displayed significantly higher expression levels and *RK11* lower expression levels in the resveratrol producing strain than in the reference strain. These transcriptional differences may result from the genetic engineering performed to channel carbon towards resveratrol formation. Resveratrol production via the oxidative branch of the pentose phosphate pathway (in which *RK11* encodes an intermediate step) results in net NADPH production (see stoichiometry). Transketolase, encoded by *TKL1*, offers a non-oxidative pathway for pentose phosphate production from glycolytic intermediates (Figure 2.1). The antagonistic regulation of *TKL1* and *RK11* may therefore respond to a need for redox balancing in the resveratrol producer. Closer to phenylalanine, expression of *ARO9* is activated by aromatic amino acids and expression of *ARO7* is repressed by tyrosine [42]. Increased expression of these two genes in the resveratrol producer may thus reflect alterations in intracellular amino acid concentrations. In addition, transcript levels of the multidrug transporter Pdr12 were consistently higher in the resveratrol producing strain than in the reference strain irrespective of growth rate. Expression of *PDR12* is induced by weak organic acids, which suggests that intermediates of the resveratrol pathway (coumaric acid, cinnamic acid and/or phloretic acid) may induce *PDR12* [156]. Even though resveratrol production levels were relatively low, genetic engineering and heterologous resveratrol production had therefore an impact on expression of key endogenous enzymes involved in the *de novo* pathway.

### **Differences in relative growth rate result in a glucose-dependent transcriptome response |**

Both the resveratrol producing strain and the congeneric reference strain showed a positive correlation between specific growth rate and expression of genes involved in anabolism, a relationship that has been identified before [225]. Furthermore,

a negative correlation was observed for genes involved in reaction to stress, a response known to decrease with growth rate [225]. Comparison of the two strains, however, showed that the most prominent differences in gene expression involved a set of genes known to respond to extracellular glucose concentration. This response agreed with the residual glucose concentration, which showed a pronounced correlation with specific growth rate in cultures of the resveratrol producer (Figure 2.2B).

In steady-state glucose-limited chemostat cultures, the residual glucose concentration ( $C_S$ ) is dependent on the specific growth rate ( $\mu$ ) (which in steady-state chemostats equals the dilution rate), the maximum specific growth rate ( $\mu_{max}$ ) under the experimental conditions, and the microorganism's substrate saturation constant for glucose ( $K_S$ ), according to kinetics first proposed by Monod [194].

$$\mu = \mu_{max} \frac{C_S}{K_S + C_S} \quad (2.3)$$

The maximum specific growth rate of the resveratrol producer was 38% lower than that of the reference strain. At each growth rate tested in chemostat, this strain therefore operated closer to its  $\mu_{max}$  than the reference strain. The resulting higher relative specific growth rate ( $\frac{\mu}{\mu_{max}}$ ) is consistent with the higher residual glucose concentrations in cultures of the resveratrol producing strain [119]. While chemostat cultivation is a powerful and widely used tool to compare strains with different  $\mu_{max}$  at the same specific growth rate, the potential impact of differences in relative growth rate has hitherto been largely overlooked. In a recent study, Hebly and co-workers, exposing *S. cerevisiae* to temperature oscillations in glucose-limited continuous cultures, observed that the relative growth rate of yeast at different temperatures had a stronger impact on physiology and transcriptome than temperature itself [119]. The present study provides a clear illustration of the importance of considering relative as well as absolute growth rates in chemostat-based comparisons of different microbial strains.

## Conclusions

Low specific growth rates are a common constraint in industrial fed-batch processes for the microbial production of compounds whose formation from glucose requires a net input of ATP. Glucose-limited chemostat cultivation of a recombinant resveratrol-producing *S. cerevisiae* strain demonstrated a strong correlation between recombinant resveratrol production from glucose and specific growth rate. By-product formation was identified as a clear priority for future research on improving resveratrol yields. Furthermore, this study underlined the impact of specific growth rate on the distribution of glucose, the carbon and energy source, over growth, maintenance requirements and product formation. The results emphasize the importance of metabolic engineering



strategies that enable uncoupling of product formation and growth in the microbial production of ATP-requiring compounds and of minimizing maintenance energy requirements in such processes.

## Acknowledgements

This research was supported by EU FP7 grant RoBoYeast, CP 289137. We would like to thank Prof. Jochen Förster (now at the Novo-Nordisk Foundation's Biosustainability Centre in Hørsholm, Denmark) for initiating this study and Prof. Dr.-Ing Ralf Takors (University of Stuttgart) for coordinating the RoBoYeast project.

## Methods

**Strains |** The prototrophic resveratrol-producing strain *Saccharomyces cerevisiae* FS09322 [143], was obtained from Fluxome Sciences, Stenløse, Denmark. The congeneric prototrophic strain CEN.PK113-7D (*MATa*, *MAL2-8c*, *SUC2*) was used as a reference [197]. Stock cultures of *S. cerevisiae* CEN.PK113-7D were grown in 500 mL shake flasks on 100 mL YPD medium (10 g L<sup>-1</sup> Bacto yeast extract, 20 g L<sup>-1</sup> Bacto peptone and 20 g L<sup>-1</sup> D-glucose). After addition of glycerol (20% v/v) to early stationary phase cultures, 2 mL aliquots were stored at -80°C. Stock cultures of *S. cerevisiae* FS09322 were grown in 500 mL shake flasks on 100 mL synthetic medium [290] set to pH 6.0 with 2M KOH, and containing 20 g L<sup>-1</sup> D-glucose. 2 mL aliquots were stored at -80°C.

**Media and cultivation methods |** Shake-flask cultures were grown in an orbital shaker at 200 rpm and at 30°C in synthetic medium [290], set to pH 6.0 with 2M KOH prior to sterilization and supplemented with 20 g L<sup>-1</sup> D-glucose. Pre-cultures were grown in 500 mL shake flasks containing 100 mL of the same medium, inoculated with a 2-mL glycerol stock. Aerobic chemostat cultivation was performed in 2 litre bioreactors (Applikon, Delft, the Netherlands) equipped with a level sensor to maintain a constant working volume of 1 litre. The culture temperature was controlled at 30°C and dilution rates between 0.025 h<sup>-1</sup> and 0.15 h<sup>-1</sup> were set by controlling the flow rate. Chemostat cultures of both CEN.PK113-7D and FS09322 were grown on synthetic medium [290], supplemented with 7.5 g L<sup>-1</sup> D-glucose, 0.3 g L<sup>-1</sup> Struktol J673 antifoam (Schill and Scheilacher AG, Hamburg, Germany), and 0.015 g L<sup>-1</sup> copper sulfate pentahydrate (copper concentrations in the medium required for induction of CUP1p controlled PAL2 were optimized for specific resveratrol production rate in batch to a concentration of 0.015 g L<sup>-1</sup>, without affecting the  $\mu_{\max}$  of FS09322). The pH was kept constant at 6.5 by automatic addition of 2M KOH. Cultures were sparged with air (0.5 L.min<sup>-1</sup>) and stirred at 800 rpm. Chemostat cultures were assumed to be in steady state when, after at least 6 volume changes, the culture dry weight and specific carbon-dioxide production rate changed by less than 3% over 2 consecutive volume changes. Steady-state samples were taken between 10 and 16 volume changes after inoculation to minimize the impact of evolutionary adaptation. Carbon recoveries for independent chemostats were >95%. For the growth rate range study, 15 independent chemostats were performed with FS09322, three at a dilution rate of 0.025

$\text{h}^{-1}$ , three at  $0.05 \text{ h}^{-1}$ , two at  $0.075 \text{ h}^{-1}$ , five at  $0.10 \text{ h}^{-1}$ , and two at  $0.15 \text{ h}^{-1}$ . For CEN.PK113-7D, ten independent chemostats were performed, two at  $0.025 \text{ h}^{-1}$ , four at  $0.05 \text{ h}^{-1}$ , two at  $0.10 \text{ h}^{-1}$  and two at  $0.15 \text{ h}^{-1}$ . For the study on the effect of (by-)products, reference strain CEN.PK113-7D was grown in independent duplicate glucose-limited chemostats performed at a dilution rate of  $0.10 \text{ h}^{-1}$  in synthetic medium [48] supplemented with either resveratrol ( $6.3 \pm 0.8 \text{ mM}$ ), coumaric acid ( $91 \pm 5 \text{ mM}$ ), phloretic acid ( $253 \pm 1 \text{ mM}$ ) or cinnamic acid ( $154 \pm 18 \text{ mM}$ ).

**Determination of substrate, metabolites and biomass concentration** | Culture dry weight was calculated by filtering 10 mL of culture broth over pre-dried and pre-weighed membrane filters (pore size  $0.45 \mu\text{m}$ , Gelman Science), which were then washed with demineralized water, dried in a microwave oven (20 min, 350W) and weighed again. Supernatants were obtained by centrifugation of culture samples (3 min at  $20.000 \text{ g}$ ) and analysed by high-performance liquid chromatograph (HPLC) analysis on a Waters Alliance 2690 HPLC (Waters, Milford, MA) equipped with a Bio-Rad HPX 87H column (BioRad, Veenendaal, The Netherlands), operated at  $60^\circ\text{C}$  with  $5 \text{ mM H}_2\text{SO}_4$  as the mobile phase at a flow rate of  $0.6 \text{ mL}\cdot\text{min}^{-1}$ . Detection was by means of a dual-wavelength absorbance detector (Waters 2487) and a refractive index detector (Waters 2410). For measurement of phenylpropanoic compounds, culture samples were diluted with an equal volume of 50% ethanol. After vigorous mixing, cells were spun down at  $20.000 \text{ g}$  for 3 min. The supernatant was analysed on a Waters 2695 separation module and a Waters 996 photodiode array detector. Resveratrol, phloretic acid, coumaric acid, phenylethanol, and cinnamic acid were measured at 306, 275, 309, 214 and  $277 \text{ nm}$ , respectively, using an Agilent Zorbax SB-C18 column ( $4.6 \times 5.0, 3.5 \text{ micron}$ ) operated at  $30^\circ\text{C}$ . A gradient of acetonitrile and  $20 \text{ mM KH}_2\text{PO}_4$  (pH 2) with 1% acetonitrile was used as eluent, at a flow rate of  $1 \text{ mL}\cdot\text{min}^{-1}$ , increasing from 0 to 10% acetonitrile in 6 min followed by an increase to 40% acetonitrile until 23 min. From 23 min to 27 min, 100%  $\text{KH}_2\text{PO}_4$  was used as eluent. Resveratrol, coumaric acid, cinnamic acid, phloretic acid and phenylethanol standards for calibration were obtained from Sigma Aldrich (Sigma-Aldrich, Zwijndrecht, The Netherlands). Residual glucose concentrations in glucose-limited chemostat cultures were analysed after rapid quenching with cold steel beads [183], using an enzymatic glucose kit (Roche, Almere, The Netherlands, no. 0716251).

**Gas analysis** | The exhaust gas from chemostat cultures was cooled with a condenser ( $2^\circ\text{C}$ ) and dried with a PermaPure Dryer (model MD 110-8P-4; Inacom Instruments, Veenendaal, the Netherlands) prior to online analysis of carbon dioxide and oxygen with a Rosemount NGA 2000 Analyser (Baar, Switzerland). Exhaust gas flow rates, biomass-specific carbon dioxide production rates and oxygen consumption rates were calculated as described previously [282].

**Viability assays** | Chemostat cultures were assayed for viability using the FungaLight AM-CFDA (acetoxymethyl ester 5-carboxyfluorescein diacetate)/propidium iodide yeast viability kit (Invitrogen, Carlsbad, CA) by counting 10,000 cells on a Cell Lab Quanta SC MPL flow cytometer (Beckman Coulter, Woerden, Netherlands) as described previously [27]. AM-CFDA is a cell-permeant substrate for an intracellular non-specific esterase activity. Hydrolytic cleavage of the lipophilic blocking and diacetate groups of AM-CFDA results in a green fluorescence in

metabolically active cells. Propidium iodide intercalates with DNA in cells with a compromised cell membrane, which results in red fluorescence.

**Protein determination** | A fresh sample of the culture containing 50 mg biomass was centrifuged, and the pellet was washed twice with distilled water and resuspended in 5 mL of water. The concentrate was boiled in 1 M NaOH (final concentration) for 10 min and subsequently cooled on ice. Samples were 10 times diluted in distilled water and further processed according to the protocol for Bradford Quick Start Protein Assay (Bio-Rad, Veenendaal, Netherlands). Absorbance of samples was measured at 595 nm. Dried bovine serum albumin (Sigma-Aldrich, Zwijndrecht, The Netherlands) was used as a standard.

**Transcriptome analysis** | Microarray analysis was performed with samples from independent duplicate steady-state chemostat cultures of *S. cerevisiae* strains FS09322 and CEN.PK113-7D grown at four different dilution rates, comprising a total dataset of 16 microarrays. Sampling from chemostat cultures for transcriptome analysis was carried out by using liquid nitrogen for rapid quenching of mRNA turnover [214]. Prior to RNA extraction, samples were stored in a mixture of phenol/chloroform and TAE buffer at -80°C. Total RNA extraction, isolation of mRNA, cDNA synthesis, cRNA synthesis, labelling and array hybridization was performed as described previously [189], with the following modifications. To chelate the copper present at 4 mg L<sup>-1</sup> in the culture medium and thereby prevent copper-induced mRNA degradation [50], EDTA was added to defrosting samples at a final concentration of 80 mM. The quality of total RNA, cDNA, aRNA and fragmented aRNA was checked using an Agilent Bioanalyzer 2100 (Agilent Technologies, Santa Clara, CA). Hybridization of labelled fragmented aRNA to the microarrays and staining, washing and scanning of the microarrays was performed according to Affymetrix instructions (EukGE\_WS2v5). The 6383 yeast open reading frames were extracted from the 9335 transcript features on the YG-S98 microarrays. All microarray data used in this study are available via GEO series accession number GSE65942.

To allow comparison, all expression data were normalized to a target value of 240 using the average signal from all gene features. To eliminate variation in genes that are not expressed, genes with expression values below 12 were set to 12 and the gene features for which the maximum expression was below 20 for all 19 arrays were discarded. The average deviation of the mean transcript data of replicate chemostats was approximately 14%, similar to the reproducibility usually observed in replicate steady state chemostat cultures [67]. The expression of housekeeping genes *ACT1*, *HHT2*, *SHR3*, *PDA1* and *TFC1* [268] remained stable for both strains at all tested growth rates (average coefficient of variation 12% ± 2% see Supplementary Figure 2.6). EDGE version 1.1.291 [179] was used to perform a differential expression analysis based on gene expression profiles across the different dilution rates, using strains and dilution rates as covariates. Expression profiles with a false discovery rate below 0.005 (p-value 0.0025) were considered as significantly differently expressed between the two strains and were clustered with k-means clustering using positive correlation as distance metric (Expressionist Pro version 3.1, Genedata, Basel, Switzerland). Gene expression clusters were analysed for overrepresentation of functional annotation categories from the Munich Information Centre for Protein Sequences (MIPS) database (<http://mips.gsf.de/genre/proj/yeast>), based on the hypergeometric distribution

analysis tool described by Knijnenburg *et al* [150]. Additional categories were searched for enrichments, that consist of a set of 589 genes transcriptionally up-regulated (designated Glucose responsive UP) and 565 genes transcriptionally down-regulated (designated Glucose responsive DOWN) upon addition of excess glucose to glucose-limited chemostat cultures of *S. cerevisiae* (aerobic cultures, same experimental set-up and strain background as in the present study) [157].

**Stoichiometric calculations** | The maximum yield of resveratrol on glucose was calculated using a compartmented stoichiometric model for aerobic growth of *S. cerevisiae* on glucose [67]. The model was extended to allow resveratrol production by incorporating the reactions catalyzed by: L-phenylalanine ammonia lyase, cinnamate 4-hydroxylyase, coumarate CoA ligase, resveratrol synthase and the ATP-binding cassette transporter Snq2 for export of resveratrol from the cells. The list of additional reactions can be found in Additional file 2.1. The resulting model did not contain parallel reactions, and when the growth rate was set to zero the only degree of freedom was the rate of resveratrol production. By setting the growth rate to zero and the resveratrol production to a certain fixed value the flux distribution and the net requirement of glucose and oxygen were calculated for different network options, that is NADPH production via Ald6 or the pentose phosphate pathway, combined with different cofactor specificities of glutamate dehydrogenase (NADH or NADPH). From these, the maximum yields of resveratrol on glucose, and the ATP requirement for resveratrol biosynthesis were calculated. For all calculations the P/O ratio for respiratory ATP production was set to 1.0.

## Supplementary material Chapter 2

### Supplementary Figures

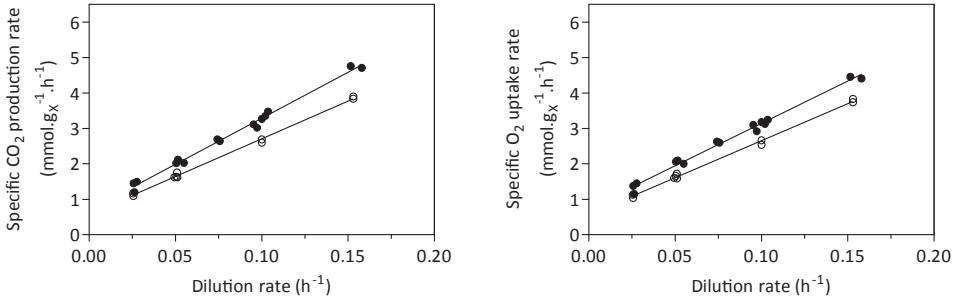


**Figure 2.4:** Specific CO<sub>2</sub> production and specific O<sub>2</sub> uptake rates of the resveratrol producing *S. cerevisiae* strain FS09322 and the isogenic strain CEN.PK113-7D. Closed symbols indicate the resveratrol producing *S. cerevisiae* strain FS09322. Open symbols indicate isogenic strain CEN.PK113-7D. Each data point represents results from an individual chemostat.

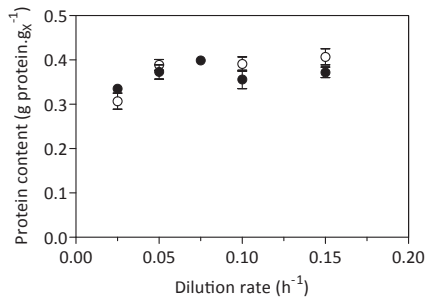


**Figure 2.5:** Protein content of the resveratrol producing *S. cerevisiae* strain FS09322 and its isogenic strain CEN.PK113-7D. Open symbols indicate strain CEN.PK113-7D, close symbols indicate strain FS09322. The shown data represent the average and standard deviation of two independent culture replicates for each dilution rate and each strain.

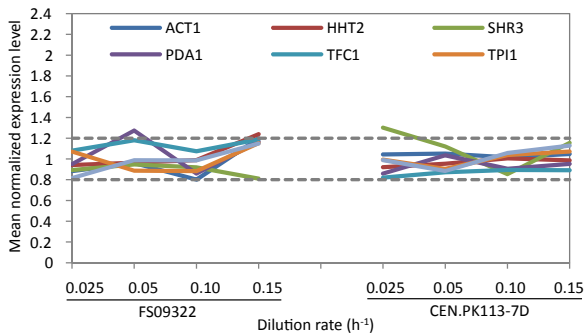
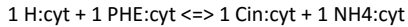


**Figure 2.6:** Averaged normalized gene expression of housekeeping genes [268] for *S. cerevisiae* strain FS09322 and CEN.PK113-7D. Dotted bars indicate 20% variation around normalized expression.

**Additional files**

**Additional file 2.1.** Additional reactions for incorporation of resveratrol biosynthesis in the stoichiometric model.

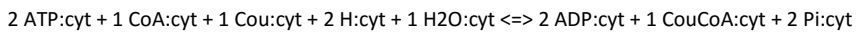
L-phenylalanine ammonia-lyase



Cinnamate 4-hydroxylase



Coumarate CoA ligase



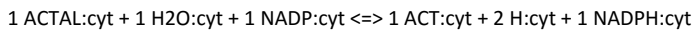
Resveratrol synthase



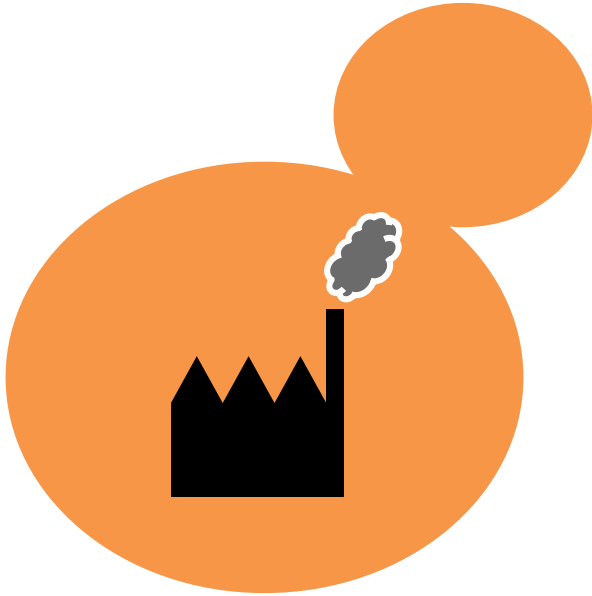
NAD glutamate dehydrogenase; Gdh2



NAD acetaldehyde dehydrogenase, Ald2/3



acetaldehyde	ACTAL	C2H4O
acetyl-CoA	ACCoA	C23H34N7O17P3S-4
ADP	ADP	C10H12N5O10P2-3
carbondioxide	CO2	CO2
chorismate	CHO	C10H8O6-2
Cinnamate	Cin	C9H8O2
CoA	CoA	C21H32N7O16P3S-4
Coumarate	Cou	C9H8O3
CoumaroylCoA	CouCoA	C30H42N7O18P3S
glutamate	GLM	C5H8NO4-1
hydrogen	H	H+1
malonyl-CoA	MACoA	C24H33N7O19P3S-5
NAD	NAD	+1
NADH	NADH	H
NADP	NADP	+1
NADPH	NADPH	H
NH4	NH4	H4N+1
oxoglutarate	OGL	C5H4O5-2
oxygen	O2	O2
phenylalanine	PHE	C9H11NO2
phosphate	Pi	HO4P-2
reservatrol	res	C14H12O3
water	H2O	H2O



Oxygen availability strongly affects chronological lifespan and thermotolerance in batch cultures of *Saccharomyces cerevisiae*

Markus M.M. Bisschops\*, Tim Vos\*, Rubén Martínez-Moreno, Pilar de la Torre Cortés, Jack T. Pronk, Pascale Daran-Lapujade

\* Joint first authorship

Published in *Microbial Cell* 2015, 2:429-444



### Abstract

Stationary-phase (SP) batch cultures of *Saccharomyces cerevisiae*, in which growth has been arrested by carbon-source depletion, are widely applied to study chronological lifespan, quiescence and SP-associated robustness. Based on this type of experiments, typically performed under aerobic conditions, several roles of oxygen in aging have been proposed. However, SP in anaerobic yeast cultures has not been investigated in detail. Here, we use the unique capability of *S. cerevisiae* to grow in the complete absence of oxygen to directly compare SP in aerobic and anaerobic bioreactor cultures. This comparison revealed strong positive effects of oxygen availability on adenylate energy charge, longevity and thermotolerance during SP. A low thermotolerance of anaerobic batch cultures was already evident during the exponential growth phase and, in contrast to the situation in aerobic cultures, was not substantially increased during transition into SP. A combination of physiological and transcriptome analysis showed that the slow post-diauxic growth phase on ethanol, which precedes SP in aerobic, but not in anaerobic cultures, endowed cells with the time and resources needed for inducing longevity and thermotolerance. When combined with literature data on acquisition of longevity and thermotolerance in retentostat cultures, the present study indicates that the fast transition from glucose excess to SP in anaerobic cultures precludes acquisition of longevity and thermotolerance. Moreover, this study demonstrates the importance of a preceding, calorie-restricted conditioning phase in the acquisition of longevity and stress tolerance in SP yeast cultures, irrespective of oxygen availability.

## Introduction

Just like other living organisms, *Saccharomyces cerevisiae* cells age and have a finite chronological lifespan. The similarity of cellular processes in *S. cerevisiae* to those in higher eukaryotes and its accessibility to a wide range of experimental techniques have made this yeast a popular model for studying chronological aging of metazoan cells [76, 172, 37, 192]. Chronological aging of *S. cerevisiae* is typically studied in aerobic batch cultures, in which growth arrest and quiescence are triggered by exhaustion of the available carbon sources in the growth medium [171, 108]. Survival of individual yeast cells in such non-growing, stationary-phase (SP) cultures is then taken as a measure for their chronological lifespan (CLS). Over the past decade, studies on SP yeast cultures have contributed to our understanding of cellular mechanisms involved in aging, and several underlying cellular mechanisms were also found in higher eukaryotes [87].

Calorie restriction has been shown to extend lifespan in organisms ranging from yeast to man, with studies on many organisms pointing at an important role of nutrient-signaling cascades [248]. Turn-over of damaged macromolecules, and in particular proteins, has similarly been identified as a key process in aging in many organisms [236]. A third universal factor implicated in aging is respiration and, in particular, the associated formation of reactive oxygen species (ROS), which has been shown to enhance aging-related cellular deterioration in many organisms [14]. However, ROS have also been implicated in beneficial effects. In particular, mild ROS stress has been proposed to contribute to CLS extension by inducing stress-resistance genes, a phenomenon known as hormesis [175, 243]. Similarly, increased mitochondrial respiration and ROS production rates in calorie-restricted yeast cultures have been linked to CLS extension [191, 199, 251].

ROS generation is not necessarily the only mechanism by which respiration and oxygen can affect CLS. In aerobic, glucose-grown batch cultures of *S. cerevisiae*, a fast and predominantly fermentative growth phase on glucose is followed by a second, respiratory growth phase in which the fermentation products ethanol and acetate are consumed [276]. This second growth phase, known as post-diauxic phase, is characterized by slow growth. During the post-diauxic phase, genes involved in SP are already expressed at an elevated level, as well as some features associated with SP cultures, such as increased stress resistance [108]. In anaerobic cultures of *S. cerevisiae*, the absence of oxygen prevents a respiratory post-diauxic growth phase. Instead, a phase of fast, fermentative exponential growth on glucose is immediately followed by SP, in which maintenance of viability and cellular integrity depends on metabolism of storage compounds. *S. cerevisiae* cells can contain two types of storage polymers: the storage carbohydrates trehalose and glycogen, and fatty acids, which are mostly stored in the form of di- and triacylglycerol esters [93, 304]. In the absence of oxygen, yeast cells cannot catabolize fatty

acids by  $\beta$ -oxidation and, moreover, conversion of storage carbohydrates via alcoholic fermentation yields 5-8 fold less ATP than their respiratory dissimilation [27].

Previous studies on the role of respiration in aging were predominantly based on the use of respiration-deficient *S. cerevisiae* mutants (e.g.  $\rho^0$  strains and other mutants) [263, 167, 32, 3, 16] and respiratory inhibitors [199]. These approaches, however, have several drawbacks. Firstly, mitochondria are not only involved in respiration, but also in essential anabolic reactions (e.g., assembly of iron-sulfur complexes, amino acid biosynthesis and long-chain lipid biosynthesis [38]). Studies on petite or  $\rho^0$  mutants may therefore cause unwanted 'side-effects' resulting from the absence or inefficiency of mitochondrial processes, rather than from direct effects of oxygen or respiration on aging. For example, the absence of mitochondrial DNA influences crosstalk between these organelles and the nucleus [306]. Furthermore, inhibition of respiration may result in reduced ROS levels [199], but can also result in ROS accumulation [161], depending on the intervention chosen. In addition, ROS may still be produced by other oxygen-consuming processes in yeast, such as disulfide-bond formation during oxidative protein folding [235].

Surprisingly, while *S. cerevisiae* is unique among yeasts and eukaryotes for its ability to grow fast under fully aerobic as well as strictly anaerobic conditions [293], this ability has not been used to systematically investigate the impact of oxygen availability on entry into SP, on longevity and on robustness. The goal of the present study was therefore to investigate the impact of oxygen availability on yeast physiology in SP cultures. More specifically, we investigated whether the post-diauxic phase and respiratory mobilization of storage compounds in aerobic cultures affects CLS and thermotolerance during SP. To this end, aerobic and anaerobic bioreactor batch cultures of *S. cerevisiae* were grown into SP and subjected to detailed physiological and transcriptome analyses.

## Results

### **Anaerobicity reduces chronological lifespan and stress resistance in stationary phase cultures**

To investigate the impact of oxygen availability on chronological lifespan in SP cultures of *S. cerevisiae*, survival kinetics were analyzed during SP in aerobic and anaerobic, glucose-grown bioreactor cultures. In aerobic cultures, the percentage of cells capable of colony formation on complex-medium agar plates typically decreased to ca. 2% in the 8 days following onset of SP, i.e. after exhaustion of all exogenous carbon sources including ethanol and organic acids (Figure 3.1). Viability of anaerobic cultures decreased much faster, reaching values below 1% within 4.5 days after the onset of SP, that is after all exogenous glucose was consumed (Figure 3.1).

Increased thermotolerance is a well-documented characteristic of SP cultures of *S. cerevisiae* [301, 5]. Indeed, half of the cells in samples from aerobic, early-SP cultures

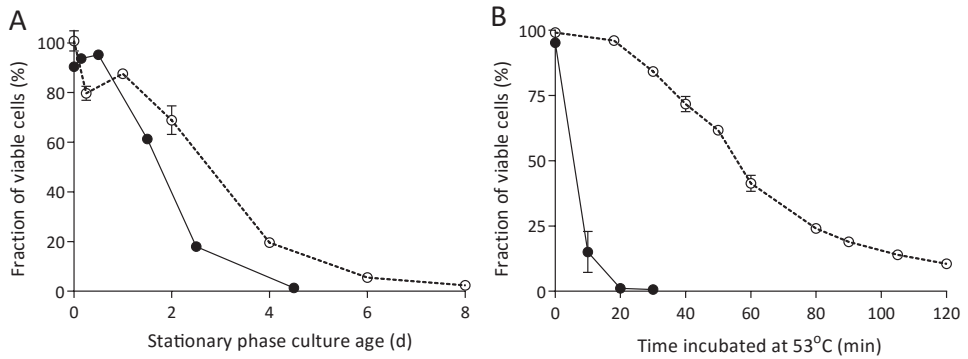


**Figure 3.1:** Chronological life span and thermotolerance of stationary-phase cultures is much lower under anaerobic than under aerobic conditions. Chronological life span (A): survival expressed as ratio of colony forming units divided by the number of cells plated, during aerobic and anaerobic SP cultures. Time point zero indicates the onset of SP, which corresponds to exogenous glucose exhaustion in anaerobic cultures and exhaustion of all exogenous carbon sources including ethanol and organic acids in aerobic cultures. Thermotolerance (B): loss of viability after sudden exposure of cells from aerobic and anaerobic cultures during early SP to 53°C. Open symbols represent aerobic cultures, closed symbols anaerobic cultures. Data represent the average and SEM of measurements on independent duplicate cultures.

survived a 60-min exposure to 53°C. Notably, up to 20 minutes incubation at 53°C hardly affected viability, suggesting that cells were well capable of repairing heat-induced damage during this period. In contrast, fewer than 20% of the cells from anaerobic early-SP cultures survived a 10-min incubation at this temperature (Figure 3.1). Implementation of anaerobic conditions during sampling and heat-shock assays did not significantly affect this difference, indicating that heat-induced loss of viability was not influenced by exposure of anaerobically grown cells to oxygen during the assays (data not shown). Furthermore, washing of cells prior to the heat-shock experiments did not influence heat-shock resistance, indicating that the presence of low (< 1 g L<sup>-1</sup>) ethanol concentrations in the assays did not cause the low thermotolerance of cells from anaerobic SP cultures.

**Oxygen availability strongly affects the transcriptome of SP cultures** | In aerobic yeast cultures, entry into SP is accompanied by a range of physiological changes that enhance survival in harsh, nutrient-poor environments [301]. This adaptation coincides with a vast transcriptional reprogramming [298, 181, 95] that includes up-regulation of genes involved in resistance mechanisms to a wide array of stresses. Currently, no transcriptome data are available in the literature on anaerobic SP cultures of *S. cerevisiae*.

A transcriptome analysis, performed on culture samples taken 4 h after the onset of SP, revealed that a quarter of the yeast genome (1452 genes, Supplementary Table 3.1) was differentially expressed (fold-change cut-off of 2.0 and adjusted P-value below 0.05) in aerobic and anaerobic SP cultures. Among these genes were several genes known to be regulated by the heme and oxygen dependent transcription factors Hap1 and Rox1

**Table 3.1:** Functional categories overrepresented among genes with different expression levels in aerobic and anaerobic stationary phase cultures. <sup>a</sup>Bonferroni-corrected P-value cut-off of 0.05 was used and P-values indicate the probability of finding the same numbers of genes in a random set of genes. Functional categories are obtained from the Gene Ontology set or, in italic font, directly from literature references. Details can be found in Supplementary Table 3.2.

Category description	# of genes in dataset	# of genes in category	p-value <sup>a</sup>
<i>574 genes with higher expression in aerobic stationary phase cultures</i>			
<i>Genes induced in stationary phase</i> [181]	53	122	$1.2 \cdot 10^{-22}$
<i>Genes induced by environmental stress response</i> [97]	54	281	$3.2 \cdot 10^{-6}$
Fatty acid metabolic process	13	29	$5.4 \cdot 10^{-4}$
Fatty acid beta-oxidation	7	9	$2.0 \cdot 10^{-3}$
Transmembrane transport	52	303	$3.8 \cdot 10^{-3}$
Glyoxylate cycle	6	8	$1.7 \cdot 10^{-2}$
<i>878 genes with higher expression in anaerobic stationary phase cultures</i>			
Translation	131	345	$4.1 \cdot 10^{-28}$
<i>Genes induced by environmental stress response</i> [97]	78	281	$1.7 \cdot 10^{-8}$
Mitochondrial translation	36	81	$1.9 \cdot 10^{-8}$
Oxidation reduction	74	270	$1.6 \cdot 10^{-6}$
Metabolic process	93	389	$2.6 \cdot 10^{-5}$
Response to stress	49	161	$3.2 \cdot 10^{-5}$
Heme biosynthetic process	10	12	$1.6 \cdot 10^{-4}$
Methionine metabolic process	11	15	$3.5 \cdot 10^{-4}$
Sulfate assimilation	9	11	$1.0 \cdot 10^{-3}$
Porphyrin biosynthetic process	8	9	$1.4 \cdot 10^{-3}$
Carbohydrate metabolic process	28	93	$4.2 \cdot 10^{-2}$
Glycolysis	14	32	$4.6 \cdot 10^{-2}$
Methionine biosynthetic process	14	32	$4.6 \cdot 10^{-2}$

[267, 115, 148]. Approximately 40% of the differentially expressed genes (574 genes, Supplementary Table 3.1) were transcribed at higher levels in the aerobic SP cultures. This gene set showed a strong overrepresentation of genes involved in fatty acid metabolism and, in particular, in  $\beta$ -oxidation (Table 3.1). This set of genes was also strongly enriched for genes that were up-regulated during SP in previous studies performed in shake flasks [181] (Table 3.1). Examples included the SP-genes *SPG1*, *SPG3*, *SPG4*, *SPG5*, and *SSA3*, which encodes a stress-induced ATPase. Furthermore, a significant number of genes (54) induced by the environmental stress response [97] was expressed at higher levels in aerobic SP cultures than in their anaerobic counterparts (Table 3.1).

Most of the genes that were differentially expressed in aerobic and anaerobic SP cultures (60%, 878 genes, Supplementary Table 3.1) showed a higher transcript level under anaerobic conditions. This gene set showed an overrepresentation of genes that were previously shown to be expressed at high levels in anaerobic yeast cultures and which

were therefore not necessarily related to SP. This subgroup included genes involved in heme synthesis [148] and members of the multi-gene seripauperin family [223] (Table 3.1 and Supplementary Table 3.2). Interestingly, a strong overrepresentation (131 out of 345 genes) was found for the GO category 'translation' (Table 3.1). This subset included many genes encoding cytosolic and mitochondrial ribosomal proteins (65 and 24 genes respectively). Furthermore, several genes involved in carbohydrate metabolism, including glycogen metabolism, were expressed at higher levels in anaerobic SP cultures (Table 3.1). Finally, the set of 878 genes with higher expression in anaerobic SP cultures showed a very strong overrepresentation of genes induced by the environmental stress response [97].

**Anaerobicity negatively affects the energy status of SP cultures** | Use of oxygen as an electron acceptor for respiration enables oxidative phosphorylation. As a consequence, ATP yields on glucose, glycogen and trehalose in respiratory cultures can be up to ca. 8-fold higher than in anaerobic, fermentative cultures [27][288]. Furthermore, since anaerobic yeast cultures cannot catabolize fatty acids, their use as energy reserves is restricted to aerobic cultures. To investigate the impact of storage metabolism and energy status on the short CLS of anaerobic SP cultures, cellular contents of storage materials and adenylate energy charge (a measure for the energetic status of living cells [9]) were analysed in aerobic and anaerobic SP cultures.

In aerobic cultures, intracellular pools of trehalose and glycogen were depleted within 1 day after entry into SP (Figure 3.2A and B). Cellular contents of the fatty acids palmitic and palmitoleic acid, also decreased during aerobic SP, but at a much slower rate than the storage carbohydrates and approached 6% of the total fatty acids content. This level is close to the membrane-associated fatty acid content previously reported in *S. cerevisiae* [289], indicating that yeast cells had exhausted most of their reserve lipids after 2 days in SP (Figure 3.2C). Together with the increased expression of genes involved in  $\beta$ -oxidation in aerobic SP cultures (Table 2.4), this observation indicates that aerobic SP cells use part of their fatty acids as an endogenous carbon and energy source. In aerobic cultures, the adenylate energy charge was  $0.70 (\pm 0.08)$  and the intracellular ATP concentration was  $5.45 (\pm 0.76)$  mM at the onset of SP. These results are in good agreement with published data [55, 15]. In the days after the onset of SP, both parameters gradually decreased. Two full days after the onset of SP, the adenylate energy charge was still above 0.25 (Figure 3.3).

Trehalose and glycogen are the only known carbon and energy reserves in anaerobic *S. cerevisiae* cultures. The initial trehalose content and utilization profile in anaerobic SP cultures strongly resembled those observed in aerobic cultures. The initial glycogen concentration in anaerobic SP cultures was ca. four-fold higher than in aerobic SP cultures. Nevertheless, intracellular glycogen was exhausted after 2 days in SP (Figure 3.2A and B). At the onset of SP, intracellular ATP concentration and adenylate energy

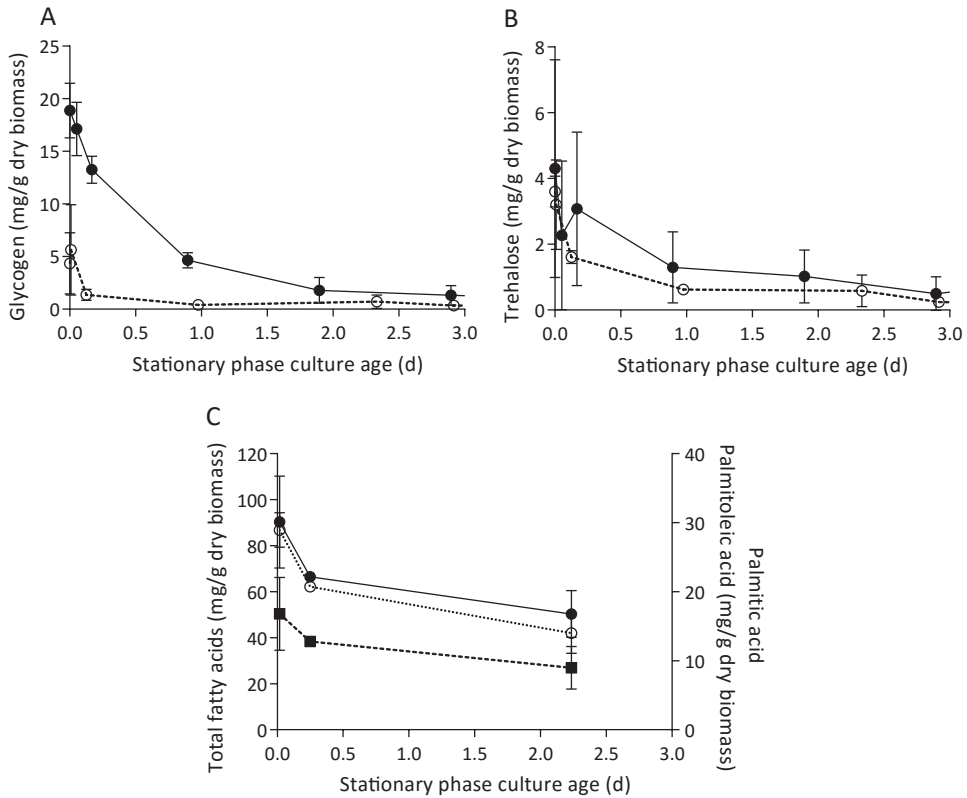


**Figure 3.2:** Utilization of carbohydrate and lipid storage compounds in aerobic and anaerobic stationary-phase cultures. Cellular contents of glycogen (A) and trehalose (B) are shown for the SP of glucose-grown batch cultures of *S. cerevisiae*, grown under aerobic (open symbols) or anaerobic (closed symbols) conditions. Panel (C) shows cellular contents of total fatty acids (closed circles), palmitoleic acid (open circles) and palmitic acid (closed squares) in aerobic SP cultures. Time point zero indicates the onset of SP, which corresponds to exogenous glucose exhaustion in anaerobic cultures and exhaustion of all exogenous carbon sources including ethanol and organic acids in aerobic cultures. Average and SD or SEM are shown, calculated from either quadruplicate cultures (glycogen and trehalose) or duplicate cultures (fatty acids), respectively.

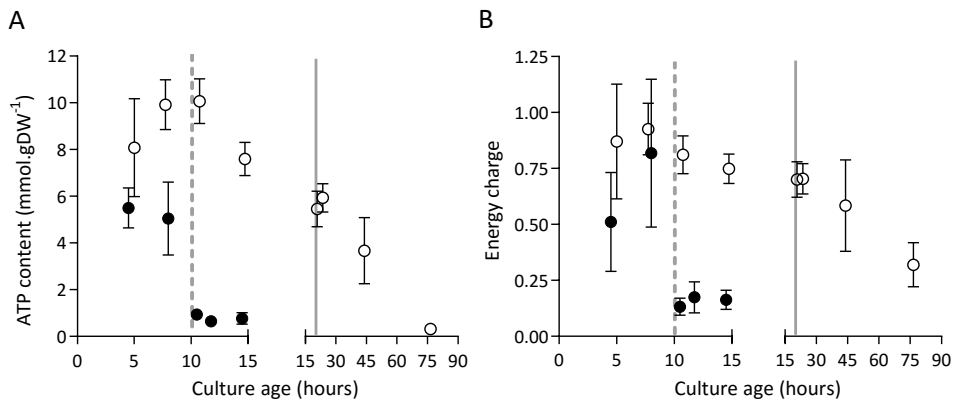


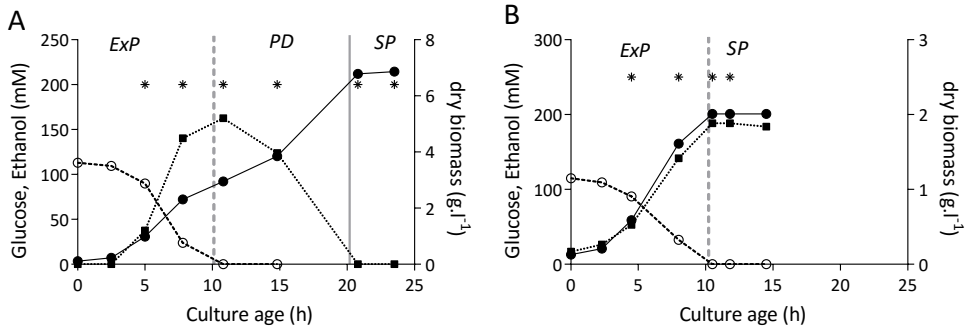
**Figure 3.3:** Intracellular ATP concentration and adenylate energy charge in aerobic and anaerobic stationary-phase cultures. Cellular ATP content (A) and adenylate energy charge (B) in aerobic (open symbols) and anaerobic (closed symbols) cultures. The dashed vertical line represents glucose exhaustion and the onset of anaerobic SP, the solid vertical line represents ethanol exhaustion and the onset of aerobic SP. Values are shown as averages of duplicate cultures (+/- SEM).

charge of anaerobic SP cultures were already lower than in aerobic cultures. Moreover, they decreased to very low levels within half a day after the onset of SP (Figure 3.3).

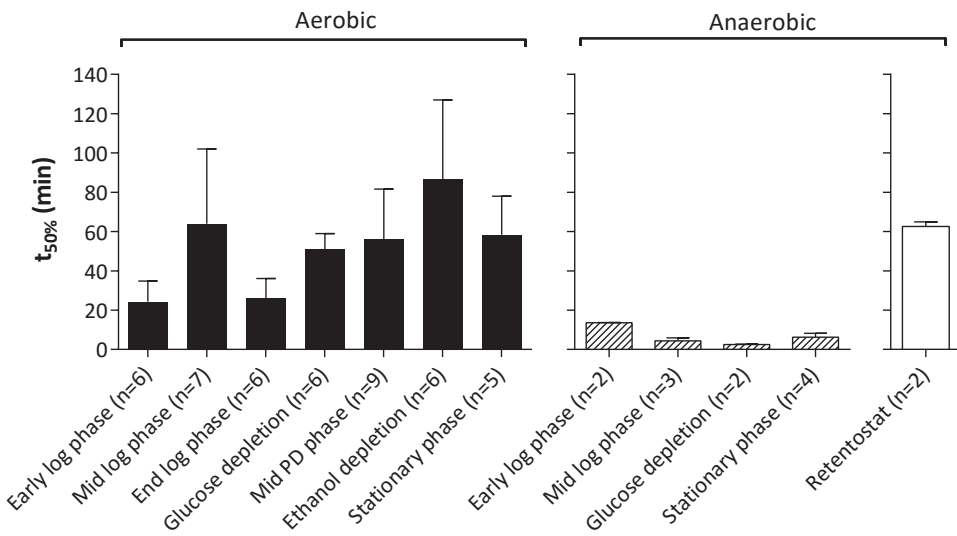
**Different entry trajectories into SP in aerobic and anaerobic cultures** | The results described above reveal clear differences in transcriptome, energy status, thermotolerance and CLS of aerobic and anaerobic SP cultures. Some of these parameters already differed at the onset of SP, indicating the importance of different ‘entry trajectories’ of aerobic and anaerobic cultures into SP. A major difference between aerobic and anaerobic batch cultures is the absence, in the latter, of a respiratory post-diauxic phase, in which ethanol and minor fermentation products acetate and glycerol are consumed. Growth in the post-diauxic phase, in which metabolism is completely respiratory, is slower than during the preceding glucose phase [258]. In this study, the maximum specific growth rate of anaerobic cultures ( $0.31 \pm 0.01 \text{ h}^{-1}$ ) during the glucose phase was lower than that of aerobic cultures ( $0.39 \pm 0.02 \text{ h}^{-1}$ , Figure 3.4). In aerobic cultures, the specific growth rate during the post-diauxic phase ( $0.10 \pm 0.01 \text{ h}^{-1}$ ) was ca. four-fold lower than during the fast growth phase on glucose. As a consequence, the specific growth rate in the hours preceding the onset of SP was ca. three-fold lower in aerobic cultures than in anaerobic cultures. To investigate whether the post-diauxic phase may have ‘conditioned’ aerobic cultures for entry into SP, analysis of aerobic and anaerobic batch cultures was extended to include the growth phases that precede SP.

A much higher thermotolerance in aerobic cultures was already evident in the exponential growth phase and further increased during the post-diauxic phase, to reach a maximum upon entry into SP (Figure 3.5). Conversely, thermotolerance of anaerobic





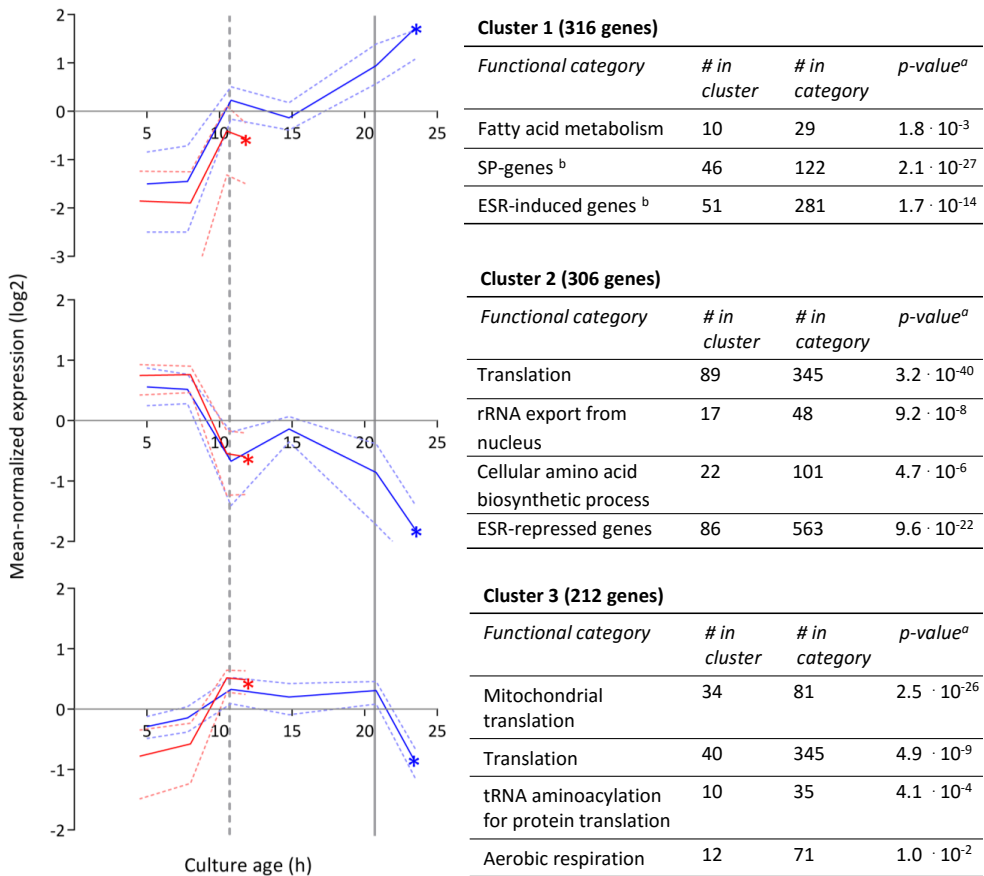
**Figure 3.4:** Growth phases in aerobic and anaerobic batch cultures. Biomass (closed circles), glucose (open circles) and ethanol (closed squares) concentration during the different growth phases of aerobic (A) and anaerobic (B) batch cultures of *S. cerevisiae*. The initial phase of exponential growth on glucose (ExP), the following post-diauxic phase of slower growth on non-fermentable carbon sources (PD) and final stationary phase (SP) are indicated. Values shown are from single representative batch cultures, independent replicate cultures yielded essentially the same results. Vertical lines indicate depletion of glucose (dashed line) and of fermentation products (solid line). Asterisks (\*) indicate time points at which samples were taken for transcriptome analysis.



**Figure 3.5:** Thermotolerance of aerobic and anaerobic cultures during different growth phases. Thermotolerance of cells during different growth phases of aerobic (black bars) and anaerobic (hatched bars) batch cultures of *S. cerevisiae* (Figure 3.4). The white bar depicts the thermotolerance of *S. cerevisiae* grown for 8 days in anaerobic retentostats [20]. Thermotolerance was assayed by monitoring viability during incubation at 53°C and is shown as the incubation time resulting in a 50% decrease in viability ( $t_{50\%}$ ) (see Materials and Methods for more details). The number of independent culture replicates for each of the growth phases is denoted on the x-axis labels.

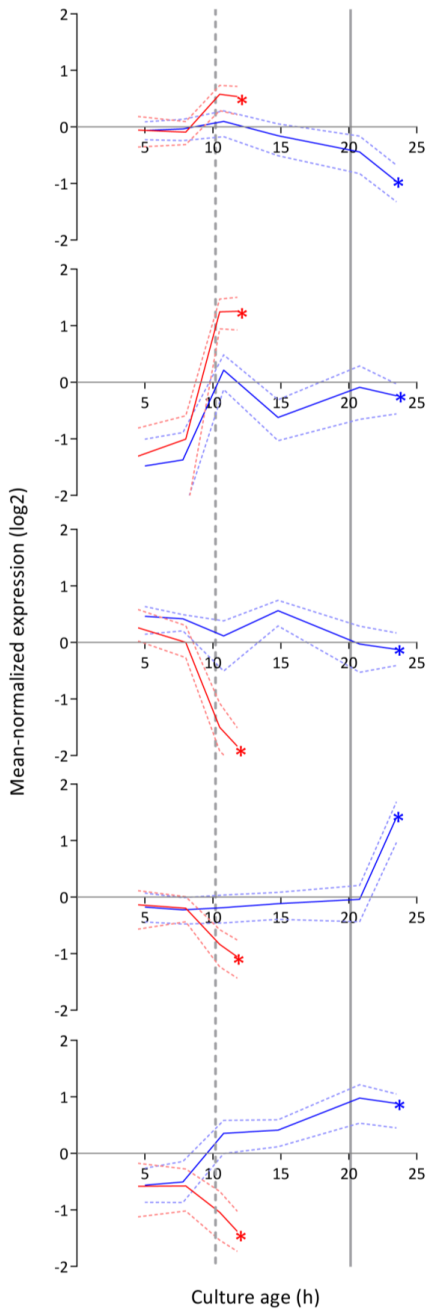
cultures did not increase during entry into SP and, consequently, remained much lower than that of aerobic cultures (Figure 3.5).

To further compare the different ‘entry trajectories’ into SP of aerobic and anaerobic



**Figure 3.6:** Clustering of genes differentially expressed between aerobic and anaerobic SP cultures according to their expression profiles during the growth phases preceding SP. Genes whose differential expression between aerobic and anaerobic SP cultures originated from changes after glucose depletion. Each graph presents the expression profiles of genes from aerobic culture (blue lines) and anaerobic cultures (red lines) in a particular gene cluster. The solid lines represent the average of the mean-normalized expression of all genes in the cluster. The dashed lines represent the first and third quartile of these mean-normalized expression values, giving information on the scatter in the expression of genes in the cluster. Asterisks (\*) indicate the SP samples from anaerobic and aerobic batches. Vertical lines indicate glucose exhaustion (dashed line) and carbon exhaustion (solid line, for aerobic cultures only). For each cluster a table reports the overrepresentation of functional categories, including the number of genes in the cluster belonging to a specific functional category (# in cluster), the total number of genes in this functional category (# in category), and the a Bonferroni-corrected P-values that indicate the likelihood of obtaining such enrichment in a random set of genes. <sup>a</sup>Only categories with a Bonferroni-corrected P-value below 0.05 were deemed significant and presented in the tables. <sup>b</sup>SP-genes and ESR induced or repressed genes were obtained from [181] and [97] respectively. More details can be found in Supplementary Table 3.3.

batch cultures, transcriptome analyses were performed at different time points during exponential phase, post-diauxic phase (aerobic cultures only) and SP. Genes were grouped in 9 clusters, based on their time-dependent expression profiles in aerobic and anaerobic cultures (Figure 3.6 and 3.7). A full dataset is available in Supplemental Data (Supplementary Tables 3.3 and 3.4).

**Cluster 4 (83 genes)**

<i>Functional category</i>	<i># in cluster</i>	<i># in category</i>	<i>p-value<sup>a</sup></i>
No significant terms			

**Cluster 5 (254 genes)**

<i>Functional category</i>	<i># in cluster</i>	<i># in category</i>	<i>p-value<sup>a</sup></i>
Response to stress	20	161	$1.7 \cdot 10^{-2}$
ESR-induced genes <sup>b</sup>	69	281	$2.9 \cdot 10^{-35}$

**Cluster 6 (53 genes)**

<i>Functional category</i>	<i># in cluster</i>	<i># in category</i>	<i>p-value<sup>a</sup></i>
tRNA transcription from RNA polymerase III promoter	4	15	$1.5 \cdot 10^{-2}$

**Cluster 7 (84 genes)**

<i>Functional category</i>	<i># in cluster</i>	<i># in category</i>	<i>p-value<sup>a</sup></i>
Regulation of transcription	20	505	$1.6 \cdot 10^{-2}$

**Cluster 8 (121 genes)**

<i>Functional category</i>	<i># in cluster</i>	<i># in category</i>	<i>p-value<sup>a</sup></i>
Carboxylic acid metabolic process	4	9	$4.0 \cdot 10^{-2}$

**Figure 3.7:** Clustering of genes differentially expressed between aerobic and anaerobic SP cultures according to their expression profiles during the growth phases preceding SP. Clusters of genes whose differential expression between aerobic and anaerobic stationary phase cultures originated from changes upon glucose exhaustion. For further description, see Figure 3.6

Less than one tenth (126 of 1452) of the genes that were differentially expressed in aerobic and anaerobic SP cultures (Table 3.1) already showed corresponding differences during the mid-exponential growth phase in aerobic and anaerobic cultures. For over half (834 of 1452) of the differentially expressed genes in SP cultures, the differences rose after glucose exhaustion, i.e. during the post-diauxic phase in aerobic cultures (Figure 3.6A, clusters 1-3). Cluster 1 comprises genes whose expression increased during the aerobic and anaerobic exponential growth phases, with a further increase during the aerobic post-diauxic phase (Figure 3.6A). Genes involved in fatty acid catabolism were overrepresented in this cluster, as well as genes that were previously shown to be induced in aerobic SP (including *SPG1*, *SPG3*, *SPG4*, *SPG5* and Hsp70-family-member *SSA3* [181]) (Figures 3.6A and 3.8). Genes in cluster 2 showed similar transcript levels during the aerobic and anaerobic exponential growth phases on glucose. However, due to a pronounced decrease in expression during the post-diauxic phase in aerobic cultures, expression levels were higher in anaerobic SP cultures than in aerobic SP cultures. This cluster was markedly enriched for genes involved in amino acid synthesis and translation (Figure 3.6A), suggesting that a down-regulation of protein synthesis occurred during the post-diauxic phase. Cluster 3 comprised of genes whose transcript levels increased during the exponential phase of both aerobic and anaerobic cultures but, subsequently, only decreased in aerobic SP cultures. Cluster 3 showed an overrepresentation of genes involved in mitochondrial translation and respiration (Figure 3.6A).

For 595 of the 'oxygen-responsive in SP' genes listed in Table 3.1, differences in expression occurred already upon glucose exhaustion (Figure 3.7, cluster 4-8). Genes in Cluster 5, characterized by a specific up-regulation upon entry into anaerobic SP, showed an overrepresentation of stress-responsive genes (Figure 3.7, cluster 5). Several of these are known to be specifically expressed under anaerobic conditions (e.g., the cell-wall mannoprotein-encoding gene *DAN4* and members of the seripauperin family [223]), but cluster 5 also included heat-shock genes whose expression is not specifically linked to anoxic conditions (e.g. *HSP30* and *SSA4*). Genes that showed a specific downregulation during anaerobic SP, but a constant (Figure 3.7, cluster 6) or increased expression in aerobic SP (Figure 3.7, clusters 7 and 8) showed an overrepresentation of genes involved in transcription-related processes and carboxylic acid metabolism. The latter of which plays a role in the respiration of exogenous carboxylic acids during the post-diauxic phase (Figure 3.7, cluster 8). All 23 genes whose transcript levels were higher under anaerobic conditions, irrespective of the growth phase (Supplementary Table 3.4), were previously described to be upregulated under anaerobic conditions. The majority (14) of these genes belonged to the seripauperin family .

Two clusters (Figure 3.6, cluster 1 and 5) comprised genes whose transcript levels increased in aerobic as well as in anaerobic batch cultivation, but to different final levels. These clusters were enriched for genes induced by the environmental stress response [97]. The extreme differences in thermotolerance of aerobic and anaerobic SP cultures (Figure

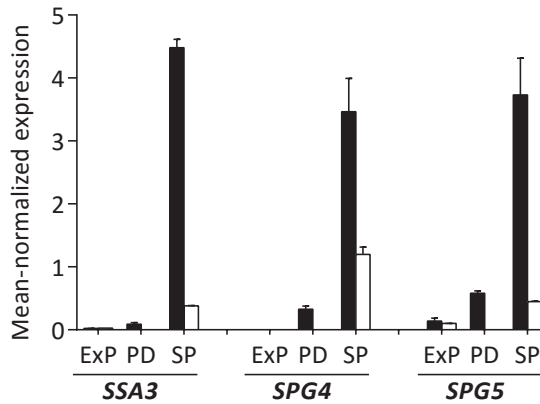


**Figure 3.8:** Expression levels of the SP-associated genes *SSA3*, *SPG4* and *SPG5* during different growth phases in aerobic and anaerobic batch cultures. The mean-normalized expression values during exponential growth on glucose phase (Exp), post-diauxic growth phase (PD, only aerobic cultures) and stationary phase (SP, i.e. 4 hours after exhaustion of exogenous consumable carbon-sources) in aerobic (black bars) and anaerobic (white bars) cultures of *S. cerevisiae* of the genes *SSA3*, *SPG4* and *SPG5*. Average values of duplicate cultures are shown ( $\pm$  SEM).

3.5) were therefore only partially mirrored at the transcript level, indicating that factors other than transcriptional reprogramming contribute to these differences.

## Discussion

This study demonstrates a strong impact of oxygen availability on chronological lifespan and stress tolerance in SP batch cultures of *S. cerevisiae* and, thereby, confirms and extends earlier observations on its physiology in aerobic and anaerobic cultures [191, 304, 269]. The CLS of anaerobically grown SP cultures was much shorter than that of their aerobic counterparts and an even more dramatic difference was observed for thermotolerance. As will be discussed below, these differences involved a different conditioning of aerobic and aerobic cultures during the growth phases preceding SP, as well as energetic constraints imposed on yeast cells in anaerobic SP cultures.

**The post-diauxic growth phase enables transcriptional conditioning of aerobic yeast cultures for stationary phase** | Our transcriptome data revealed that 57% of the transcriptional differences between aerobic and anaerobic SP cultures originated from transcriptional reprogramming during the aerobic post-diauxic growth phase. Although several well-known hallmark transcripts of SP cultures, previously identified in (semi) aerobic shake-flask cultures, such as *SPG4*, *SPG5* and *SSA3* [181], showed increased levels in anaerobic SP cultures, their levels did not reach those observed in aerobic cultures (Figure 3.8). Moreover, many genes involved in biosynthesis were strongly down-regulated during the aerobic post-diauxic phase and SP, but retained expression levels

close to those in the exponential growth phase in anaerobic cultures (Figure 3.6). These transcriptome data are consistent with the hypothesis that the post-diauxic phase in aerobic cultures conditions cells for entry into SP and that, conversely, absence of a post-diauxic phase prevents anaerobic batch cultures from adequately adapting to SP and starvation.

Hormesis could potentially explain the difference in robustness between aerobic and anaerobic cultures. Indeed respiration can generate low levels of ROS and thereby induce stress tolerance via increased expression of stress tolerance genes [191, 263]. However, among a set of 22 genes encoding enzymes involved in ROS-protective mechanisms [209], including the superoxide dismutase genes *SOD1* and *SOD2*, whose expression is strongly upregulated during exposure to ROS [97, 191], only the peroxisomal catalase *CTA1* was higher expressed in aerobic SP cultures. These findings argue against a dominant role of ROS-based hormesis in the acquisition of increased robustness by aerobic SP cultures.

**Caloric restriction: a key factor in conditioning yeast cells for stationary phase and starvation** |

Thermotolerance is negatively correlated with specific growth rate in *S. cerevisiae* as Lu *et al.* (2009) demonstrated in nutrient-limited chemostat cultures [174]. Although these authors did not evaluate the impact of specific growth rate on CLS nor investigate anaerobic growth, they showed that the negative correlation between thermotolerance and growth rate also held in a respiratory-deficient *S. cerevisiae* strain [174]. Our data are fully consistent with the hypothesis that the strong reduction of specific growth rate (from 0.39 to 0.10 h<sup>-1</sup>) during transition from fast exponential growth on glucose to the post-diauxic phase in aerobic batch cultures could similarly trigger increased thermotolerance and extended CLS during the starvation phase. We have also recently shown that a gradual decrease of the specific growth rate to near-zero values in glucose-limited retentostats [28] yielded yeast cells with a thermotolerance that is as high as that of aerobic SP cultures (Figure 3.5), and with an even longer CLS during subsequent starvation [27]. The transcriptional reprogramming observed in these anaerobic severely calorie-restricted cultures [29] strongly resembled the transcriptome changes observed in the present study for aerobic cultures entering SP and proteome analysis showed increased levels of proteins involved in stress resistance [24]. Deletion of Rim15, a kinase under control of several nutrient signaling pathways [262], strongly reduced the acquisition of robustness in both anaerobic and aerobic calorie-restricted cultures [299, 26], suggesting a strong role for nutrient signaling independent of oxygen availability.

The present study, combined with our previous retentostat studies, therefore clearly demonstrates that prior conditioning by a period of caloric restriction (e.g. by slow growth during the aerobic post-diauxic phase or in extremely glucose-limited cultures) is a prerequisite for acquisition of a prolonged CLS by non-growing, starving cultures

of *S. cerevisiae*. This conclusion, which supports earlier proposals based on starvation experiments by Thomsson *et al.* [269, 270], has important implications for the design and interpretation of yeast studies on chronological aging, for example when such studies involve mutants that are impeded in energy metabolism.

**The low thermotolerance of exponentially growing anaerobic cultures does not correlate with expression of heat shock genes** | Although both aerobic and anaerobic, non-growing yeast cultures can acquire a similar thermotolerance by an appropriate preceding conditioning phase, a drastic difference was observed in the thermotolerance of exponentially growing aerobic and anaerobic cultures (Figure 3.5). The similar adenylate energy charge and intracellular ATP concentrations of aerobic and anaerobic cultures during exponential growth on glucose appear to rule out cellular energy status as a major cause of this difference. Since the high temperature (53°C) during the thermotolerance assays precludes *de novo* synthesis of mRNA or protein synthesis [100], this difference must already be expressed in the batch cultures themselves. Transcript levels of genes that were previously implicated in heat-shock resistance (including HSP genes [303] such as *HSP104* [168], *HSP26* [118], *HSP12* [220], *SSA3* [302]) were similar during the exponential growth phase on glucose in aerobic and anaerobic cultures. Moreover, of 59 genes identified as essential for heat-shock survival by Gibney and coworkers [100], only one gene was differentially expressed, *LIA1*, and showed a higher transcript level in anaerobic cultures.

Oxygen availability strongly influences sterol and unsaturated fatty acid composition of yeast cells [304], especially because these compounds have to be added to growth media as anaerobic growth factors [289]. These differences in membrane composition might partially explain the observed differences in thermotolerance between aerobically and anaerobically grown *S. cerevisiae* cells. The hypothesis that membrane composition is a key determinant in thermotolerance of *S. cerevisiae* [79, 110] is consistent with a recent study, in which the acquisition of increased thermotolerance by laboratory-evolved strains was shown to be caused by changes in their sterol composition [46].

**A low energy status of anaerobic SP cultures limits metabolic flexibility** | Consistent with earlier reports [304, 54], anaerobic batch cultures of *S. cerevisiae* displayed a substantially higher glycogen content than aerobic cultures. However, after the onset of SP, anaerobic cultures showed a much faster decrease of the adenylate energy charge. This difference can be attributed to several factors. Firstly, since *S. cerevisiae* cannot derive metabolic energy from lipids and amino acids in the absence of oxygen [281], anaerobic cultures are entirely dependent on glycogen and trehalose as energy storage compounds and anaerobic catabolism of these storage carbohydrates yields less ATP than respiration. The estimated ATP synthesis rate from anaerobic glycogen dissimilation of ca. 5  $\mu\text{mol}$  per

g biomass dry weight per hour during the first day in SP (based on a maximum ATP yield of 3 ATP per glucose residue [27]), was two orders of magnitude lower than the cellular ATP demand for maintenance estimated from chemostat and retentostat cultures ( $m_{\text{ATP}} = 1 \text{ mmol ATP per g biomass dry weight per hour}$  [28]). A similar extreme reduction of ATP turnover rates was observed when anaerobic retentostat cultures were switched to carbon starvation [27]. Together, these observations indicate that an extremely low ATP turnover is an intrinsic feature of anaerobic, starving yeast cultures. In addition to this extreme low ATP-turnover, it is even conceivable that the apparent inability of anaerobic batch cultures to efficiently down-regulate energy-consuming processes, including protein synthesis, the single most expensive biosynthetic process in living cells [291, 259], may have exacerbated the fast decline of their energy status after entry into SP (Figure 3.3).

The low energy status of cells may at the same time have put strong constraints on these energy consuming processes. Proteome analyses should reveal whether the increased transcription of *HSP* genes, implicated in thermotolerance, which took place late in the exponential growth phase (Figure 3.6), was too late to enable synthesis of the corresponding proteins before the decline in cellular energy status in anaerobic SP cultures. Such a scenario would explain the discrepancy between the oxygen-independent upregulation of these genes (with notable exception of *SSA3*) and the absence of increased thermotolerance in anaerobic SP cultures.

Taken together, the results from the present study indicate that, in the short time lapse between the moment at which anaerobic cultures sense that glucose reaches critically low levels and the actual exhaustion of glucose, they lack the time and resources to perform the energy-intensive remodeling of their transcriptome and proteome required to robustly face starvation. Our data are therefore entirely consistent with the notion that the low CLS and thermotolerance of anaerobic SP cultures, in comparison with aerobic cultures, is due to the absence of a proper conditioning phase and a limited metabolic flexibility due to a lower cellular energy status.

**Outlook |** Many studies in which SP yeast cultures are used as a model system to investigate aspects of aging, still rely on shake-flask cultures. Due to their low and poorly controlled oxygen-transfer capacity, the aeration status of shake-flask cultures is generally unclear. The strong impact of oxygen availability on aging-related characteristics [199] underlines the value of controlled cultivation techniques, e.g. in bioreactors, including batch, chemostat and retentostat cultures [28, 309, 43, 195] or flow-through cells [163], in yeast-based aging studies. In particular, the use of anaerobic cultures as a model offers interesting possibilities to clarify the role of respiration and ROS in aging, apoptosis and longevity.

The short life span and low robustness of anaerobic SP cultures of *S. cerevisiae* is directly relevant for industrial applications. Robustness of SP cultures is especially important for



processes in which biomass from anaerobic batch cultures is recycled, e.g. in industrial bioethanol production and beer brewing [18, 101]. Clearly, results from (semi-)aerobic shake-flask cultures cannot be used to predict the performance of such anaerobic processes and improvement of robustness in these industrial processes will have to be based on studies in anaerobic systems.

*Saccharomyces* yeasts have the capability, rare among eukaryotes, to grow fast in the complete absence of oxygen and it is often assumed that they are well adapted to anaerobic environments [293, 111, 104]. While the natural habitat of *S. cerevisiae* is still a matter of debate [104], lower biomass concentrations frequently encountered in natural environments combined with the low affinity of yeast glucose transporters [227] may lead to a transition into SP that is sufficiently slow to enable acquisition of longevity and robustness under anaerobic conditions. Further research is therefore needed to investigate the ecological relevance of this laboratory study.

## Acknowledgements

We thank Mervin Pieterse, Pauline Folch, Nuria Barrajon-Simanca, Xavier Hakkaart for assistance in performing the experiments. Ruben Martínez-Moreno is recipient of a CSIC JAE-Predoc grant co-funded by the European Social Fund of the EU.

## Methods

**Strains and cultivation** | The prototrophic *Saccharomyces cerevisiae* strain CEN.PK113-7D (MATA MAL2-8c SUC2) used in this study is a congeneric member of the CEN.PK family [197, 84]. Stock cultures were grown at 30°C in shake flasks containing yeast extract (1% w/v), peptone (2% w/v) and dextrose (2% w/v) (YPD) medium. Glycerol, final concentration 20% (v/v), was added to overnight cultures and 1 mL aliquots were stored at -80°C.

Previously described synthetic medium [290] was used with 20 g/L glucose as sole carbon-source and 0.2 g L<sup>-1</sup> antifoam Emulsion C (Sigma, St. Louise, USA). In case of anaerobic cultivations, the medium was supplemented with anaerobic growth factors ergosterol (10 mg L<sup>-1</sup>) and Tween 80 (420 mg L<sup>-1</sup>) dissolved in ethanol. Inocula for batch fermentations consisted of 100 mL yeast culture grown overnight to an OD<sub>660</sub> of 4 in synthetic medium with 20 g L<sup>-1</sup> glucose. Aerobic and anaerobic batch fermentations were carried out at 30°C in 2 L bioreactors (Applikon, Schiedam, The Netherlands), with a working volume of 1.4 L. Cultures were stirred at 800 rpm and sparged at a flow-rate of 700 mL min<sup>-1</sup> with either dried air or nitrogen gas (< 10 ppm oxygen, Linde Gas Benelux, The Netherlands). The bioreactors were equipped with Norprene tubing (Saint-Gobain Performance Plastics, Courbevoie, France) and Viton O-rings (Eriks, Alkmaar, The Netherlands) to minimize diffusion of oxygen. During aerobic cultivations, dissolved oxygen levels remained above 40% of the initial saturation level as measured by Clark electrodes (Mettler Toledo, Greifensee, Switzerland). The culture pH was maintained at 5.0 by automatic addition of 2 M KOH and 2 M H<sub>2</sub>SO<sub>4</sub>.

**Analysis of biomass, metabolites, substrate and exhaust gas** | Biomass concentration as culture dry weight was determined as described previously [219]. For substrate and extracellular metabolite concentration determination, culture supernatants were obtained by centrifugation of culture samples (3 min at 20.000 g) and analysed by high-performance liquid chromatograph (HPLC) analysis on a Waters Alliance 2690 HPLC (Waters, Milford, MA) equipped with a Bio-Rad HPX 87H column (BioRad, Veenendaal, The Netherlands), operated at 60°C with 5 mM H<sub>2</sub>SO<sub>4</sub> as the mobile phase at a flow rate of 0.6 ml min<sup>-1</sup>. Detection was by means of a dual-wavelength absorbance detector (Waters 2487) and a refractive index detector (Waters 2410).

The exhaust gas from batch cultures was cooled with a condenser (2°C) and dried with a PermaPure Dryer (model MD 110-8P-4; Inacom Instruments, Veenendaal, the Netherlands) prior to online analysis of carbon dioxide and oxygen with a Rosemount NGA 2000 Analyser (Baar, Switzerland).

**Colony forming units** | To determine culture viability, small aliquots of culture broth were taken from the reactor and cells were counted on a Z2 Coulter Counter (Beckman Coulter, Woerden, Netherlands) equipped with a 50 µm orifice (Multisizer II, Beckman Coulter, Woerden, Netherlands). Cells were diluted in 0.1% peptone and 100 µL suspensions containing approximately 30, 300 and 3000 cells were plated on yeast extract (1% w/v), peptone (2% w/v) and dextrose (0.5% w/v) (YPD) agar plates and incubated at 30°C for at least 3 days before counting the colonies. CFU was calculated as the number of colonies formed divided by the number of plated cells.

**Thermotolerance assay** | Cells from culture broth were counted with a Z2 Coulter Counter and diluted in pre-warmed (53°C) isotone diluent II (Beckman Coulter, Woerden, Netherlands) to yield 50 mL cell suspensions with a density of 1.10<sup>7</sup> cells mL<sup>-1</sup>. Cell suspensions were incubated in a waterbath at 53°C and 4 mL aliquots were sampled in 10 min intervals. Samples were cooled on ice and assayed for viability using the FungaLight 5-CFDA, AM (acetoxymethyl ester 5-carboxyfluorescein diacetate)/propidium iodide (PI) yeast viability kit (Invitrogen, Carlsbad, CA) by counting 10,000 cells on a Cell Lab Quanta SC MPL flow cytometer (Beckman Coulter, Woerden, Netherlands) as described previously [27]. 5-CFDA, AM is a cell-permeant substrate for intracellular non-specific esterase activity. Hydrolytic cleavage of the lipophilic blocking acetoxymethyl and diacetate groups of 5-CFDA, AM results in a green fluorescent signal in metabolically active cells. Propidium iodide intercalates with DNA in cells with a compromised cell membrane, which results in red fluorescence. Cells stained with PI were considered dead cells. For each independent sample, the t<sub>50</sub> value (the time after which 50% of the initial viable population was dead) was estimated by fitting the viability data with a sigmoidal dose-response curve in Graphpad Prism 4.03. Both measurements of viability, i.e. metabolic activity based on 5-CFDA, AM and membrane integrity based on PI gave similar t<sub>50</sub>-values, therefore only results based on PI are shown.

**Storage carbohydrate measurements** | 1.2 mL culture broth was quenched in 5 mL of cold methanol (-40°C) using a rapid sampling setup described previously [45], mixed and subsequently pelleted (4,400 g, 5 min) at -19°C. Cells were washed with 5 mL of cold methanol (-40°C) and pellets stored at -80°C. Pellets were resuspended in Na<sub>2</sub>CO<sub>3</sub> (0.25 M) and further processed according to a previously described procedure [206].

**Fatty acids measurements** | Culture volumes corresponding to 50 mg biomass were sampled on ice, centrifuged (10,000 g, 10 min at 4°C), washed twice, resuspended in 5 ml ice-cold water and stored at -20°C. Lipid extraction was performed as described previously [138]. Aliquots of 0.15 mL were added to 15 mL tubes and 1.5 mL of a mixture of concentrated HCl and 1-propanol (1:4) and 1.5 mL of dichloroethane were added. 400 µg of myristic acid (a 15:0 fatty acid) was included as internal standard. Samples were incubated at 100°C for 2 h. Subsequently, 3 mL of water was added to cooled samples. 1 mL of the organic phase was filtered over water-free sodium sulfate into GC vials. The fatty acid propyl esters in the organic phase were analyzed by gas chromatography (model 6890N, Agilent, U.S.A.) using a DB-wax column (length, 30 m; inside diameter, 0.25 mm; film thickness, 0.25 µm; J&W Scientific, Folsom, CA) and helium as the carrier gas. The sample volume was 1 µL, and the split was set to 1:20. The injection temperature was 230°C, and the following temperature gradient was used: 120°C at the start, increasing at a rate of 10°C/min up to 240°C, and then 240°C for 8 min. The fatty acid propyl esters were detected using a flame ionization detector at 250°C.

**Analysis of intracellular adenosine-phosphate concentrations** | Samples for internal metabolite analysis were obtained by rapid sampling [45]. 1.2 mL of culture broth was rapidly quenched into 5 mL of 100% methanol, pre-cooled to -40°C. Samples were washed with cold methanol and extracted with boiling ethanol. Intracellular AMP and ADP were determined enzymatically, using a previously described assay based on myokinase, pyruvate kinase and lactate dehydrogenase reactions [133]. Assays were performed in white, flat bottom 96-well microtiter plates (Corning Inc., USA). NADH fluorescence was measured in a TECAN GENios Pro microtiterplate reader (Tecan, Männedorf, Switzerland) as previously described [45]. Intracellular ATP was also assessed enzymatically. The assay contained 115 mM triethanolamine (pH 7.6), 11.5 mM MgSO<sub>4</sub>·7H<sub>2</sub>O, 1.15 mM NADP<sup>+</sup> per well including sample extract, total volume was 205 µL per well. The reaction to measure ATP was initiated by adding 12 mM glucose and 30 U hexokinase (Sigma-Aldrich Chemie B.V, Zwijndrecht, The Netherlands). Assays were performed in black, flat bottom 96-well microtiter plates (Corning Inc., USA). NADPH fluorescence was measured in a TECAN GENios Pro microtiterplate reader. The adenylate energy charge was calculated according to the previously described equation [9]:

$$EC = \frac{[ATP] + 0.5[ADP]}{[ATP] + [ADP] + [AMP]}$$

**Transcriptome analysis** | Independent duplicate aerobic and anaerobic batch cultures were sampled at six and four different time points respectively (see Figure 3.4A and B) for microarray analysis, resulting in a total dataset of 20 microarrays. Sampling from batch cultures for transcriptome analysis was performed using liquid nitrogen for rapid quenching of mRNA turnover [216]. Prior to RNA extraction, samples were stored in a mixture of phenol/chloroform and TEA buffer at -80°C. Total RNA extraction, isolation of mRNA, cDNA synthesis, rRNA synthesis, labelling and array hybridization was performed as previously described [189]. The quality of total RNA, cDNA, rRNA and fragmented rRNA was checked using an Agilent Bioanalyzer 2100 (Agilent Technologies, Santa Clara, CA). Hybridization of labelled fragmented rRNA to the microarrays and staining, washing and scanning of the microarrays was performed according to Affymetrix instructions (EukGE\_WS2v5).

The 6383 yeast open reading frames were extracted from the 9335 transcript features on the YG-S98 microarrays. To allow comparison, all expression data were normalized to a target value of 240 using the average signal from all gene features [119]. The microarray data used in this study are available via GEO series accession number GSE69485. To eliminate variation in genes that are not expressed, genes with expression values below 12 were set to 12 and the gene features for which the maximum expression was below 20 for all 20 arrays were discarded [29]. The average deviation of the mean transcript data of replicate batches was ca. 11%, similar to the reproducibility usually observed in replicate steady state chemostat cultures [67]. The expression of housekeeping genes *ACT1*, *PDA1*, *TFC1*, *ALG9*, *TAF10* and *UBC6* [268] remained stable for both conditions and all sample points (average coefficient of variation  $17\% \pm 5\%$ ).

To identify genes that were differentially expressed between aerobic and anaerobic SP cultures, a pairwise comparison was performed between aerobic samples taken at time point 6 (Figure 3.4A) and anaerobic samples taken at time point 4 (Figure 3.4B) as previously described [89]. Similarly, genes differently expressed during growth on glucose under aerobic or anaerobic conditions were identified through a pairwise comparison of aerobic and anaerobic samples taken at time point 1 (see Figure 3.4A and B). Differences with adjusted P-values lower than 0.05 and a fold difference of 2 or higher were considered statistically significant. Time-dependent expression profiles of selected genes were clustered according to optimal k-means clustering using positive correlation as distance metric (Expressionist Pro version 3.1, Genedata, Basel, Switzerland) resulting in an optimal number of 9 clusters. For display of time-dependent transcript levels, expression values were normalized per gene by dividing single expression values by the average expression value of both conditions and all time points. Mean values of these average-normalized values for all genes in each cluster are shown, as well as the first and third quartile of average-normalized values.

Gene expression clusters were analysed for overrepresentation of functional annotation categories of the Gene Ontology (GO) database (<http://www.geneontology.org/>), based on a hypergeometric distribution analysis tool [150]. Additional categories describing genes expressed in SP cultures [181], genes commonly induced by several environmental stresses [97] or essential for heat-shock survival [100] were extracted from the respective references.

## **Supplementary material Chapter 3**

Supplementary materials are freely available on the website of Microbial Cell in which the original publication was published online on October 21, 2015, in Volume 2, Number 11, October 2015, Pages 429–444 (doi: 10.15698/mic2015.11.238).

### **Supplementary Table 3.1**

For the list of genes differentially expressed between aerobic and anaerobic stationary phase cultures the reader is referred to the Excel spread sheet that can be found online.

### **Supplementary Table 3.2**

For the list of genes in functional categories overrepresented among genes with higher expression in (1) aerobic or (2) anaerobic stationary phase cultures the reader is referred to the Excel spread sheet that can be found online.

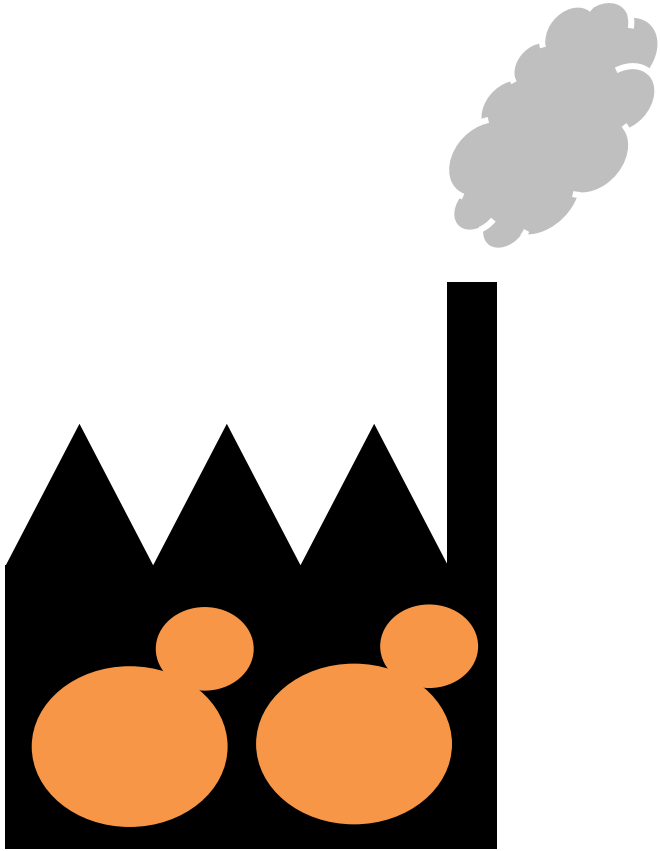
### **Supplementary Table 3.3**

For the list of genes differentially expressed between aerobic and anaerobic SP cultures per cluster for clusters 1-8 the reader is referred to the Excel spread sheet that can be found online.

### **Supplementary Table 3.4**

For the list of genes with constitutive higher expression in anaerobic batch cultures including stationary phase the reader is referred to the Excel spread sheet that can be found online.





# 4

## Maintenance-energy requirements and robustness of *Saccharomyces cerevisiae* at aerobic near-zero specific growth rates

Tim Vos, Xavier D.V. Hakkaart, Erik A.F. de Hulster, Antonius J. A. van Maris, Jack T. Pronk, Pascale Daran-Lapujade

Published in *Microbial Cell Factories* 2016, 15:111



### Abstract

*Saccharomyces cerevisiae* is an established microbial platform for production of native and non-native compounds. When product pathways compete with growth for precursors and energy, uncoupling of growth and product formation could increase product yields and decrease formation of biomass as a by-product. Studying non-growing, metabolically active yeast cultures is a first step towards developing *S. cerevisiae* as a robust, non-growing cell factory. Microbial physiology at near-zero growth rates can be studied in retentostats, which are continuous-cultivation systems with full biomass retention. Hitherto, retentostat studies on *S. cerevisiae* have focused on anaerobic conditions, which bear limited relevance for aerobic industrial processes. The present study uses aerobic, glucose-limited retentostats to explore the physiology of non-dividing, respiring *S. cerevisiae* cultures, with a focus on industrially relevant features.

Retentostat feeding regimes for smooth transition from exponential growth in glucose-limited chemostat cultures to near-zero growth rates were obtained by model-aided experimental design. During 20 days of retentostats cultivation, the specific growth rate gradually decreased from  $0.025 \text{ h}^{-1}$  to below  $0.001 \text{ h}^{-1}$ , while culture viability remained above 80%. The maintenance requirement for ATP ( $m_{\text{ATP}}$ ) was estimated at  $0.63 \text{ mmol ATP (g biomass)}^{-1} \text{ h}^{-1}$ , which is ca. 35% lower than previously calculated for anaerobic retentostats. Concomitant with decreasing growth rate in aerobic retentostats, transcriptional down-regulation of genes involved in biosynthesis and up-regulation of stress-responsive genes resembled transcriptional regulation patterns observed for anaerobic retentostats. The heat-shock tolerance in aerobic retentostats far exceeded previously reported levels in stationary-phase batch cultures. While *in situ* metabolic fluxes in retentostats were intentionally low due to extreme caloric restriction, off-line measurements revealed that cultures retained a high metabolic capacity.

This study provides the most accurate estimation yet of the maintenance-energy coefficient in aerobic cultures of *S. cerevisiae*, which is a key parameter for modelling of industrial aerobic, glucose-limited fed-batch processes. The observed extreme heat-shock tolerance and high metabolic capacity at near-zero growth rates demonstrate the intrinsic potential of *S. cerevisiae* as a robust, non-dividing microbial cell factory for energy-intensive products.

## Introduction

The yeast *Saccharomyces cerevisiae* is an established microbial host for the production of native yeast metabolites as well as non-native products [144]. Production of many of these compounds, including phenylpropanoids, isoprenoids, heterologous proteins and lipids [51, 295, 170] from glucose requires a net input of ATP. The maximum ATP yield from glucose is obtained when its dissimilation occurs exclusively via respiration. In *S. cerevisiae*, a completely respiratory sugar metabolism requires aerobic conditions and sugar-limited cultivation at low to intermediate specific growth rates [276]. In industry, these requirements are usually met by sugar-limited, aerobic fed-batch cultivation. Due to oxygen-transfer and cooling constraints, aerobic fed-batch processes typically involve low specific growth rates [277, 122]. However, biomass-specific production rates ( $q_p$ ) of products whose biosynthesis from sugar requires a net input of ATP typically show a positive correlation with specific growth rate [295, 170, 151, 136]. Understanding and, ultimately, breaking this correlation between growth and product formation by improving specific rates of product formation at low specific growth rates, is an important target for optimizing productivity and product yields in aerobic, sugar-limited fed-batch cultures.

In addition to the relation between  $q_p$  and specific growth rate, microbial product formation at low specific growth rates is strongly influenced by the metabolic-energy requirement of microorganisms for maintaining cellular integrity and viability. In a first analysis, this maintenance-energy requirement is often assumed to be growth-rate independent [295, 265]. Distribution of carbon- and energy substrate over growth and cellular maintenance can then be described by the Pirt equation [217], which can be modified to include ATP-requiring product formation (See equation in Figure 4.1). The Pirt equation describes how the fraction of the energy substrate that needs to be dissimilated to fulfil maintenance energy requirements increases as the specific growth rate in, for example, an aerobic, sugar-limited fed-batch process decreases. In slow-growing aerobic industrial fed-batch processes this increasing impact of maintenance requirements has a major negative impact on product yields and productivities [295].

Analysis of the physiology of extremely slow growing yeast cultures can provide relevant, quantitative information on the maintenance-energy requirements of *S. cerevisiae* and for developing this yeast into a non-growing cell factory [28, 29, 27, 26, 24]. Retentostats are continuous cultivation devices with full biomass retention that have been designed to study microbial physiology at near-zero growth rates [286, 85]. Retentostat cultivation typically starts with a steady-state chemostat culture, operated at a low dilution rate. After reaching steady state, the chemostat culture is switched to retentostat mode by redirecting the effluent through a filter unit that ensures full biomass retention (Figure 4.1). The constant, growth-limiting feed of glucose will then result in biomass accumulation, while the amount of substrate available per cell per unit of time decreases over time (Figure 4.1). This decreased substrate availability results in decreasing

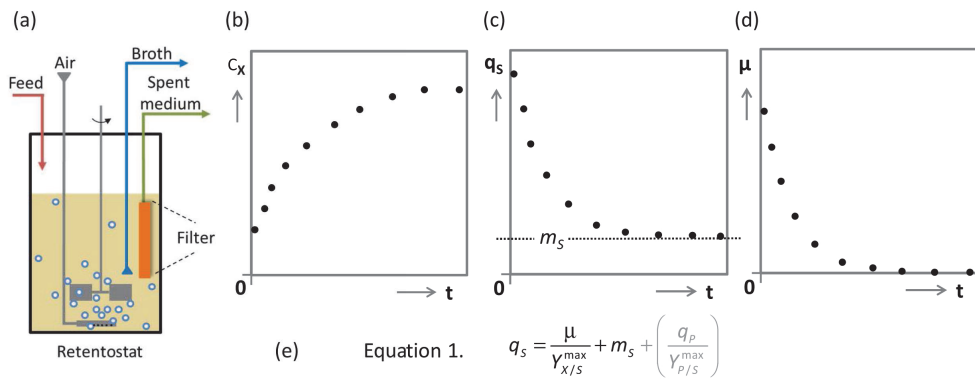


**Figure 4.1:** Schematic representation of retentostat set-up and simulated profiles of biomass accumulation ( $C_x$ ), glucose consumption rate ( $q_s$ ) and specific growth rate ( $\mu$ ) during prolonged retentostat cultivation. The retentostat is a continuous bioreactor system in which the outflow can be switched from whole-broth removal to complete cell retention through a filter probe (a). After switching from chemostat cultivation to retentostat mode, biomass accumulates in the bioreactor (b), which gradually decreases the glucose availability per unit of biomass. This decrease ultimately results (c) in specific glucose consumption rates that can only meet energy demands for cellular maintenance ( $m_s$ ), thereby causing near-zero specific growth rates (d). The distribution of the carbon and energy source over growth, maintenance and product formation (not indicated in the plots) is mathematically captured by an extended Pirt equation (e), in which  $Y_{X/S}^{\max}$  is the maximum theoretical biomass yield,  $q_p$  is the specific production rate of a product whose synthesis requires metabolic energy, and  $Y_{P/S}^{\max}$  is the maximum theoretical yield of this product on substrate.

specific substrate consumption rates ( $q_s$ ) which, after prolonged retentostat cultivation, asymptotically approach the cellular energy-substrate requirement for maintenance ( $m_s$ ). Since, in this situation, no energy substrate is available for growth the specific growth rate ( $\mu$ ) asymptotically approaches zero (Figure 4.1).

Retentostat cultures have mostly been used in the early 1990's to investigate the response of prokaryotes to extreme energy limitation. At extremely low growth rates, many bacteria, including *Escherichia coli*, display an alarmone-mediated stringent response. This coordinated response enables cultures to more efficiently withstand nutrient scarcity by down regulation of energy-intensive cellular processes and, therefore, a reduction of the maintenance-energy requirement [286, 8]. Retentostats have recently been used to study the physiology of *S. cerevisiae* at near-zero growth rates under anaerobic conditions [28, 29, 27, 26, 24]. Even at extremely low specific growth rates, the maintenance requirement of *S. cerevisiae* in these anaerobic chemostat cultures was shown to be growth-rate independent [28]. A decrease of the ATP-turnover of non-growing cultures was only observed when anaerobic, retentostat-grown *S. cerevisiae* cultures were switched to glucose starvation and energy metabolism became dependent on metabolism of storage carbohydrates [27]. Transcriptome responses during anaerobic retentostats encompassed many genes whose transcription was previously shown to be growth-rate correlated in faster growing cultures, as well as an increased expression of genes involved in resistance to a variety of stresses [29]. Consistent with the latter observation, yeast cells grown at low specific growth rates acquire a strongly increased

robustness towards heat shock and an increased chronological life span [27, 174].

Since previous retentostat studies on *S. cerevisiae* were exclusively performed under anaerobic conditions, it remains unclear how oxygen availability affects its physiology at extremely low specific growth rates. Oxygen is known to have multiple effects on cellular biology. Even in *S. cerevisiae*, which has a rather low efficiency of oxidative phosphorylation, fully respiratory dissimilation of glucose yields eight-fold more ATP than alcoholic fermentation, which is the sole dissimilatory pathway under anaerobic conditions [291]. This higher ATP yield supports higher biomass yields and, if the maintenance-requirement for ATP ( $m_{\text{ATP}}$ ) is the same in aerobic and anaerobic cultures, should lead to a lower  $m_S$  than observed in anaerobic cultures. Since biomass yield and maintenance-energy requirement affect the dynamics of retentostats, these differences should also be taken into account in the design of feed regimes that result in a smooth transition from exponential growth to near-zero growth rates. Despite the industrial relevance of maintenance-energy requirements, accurate experimental estimates of  $m_S$  and  $m_{\text{ATP}}$  for aerobic, sugar-limited cultures of *S. cerevisiae* on synthetic medium are not available. The assumption that  $m_{\text{ATP}}$  in aerobic cultures is the same as in anaerobic cultures [272], can result in over- or underestimation of the  $m_S$  of aerobic cultures. In anaerobic cultures, presence of the anaerobic growth factor oleic acid [289] and of ethanol and organic acids might increase  $m_{\text{ATP}}$ . Similarly, detoxification of reactive oxygen species (ROS) and repair of ROS-induced damage may lead to increased maintenance energy requirements in aerobic cultures [131]. ROS, which can contribute to cellular aging, could also accelerate cell death of aerobic, non-dividing and chronologically aging yeast cultures [52]. A further question that remains to be addressed is whether and to what extent extremely slow-growing *S. cerevisiae* cultures retain a high metabolic capacity, which is a prerequisite for efficient product formation.

Previous studies showed that glucose-limited aerobic cultures of *S. cerevisiae* retain a high capacity of glycolysis (the highway for sugar assimilation) at specific growth rates down to  $0.05 \text{ h}^{-1}$  [279], but no data are available on the glycolytic capacity at near-zero growth rates. The goal of the present study is to quantitatively analyse maintenance-energy requirement, robustness and glycolytic capacity of *S. cerevisiae* in aerobic cultures grown at near-zero growth rate. To this end, regimes for aerobic retentostat cultivation were designed and implemented that enabled a smooth transition from exponential growth to near-zero growth rates. In addition to quantitative physiological analyses, transcriptome analysis was performed to investigate cellular responses to near-zero growth in aerobic cultures and to compare these with previously published transcriptome data obtained from anaerobic retentostats.

## Results

**Design of a regime for smooth transition to near-zero growth rates in aerobic retentostats** | Growth rate dynamics and biomass accumulation in retentostat cultures mainly depends on two condition-dependent and strain-specific parameters: the theoretical maximal biomass yield ( $Y_{X/S}^{\max}$ ) and the maintenance coefficient ( $m_S$ ). To predict the impact of these parameters on growth dynamics in aerobic retentostat cultures, a model based on the Pirt definition of resource allocation (see Figure 4.1) was used.  $Y_{X/S}^{\max}$  was estimated from published data on aerobic, glucose-limited chemostat cultures of the *S. cerevisiae* strain used in this study ( $0.5 \text{ g g}^{-1}$  [279]). Since no accurate estimates for the aerobic  $m_S$  are available, model-based simulations were performed with a range of  $m_S$  values that were based on the  $m_S$  calculated from anaerobic retentostat experiments (biomass-specific glucose consumption for maintenance:  $0.5 \text{ mmol g}_X^{-1} \text{ h}^{-1}$ , [28]) and assuming a P/O ratio of 1.0 for aerobic, respiring cultures of *S. cerevisiae* [291, 89], which leads to an 8-fold higher ATP yield from respiratory sugar dissimilation than from alcoholic fermentation.

Initial model simulations were performed based on the assumption that no loss of viability occurs during retentostat cultivation and with the same feed regime that was previously used for anaerobic retentostats (constant dilution rate of  $0.025 \text{ h}^{-1}$  and a glucose concentration in the feed of  $20 \text{ g L}^{-1}$  [28]). This resulted in a predicted accumulation of biomass to a concentration of ca.  $45 \text{ g L}^{-1}$ , Figure 4.2, blue line), which was considered to present a substantial risk of clogging the filter unit. Moreover, in this simulation, near-zero growth rates (i.e. specific growth rates below  $0.001 \text{ h}^{-1}$ ) were only reached after multiple weeks of operation (Figure 4.2, blue line), which was considered to be impracticable.

Near-zero growth rates can be reached faster by decreasing the glucose concentration in the medium for the retentostat culture ( $C_{S,MR}$ ) compared to the glucose concentration in the medium for the chemostat culture ( $C_{S,MC}$ ). However, care should be taken to avoid scenarios in which the glucose supply changes suddenly or transiently decreases below the culture's maintenance-energy demand, which might affect cellular viability. Introduction of an additional medium mixing vessel (Figure 4.2), allowed for a controlled, smooth transition of the ingoing glucose concentration ( $C_{S,in}$ ) into the retentostat culture, whilst maintaining a constant flow of medium ( $\Phi_V$ ) and thereby a constant dilution rate. To incorporate the mixing vessel the model was expanded with Equation 4.1 and simulations were performed for experimental design of  $C_{S,MR}$  and the volume of the mixing vessel ( $V_S$  in liters) (Figure 4.2).

$$\frac{dC_{S,in}}{dt} = \frac{\Phi_V}{V_S} C_{S,MR} - \frac{\Phi_V}{V_S} C_{S,in} \quad (4.1)$$

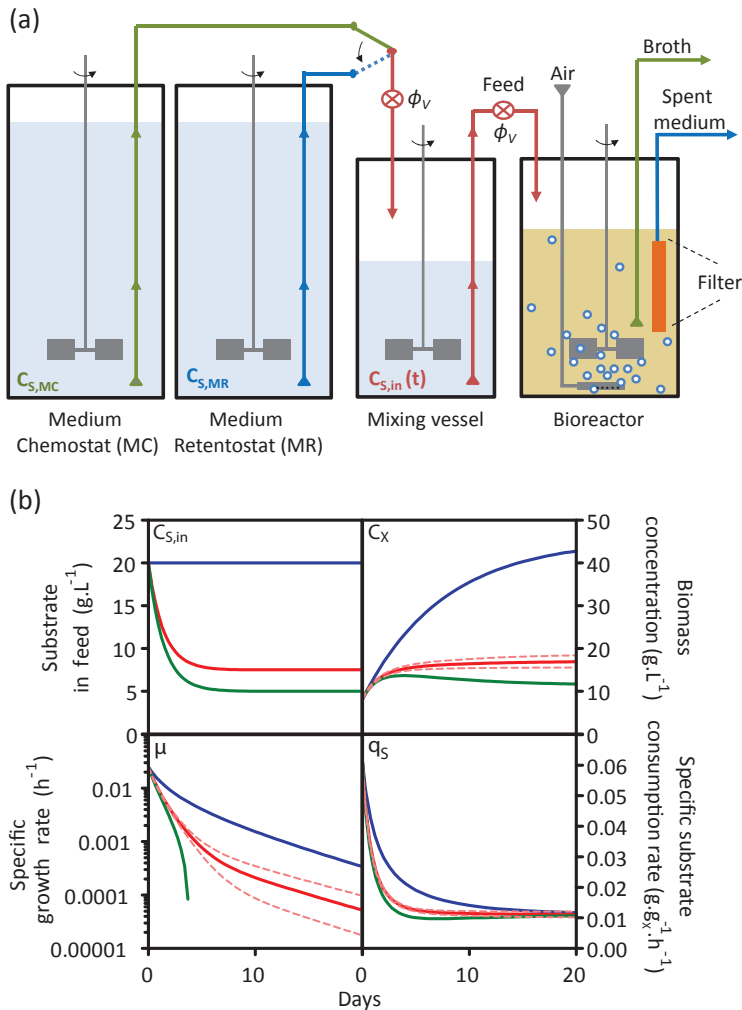


**Figure 4.2:** Setting up aerobic retentostat cultures. (a) Retentostat cultures (bioreactors) were started from a steady-state chemostat culture with an ongoing glucose concentration ( $C_{S,MC}$ ) of  $20 \text{ g L}^{-1}$ . At the start of the retentostats ( $t = 0 \text{ h}$ ), the feed to the mixing vessel was switched to the medium reservoir for the retentostat cultivation (as indicated by the arrow). The process was modelled for three different concentrations of glucose in the medium reservoir for the retentostat cultures ( $C_{S,MR}$ ). (b) Profiles of biomass accumulation ( $C_X$ ), specific glucose consumption rate ( $q_S$ ) and specific growth rate ( $\mu$ ) in time were predicted with a mathematical model, based on glucose concentration in the feed coming from the mixing vessel. Blue lines indicate a scenario in which  $C_{S,MC} = C_{S,MR} = 20 \text{ g L}^{-1}$ , green lines indicate  $C_{S,MR} = 5 \text{ g L}^{-1}$ , and red lines indicate  $C_{S,MR} = 7.5 \text{ g L}^{-1}$ . Dotted lines indicate simulations for which 10% higher or lower maintenance values were considered in the model (see Methods section). The operational conditions applied in the experiments in this study correspond to the red lines.

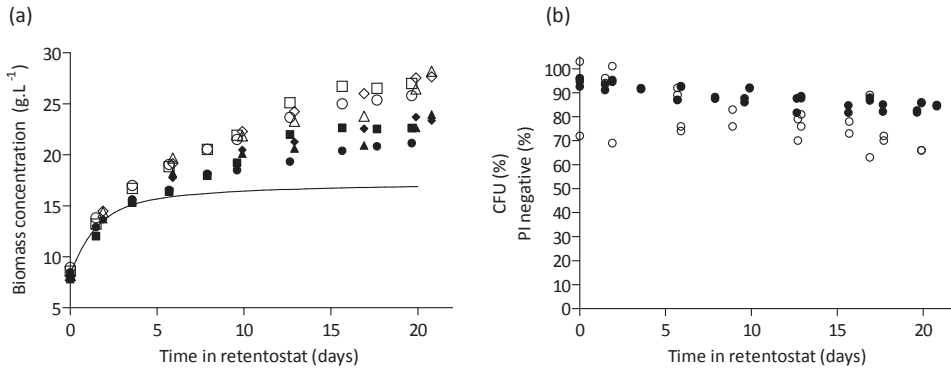


**Figure 4.3:** Biomass accumulation and culture viability during prolonged retentostat cultivation. (a) Predicted biomass accumulation profile (line), measured biomass dry weight concentrations (open symbols), and viable biomass concentration (closed symbols) from four replicate retentostat cultures. (b) Culture viability estimated by flow cytometric analysis of propidium iodide-stained cells (closed symbols), and viability estimated from colony-forming unit counts (open symbols).

Figure 4.2 depicts the modelling output when  $C_{S,MR}$  equals  $C_{S,MC}$  (blue lines) and when  $C_{S,MR}$  was decreased to 7.5 or 5 g L<sup>-1</sup> (solid red and green lines, respectively) assuming an  $m_S$  of 0.011 g g<sup>-1</sup> h<sup>-1</sup>.

In the simulations, values of  $C_{S,MR}$  of 5 g L<sup>-1</sup> and lower resulted in ‘negative growth’, indicating that the model predicted glucose starvation and cell death. Since, in extremely slow growing cultures, glucose is predominantly used for maintenance, growth dynamics in retentostats are particularly sensitive to variations in  $m_S$ . Accordingly, a 20% change in  $m_S$  resulted in a five-fold difference in the predicted specific growth rates after 20 d of retentostat cultivation (dashed lines in Figure 4.2). Based on these simulations, operational conditions were chosen such that the prediction complied to the following requirements: i) near-zero growth rates ( $\mu < 0.001$  h<sup>-1</sup>) achieved within two weeks of retentostat cultivation, ii) prevention of sudden changes in  $q_S$  and glucose starvation, iii) the conditions led to a sizeable difference between initial and final biomass concentrations, iv) previous criteria met for a range of  $m_S$  values, and v) final biomass concentration kept below 30 g L<sup>-1</sup> to prevent filter clogging (Figure 4.2, red line). The chosen operational conditions are described in Figure 4.2, and correspond to the red line.

**Maintenance-energy requirements in aerobic retentostat cultures** | In four independent retentostat cultures, biomass accumulated reproducibly over a period of ca. 20 days. The final biomass concentrations were ca. 3-fold higher than those in the preceding chemostat culture (Figure 4.3a). However, the experimentally observed biomass accumulation was substantially higher than predicted from model simulations (Figure 4.3a). One factor that might contribute to this apparent discrepancy was the biomass viability which, in the model simulations, was assumed to remain at 100% throughout the retentostats experiments. Indeed, flow-cytometric analysis of cellular

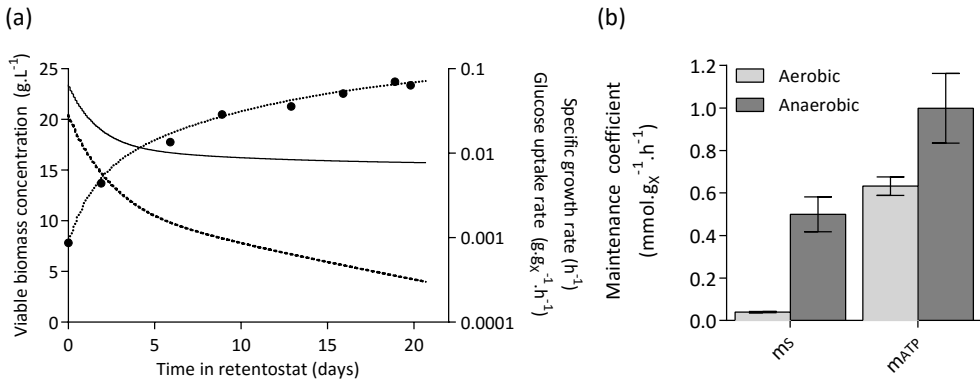


**Figure 4.4:** Growth kinetics and  $m_S$  in retentostat cultures. (a) Specific glucose-consumption rate ( $q_S$ , solid line) and specific growth rate ( $\mu$ , dashed line) calculated by non-linear regression of the accumulation of viable- and total biomass over time (see Methods section). The closed symbols and dotted line represent the viable biomass and linear regression of the viable biomass, respectively. Data are shown for a single representative retentostat experiment. (b) Glucose and ATP requirements for maintenance ( $m_S$  and  $m_{ATP}$ , respectively) of aerobic and anaerobic retentostat cultures (anaerobic data obtained from [28]). The aerobic  $m_{ATP}$  was calculated based on a P/O ratio of respiring *S. cerevisiae* cultures of 1.0 [291].

integrity indicated that, over 20 d of retentostat cultivation, culture viability decreased to ca. 85% (Figure 4.3b). Colony-forming unit counts confirmed that ca. 70% of the cells in the population were able to sustain growth after 20 d in retentostat culture. This apparent loss of cells' capacity to divide contrasts with the retention of cellular integrity and has been previously reported for anaerobic retentostat cultures. It may result from various factors, such as the irreversible degradation of macromolecules necessary for duplication, but may also result from loss of reproductive capacity during CFU plating assays. To prevent the risk of underestimating culture viability resulting from loss of reproductive capacity during CFU plating assays, viable biomass concentrations were therefore calculated based on flow cytometry-based viability assays (Figure 4.3b). Based on these observations, a low but significant death rate of  $4.7 \cdot 10^{-4} \text{ h}^{-1}$  was calculated. However, correcting for viability only explained part of the difference between the observed and modelled biomass accumulation profiles.

As mentioned above, the exact value of  $m_S$  is expected to have a strong impact on biomass accumulation profiles in retentostat cultures. Assuming specific growth-rate independent maintenance, the aerobic  $m_S$  was estimated from the calculated specific growth rate and glucose consumption rates of *S. cerevisiae* in the aerobic retentostats, using biomass concentrations corrected for viability (Figure 4.4a). During 20 d of retentostat cultivation, specific growth rates in all four replicate experiments decreased from  $0.025 \text{ h}^{-1}$  in steady-state to values below  $8 \cdot 10^{-4} \text{ h}^{-1}$ , representing doubling times of over 36 d. The average specific glucose-consumption rate converged to  $0.039 \pm 0.003 \text{ mmol g}_X^{-1} \text{ h}^{-1}$ , representing the cellular substrate requirement exclusively necessary for maintenance energy purposes (Figure 4.4b). Considering an *in vivo* P/O ratio in



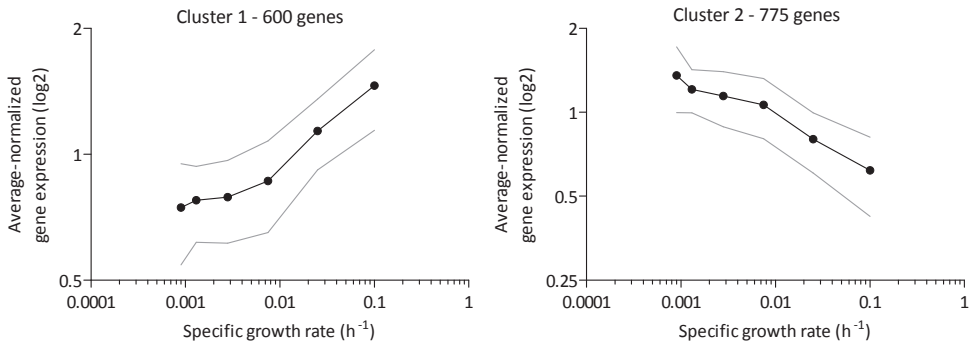


**Figure 4.5:** K-mean clustering of the 1375 genes with significant growth-rate dependent expression profiles. Retentostat data were combined with data from aerobic glucose-limited chemostats grown at  $\mu = 0.10 \text{ h}^{-1}$  (see Methods section). The p-value threshold for significant differential expression was set to 0.01. For each cluster, averaged-normalized expression values are depicted as a function of specific growth rate (see Methods section). Grey dotted lines show the standard deviation of averaged expression values.

*S. cerevisiae* of 1.0 [291], the aerobic ATP requirement of *S. cerevisiae* for maintenance ( $m_{\text{ATP}}$ ) calculated from these experiments was  $0.63 \pm 0.04 \text{ mmol ATP g}_X^{-1} \text{ h}^{-1}$ . This value is ca. 30% lower than the  $m_{\text{ATP}}$  previously estimated from anaerobic retentostat cultures [28] (Figure 4.4b).

**Transcriptional reprogramming in aerobic retentostats: involvement of ‘growth-rate responsive’ genes** | Over the course of the aerobic retentostat experiments, 1375 genes (ca. one-fifth of the genome) were differentially expressed. In comparison, aerobic batch cultures transitioning from exponential growth, through a post-diauxic phase, into stationary phase, resulted in 1690 differentially expressed genes (using the same analysis software and statistical criteria as in the present work, see Chapter 3). One third (458 genes) of the 1375 genes identified in the present retentostat dataset overlapped with the aerobic batch dataset. The 1375 differentially expressed genes identified in the present study could be separated in two clusters with clear, specific-growth-rate dependent transcript profiles (Figure 4.5). Cluster 1 harboured 600 genes whose expression displayed a positive correlation with specific growth rate (Figure 4.5). As anticipated, this cluster showed an overrepresentation of genes involved in typical growth-related processes, including protein, ribosome, amino acid, nucleotide and lipid biosynthesis (Table 4.1). Consistent with this observation, Cluster 1 also showed an overrepresentation of genes whose expression is controlled by transcription factors that are involved in this response: Fhl1, Rap1 and Sfp1, Gcn4 and Met32 (Table 4.1). Genes involved in sterol metabolism (including 15 of the 19 *ERG* genes involved in ergosterol synthesis) and pentose-phosphate pathway were also overrepresented in Cluster 1. Cluster 2 grouped the remaining 775 differentially expressed genes, whose transcript levels showed a negative correlation with specific growth rate (Figure 4.5). This cluster was most strongly

**Table 4.1:** Overrepresentation of functional categories among the differentially expressed genes in Cluster 1 (see Figure 4.5).

Cluster 1	Functional category	k <sup>a</sup>	n <sup>b</sup>	p-value <sup>c</sup>
MIPS <sup>d</sup>	PROTEIN SYNTHESIS	138	511	4.98·10 <sup>-31</sup>
	Ribosomal proteins	95	277	4.29·10 <sup>-29</sup>
	Ribosome biogenesis	106	343	2.46·10 <sup>-28</sup>
	Amino acid metabolism	69	243	3.31·10 <sup>-15</sup>
	METABOLISM	221	1530	5.87·10 <sup>-11</sup>
	Metabolism of the aspartate family	26	64	1.75·10 <sup>-8</sup>
	Metabolism of methionine	18	36	3.52·10 <sup>-7</sup>
	Tetracyclic and pentacyclic triterpenes metabolism	16	36	2.84·10 <sup>-5</sup>
	Purine nucleotide/nucleoside/nucleobase metabolism	22	66	4.58·10 <sup>-5</sup>
	Nucleotide/nucleoside/nucleobase metabolism	48	230	4.81·10 <sup>-5</sup>
	Isoprenoid metabolism	16	41	2.55·10 <sup>-4</sup>
	Sulfur metabolism	7	8	3.51·10 <sup>-4</sup>
	Sulfate assimilation	7	8	3.51·10 <sup>-4</sup>
	Metabolism of the cysteine-aromatic group	23	80	4.79·10 <sup>-4</sup>
	Aminoacyl-tRNA-synthetases	15	39	7.46·10 <sup>-4</sup>
	ENERGY	58	360	1.69·10 <sup>-2</sup>
Pentose-phosphate pathway	10	24	2.20·10 <sup>-2</sup>	
GO <sup>d</sup>	Translation	117	345	6.31·10 <sup>-36</sup>
	Cellular amino acid biosynthetic process	44	101	1.10·10 <sup>-16</sup>
	Ribosome biogenesis	46	178	1.13·10 <sup>-7</sup>
	Oxidation reduction	60	270	1.24·10 <sup>-7</sup>
	Metabolic process	76	389	2.49·10 <sup>-7</sup>
	Steroid biosynthetic process	15	24	2.73·10 <sup>-7</sup>
	Sterol biosynthetic process	15	28	5.46·10 <sup>-6</sup>
	Methionine biosynthetic process	16	32	6.13·10 <sup>-6</sup>
	Maturation of SSU-rRNA	22	62	2.28·10 <sup>-5</sup>
	Sulfate assimilation	9	11	3.49·10 <sup>-5</sup>
	rRNA processing	43	195	8.44·10 <sup>-5</sup>
	Methionine metabolic process	10	15	1.36·10 <sup>-4</sup>
	Lipid biosynthetic process	18	52	7.16·10 <sup>-4</sup>
Ergosterol biosynthetic process	7	9	2.66·10 <sup>-3</sup>	
TF <sup>d</sup>	<i>FHL1</i>	75	208	1.64·10 <sup>-24</sup>
	<i>RAP1</i>	51	145	1.31·10 <sup>-15</sup>
	<i>SFP1</i>	20	50	1.41·10 <sup>-6</sup>
	<i>GCN4</i>	37	182	8.70·10 <sup>-4</sup>
	<i>HAP1</i>	27	120	2.60·10 <sup>-3</sup>
	<i>MET32</i>	9	24	4.06·10 <sup>-2</sup>

<sup>a</sup> Number of genes present in both the cluster and the functional category.

<sup>b</sup> Total number of genes in the functional category.

<sup>c</sup> A Bonferroni corrected p-value cut-off of 0.05 was used and p-values indicate the probability of finding the same number of genes in a random set.

<sup>d</sup> Functional categories originate from the Munich Information Centre for Protein Sequences (MIPS), Gene Ontology (GO) or transcription factor binding datasets (TF) described in the Methods section.

**Table 4.2:** Overrepresentation of functional categories among the differentially expressed genes in Cluster 2 (see Figure 4.5).

Cluster 2	Functional category	k <sup>a</sup>	n <sup>b</sup>	p-value <sup>c</sup>
MIPS <sup>d</sup>	UNCLASSIFIED PROTEINS	194	1140	4.13·10 <sup>-5</sup>
	Oxidative stress response	21	56	7.17·10 <sup>-4</sup>
	CELL RESCUE, DEFENSE AND VIRULENCE	101	558	9.06·10 <sup>-3</sup>
	Degradation of polyamines	5	5	1.98·10 <sup>-2</sup>
	ENERGY	70	360	2.14·10 <sup>-2</sup>
	CELLULAR COMMUNICATION	50	239	4.60·10 <sup>-2</sup>
	Cellular signalling	44	202	4.71·10 <sup>-2</sup>
GO <sup>d</sup>	Signal transduction	24	74	4.64·10 <sup>-3</sup>
	Protein amino acid phosphorylation	36	141	1.11·10 <sup>-2</sup>
	Proteasomal ubiquitin-dependent protein catabolic process	9	16	3.95·10 <sup>-2</sup>
	Oxidation reduction	56	270	3.96·10 <sup>-2</sup>
	Negative regulation of gluconeogenesis	7	10	4.55·10 <sup>-2</sup>
TF <sup>d</sup>	<i>MSN2/MSN4</i> <sup>e</sup>	55	166	4.29·10 <sup>-11</sup>
	<i>SKN7</i>	43	175	6.59·10 <sup>-4</sup>
	<i>YAP7</i>	36	152	9.78·10 <sup>-3</sup>
	<i>CAD1</i>	12	32	4.40·10 <sup>-2</sup>

a, b, c, d See Table 4.1.

e *MSN2/4* transcription factor dataset originates from [97].

enriched for genes involved in stress response, and more specifically targets of *Skn7* and *Cad1*, as well as for genes involved in signal transduction and protein turnover (Table 4.2). Accordingly, Cluster 2 was strongly enriched for targets of the stress-responsive transcription factor pair *Msn2/Msn4* (55 out of 166 genes, p-value 4.29 10<sup>-11</sup>) [97].

A positive correlation with specific growth rate of the expression levels of genes involved in anabolic processes and a negative correlation of those of stress-responsive genes, was previously shown in aerobic chemostat cultures grown at specific growth rates of 0.05 h<sup>-1</sup> and above [47, 225, 36]. Clusters 1 and 2 showed a substantial overlap with these previously identified sets of growth-rate responsive genes (Supplementary figure 4.9).

To investigate how cellular responses to near-zero growth rates differed between aerobic and anaerobic cultures, we compared transcriptome data from the present study with those obtained in a previous transcriptome analysis of anaerobic retentostats of the same *S. cerevisiae* strain [29]. Anaerobic retentostat cultivation yielded 2661 differentially expressed genes, based on the same range of specific growth rates and applying the same statistical criteria as in the present study. This number of genes is almost two-fold higher than observed in the aerobic retentostats. Synthetic medium, pH and temperature in the anaerobic retentostats were the same as those used in the present study, except for the addition of the anaerobic growth factors Tween-80 (a source of oleic acid) and ergosterol in the previous study.

Differences in the responses of anaerobic and aerobic retentostats were investigated by

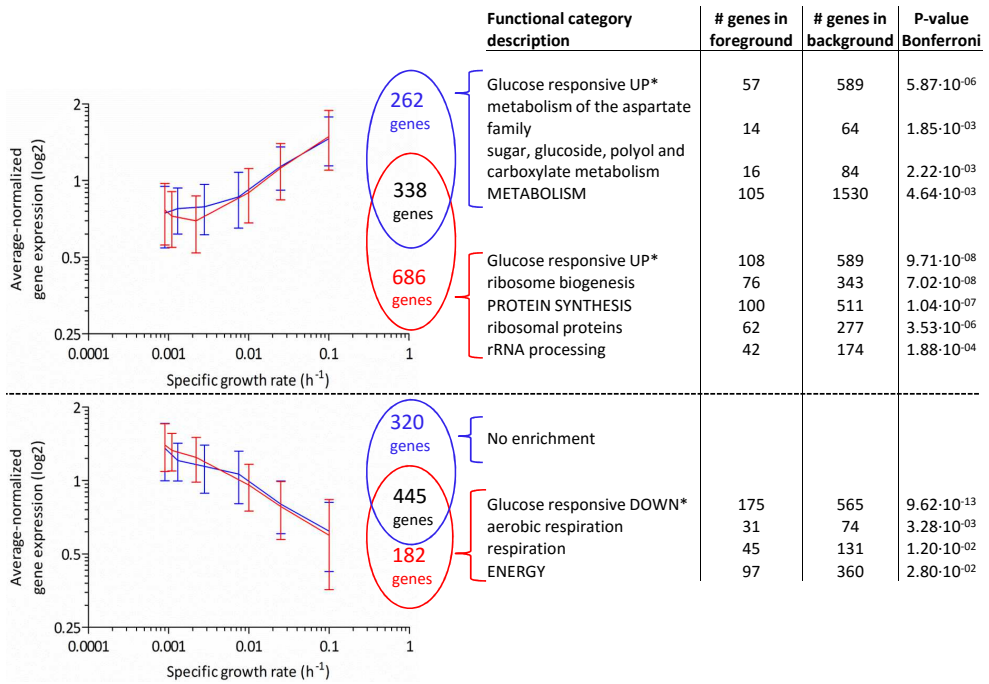


**Figure 4.6:** Comparison between aerobic (blue) and anaerobic (red) growth-rate dependent gene expression at near-zero growth rates. Transcriptome datasets of aerobic (blue) and anaerobic experiments (red) covered a specific growth rate range between  $0.1 \text{ h}^{-1}$  and values below  $0.001 \text{ h}^{-1}$ , with an equal number of data points ([29] and Figure 4.5). The p-value threshold for significant differential expression was 0.01. Overlapping and exclusive gene groups within the clusters, presented as Venn diagrams, were mined for overrepresentation of genes involved in specific functional categories with a Bonferroni-corrected p-value threshold of 0.05 (see Methods section). Genes in foreground represent number of genes present in both the cluster and the functional category, Genes in the background represent the total number of genes in the functional category. \*Glucose-responsive gene sets are derived from [157].

identifying genes that showed a specific transcriptional response to near-zero growth rates in either aerobic or anaerobic retentostats (Figure 4.6). Among 182 genes whose expression increased at extremely low growth rates in anaerobic retentostat cultures, only functional categories related to aerobic respiration, were significantly enriched (Figure 4.6). 31 Out of 74 genes involved in the cellular function Aerobic Respiration were specifically up-regulated in anaerobic retentostats, including 8 *COX* genes, which encode subunits of the mitochondrial inner-membrane cytochrome *c* oxidase. Genes involved in this functional category were not overrepresented among the responsive genes identified in aerobic retentostat cultures, indicating that up-regulation of respiration-related genes is a specific adaptation to anaerobic slow growing and/or aging cultures. Among the 686 genes whose expression showed a reduced expression at near-zero growth rates under anaerobic conditions, functional categories related to protein synthesis were significantly enriched (Figure 4.6).

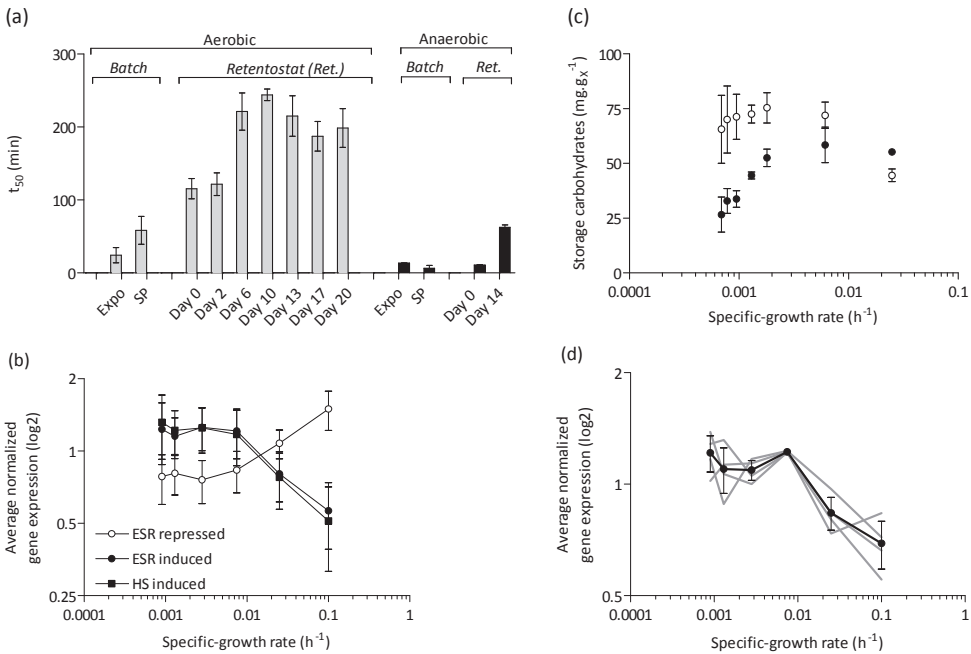


**Figure 4.7:** Heat-shock tolerance of aerobic and anaerobic retentostat and batch cultures. (a) Data on heat shock tolerance of anaerobic retentostat cultures and from batch cultures are taken from previous studies [25, 27]. Batch cultures were characterized during the exponential growth phase (expo) and after ca. 2 h in stationary phase (SP) [25].  $t_{50}$  represents incubation time at 53 °C at which 50 % of the initial viable cell population was still alive. (b) Transcript levels of genes that exhibit a significant growth-rate dependent expression in retentostat, and are also known to respond to environmental stress and heat shock according to [97, 80]. (c) Cellular contents of trehalose (open symbols) and glycogen (closed symbols) during prolonged retentostat cultivation. (d) Average-normalized expression profiles of genes involved in trehalose metabolism (see Methods section).

**Extreme heat-shock tolerance of yeast cells grown in aerobic retentostats** | Studies in aerobic chemostats, anaerobic retentostats and aerobic stationary-phase batch cultures showed that slow growth of *S. cerevisiae* increases its stress tolerance, most often measured as its ability to survive exposure to high temperatures [27, 174, 25]. The aerobic chemostat cultures, grown at a specific growth rate of 0.025 h<sup>-1</sup>, which preceded the retentostat cultures were already remarkably heat-shock tolerant, with 50% of the population surviving a 115 min exposure to a temperature of 53 °C (Figure 4.7a). After 10 d of retentostat cultivation, when the specific growth rate had decreased below 0.001 h<sup>-1</sup>, this  $t_{50}$  had increased to 4 h. This  $t_{50}$  value is approximately four-fold higher than previously described for extremely heat-shock tolerant cultures, such as aerobic stationary-phase and anaerobic retentostat cultures (Figure 4.7a). To the best of our knowledge, this heat-shock tolerance is the highest measured to date in *S. cerevisiae*.

In previous studies, a high heat-shock tolerance of *S. cerevisiae* was found to correlate with increased transcript levels of many known stress-responsive genes [25, 27]. Consistent with these earlier observations, transcript levels of Msn2/4 gene targets, as

well as genes that were previously shown to be responsive to environmental stresses (ESR induced: 110 out of 281, p-value  $1.17 \cdot 10^{-30}$ ; ESR repressed: 170 out of 563, p-value  $3.31 \cdot 10^{-48}$ ) or to heat shock in an *Msn2/4*-independent manner (125 out of 427, p-value  $3.11 \cdot 10^{-21}$ ), correlated with specific growth rate and, therefore, with heat-shock tolerance in the aerobic retentostat cultures (Figure 4.7b) [97, 80]. Heat-shock proteins function as chaperones that prevent aggregation of thermally damaged proteins, unfold them, or mark them for degradation [292]. Of 76 genes known to encode heat-shock proteins, seven showed increased mRNA levels at near-zero growth rates (*SSA3*, *HSP26*, *HSP42*, *XDJ1*, *CWC23*, *EUG1* and *HSP60*) [292]. Disaggregation and (re)folding activities of heat-shock proteins are ATP dependent and maintaining intracellular ATP levels has been shown to be crucial for heat-shock survival of stationary-phase batch cultures [25, 211]. High contents of the intracellular carbohydrate storage materials trehalose and glycogen (>10% of biomass dry-weight, Figure 4.7c) may have contributed to the extreme heat-shock tolerance of yeast cells grown in aerobic retentostat cultures by supplying the ATP that is required to combat heat stress (Figure 4.7c). In addition to intracellular trehalose concentrations, expression of the trehalose-metabolism related genes *TPS1*, *TPS2*, *ATH1* and *NTH1* increased substantially when retentostat cultures approached near-zero growth rates (Figure 4.7c,d) [211, 62]. The strong increase of intracellular trehalose concentrations in the aerobic retentostat cultures represents a marked difference with published data on anaerobic retentostats, in which intracellular trehalose levels were low and glycogen was the predominant storage carbohydrate [29].

### **Aerobic retentostat cultures retain a high glycolytic capacity at near-zero growth rates**

Glycolysis, together with glucose transport, pyruvate decarboxylase and alcohol dehydrogenase, represents the pathway for alcoholic fermentation in *S. cerevisiae*. Respiratory cultures of this yeast maintain a high capacity for fermentative metabolism (fermentative capacity), which allows *S. cerevisiae* to rapidly increase its glycolytic flux in response to, for example, oxygen depletion and/or exposure to high sugar concentrations [274, 68, 278]. In aerobic glucose-limited chemostat cultures of the *S. cerevisiae* CEN.PK113-7D strain, fermentative capacity is essentially growth-rate independent at specific growth rates between  $0.05 \text{ h}^{-1}$  and  $0.3 \text{ h}^{-1}$ , [279]. The fermentative capacity of  $7.5 \text{ mmol ethanol g}_x^{-1} \text{ h}^{-1}$  measured in the aerobic chemostats ( $D = 0.025 \text{ h}^{-1}$ , Figure 4.8a), matched well with the fermentative capacity found previously at these higher specific growth rates [279]. After 18 d of aerobic retentostat cultivation a significantly lower ( $p < 0.05$ ) fermentative capacity of  $4.5 \text{ mmol ethanol g}_x^{-1} \text{ h}^{-1}$  was measured (Figure 4.8a). The corresponding glucose-consumption rate was 45-fold higher than the specific rate of glucose consumption measured in the retentostat at this time point.

The decrease of the fermentative capacity in the aerobic retentostats coincided with a decrease of the transcript levels of a subset of glycolytic genes, some of which encoded major isoforms of glycolytic enzymes [256]. Expression levels of *HXX2*, encoding

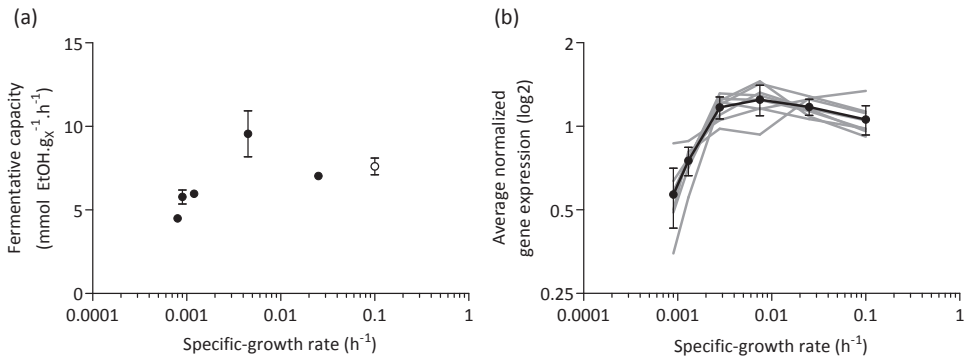


**Figure 4.8:** Fermentative capacity and expression levels of glycolytic genes in *S. cerevisiae* at near-zero growth rates. (a) Fermentative capacity, measured off-line as the specific rate of ethanol formation upon exposure of anaerobic cell suspensions to excess glucose. Fermentative capacity assays were performed on independent duplicate retentostat cultures, sampled at different time points. The open symbol corresponds to data from [279]. (b) Log<sub>2</sub> average-normalized gene expression of *HXK2*, *FBA1*, *PGK1*, *GPM1*, *ENO1*, *ENO2*, *PYK1*, and *PDC1* during retentostat cultivation, plotted as a function of specific growth rate (see Methods section).

hexokinase 2, first step in glycolysis, *FBA1* encoding the single fructose-bisphosphate aldolase, *PGK1* encoding the single phosphoglycerate kinase, *GPM1* encoding the major phosphoglucomutase/yeast phosphoglycerate isoenzymemutase, *ENO1*, and *ENO2* paralogs encoding the two yeast enolases, *PYK1* also known as *CDC19*, encoding the major pyruvate kinase, last step in glycolysis, and *PDC1* encoding pyruvate decarboxylase 1 responsible for the 1<sup>st</sup> step in the fermentative pathway leading to ethanol, were stable during the initial phase of the retentostat cultures, but significantly and substantially decreased at growth rates below 0.002 h<sup>-1</sup> (Figure 4.8b). Pair-wise comparison of transcriptome data for day 0 and day 16 of the retentostats (corresponding to specific growth rates of 0.025 h<sup>-1</sup> and 0.0009 h<sup>-1</sup>, respectively) showed at least a two-fold difference in expression levels of *HXK2*, *PGK1*, *GPM1*, *ENO2* and *PDC1*. Overrepresentation of binding sites for Rap1/Gcr1 in their promoter regions suggests that these transcription factors may be involved in their transcriptional regulation at near-zero growth rates. This hypothesis is further supported by the observation that 51 of the 145 gene targets of the transcription factor Rap1 were part of Cluster 1 (Figure 4.5, Table 4.1). While we cannot exclude that decreased glucose transport was also involved in the reduction of fermentative capacity, no difference was observed in *HXT* gene expression at near-zero growth rates.

## Discussion

**Estimation of maintenance-energy requirements from aerobic retentostats** | Initially developed by microbial ecologists to explore the ‘twilight zone’ between exponential growth and starvation [284, 286, 8, 241, 242], the retentostat has recently seen a revival in studies on industrial microorganisms [85]. A key advantage of retentostat cultivation

for application-inspired research is that it enables an accurate, quantitative estimation of microbial maintenance-energy requirements [85]. The conventional method for determining  $m_S$  does not measure, but estimates the specific rate of energy-substrate consumption in non-growing cultures, based on extrapolation of measurements on chemostat cultures that are actively growing (often at specific growth rates of  $0.05 \text{ h}^{-1}$  and above). Since, at these specific growth rates, substrate consumption for maintenance is relatively small as compared to the overall consumption rate of the energy substrate,  $m_S$  values calculated via this procedure are sensitive to small measurement errors [295, 85]. Moreover, chemostat-based estimation of  $m_S$  is based on the assumption that this parameter is growth-rate independent. Studies on several prokaryotes have shown that this assumption is not always valid and that, at extremely slow growth rates, several bacteria downregulate ATP turnover and thereby reduce substrate consumption for maintenance [8, 53].

Even at extremely low specific growth rates, the energetics of aerobic, glucose-limited retentostat cultures of *S. cerevisiae* could be adequately described with a growth-rate independent  $m_S$ . The same conclusion was drawn earlier for anaerobic, glucose-limited retentostat cultures of this yeast [28]. The value of  $m_S$  estimated from the aerobic retentostat cultures was  $0.039 \text{ mmol}_{\text{glucose}} \text{ gX}^{-1} \text{ h}^{-1}$ . There are surprisingly few, invariably chemostat-based, estimates of the  $m_S$  of aerobically grown *S. cerevisiae*. Four decades ago, Rogers and Stewart [230] calculated an  $m_S$  of  $0.07 \text{ mmol}_{\text{glucose}} \text{ gX}^{-1} \text{ h}^{-1}$  based on aerobic chemostat cultures of a diploid *S. cerevisiae* strain, grown at pH 5.5 on a complex medium. This value is 75% higher than the  $m_S$  found in the present study. Recently, based on aerobic chemostat cultures of the same haploid *S. cerevisiae* strain that is used in the present study, grown at pH 5.5, we estimated an  $m_S$  that was even 2.5-fold higher than calculated from the aerobic retentostats [295]. It should, however, be noted that the latter study used a growth medium that contained high concentrations of copper, which may have negatively affected cellular energetics.

Based on an assumed P/O ratio of 1.0 [291, 89, 244, 287], the maintenance requirement for ATP ( $m_{\text{ATP}}$ ) estimated from the aerobic retentostat cultures was  $0.63 \text{ mmol}_{\text{ATP}} \text{ gX}^{-1} \text{ h}^{-1}$ , a value 35% lower than previously estimated based on anaerobic retentostat cultures of the same *S. cerevisiae* strain [28]. One possible explanation for this difference is that anaerobic growth indeed results in a higher  $m_S$ , for instance as a result of increasing proton leakage across membranes due to the presence of the fermentation products ethanol and acetic acid. Additionally, the anaerobic growth factor oleic acid, which is added to anaerobic chemostat media as the oleate ester Tween-80, has been shown to negatively affect growth energetics [289]. Alternatively, the assumed P/O value of 1.0 might be wrong. However, if this were the sole reason for the observed difference, the actual P/O ratio would have to be close to 1.7, which falls outside the range of estimates for this parameter from several quantitative physiological studies on *S. cerevisiae* [291, 89,



244, 287]. The lower  $m_{\text{ATP}}$  under aerobic conditions, makes it unlikely that the presence of oxygen or generation of ROS in respiration increases maintenance-energy requirements.

Maintenance-energy requirements are well known to depend on growth conditions, for example on the presence of weak organic acids [215, 290, 1], and may additionally be strain dependent. The present study demonstrates that retentostat cultivation offers a robust way to estimate  $m_s$ . The large impact of this parameter on the performance of large-scale industrial fed-batch processes provides a strong impetus for using this, somewhat technically demanding, approach for determining and comparing maintenance-energy requirements of different production hosts under carefully controlled, industrially relevant experimental conditions.

**Extreme heat-shock tolerance of aerobic retentostat cultures** | In industrial processes, yeast cells face a variety of stresses, including high concentrations of  $\text{CO}_2$  and other products, inhibitors in low-grade media, fluctuations in nutrient availability (e.g. during biomass recycling and ‘repitching’ in beer fermentation) and high as well as low temperatures [240, 101]. Here we show that aerobic retentostat cultures of *S. cerevisiae* grown at near-zero growth rates acquire an extreme resilience to heat shock. We recently reported that stationary-phase, glucose-grown aerobic batch cultures of *S. cerevisiae* are much more heat-shock tolerant than the corresponding anaerobic cultures [25]. This difference was tentatively attributed to the much faster transition from exponential growth to nutrient depletion in anaerobic batch cultures, which do not exhibit the second, slow growth phase on ethanol that is characteristic for aerobic glucose-grown batch cultures of *S. cerevisiae*. The hypothesis that this fast transition prevented a full induction of heat-shock tolerance was consistent with the earlier observation that anaerobic retentostat cultures, which undergo a slow transition to near-zero growth rates, exhibit a much higher heat-shock tolerance than anaerobic stationary-phase batch cultures [25]. The present study shows that, despite a very similar ‘conditioning’, the heat-shock tolerance of aerobic retentostat cultures is much more pronounced than in anaerobic retentostats (four to five-fold higher  $t_{50}$ , Figure 4.7a). Indeed, to our knowledge, the heat-shock tolerance of the aerobic retentostat cultures is the highest reported to date for *S. cerevisiae*. These observations indicated that a smooth transition from exponential growth to (near-)zero growth in aerobic cultures provides an optimal conditioning for heat-shock tolerance in this yeast. Further research is required to assess whether this conclusion can be extended to include conditioning for other industrially relevant stresses, such as freezing/drying, osmotic stress and oxidative stress.

Intracellular concentrations of trehalose and regulation of genes involved in its metabolism showed a remarkable correlation with the different levels of heat-shock tolerance in aerobic retentostats. Trehalose can act as an energy reserve, and has also been proposed to be directly involved in heat shock resistance [73, 140, 245].

However, recent evidence suggests that secondary, so called 'moonlighting' functions of the trehalose-6-phosphate synthase Tps1, rather than trehalose itself, contribute to cell integrity during heat shock [211]. Additionally, different expression levels of other stress-induced proteins and different membrane composition, resulting from the inability of anaerobic cultures to synthesize unsaturated fatty acid and sterols, may contribute to the different heat-shock tolerance of aerobic and anaerobic *S. cerevisiae* cultures [289, 46, 304].

***S. cerevisiae* down-regulates glycolytic gene expression but maintains a high fermentative capacity at near-zero growth** | Protein synthesis is the single most ATP-intensive process in living cells [259], and especially proteins with relatively high expression levels and short turnover times are expected to represent a significant metabolic burden to cells grown under severely calorie-restricted retentostat cultivation regimes. In actively growing *S. cerevisiae* cultures, glycolytic enzymes make up a significant fraction of the total cellular protein [71]. The half-life of most glycolytic proteins in *S. cerevisiae* grown in glucose-excess conditions range between 5 and 20 hours, excluding Tdh1, Tdh2, Gpm2, and Eno1, for which half-lives of over 100 hours have been determined [56]. These reported half-lives are much lower than the amount of time that the cells reside in retentostat; protein turnover of glycolytic proteins could therefore significantly contribute to the energy requirements of *S. cerevisiae* at near-zero growth. Under many conditions, this yeast exhibits a large overcapacity of the glycolytic pathway. Indeed, a substantial loss of fermentative capacity has previously been observed during prolonged cultivation of *S. cerevisiae* in aerobic, glucose-limited chemostat cultures (50% after 100 generations) [132]. This loss was attributed to mutations that reduced the metabolic burden of synthesizing large amounts of glycolytic proteins. Although retentostat-grown cells retained a high glycolytic capacity, this decreased by ca. 40% at extremely low specific growth rates. It is, however, unlikely that evolutionary adaptation caused this reduction in glycolytic capacity, since the average number of generations in the retentostat experiments was approximately three as a consequence of the biomass retention. Instead, the reduced mRNA levels of several glycolytic genes suggest a transcriptional downregulation of this key pathway at extremely low growth rates. Furthermore, glycolytic genes *PGK1* and *PYK1* that are considered to be constitutively expressed at high levels [207], displayed ca. two-fold reduced transcript levels at near-zero growth (Figure 4.8), and shows that glycolytic promoters for the expression of (heterologous) proteins should be carefully selected.

**Impact of oxygen availability on transcriptional reprogramming at near-zero growth rates** | The specific growth rate profiles and experimental conditions employed in the aerobic retentostat cultures very strongly resembled those applied in a previous study on anaerobic retentostats of the same *S. cerevisiae* strain. Gene sets that

showed a transcriptional response in these retentostat experiments showed a strong overrepresentation of growth-rate responsive genes identified by Fazio *et al.* [90]. These authors used chemostats, grown at specific growth rates of  $0.03 \text{ h}^{-1}$  and higher, to explore transcriptional responses under different aerobic and anaerobic nutrient-limitation. Of the set of 268 growth-rate-responsive genes identified in their study, 115 genes were also found to show growth-rate dependent expression at the very low specific growth rates studied in the aerobic and anaerobic retentostats. Despite this clear overlap in transcriptional responses, the number of genes that showed a transcriptional response to the shift to near-zero growth rates was two-fold higher in the anaerobic retentostats than in the aerobic retentostats. As discussed above, ATP yields from respiratory and fermentative glucose dissimilation differ by a factor of approximately 8. As a consequence, at any specific growth rate, specific rates of glucose consumption ( $q_S$ ) in anaerobic glucose-limited cultures are higher than in the corresponding aerobic cultures. For example, at a specific growth rate of  $0.025 \text{ h}^{-1}$ , the  $q_S$  in anaerobic glucose-limited chemostat cultures ( $2.3 \text{ mmol}_{\text{glucose}} \text{ g}_X^{-1} \text{ h}^{-1}$  (Supplementary figure 4.10, [28]), was ca. 8-fold higher than in the corresponding aerobic chemostat cultures ( $0.3 \text{ mmol}_{\text{glucose}} \text{ g}_X^{-1} \text{ h}^{-1}$  (Supplementary figure 4.10). Simple Monod kinetics [194] predict that this difference should also be reflected in the concentration of the growth-limiting nutrient. Indeed, residual glucose concentrations in these anaerobic and aerobic cultures were 0.3 mM and 0.07 mM, respectively (Supplementary figure 4.10 and [27]). The consequence of these differences is that aerobic and anaerobic retentostat cultures operate in a different range of residual glucose concentrations. Concomitantly, a set of previously identified glucose-responsive transcripts were specifically overrepresented under anaerobiosis among genes which were transcriptionally up and down regulated with specific growth rate in retentostat cultures (Figure 4.6) [157]. This comparison identifies differences in glucose concentration as a major cause of the different transcriptome profiles of aerobic and anaerobic retentostat cultures.

## Conclusion

Glucose-feeding regimes of retentostat cultures were optimized by model simulations to enable a first characterization of glucose-limited, aerobic cultures of *S. cerevisiae* during a smooth transition to extremely low specific growth rates. Quantitative analysis of these retentostats enabled the most accurate estimation to date of the growth-rate-independent maintenance-energy requirement of this yeast. Aerobic, glucose-limited retentostat cultures of *S. cerevisiae* showed a high viability, an extremely high heat-shock tolerance and retained an overcapacity of the fermentative pathway, thus illustrating the potential of this yeast to be developed for robust product formation in the absence of growth. This study shows that retentostat cultures, although technically demanding, offer

unique possibilities for quantitative analysis of industrially relevant aspects of microbial physiology.

## Acknowledgements

We would like to thank Corinna Rebnegger, Rinke van Tatenhove-Pel and Pilar de la Torre Cortes for assistance in the experiments. This work was supported by the B-Basic research programme, which was financed by the Netherlands Organisation for Scientific Research (NWO), and by the European Union's Framework VII programme (RoBoYeast project).

## Methods

**Yeast strain and shake-flask cultivation** | The prototrophic strain *Saccharomyces cerevisiae* CEN.PK113-7D (*MATa*, *MAL2-8c*, *SUC2*; [84, 197]) was used in this study. Stock cultures were grown in 500 mL shake flasks containing 100 mL YPD medium (10 g L<sup>-1</sup> Bacto yeast extract, 20 g L<sup>-1</sup> Bacto peptone and 20 g L<sup>-1</sup> D-glucose). After addition of glycerol (20% v/v) to early stationary-phase cultures, 2 mL aliquots were stored at -80°C. Shake-flask precultures for chemostat experiments were grown in 500 mL shake flasks containing 100 mL of synthetic medium, set to pH 6.0 with 2 M KOH prior to autoclaving and supplemented with 20 g L<sup>-1</sup> D-glucose [290]. These shake-flask cultures were inoculated with 2 mL of frozen stock culture and incubated in an orbital shaker at 200 rpm and at 30°C.

**Chemostat cultivation** | Chemostat cultivation was performed in 2-liter bioreactors (Applikon, Delft, the Netherlands) equipped with a level sensor to maintain a constant working volume of 1.4 L. The culture temperature was controlled at 30°C and the dilution rate was set at 0.025 h<sup>-1</sup> by controlling the medium inflow rate. Cultures were grown on synthetic medium, prepared as described previously [290] but with the following modifications: the glucose concentration was increased to 20 g L<sup>-1</sup> glucose ( $C_{S,MC}$ ), the amount of trace-element and vitamin solutions were increased to 1.5 mL L<sup>-1</sup>, and 2 mL L<sup>-1</sup> respectively [290], and 0.25 g L<sup>-1</sup> Pluronic 6100 PE antifoaming agent (BASE, Ludwigshafen, Germany) was used. Fresh medium was supplied to the bioreactor from a 3 L stirred mixing vessel (Applikon, Delft, The Netherlands) whose working volume ( $V_S$ ) of 1.2 L was controlled by a level sensor and which was stirred continuously at 500 rpm. The mixing vessel was equipped with a sampling port. Medium was added to the mixing reactor by automatic addition from a medium reservoir, with a flow rate ( $\phi_V$ ) of 35 mL h<sup>-1</sup> corresponding to the dilution rate in the bioreactor. Cultures were sparged with air (0.5 vvm) and stirred at 800 rpm. Culture pH was kept constant at 5.0 by automatic addition of 10% NH<sub>4</sub>OH. Chemostat cultures were assumed to be in steady state when, after at least 6 volume changes, culture dry weight and the specific carbon dioxide production rates changed by less than 3% over 2 consecutive volume changes. Steady-state carbon recoveries of chemostat cultures included in this study were above 98%. Chemostat experiments performed at a dilution rate of 0.10 h<sup>-1</sup> were performed as described above, with the following modifications: cultures were grown on synthetic medium [290] without

modifications, with  $7.5 \text{ g L}^{-1}$  glucose,  $1 \text{ mL L}^{-1}$  trace elements solution, and  $1 \text{ mL L}^{-1}$  vitamin stock solution.

**Retentostat** | After reaching a steady-state in chemostat cultures, the retentostat phase was started by switching the reactor effluent to an outflow port equipped with an autoclavable Applisense filter assembly (Applikon), consisting of a hydrophobic polypropylene filter with a pore size of  $0.22 \text{ }\mu\text{m}$  and a stainless steel hollow filter support. Prior to autoclaving, the filter was wetted by overnight incubation in 96% ethanol, and subsequently rinsed with a phosphate buffer saline solution (containing per 1 L demi-water: 8 g NaCl, 0.2 g KCl, 1.44 g  $\text{Na}_2\text{HPO}_4$ , 0.24 g  $\text{KH}_2\text{PO}_4$ , and HCl to adjust the final pH to 7.4). To control biomass accumulation, the medium reservoir connected to the mixing vessel (see above) was exchanged for a reservoir containing standard synthetic medium [49] supplemented with  $7.5 \text{ g L}^{-1}$  glucose ( $C_{S,MR}$ ) and  $0.25 \text{ g L}^{-1}$  pluronic 6100 PE antifoam. Consequently, the concentration of growth-limiting substrate glucose entering the bioreactor ( $C_{S,in}$  in  $\text{g L}^{-1}$ ) decreased over time ( $t$  in [h]) according to Equation 4.2.

$$C_{S,in} = (C_{S,MC} - C_{S,MR}) \cdot e^{-\frac{\Phi_V t}{V_S}} + C_{S,MR} \quad (4.2)$$

In this equation,  $C_{S,MC}$  and  $C_{S,MR}$  correspond to the glucose concentrations in the medium entering the mixing vessel during the chemostat and the retentostat phase respectively. During retentostat cultivation, culture pH was controlled by automatic addition of 2M KOH. Sampling frequency and sample volume were minimized to limit the impact of sampling on biomass accumulation inside the reactor. Culture purity was routinely checked by microscopy and by plating on synthetic medium agar containing  $20 \text{ g L}^{-1}$  glucose and 20 mM LiCl [66]. Full biomass retention was confirmed by plating filtered effluent on YPD containing 2 % (w/v) agar.

**Predicting retentostat growth kinetics** | Operational conditions to enable a smooth transition of the retentostat cultures to near-zero growth rates, were defined with a mathematical model that simulates growth kinetics of yeast during aerobic retentostat cultivation (See Additional file 4.1). Essentially, the mass balance equation for biomass (Equation 4.3) was solved using MATLAB® ode45 solver, by incorporating the substrate mass balance (Equation 4.4), with the Pirt relation [217] (Figure 4.1).

$$\frac{dC_X}{dt} = \mu C_X \quad (4.3)$$

$$\frac{dC_S}{dt} = \frac{\Phi_V}{V} (C_{S,in} - C_S) - q_S C_X \quad (4.4)$$

In these equations,  $C_X$  [ $\text{g L}^{-1}$ ] is the biomass concentration in the retentostat,  $\mu$  [ $\text{h}^{-1}$ ] is the specific growth rate,  $C_S$  [ $\text{g L}^{-1}$ ] is the residual substrate concentration,  $C_{S,in}$  [ $\text{g L}^{-1}$ ] is the substrate concentration in the feed,  $\Phi_V/V$  [ $\text{h}^{-1}$ ] is the dilution rate, and  $q_S$  [ $\text{g g}_X^{-1} \text{ h}^{-1}$ ] is the biomass-specific glucose consumption rate. The specific substrate consumption rate can be described by the Pirt relation (Figure 4.1), in which  $Y_{X/S}^{\max}$  [ $\text{g g}^{-1}$ ] is the maximum biomass yield on glucose, and  $m_S$

[g g<sub>X</sub><sup>-1</sup> h<sup>-1</sup>] is the maintenance coefficient. Because retentostats were glucose limited and C<sub>S,in</sub> >> C<sub>S</sub>, the glucose concentration in the retentostat was assumed to be in a pseudo-steady state such that  $\frac{dC_S}{dt} \approx 0$ . To run simulations, the model required inputs for variables V (bioreactor volume) [L],  $\Phi_V$  (flow rate) [L h<sup>-1</sup>], C<sub>S,MC</sub> [g L<sup>-1</sup>], C<sub>S,MR</sub> [g L<sup>-1</sup>], and V<sub>S</sub> [L], and generated time-dependent profiles for biomass accumulation, glucose concentration in the feed, specific glucose consumption rates, and specific growth rates for a range of m<sub>S</sub> values. The final operational conditions chosen for the retentostat experiments are indicated in Figure 4.2.

**Regression analysis of biomass accumulation in retentostat** | The maintenance-energy requirements and biomass-specific death rate of *S. cerevisiae* in aerobic retentostat were estimated from a least-squares regression analysis of data points for the biomass concentration (dry-weight) and the viable biomass concentration over time, using a MATLAB model (See Additional file 4.2). From these parameters, the specific growth rate and substrate consumption rates were derived. The curve shape was determined by the solution of the following ordinary differential equations with the smallest sum of square errors:

$$\frac{dC_{X_V}}{dt} = \mu C_{X_V} - k_d C_{X_V} \quad (4.5)$$

$$\frac{dC_{X_d}}{dt} = k_d C_{X_V} \quad (4.6)$$

$$\frac{dC_S}{dt} = \frac{\Phi_V}{V} (C_{S,in} - C_S) - q_S C_X \quad (4.7)$$

In these equations, C<sub>X\_V</sub> is the viable biomass concentration [g L<sup>-1</sup>], k<sub>d</sub> is the death rate [h<sup>-1</sup>]. The equation in Figure 4.1 was used to define the specific substrate consumption rate (q<sub>S</sub>). The model required input for the biomass concentrations measured at different time points, and the following variables: V [L],  $\Phi_V$  [L h<sup>-1</sup>], C<sub>S,MC</sub> [g L<sup>-1</sup>], C<sub>S,MR</sub> [g L<sup>-1</sup>], V<sub>S</sub> [L] and Y<sub>X/S</sub><sup>max</sup>. A value for m<sub>S</sub> was approximated using parameter estimation. The time-dependent change of q<sub>S</sub> and  $\mu$  during the course of the retentostat followed from the regression analysis (See Additional file 4.2). To respect small differences in operational variables per experiment, regression analyses were performed separately on each independent retentostat experiment.

**Determination of substrate, metabolites and biomass concentration** | Prior to culture dry weight assays, retentostat samples were diluted in demineralized water. Culture dry weight was measured by filtering exactly 10 mL of an appropriate dilution of culture broth over pre-dried and pre-weighed membrane filters (pore size 0.45  $\mu$ m, Gelman Science), which were then washed with demineralized water, dried in a microwave oven (20 min, 350W) and reweighed. Supernatants were obtained by centrifugation of culture samples (3 min at 16,000 x g) and analysed by high-performance liquid chromatography (HPLC) analysis on a Agilent 1100 HPLC (Agilent Technologies, Santa Clara, CA, USA), equipped with an Aminex HPX 87H column (BioRad, Veenendaal, The Netherlands), operated with 5 mM H<sub>2</sub>SO<sub>4</sub> as the mobile phase at a flow rate of

0.6 mL min<sup>-1</sup> and at 60°C. Detection was by means of a dual-wavelength absorbance detector (Agilent G1314A) and a refractive-index detector (Agilent G1362A). Residual glucose concentrations in chemostat and retentostat cultures were analysed by HPLC after rapid quenching of culture samples with cold steel beads [183].

**Gas analysis |** The exhaust gas from chemostat cultures was cooled with a condenser (2°C) and dried with a PermaPure Dryer (model MD 110-8P-4; Inacom Instruments, Veenendaal, the Netherlands) prior to online analysis of carbon dioxide and oxygen with a Rosemount NGA 2000 Analyser (Baar, Switzerland).

**Viability assays|** Small aliquots of culture broth (< 1 mL) were sampled in a 10 mM Na-Hepes buffer (pH 7.2) with 2% glucose. Cell numbers were determined with a Coulter counter using a 50 µm orifice (Multisizer II, Beckman, Fullerton, CA). Colony-forming units (CFU) in culture samples were quantified by triplicate plating of ten-fold dilution series in 0.1% peptone on 2% YPD agar plates. At least 150 colonies were counted after 2 d of incubation at 30 °C to calculate CFU. Viability was then calculated by comparing CFU counts with total cell counts. Additionally culture viability was assayed by propidium iodide (PI) staining with the FungaLight yeast viability kit (Invitrogen, Carlsbad, CA) by counting 10,000 cells on a Cell Lab Quanta SC MPL flow cytometer (Beckman Coulter, Woerden, Netherlands) as described previously [27]. PI intercalates with DNA in cells with a compromised cell membrane, causing a red fluorescence.

**Heat shock resistance assays |** Samples from retentostat cultures were added to Isoton II diluent (Beckman Coulter, Woerden, Netherlands), pre-heated at 53 °C, to a final concentration of 10<sup>7</sup> cells mL<sup>-1</sup>, and incubated at 53 °C for at least 200 min. Loss of viability was monitored by sampling at 20 min intervals. Samples were immediately cooled on ice and subsequently stained with PI and analysed by flow cytometry as described above. Heat-shock resistance was represented by t<sub>50</sub>, the incubation time at 53 °C that lead to a 50% decrease in viability. To calculate t<sub>50</sub>, survival curves were fitted with a sigmoidal dose-response curve in Graphpad® Prism, version 4.03. Glycogen and trehalose assays 1 mL broth was sampled from the retentostat or chemostat and immediately added to 5 mL of cold methanol (-40 °C), mixed and centrifuged (4,400 x g, -19 °C, 5 min). The supernatant was decanted and pellets were resuspended in 5 mL cold methanol, pelleted again and stored at -80 °C. Pellets were then resuspended and diluted in 0.25 M Na<sub>2</sub>CO<sub>3</sub>, and further processed as previously described [206]. Trehalose was directly measured by HPLC. Glucose released from glycogen was measured by HPLC after overnight incubation of samples at 57 °C with α-amylglucosidase (from *Aspergillus niger*, Sigma-Aldrich, Zwijndrecht, Netherlands).

**Fermentative capacity assays |** Samples containing exactly 100 mg dry weight of biomass from retentostat cultures were harvested by centrifugation at 5,000 x g for 5 min, washed once, and resuspended in 10 mL five-fold concentrated synthetic medium (pH 6, [290]). Subsequently, these cell suspensions were introduced into a 100 mL reaction vessel maintained at 30°C, which was kept anaerobic with a constant flow (10 mL min<sup>-1</sup>) of water-saturated CO<sub>2</sub>. After addition of 40 mL demineralized water and 10 min of pre-incubation, 10 mL glucose solution (100 g L<sup>-1</sup>) was added,

and 1 mL samples were taken at 5 min intervals. After centrifugation, ethanol concentrations in supernatants were determined by HPLC. Fermentative capacity, calculated from the increase in ethanol concentration during the first 30 min of the experiments, was expressed as  $\text{mmol}_{\text{ethanol}} \text{g}_X^{-1} \text{h}^{-1}$ . During the assay period, the increase in biomass concentration was negligible, and the increase in ethanol concentration was linear with time and proportional to the amount of biomass added.

**Transcriptome analysis** | Microarray analysis was performed with samples from independent triplicate steady-state chemostat cultures and duplicate retentostat cultures of *S. cerevisiae* strain CEN.PK113-7D sampled at 5 time points, comprising a total dataset of 13 microarrays. Sampling for transcriptome analysis was carried out by using liquid nitrogen for rapid quenching of mRNA turnover [214]. Prior to RNA extraction, samples were stored in a mixture of phenol/chloroform and TAE buffer at  $-80^\circ\text{C}$ . Total RNA extraction, isolation of mRNA, cDNA synthesis, cRNA synthesis, labelling and array hybridization was performed as described previously [189], with the following modifications. The quality of total RNA, cDNA, aRNA and fragmented aRNA was checked using an Agilent Bioanalyzer 2100 (Agilent Technologies, Santa Clara, CA). Hybridization of labelled fragmented aRNA to the microarrays and staining, washing and scanning of the microarrays was performed according to Affymetrix instructions (EukGE\_WS2v5). The 6383 yeast open reading frames were extracted from the 9335 transcript features on the YG-S98 microarrays. To allow comparison, all expression data were normalized to a target value of 240 using the average signal from all gene features. The transcriptome data have been made available at the GEO data repository under accession number GSE77842. To eliminate variation in genes that are essentially not expressed, genes with expression values below 12 were set to 12 and the genes for which the average expression was below 20 for all 13 arrays were discarded. The average deviation of the mean transcript data of replicate retentostats was approximately 10%, similar to the reproducibility usually observed in replicate steady state chemostat cultures [67]. The expression of housekeeping genes *ACT1*, *HHT2*, *SHR3*, *PDA1*, *TPI* and *TFC1* [268] remained stable for both strains at all tested growth rates (average coefficient of variation  $11\% \pm 4\%$  see Supplementary figure 4.11). To perform a differential expression analysis based on gene expression profiles across the different growth rates, EDGE version 1.1.291 [179] was used with growth rate as covariate. Genes with expression profiles with a p-value below 0.01 were considered to significantly correlate with growth rate, and were clustered with k-means clustering using Consensus Clustering (GenePattern 2.0, Broad Institute, [226]). For display of specific growth rate dependent expression profiles, expression values were normalized per gene by dividing single expression values by the average expression value at all different growth rates. Averages  $\pm$  standard deviation of these average-normalized values are shown in Figures 4.5, 4.6, 4.7 and 4.8. Gene expression clusters were analysed for overrepresentation of functional annotation categories from the Munich Information Centre for Protein Sequences (MIPS) database (<http://mips.gsf.de/genre/proj/yeast>), the Gene Ontology (GO) database (<http://geneontology.org/>) and transcription factor binding (TF) according to [115], based on the hypergeometric distribution analysis tool described by Knijnenburg et al [150]. Additional functional categories that were searched for enrichment originate from [97, 80, 292, 100].



## Supplementary material Chapter 4

### Supplementary figures

Cluster 1 600 genes			Cluster 2 775 genes	
452	110	Regenberg <i>et al</i> , 2006	111	122
153	84	Brauer <i>et al</i> , 2008	122	216
347	166	Castrillo <i>et al</i> , 2007	131	273
Repressed			Induced	

**Figure 4.9:** Number of genes identified in cluster 1 and 2 that overlap with genes identified in previous growth studies of which the expression correlated with specific growth rate. “Repressed” indicates a positive correlation, “induced” indicates a negative correlation, referring to the mode of regulation at low specific growth rates. Numbers outside the circle indicate the number of genes identified by the corresponding study, but not identified in the present study.

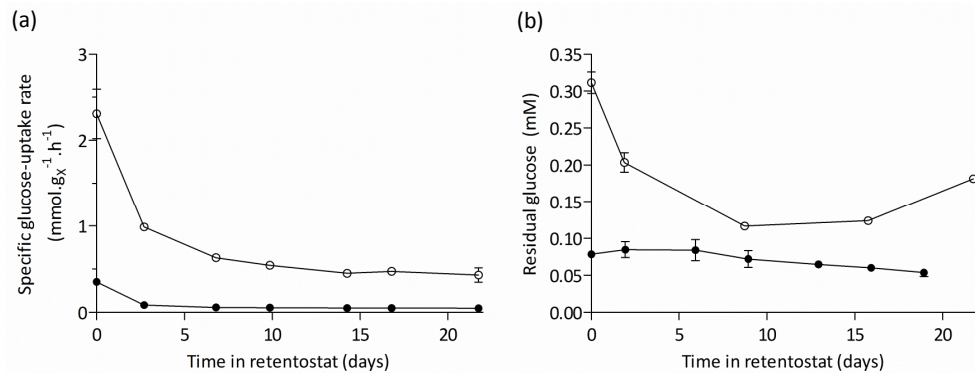


**Figure 4.10:** Specific glucose-consumption rate (a) and residual glucose concentrations (b) of aerobic (closed symbols) and anaerobic cultures (open symbols) during prolonged retentostat. The data is represented as the average  $\pm$  standard deviation of replicate independent retentostat samples. The residual glucose concentration data point at  $0.1 \text{ h}^{-1}$  originates from aerobic glucose-limited chemostat cultures described here [155], operated and sampled under the same conditions as reported in the methods section of this work.

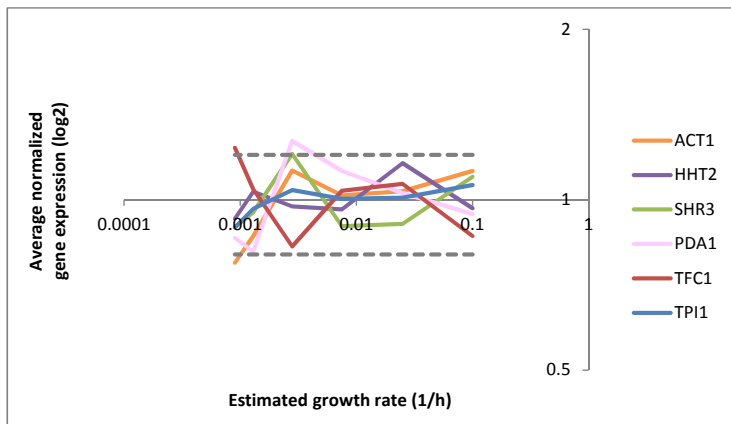
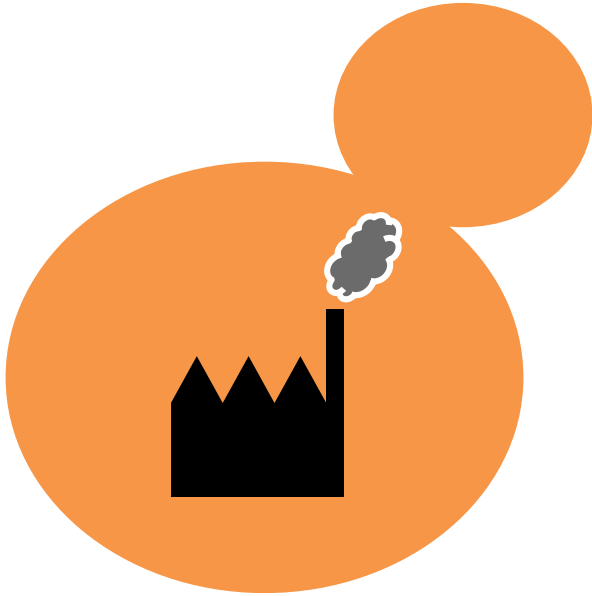


**Figure 4.11:** Averaged normalized gene expression of housekeeping genes for *S. cerevisiae* strain CEN.PK113-7D [268]. Dotted bars indicate 20% variation around normalized expression.

### Additional files

**Additional file 4.1 (a, b, c).** Three files encompassing the MATLAB model to predict biomass accumulation, specific growth rate, and specific glucose consumption rates over the course of retentostat (see Methods section). Additional file 4.1a describes how to run or adapt the prediction model. The model itself is contained in two Matlab files (Additional files 4.1b and 4.1c). *These files are available upon request.*

**Additional file 4.2 (a, b, c, d, e).** Five files encompassing the MATLAB model for non-linear regression of biomass accumulation in retentostat (see Methods section). Additional file 4.2a describes how to run or adapt the regression model. Additional file 2b is an example Excel file that can be adapted to include (hypothetical) experimental data. In addition, MATLAB writes the output of the regression model to this Excel file. The model itself is contained in three Matlab files (Additional files 4.2c, 4.2d and 4.2e) which operate together with Additional file 4.2b. *These files are available upon request.*



*Pichia pastoris* exhibits high viability and low maintenance-energy requirement at near-zero specific growth rates

Corinna Rebnegger\*, Tim Vos\*, Alexandra B. Graf, Minoska Valli, Jack T. Pronk, Pascale Daran-Lapujade, Diethard Mattanovich

\* Joint first authorship

Published in *Applied and Environmental Microbiology* 2016, 82:4570-4583

### Abstract

The yeast *Pichia pastoris* is a widely used host for recombinant protein production. Understanding its physiology at extremely low growth rates is a first step in the direction of decoupling product formation from cellular growth and therefore of biotechnological relevance. Retentostat cultivation is an excellent tool for studying microbes at extremely low specific growth rates but has so far not been implemented for *P. pastoris*. Retentostat feeding regimes were based on maintenance-energy requirement ( $m_S$ ) and maximum biomass yield on glucose ( $Y_{X/S}^{\max}$ ) estimated from steady-state glucose-limited chemostat cultures. Aerobic retentostat cultivation enabled reproducible, smooth transitions from a specific growth rate ( $\mu$ ) of  $0.025 \text{ h}^{-1}$  to near-zero specific growth rates ( $\mu < 0.001 \text{ h}^{-1}$ ). At these near-zero specific growth rates, viability remained at least 97 %. The value of  $m_S$  at near-zero growth rates was  $3.1 \pm 0.1 \text{ mg glucose per gram biomass and per hour}$ , which was three-fold lower than the  $m_S$  estimated from faster-growing chemostat cultures. This difference indicated that *P. pastoris* reduces its maintenance-energy requirement at extremely low  $\mu$ , a phenomenon not previously observed in eukaryotes. Intracellular levels of glycogen and trehalose increased while  $\mu$  progressively declined during retentostat cultivation. Transcriptional reprogramming towards zero growth included upregulation of many transcription factors as well as stress related genes and downregulation of cell cycle genes. This study underlines the relevance of comparative analysis of maintenance-energy metabolism, which has an important impact on large-scale industrial processes.

## Introduction

The methylotrophic yeast *Pichia pastoris* (syn. *Komagataella sp.*) has become increasingly popular as a host for recombinant protein production. Commercial products synthesized in *P. pastoris* include the recently FDA-approved biopharmaceuticals Jetrea® (ocriplasmin) and Kalbitor® (ecallantide) [296], as well as enzymes employed in research (trypsin, proteinase K) and industry (phospholipase C, phytase) [4]. The vast majority of heterologous proteins produced by *P. pastoris* are secreted, which enables post-translational modifications and facilitates down-stream processing. The genetic toolbox for *P. pastoris* continues to expand, with glycoengineered strains [113] as a major breakthrough to establish *P. pastoris* as a preferred host for future production of glycosylated therapeutic proteins.

Several studies have indicated that production of secreted recombinant proteins by yeasts is growth-rate-dependent [173, 170, 103, 224, 186]. The low specific secretion rate of yeasts, as compared to those of mammalian host systems [178] requires industrial production processes to be operated at high cell densities in order for them to be cost effective. However, at high biomass concentrations, the rate at which respiratory growth can be sustained is restricted by the oxygen and heat-transfer capacities of industrial bioreactors [122]. The resulting low specific growth rates in industrial fed-batch processes negatively affect biomass yield and protein productivity, thereby limiting product yields and titers [122, 184]. On the other hand, excess biomass represents an undesirable by-product, as its formation requires non-productive substrate consumption. Clearly, breaking the correlation of growth and productivity would be an attractive asset for *P. pastoris* as a protein-production platform. Gaining insights in the physiology of non-growing, metabolically active *P. pastoris* at extremely low growth rates may serve as a first step into this direction.

Controlled cultivation of microorganisms can be achieved in a chemostat. However, technical constraints limit the range of dilution rates at which a true continuous feed can be realized. Below a certain dilution rate set-point inherent to the system in use the supply of fresh media is only possible in a dropwise manner with increasing intervals between single drops, creating eventually a “feast and famine” scenario. Zero growth in chemostat cannot be achieved at all, as cells would wash out. A suitable tool for the cultivation of microbes in a controlled manner at extremely low specific growth rates or even under zero-growth regimes is the retentostat. This continuous-cultivation tool, first proposed by Herbert in 1961 [124], has recently been used to study several industrially relevant organisms, including the yeast *Saccharomyces cerevisiae* [85]. Retentostats are modified chemostats, in which biomass is fully retained by channeling the culture effluent through an internal or external filter device. In this continuous culture, the resulting accumulation of biomass is accompanied by a decreasing availability of energy substrate per cell per unit of time. This decrease inevitably causes a progressive

decrease of specific substrate-uptake rates and, consequently, of the specific growth rate. Theoretically, prolonged retentostat cultivation theoretically culminates in a situation in which the energy derived from the consumed substrate just suffices to sustain cellular maintenance but can no longer support biomass proliferation. Cellular processes related to maintenance, such as turnover of cellular components, osmoregulation and defense mechanisms (e.g. against reactive oxygen species) [272] can therefore be maintained while cell division has ceased. This non-growing state is fundamentally distinct from starvation in stationary-phase batch cultures, in which depletion of an essential nutrient causes cellular deterioration and, eventually, cell death [27]. Anaerobic retentostat cultivation of *S. cerevisiae* demonstrated that the maintenance-energy requirement of this yeast is independent of specific growth rate [29]. The energy demand for maintenance varies with the organism and, moreover, depends on culture conditions [85, 271]. Low maintenance requirements are especially advantageous for anabolic product formation at low growth rates, where maintenance metabolism accounts for a high percentage of the consumed substrate [265, 120].

Recent studies showed that *P. pastoris* reacts to decreasing growth rates and glucose supply by downregulation of biosynthetic processes such as gene expression and translation, and upregulation of catabolic processes and stress-responsive genes [224, 222]. However, to date, no information is available on how *P. pastoris* adjusts its physiology at near-zero specific growth rates. Growth of the yeast *S. cerevisiae* at near-zero growth rates has been investigated in aerobic and anaerobic retentostat cultures, in which it remained highly viable, metabolically active and remarkably stress-tolerant (Chapter 4) [28]. Transcriptome analyses on these near-zero growth rate cultures of *S. cerevisiae* pointed towards an extension of growth-rate dependent expression trends observed at higher specific growth rates. As the growth rate in the retentostat cultures decreased, biosynthetic processes were downregulated and genes involved in general stress resistance were induced, which was accompanied by an increased resistance to heat stress (Chapter 4) [29].

The Crabtree-negative [112] yeast *P. pastoris* exhibits an approximately 10-fold lower maximum sugar uptake rate than *S. cerevisiae* [125, 255] and its maximum specific growth rate on glucose in synthetic media under comparable conditions is approximately 30 % lower [126, 25]. Therefore, although *S. cerevisiae* and *P. pastoris* show similar growth-rate-dependent transcriptional regulation patterns at higher specific growth rates, their physiological and transcriptional adaptations at near-zero specific growth rates may well be different.

The aim of the present study was to study the physiology and transcriptional responses of *P. pastoris* to aerobic, glucose-limited growth. To this end, aerobic retentostat cultures of this yeast were implemented and used to investigate its growth energetics, robustness and genome-wide transcriptional responses during extremely slow growth. Based on initial

experiments a strain deleted in the flocculation and filamentous growth regulator gene *FLO8* was used to avoid filter clogging.

## Results

**A model strain for aerobic retentostat cultivation of *P. pastoris* |** In recent retentostat studies with *S. cerevisiae*, biomass retention was achieved by redirecting the effluent of steady-state chemostats through a membrane-filter probe (Chapter 4) [28, 26]. When the same set-up was used to grow a recombinant *P. pastoris* strain that secreted human serum albumin (HSA), the filter probe clogged within a few hours after switching to retentostat mode (data not shown). Since protein aggregation and adsorption are known causes of membrane-filter fouling and blockage [147, 177], secreted HSA might have contributed to this problem. However, the total protein concentration in the culture supernatants was only about 115 mg L<sup>-1</sup>, of which HSA 20 - 30 mg L<sup>-1</sup> and clogging occurred soon after switching to retentostat mode, so that we regarded filter clogging by extracellular protein as improbable. An alternative cause was attachment of *P. pastoris* to surfaces, a feature previously observed in bioreactor cultures of this yeast (unpublished observations). Growth on or into the filter probe, which was already present in the bioreactor during the chemostat phase that preceded retentostat cultivation, poses a major risk for its functionality. To eliminate both potential causes of membrane-filter obstruction, we set out to construct a non-producing *P. pastoris* strain with reduced growth on surfaces.

Laboratory strains of *S. cerevisiae* have been selected for unicellular, non-invasive growth, without flocculation or attachment to surfaces. Loss of these traits has been ascribed to a single nonsense mutation in *FLO8* [169]. The transcription factor Flo8 plays an important role in regulation of flocculation [92, 253] and is part of the filamentous growth signaling pathway [63]. Only one putative *P. pastoris* homolog to *S. cerevisiae* Flo8 was found by BLAST search. The ORF encoding this protein, PP7435\_Chr4-0252, tentatively called *FLO8*, was deleted in *P. pastoris* CBS 7435 with the split-marker cassette method [88, 99]. The impact of the  $\Delta flo8$  mutation was investigated by growing the mutant strain and its *FLO8* parent in glucose-limited chemostat cultures at a dilution rate of 0.05 h<sup>-1</sup> for 8 residence times (approximately one week). In cultures of the *FLO8* wild-type strain, a considerable fraction of the population showed a pseudohyphal morphology, while  $\Delta flo8$  cultures retained an ovoid, budding morphology (Figure 5.1A). Furthermore, attachment of biomass on reactor walls and other reactor components was much less pronounced in the  $\Delta flo8$  strain than in the parental strain (Figure 5.1B). Deletion of *FLO8* resulted in a 4 % decrease in the biomass yield on glucose in chemostat cultures ( $D = 0.05 \text{ h}^{-1}$ , see Supplementary Table 5.3) and a 12 % decrease in specific growth rate in duplicate shake flask batch cultures (see Table S1). These minor effects might be caused by expression of the dominant selection marker gene *KanMX* [12]. Because the pseudohyphal and



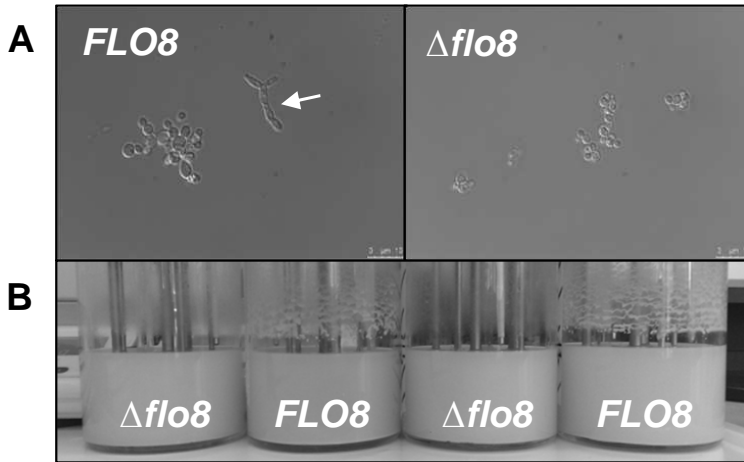


**Figure 5.1:** Morphology and surface attachment of wild-type *P. pastoris* CBS 7435 (FLO8) and an isogenic  $\Delta flo8$  strain after 7 days of cultivation in glucose-limited, aerobic chemostat cultures (dilution rate  $0.05 \text{ h}^{-1}$ ). (A) Phase-contrast micrographs. (B) Growth on bioreactor surfaces.

invasive phenotype prevented retentostat operation, the  $\Delta flo8$  strain was used for further chemostat and retentostat studies.

**Maintenance-energy requirement in glucose-limited chemostat cultures** | When microbial growth is limited by availability of the energy substrate and specific growth rates are low, a large fraction of the energy-substrate consumption is invested in cellular maintenance [217]. Maintenance includes essential aspects of cellular metabolism that are not coupled to growth, such as macromolecule turnover and homeostasis of electrochemical potential gradients across membranes [272, 120, 129]. Biomass accumulation profiles in retentostats strongly depend on the specific maintenance-energy requirement under the experimental conditions [28]. Estimation of the specific rate of energy-substrate consumption required for maintenance ( $m_s$ , in gram substrate per gram biomass and hour [ $\text{g}_S \text{ g}_X^{-1} \text{ h}^{-1}$ ]) is therefore a prerequisite for the design of feed profiles for retentostat experiments.

During growth under energy-substrate limited conditions, microorganisms in which the maintenance-energy requirement is growth-rate independent, show a linear relationship between the specific carbon and energy consumption rate ( $q_s$ ) and the specific growth rate ( $\mu$ ) according to Pirt [217]:

$$q_s = \frac{\mu}{Y_{X/S}^{\max}} + m_s \quad (5.1)$$

In this equation,  $m_s$  represents the growth-rate-independent energy-substrate requirement for maintenance and  $Y_{X/S}^{\max}$  (in  $\text{g g}^{-1}$ ) is the maximum theoretical biomass yield

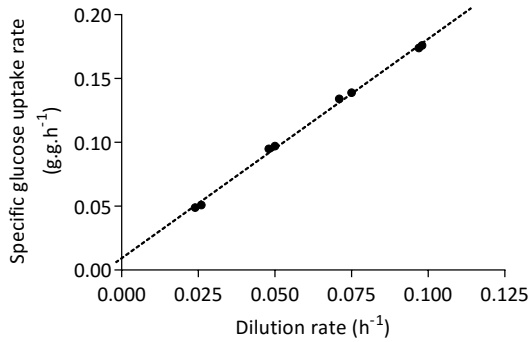


**Figure 5.2:** Specific glucose-uptake rate ( $q_s$ ) in aerobic, steady-state glucose-limited chemostat cultures of *P. pastoris* grown at different dilution rates. Linear regression was used to calculate the maintenance coefficient  $m_s$  (intercept with y-axis) and maximum biomass yield on glucose  $Y_{X/S}^{max}$  (reciprocal of the slope). The  $R^2$  value of the regression line was 0.99 and the standard error of the maintenance coefficient was determined by the LINEST function to be 23 %.

on glucose under the conditions applied. When this equation holds, both parameters can be estimated from a set of steady-state glucose-limited chemostat cultures (in which  $\mu$  equals the dilution rate) operated at different dilution rates, followed by linear regression of a  $q_s$ -versus- $\mu$  plot. To calculate  $m_s$  and  $Y_{X/S}^{max}$  for the *P. pastoris*  $\Delta flo8$  strain, eight independent glucose-limited aerobic chemostats were grown, at dilution rates ranging from 0.025 to 0.10  $h^{-1}$ . A linear relationship between  $q_s$  and  $\mu$  was indeed observed (Figure 5.2), yielding an estimated  $m_s$  ( $\pm$  standard deviation) of  $0.0100 \pm 0.0023$   $g_s g_X^{-1} h^{-1}$ . This estimate of  $m_s$  was similar to that calculated for *S. cerevisiae* grown in aerobic retentostat cultures (average  $\pm$  standard deviation:  $0.0071 \pm 0.0005$   $g_s g_X^{-1} h^{-1}$ ) (Chapter 4). The  $m_s$  of the non-producing *P. pastoris* strain used in this study was ca. 50 % lower than  $m_s$  values calculated for heterologous-protein-producing *P. pastoris* strains grown in glucose-limited chemostats, which ranged from  $0.0147 \pm 0.0009$   $g_s g_X^{-1} h^{-1}$  (calculated from [224]) to  $0.0161$   $g_s g_X^{-1} h^{-1}$  [186].  $Y_{X/S}^{max}$  was calculated to be  $0.584$   $g g^{-1}$ , ca. 4 % higher than  $Y_{X/S}^{max}$  values of heterologous-protein-producing *P. pastoris* strains reported previously ( $0.559$  and  $0.562 \pm 0.011$   $g g^{-1}$ , [186] and [224] respectively).

**Higher-than-expected biomass accumulation in retentostats** | A retentostat feeding regime for aerobic, glucose-limited chemostat cultures of *P. pastoris*  $\Delta flo8$  was designed, following an approach developed for aerobic retentostat cultivation of *S. cerevisiae* (Chapter 4). Model simulations were based on the  $m_s$  and  $Y_{X/S}^{max}$  values of the *P. pastoris*  $\Delta flo8$  strain estimated from chemostat cultures (see above). Dynamic, declining glucose-feeding profiles were generated by controlled dilution of the medium feed, using two medium reservoirs that contained media with different glucose concentrations and a mixing vessel upstream of the reactor (see Materials and Methods). Glucose concentrations in the two medium reservoirs ( $C_{S,MC}$  and  $C_{S,MR}$ ) and the volume of the

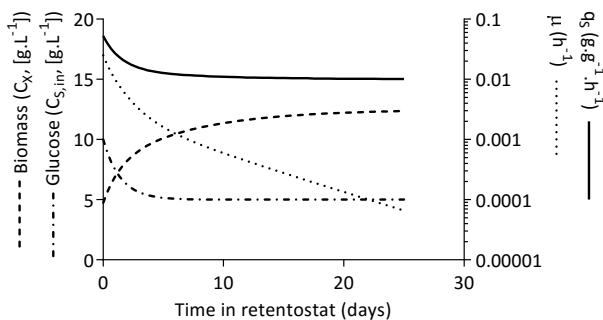


**Figure 5.3:** Model-based prediction of growth of *P. pastoris* in glucose-limited aerobic retentostat cultures. An optimized feed profile, designed to achieve a smooth decline of the specific growth rate ( $\mu$ ) from  $0.025 \text{ h}^{-1}$  to near-zero growth rates, was designed by computer simulation (see Methods). Indicated are the optimized glucose concentration profile in the feed (alternating dotted and dashed line), the resulting predicted profiles of biomass accumulation (dashed line), the specific glucose uptake rate ( $q_S$ , solid line) and  $\mu$  (dotted line).

mixing vessel were chosen such that the model-based simulations predicted a smooth transition from chemostat growth at  $0.025 \text{ h}^{-1}$  to near-zero specific growth rates in the retentostats. The optimized feeding strategy and the resulting predicted profiles of biomass accumulation,  $\mu$  and  $q_S$  are shown in Figure 5.3.

The optimized feed regime was applied in two independent, 25-day retentostat experiments with the *P. pastoris*  $\Delta flo8$  strain. Although glucose concentrations in the feed exactly matched the predicted profile, biomass accumulated to approximately 6-fold higher concentrations than predicted by model simulations (Figure 5.4A). In retentostat cultures of *S. cerevisiae*, deviation of biomass accumulation from predicted values was attributed to accumulation of metabolically inactive (non-viable) cells (Chapter 4)[28]. Since the model simulations assumed 100 % culture viability, they did not capture a possible accumulation of non-viable biomass. Culture viability of the *P. pastoris* retentostat cultures was regularly measured by fluorescence staining and flow cytometry, which yielded consistent results with plate counts of colony-forming units (see Supplementary Table 5.4). Throughout the retentostat experiments, the fraction of viable cells remained at 97% or higher (Figure 5.4B), thereby excluding loss of viability as a primary cause of the higher-than-predicted biomass accumulation. An alternative explanation for this deviation from the model predictions was that the values of  $m_S$  and/or  $Y_{X/S}^{\max}$  measured in the chemostat cultures are not representative of those at near-zero growth rates. More precisely, a lower  $m_S$  and/or a higher  $Y_{X/S}^{\max}$  at near-zero growth rates might contribute to the unexpectedly high biomass accumulation. Cell morphology remained unchanged throughout the retentostat culture (data not shown). The average cell size increased 1.2-fold from  $3.3$  to  $4.2 \mu\text{m}^2$  cross sectional area, indicating that the cell number increased nearly proportional to the biomass concentration.

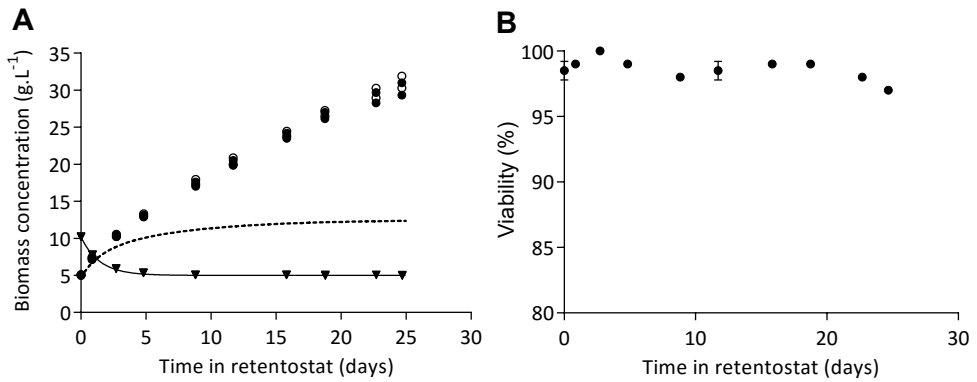


**Figure 5.4:** Biomass accumulation, glucose concentration in the feed and viability of two independent glucose-limited aerobic retentostat cultures of *P. pastoris*. (A) Retentostat cultures were initiated from chemostat cultures at time point zero. Predicted biomass accumulation profile (short dashed line), measured biomass dry-mass concentration (open circles), biomass concentration corrected for viability (closed circles), predicted glucose concentration (solid line) and measured glucose concentration in the mixing vessel (closed triangles). (B) Average culture viability based on fluorescence staining.

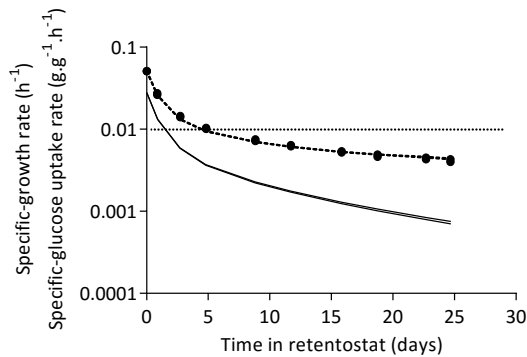


**Figure 5.5:** Glucose uptake rate ( $q_S$ ) and specific growth rate ( $\mu$ ) in two independent glucose-limited aerobic retentostat cultures of *P. pastoris*. Directly calculated  $q_S$  values (closed circles) and values for  $q_S$  derived from non-linear regression analysis of the biomass accumulation (short dashed lines) as well as  $\mu$  derived from non-linear regression analysis of the biomass accumulation (solid lines). The horizontal dotted line indicates the amount of substrate required to meet the maintenance requirement as extrapolated from chemostat cultivations at faster growth rates.

### *P. pastoris* decreases its maintenance-energy requirements at near-zero growth rates

| During the 25-day aerobic retentostat experiments, the specific growth rate of *P. pastoris* retentostat cultures, calculated by least-square regression analysis (See Material and Methods and Supplementary figure 5.11), smoothly decreased from 0.025 h<sup>-1</sup> to below 0.001 h<sup>-1</sup> (Figure 5.5). This decrease in the specific growth rate corresponded to an increase of the doubling time from 27.7 h to over 38 days. Over the same time, the specific glucose uptake rate declined to 0.004 g<sub>S</sub> g<sub>X</sub><sup>-1</sup> h<sup>-1</sup>. This extremely low  $q_S$ , which reflects the combined consumption of glucose for maintenance and growth, was only 40 % of the  $m_S$  calculated from chemostat cultures grown at specific growth rates of 0.025 h<sup>-1</sup> and

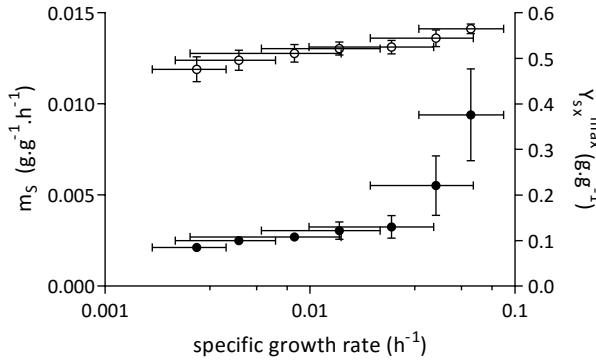


**Figure 5.6:** Dynamics of the glucose requirements for maintenance ( $m_S$ ) and maximum theoretical biomass yield ( $Y_{X/S}^{\text{max}}$ ) in relation to the specific growth rate ( $\mu$ ). Values for  $m_S$  (closed circles) and  $Y_{X/S}^{\text{max}}$  (open circles) over defined ranges of four consecutive specific growth rates were derived from linear-regression analysis performed on overlapping sets of duplicate  $\mu$ - $q_S$  relations (see Supplementary figure 5.12). The vertical error bars for  $m_S$  and  $Y_{X/S}^{\text{max}}$  indicate the standard error on the regression statistics, and the horizontal error bars indicate the defined range of specific growth rates.

above. Indeed, the average  $m_S$  calculated by least-square regression analysis of data from the retentostat cultures, equalled  $0.0031 \pm 0.0001 \text{ g}_S \text{ g}_X^{-1} \text{ h}^{-1}$ , which is three-fold lower than the  $m_S$  value calculated from the chemostat experiments. This result suggested that, in *P. pastoris*,  $m_S$  is not growth-rate-independent, but decreases strongly at extremely low specific growth rates in a way that resembles growth energetics of prokaryotes that exhibit a stringent response [8, 53, 284].

In addition to changes in  $m_S$ , a growth-rate dependency of  $Y_{X/S}^{\text{max}}$  might affect biomass accumulation profiles in the retentostats.  $Y_{X/S}^{\text{max}}$  is amongst others determined by biomass composition, which can change depending on the environment [123]. To investigate this possibility,  $q_S$ - $\mu$  relationships were determined over a range of specific growth rates in the retentostat and chemostat cultures described in this study. Chemostat data were derived from simple steady-state kinetics, while  $\mu$  and  $q_S$  in retentostat were calculated by solving biomass and substrate mass balances over defined time intervals (see Materials and Methods). Linear-regression analysis was then performed on sets of overlapping  $\mu$ - $q_S$  relations to estimate  $m_S$  and  $Y_{X/S}^{\text{max}}$  values over defined ranges of four consecutive specific growth rates in duplicate (see Supplementary figure 5.12). This analysis confirmed that  $m_S$  sharply decreased at specific growth rates between  $0.06 \text{ h}^{-1}$  and  $0.03 \text{ h}^{-1}$  (ca. three-fold), while also indicating a positive, but far less pronounced correlation of  $Y_{X/S}^{\text{max}}$  with specific growth rate (Figure 5.6).

**Glycogen and trehalose accumulation in retentostat-grown *P. pastoris*** | In glucose-limited cultures of *S. cerevisiae*, intracellular storage carbohydrate concentrations are negatively correlated with the specific growth rate [203]. To investigate if *P. pastoris* showed a similar response, the glycogen and trehalose contents in biomass were

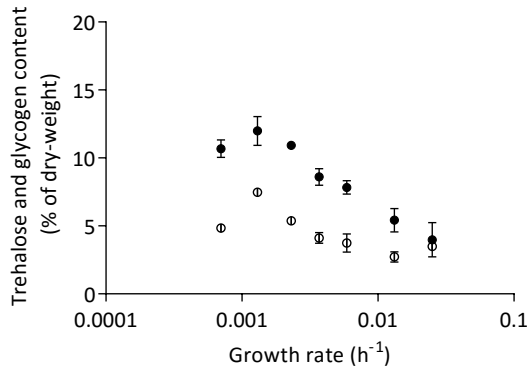


**Figure 5.7:** Storage carbohydrate accumulation in aerobic glucose-limited retentostat cultures of *P. pastoris*. Trehalose (closed circles) and glycogen (open circles) and content represented as weight-percentage of total dry biomass, plotted as a function of the specific growth rate ( $\mu$ ).

determined during the course of retentostat cultivations (Figure 5.7). For all specific growth rates, trehalose levels were higher than glycogen concentrations. Intracellular levels of both storage carbohydrates increased as  $\mu$  decreased from  $0.025 \text{ h}^{-1}$  to  $0.0013 \text{ h}^{-1}$ , reaching maximum levels of  $0.12 \text{ g g}_X^{-1}$  and  $0.07 \text{ g g}_X^{-1}$  respectively. Average trehalose and glycogen levels measured at the final sampling points, where  $\mu$  had decreased to  $0.0007 \text{ h}^{-1}$ , were 11 and 35 % lower than these maximum levels.

**Transcriptional reprogramming at near-zero growth rates** | Retentostat cultivation enabled a first exploration of the transcriptional adaptations of *P. pastoris* to near-zero specific growth rates. Microarray-based transcriptome analyses were performed on samples taken on day 1, 3, 5, 16 and 23 of retentostat cultivation, corresponding to average specific growth rates of 0.0132, 0.0059, 0.0037, 0.0013 and  $0.00082 \text{ h}^{-1}$ , respectively. To expand the range of investigated growth rates, transcriptional analysis was also performed on the set of chemostat cultures that were run to estimate  $m_S$  and  $Y_{X/S}^{\max}$  and these data were combined with the retentostat transcriptome data. Out of 5354 ORFs represented on the microarray, 1376 genes were differentially expressed (see Methods section). Two main regulation patterns were identified (Figure 5.8). The expression of genes was either negatively correlated to the specific growth rate (Cluster A, 61 % of regulated genes), or displayed the opposite trend with higher expression levels at faster growth rates (Cluster B, 39 % of regulated genes).

The gene set and the respective biological processes which were transcriptionally upregulated towards zero growth identified in this study correlate well with regulation patterns previously observed for *P. pastoris* cultivated in glucose-limited chemostat at  $\mu$  ranging from 0.15 to  $0.015 \text{ h}^{-1}$  [224]. Affected biological processes in this study (Table 5.1) were “cellular response to chemical stimulus”, “cell communication” and “response to nitrogen utilization”. Furthermore, genes with molecular functions related to aldehyde

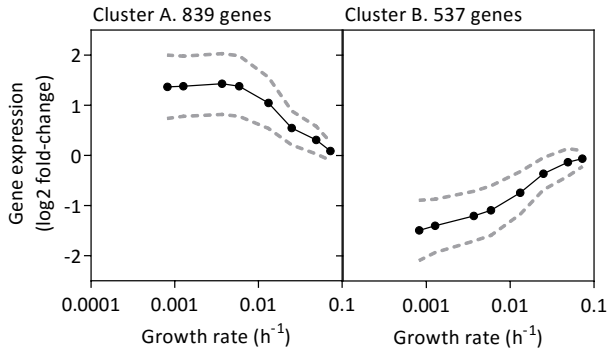


**Figure 5.8:** Global gene expression profile in *P. pastoris* over a wide range of specific growth rates ( $\mu$ ). Genes that were differentially expressed when compared to the fastest  $\mu$  of  $0.10 \text{ h}^{-1}$  in at least one comparison were grouped into two clusters by k-means clustering.

dehydrogenase activity as well as to promoter binding and transcription factor activity were significantly enriched among the genes with increasing transcript levels towards zero growth (Table 5.1). In fact, 20 % of the genes grouped in cluster A are functionally annotated as transcription factors, while in total only 10 % of all *P. pastoris* ORFs are assigned to this function. Many of the transcription factors located in cluster A are global stress response regulators (*YAP1*, *SKN7*, *SKO1*, *HAC1*, *HSF1* and *MSN4*) while others are involved in nutrient response such as glucose repression (*CAT8-2*, *MIG1-1* and *MIG1-2*) and nitrogen catabolite repression (NCR) (*MKS1*, *URE2-2*, *GAT1* and *GLN3*). Upregulation of NCR-related transcription factors towards zero growth might seem unexpected as ammonia was present in excess during chemostat and retentostat cultivation. However, for *S. cerevisiae*, it has been demonstrated that not only nitrogen but also carbon signaling is responsible for regulation of NCR [59] which might also be the case for *P. pastoris*.

Corresponding to an increase in transcript levels of stress-related transcription factors towards zero growth, higher expression levels could also be observed for a considerable number of other stress-responsive genes encoding e.g. heat shock proteins (*HSP104*, *HSP31*, *HSP42*, *HSP60*, *HSP78*, *SSA3* and *SSE1*) or proteins involved in cellular defense against oxidative stress (*CCP1-2*, *GRX3*, *MRX1-2*, *MRX2-2* and *SOD1*). Furthermore, many genes involved in alternative carbon source utilization, whose expression is known to be repressed at elevated concentrations of glucose [117, 96], were grouped into cluster A, for instance genes involved in methanol (*AOX1*, *AOX2* and *FDH1*) and ethanol (*ADH2*, *ALD2* and *ALD4*) metabolism. Expression of most of these genes continued to increase with decreasing growth rate (Figure 5.9A), although residual glucose levels during retentostat cultivation remained stable (Figure 5.9B). Transcript levels of only one of the two high affinity glucose transporters described in *P. pastoris* increased with decreasing growth rate (*HGT2*), while expression of the second one (*GTH1*) strongly decreased.

Biological processes downregulated with decreasing growth rate (Cluster B, Table 5.1)

**Table 5.1:** Enriched GO terms for the category “biological process” (BP) and “molecular function” (MF) for the clusters A and B. Redundant GO terms were excluded using the web-based tool REVIGO [261]. A file with the full length list as well as the number of significantly regulated genes per GO term and the GO term is available upon request.

Cluster	Enriched GO term (Category)	p-value <sup>a</sup>
A	RNA polymerase II regulatory region sequence-specific DNA binding (MF)	0.00
	Cellular response to chemical stimulus (BP)	0.00
	Sequence-specific DNA binding (MF)	0.00
	Nucleic acid binding transcription factor activity (MF)	0.00
	Cell communication (BP)	0.00
	Regulatory region nucleic acid binding (MF)	0.00
	Response to chemical (BP)	0.00
	Regulatory region DNA binding (MF)	0.00
	RNA polymerase II core promoter proximal region DNA binding TF activity (MF)	0.01
	Aldehyde dehydrogenase (NAD) activity (MF)	0.01
	Oxidoreductase activity, acting on the aldehyde or oxo group of donors (MF)	0.01
	Regulation of nitrogen utilization (BP)	0.01
	Oxidoreductase activity, acting on the aldehyde or oxo group of donors (MF)	0.04
	B	Mitotic nuclear division (BP)
Organelle fission (BP)		0.00
Chromosome segregation (BP)		0.00
Cell cycle (BP)		0.00
Cell division (BP)		0.00
Microtubule-based process (BP)		0.00
Cytoskeleton organization (BP)		0.00
Structural constituent of cytoskeleton (MF)		0.00
Tubulin binding (MF)		0.00
Chromosome organization (BP)		0.00
DNA-dependent DNA replication (BP)		0.00
DNA conformation change (BP)		0.00
DNA replication (BP)		0.00
Single-organism cellular process (BP)		0.00
Single organism reproductive process (BP)		0.00
Single-organism process (BP)		0.00
Cytoskeletal protein binding (MF)		0.00
DNA packaging (BP)		0.00
Nuclear migration (BP)		0.00
Double-strand break repair (BP)		0.00
Substrate-specific transmembrane transporter activity (MF)		0.01
Organic acid transmembrane transporter activity (MF)		0.01
DNA metabolic process (BP)		0.01
Small molecule metabolic process (BP)		0.01
Sterol metabolic process (BP)		0.02
Reproduction (BP)		0.02
Reproductive process (BP)		0.03

<sup>a</sup> Bonferroni corrected p-value.



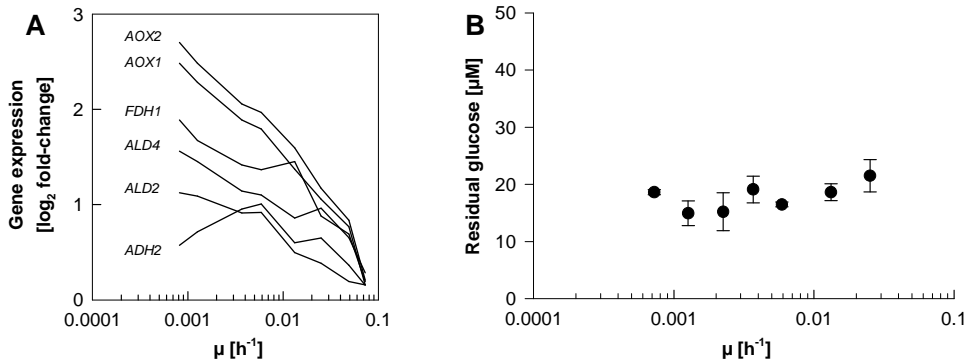


**Figure 5.9:** Expression profiles of genes involved in alternative carbon source utilization and residual glucose concentration in relation to the specific growth rate ( $\mu$ ). (A) Expression profile of 6 genes involved in methanol and ethanol utilization and (B) average residual glucose concentration.

mostly encompassed the mitotic cell cycle and related terms such as “reproduction”, “DNA metabolic process”, “chromosome segregation” and “double-strand break repair”. In total, approximately one fifth of all genes grouped into this cluster were involved in cell cycle related processes. The average expression of these cell cycle related genes steadily decreased towards zero growth (Figure 5.10A), while the ratio between cells in G1, S and G2/M phase only changed slightly at growth rates below  $0.01 \text{ h}^{-1}$  (Figure 5.10B). Further downregulation of cell cycle specific genes can therefore not be attributed to shifts in cell cycle phase distribution but can rather be explained by changes within the cell cycle phase populations. For example, a decrease in growth rate results in an increase of G1 phase duration. G1-specific cyclin expression is, however, induced just before the bud emerges [247]. Consequently, with decreasing growth rate, less and less cells in G1 phase are in the process of passing Start, resulting in an overall decrease of G1-specific gene expression.

Genes involved in sterol metabolism, and especially in ergosterol biosynthesis (10 out of 22 genes known in *P. pastoris*) or transmembrane transport were also overrepresented in Cluster B. The latter included genes involved in electron transport chain, ion transport and intra- and extracellular transport of amino acids as well as other organic compounds. Growth-rate related processes such as protein and nucleotide biosynthesis were not overrepresented within the differentially expressed genes, contrary to what has been previously reported at higher growth rates for producing and non-producing *P. pastoris* strains [224, 221]. For example, out of 179 genes annotated as being involved in “ribosome biogenesis”, only 20 were significantly regulated by growth rate in the present dataset and only 12 were grouped into cluster B. . Indeed, no significant changes in cellular RNA and protein content were detected during retentostat cultivation (data not shown). Especially the unchanged RNA content is an indication that ribosome content does not change towards zero growth. Regarding amino acid biosynthesis the expression of several genes

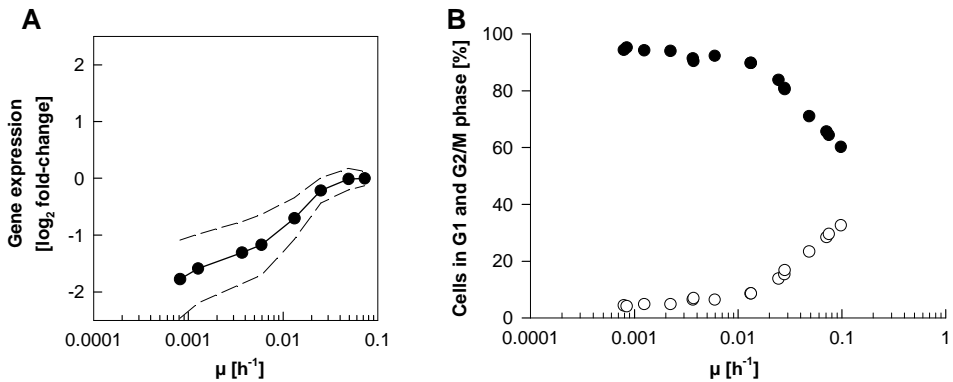


**Figure 5.10:** Expression profile of cell cycle related genes and cell cycle phase distribution of *P. pastoris* over a wide range of specific growth rates ( $\mu$ ). (A) Average expression profile of the differentially expressed genes annotated to the GO term “cell cycle” and (B) the percentage of cells in G1 phase (closed circles) and G2/M phase (open circles) based on DNA content measurements in relation to  $\mu$ .

(29 out of 119) was affected by growth rate with approximately half of the genes up- and the other half downregulated with decreasing growth rate.

## Discussion

Implementation of aerobic retentostat cultivation for *P. pastoris* allowed a first quantitative exploration of the physiology of this industrially relevant, Crabtree-negative yeast at extremely low growth rates. Retentostat cultivation reproducibly reached biomass doubling times of over five weeks, corresponding to specific growth rates below  $0.001 \text{ h}^{-1}$ . This domain of specific growth rates has previously only been explored for one other yeast, *S. cerevisiae* (Chapter 4 and [28, 26]). Similar to *S. cerevisiae* [28], *P. pastoris* exhibited an increased accumulation of storage carbohydrates with decreasing specific growth rates, with combined levels of glycogen and trehalose increasing to almost 20 % of the total biomass dry weight at near-zero growth rates. This increased accumulation of storage materials under severely calorie-restricted conditions may appear counterintuitive. However, from an evolutionary perspective, the allocation of scarce resources for storage can be interpreted as a typical ‘be prepared’ scenario [81] that conditions microorganisms to adapt their physiology to multiple different scenarios, including complete depletion of energy sources. The transcriptional derepression, in the retentostat cultures of *P. pastoris*, of pathways involved in the metabolism of alternative energy substrates, is also consistent with this adaptation strategy. Another similarity between *P. pastoris* and *S. cerevisiae* was the increased expression of genes involved in stress tolerance at low specific growth rates (Chapter 4 and [29]), a phenomenon that has also been observed in slow-growing cultures of other microorganisms grown in retentostat cultures [85].

A first marked difference between near-zero growth cultures of *P. pastoris* and *S. cerevisiae* concerned culture viability. Throughout the *P. pastoris* retentostat experiments, viability remained above 97 %. Based on this high viability, an average death rate of  $6 \times 10^{-5} \text{ h}^{-1}$  was calculated. This death rate is an order of magnitude lower than observed in aerobic retentostat cultures of *S. cerevisiae* grown in the same range of near-zero specific growth rates (Chapter 4 and [28]). Apparently, *P. pastoris* is more robust during conditions of extreme calorie restriction than *S. cerevisiae*. Moreover, in contrast to *S. cerevisiae*, which has been shown to exhibit growth-rate-independent maintenance-energy requirements in anaerobic retentostat cultures [28], *P. pastoris* showed a sharp decline of estimated maintenance-energy requirements at near-zero specific growth rates (Figure 5.6). Under these slow-growth, aerobic and glucose-limited conditions, the maintenance coefficient ( $m_s$ ) of *P. pastoris* was less than half of that of corresponding cultures of *S. cerevisiae* (Chapter 4). Its high viability and low maintenance-energy requirement in aerobic retentostat cultures indicate that *P. pastoris* has evolved to better withstand severely calorie-restricted growth than *S. cerevisiae*. This conclusion is consistent with existing knowledge on the physiology and ecology of these two industrially relevant yeasts. *P. pastoris*, like other Crabtree-negative yeast species [283], harbors high-affinity hexose transporters [185] with glucose saturation constants that are two orders of magnitude lower than the ‘high affinity’ hexose transporters of *S. cerevisiae* [283, 222, 31]. Furthermore, *P. pastoris* and other methylotrophic yeasts have been isolated from nutrient-poor environments such as decaying wood [210, 213]. An evolutionary adaptation to energy-substrate-limited growth is also illustrated by the ability of this yeast to assimilate a wide range of carbon sources including several non-sugars [159] and to simultaneously utilize binary mixtures of carbon sources which has been demonstrated amongst others for glucose and methanol under limiting conditions in continuous culture, in contrast to glucose excess where methanol utilization is repressed [208].

To our knowledge, a growth-rate-dependent maintenance-energy requirement has not been observed in a yeast or fungus so far. In *S. cerevisiae*, a sharp decrease of energy-substrate consumption for maintenance has only been reported during energy-source starvation, when metabolism becomes completely dependent on the mobilization of storage carbohydrates [27]. In contrast, growth-rate dependent maintenance energy requirements have previously been reported for several prokaryotes, for example *Escherichia coli* [53], *Bacillus polymyxa* [8], *Nitrobacter winogradskyi* and *Nitrosomonas europaea* [266]. In these organisms, low nutrient availability activates a so-called ‘stringent response’. This regulatory program, triggered by the ppGpp and pppGpp alarmones, causes an upregulation of stress-response genes and a downregulation of genes involved in energy-intensive processes such as protein turnover and cell division [285, 35]. Further research is needed to investigate if the mechanisms responsible for reducing maintenance-energy requirements in slow-growing *P. pastoris* cultures bear any

molecular or functional resemblance to this well-characterized prokaryotic mechanism. In this respect, it is remarkable that, in contrast to observations on slow-growing and energy-starved *S. cerevisiae* cultures (Chapter 4 and [27]), the retentostat cultures of *P. pastoris* did not show a marked transcriptional downregulation of genes involved in protein synthesis at near-zero growth rates, while expression levels of these genes did correlate positively with specific growth rate in faster-growing cultures [224]. Whether *P. pastoris*, an important cell factory for recombinant protein production, indeed has a higher translational capacity at low specific growth than *S. cerevisiae*, requires further research.

Retentostat studies on *P. pastoris* were enabled by the construction of a *flo8* deletion mutant, which did not show dimorphism or attachment to reactor surfaces. Since putative orthologs of *FLO8* can be found in many other biotechnologically relevant yeasts, their deletion may also prove useful for bioreactor research.

## Outlook

Yeasts are widely applied for the production of heterologous proteins and metabolites. Although physiological and molecular knowledge of *P. pastoris* is not as extensive as for *S. cerevisiae*, it holds several advantages for aerobic bioprocess applications. *P. pastoris* greatly favors respiratory metabolism [112] and, in contrast to the situation in *S. cerevisiae*, its mitochondrial respiratory chain harbors a proton-translocating complex I. The present study shows that in addition, *P. pastoris* has very low substrate requirements for maintenance at slow growth rates, a trait that is industrially relevant for production of proteins and of metabolites whose synthesis from sugar requires a net input of ATP. Furthermore, its high tolerance to caloric restriction and extremely slow growth make *P. pastoris* an interesting candidate for developing zero-growth cell factory concepts. Despite the impact of maintenance-energy requirements on productivity and product yields in large-scale, aerobic fed-batch processes, very little comparative research has been done to quantify these requirements in different microorganisms. Retentostat cultivation provides a powerful tool to gain more insight into the diversity of these requirements in industrially relevant microorganisms and, ultimately, into the molecular basis for this diversity.

## Acknowledgements

We thank Markus Buchetics for strain construction, and Brigitte Gasser for critically reading the manuscript (both BOKU Vienna). Thanks go to Xavier Hakkaart for technical assistance, and Ton van Maris for valuable discussions during this project (both TU Delft). EQ VIBT GmbH (Vienna) is acknowledged for providing bioreactor instrumentation through the VIBT-Extremophile Center.

**Table 5.2:** List of primers used for the generation of the split marker cassette.

Primer	Sequence
A_fw	CGAACATCCATCACAAAACAC
A_bw	GTTGTCGACCTGCAGCGTACGGTGTGCCGCGAAATG
D_fw	TAGGTGATATCAGATCCACTGATCAATTTGCCCAAGAGACG
D_bw	GACTGTTGCGATTGCTGGTG
B_fw	CATTCGCGGCAACACCGTACGCTGCAGGTCGACAAC
B_bw	CGGTGAGAATGGCAAAGCTTAT
C_fw	AAGCCCGATGCGCCAGAGTTG
C_bw	CGTCTCTGGGCAAATTGATCAGTGGATCTGATATCACCTA
Det_fw	ATCCAGGACACGCTCATCAAG
Det_bw	GTGTGTGCTCTGGAATTGGATC

CR was funded by the Austrian Science Fund (FWF): Doctoral Program BioToP—Biomolecular Technology of Proteins (FWF W1224). TV was funded by the B-Basic research program, which was financed by the Netherlands Organisation for Scientific Research (NWO), and by the European Union's Framework VII program (RoBoYeast project). MV was supported by the Federal Ministry of Science, Research and Economy (BMFWF), the Federal Ministry of Traffic, Innovation and Technology (bmvit), the Styrian Business Promotion Agency SFG, the Standortagentur Tirol, the Government of Lower Austria and ZIT - Technology Agency of the City of Vienna through the COMET-Funding Program managed by the Austrian Research Promotion Agency FFG.

The funders had no role in study design, data collection and interpretation, or the decision to submit the work for publication.

## Methods

**Strain and culture conditions** | *P. pastoris* CBS 7435 was obtained from the Centraal Bureau voor Schimmelcultures (The Netherlands). A mutant of this strain in which open-reading frame PP7435\_Chr4-0252 was disrupted, was constructed with the split-marker cassette method [88] as adapted for *P. pastoris* [99]. Two 1.5 kb regions located approximately 200 bp up- and downstream of the translation start of the ORF were amplified using primers A\_fw and A\_bw as well as D\_fw and D\_bw, respectively (Table 5.2). The resulting fragments A and B were used to flank two approximately 1 kb overlapping parts of the KanMX marker cassette [182] (primers B\_fw, B\_bw, C\_fw and C\_bw) by fusion PCR, using overhangs on the primers A\_bw and D\_fw that were homologous to the 5' and 3' end of the respective parts B and C of the resistance marker cassette. The two fused fragments AB and CD were simultaneously transformed into electrocompetent (28) *P. pastoris* cells by electroporation as described in [74]. Successful integration requires three different recombination events, which resulted in replacement of a 0.4 kb fragment at the 5' end of PP7435\_Chr4-0252 and its promoter by the KanMX cassette. Correct deletion mutants were verified by PCR with primers located outside of the split marker cassette (Det\_fw and Det\_bw) and gel

electrophoresis. A positive single colony isolate was selected and named CBS 7435  $\Delta flo8$ . Genomic DNA for the PCR was isolated on FTATM cards (Whatman, UK). Cultures for cryo stocks were grown overnight in 500 mL shake flasks containing either 100 mL YPG (CBS 7435) or YPG-Geneticin (CBS 7435  $\Delta flo8$ ) (per liter: 10 g yeast extract, 20 g peptone, 12.6 g glycerol and 500 mg Geneticin), under vigorous shaking (180 – 200 rpm) at 25 °C. After addition of glycerol (10 % v/v), 1 mL aliquots were stored at -80 °C. Precultures for shake-flask and bioreactor experiments were inoculated from cryo stocks and cultivated in YPD and YPD-Geneticin, respectively (per liter: 10 g yeast extract, 20 g peptone, 20 g glucose and 500 mg Geneticin) at 25 °C and 180 rpm overnight. For determination of the maximum specific growth rate ( $\mu_{max}$ ) of the  $\Delta flo8$  strain and the parental strain CBS 7435, 100 mL of buffered synthetic chemically defined medium [74] were inoculated at an OD600 of 0.8 and incubated at 25 °C and 180 rpm for 8 h.

**Chemostat cultivation** | Carbon and energy-limited aerobic chemostat cultivation for determination of specific glucose uptake rates across four dilution rates (0.025, 0.050, 0.075 and 0.100 h<sup>-1</sup>) and transcriptome analysis were performed in 1.0 L bench-top bioreactors (SR0700ODLS, DASGIP, Germany). Precultures were grown as described above, harvested, washed and resuspended in sterile demineralized water and used to inoculate the prefilled bioreactors. After completion of the batch phase (indicated by a sharp increase in dissolved oxygen concentration), chemostat cultivation was initiated at the respective dilution rate. The working volume of 400 mL was kept steady by means of a level sensor. To keep the dissolved oxygen concentration above 20%, cultures were stirred at 450 rpm and sparged with a constant air flow of 0.2 L min<sup>-1</sup>. Culture temperature was controlled at 25 °C and the pH was kept at 5.85 by automated addition of 10% ammonia solution. Chemostat media contained per liter: 10 g glucose, 5 g (NH<sub>4</sub>)<sub>2</sub>SO<sub>4</sub>, 3 g KH<sub>2</sub>PO<sub>4</sub>, 0.5 g MgSO<sub>4</sub> 7H<sub>2</sub>O, 1.5 mL trace metals solution [290], 0.4 mL of a 0.2 g L<sup>-1</sup> biotin solution (Sigma-Aldrich, USA) and 0.25 g Pluronic 6100 PE antifoaming agent (BASF, Germany).

**Retentostat cultivation** | Retentostat cultivation was preceded by a steady-state chemostat cultivation phase. The retentostat experiment was carried out in 2 L bench top bioreactors (Applikon, The Netherlands) at a working volume of 1.4 L. Main culture conditions (pH and temperature) as well as media composition were as described above. The sugar concentration in the reservoir medium ( $C_{S,MC}$ ) during the preceding chemostat phase was 10 g L<sup>-1</sup>. Cultures were sparged with air (0.7 L min<sup>-1</sup>) and stirred at 800 rpm. Fresh medium was supplied to the bioreactor from a 3 L mixing reactor (Applikon, The Netherlands) which was operated at a working volume ( $V_S$ ) of 1.2 L and continuously stirred at 500 rpm.  $V_S$  was kept constant by means of a level sensor leading to automatic addition of fresh media from an external medium vessel at a flow rate ( $\varphi_V$ ) of 35 mL h<sup>-1</sup>, corresponding to the dilution rate in the bioreactor. Chemostat cultures were considered to be in steady state when, after at least five resident times, biomass concentrations changed by less than 3 % over two consecutive volume changes. After reaching a steady-state in chemostat cultures, the retentostat phase was started by switching the reactor effluent to an outflow port equipped with an autoclavable Applisense filter assembly (Applikon, The Netherlands), consisting of a hydrophobic polypropylene filter with a pore size of 0.22  $\mu$ m and a stainless steel hollow filter support. Prior to autoclaving, the filter was wetted by overnight incubation in 96 % ethanol, and subsequently rinsed with a phosphate buffer saline solution (PBS, per liter: 8 g NaCl, 0.2 g KCl, 1.44 g

$\text{Na}_2\text{HPO}_4$ , 0.24 g  $\text{KH}_2\text{PO}_4$ , and HCl to adjust the final pH to 7.4). To control biomass accumulation, the medium reservoir connected to the mixing vessel was exchanged for a reservoir containing chemostat medium (see above) supplemented with 5 g  $\text{L}^{-1}$  instead of 10 g  $\text{L}^{-1}$  glucose ( $C_{S,MR}$ ). Consequently, the concentration of the growth-limiting substrate glucose entering the bioreactor ( $C_{S,in}$  in  $\text{g L}^{-1}$ ) decreased over time ( $t$  in [h]) according to Equation 5.2.

$$C_{S,in} = (C_{S,MC} - C_{S,MR}) \cdot e^{\frac{\Phi_V t}{V_S}} + C_{S,MR} \quad (5.2)$$

In this equation,  $C_{S,MC}$  and  $C_{S,MR}$  correspond to the glucose concentrations in the medium entering the mixing vessel during chemostat and retentostat phase respectively. Sampling frequency and sample volume were minimized to limit the impact of sampling on biomass accumulation inside the reactor. Culture purity was routinely checked by microscopy. Full biomass retention was confirmed by plating effluent on YPD containing 2 % (w/v) agar.

**Predicting retentostat growth kinetics** | To enable a smooth transition of the retentostat cultures to near-zero growth rates the operational conditions were defined with a mathematical model that simulates growth kinetics of yeast during aerobic retentostat cultivation. Essentially, the mass balance equation for biomass (Equation 5.3) was solved using MATLAB ode45 solver, by integrating the substrate mass balance (Equation 5.4), with the Herbert-Pirt relation [217] (Equation 5.5).

$$\frac{dC_X}{dt} = \mu C_X \quad (5.3)$$

$$\frac{dC_S}{dt} = \frac{\Phi_V}{V} (C_{S,in} - C_S) - q_S C_X \quad (5.4)$$

$$q_S = \frac{\mu}{Y_{X/S}^{\max}} + m_S \quad (5.5)$$

In these equations,  $C_X$  [ $\text{g L}^{-1}$ ] is the biomass concentration in the retentostat,  $\mu$  [ $\text{h}^{-1}$ ] is the specific growth rate,  $C_S$  [ $\text{g L}^{-1}$ ] is the residual substrate concentration,  $C_{S,in}$  [ $\text{g L}^{-1}$ ] is the substrate concentration in the feed,  $\Phi_V/V$  [ $\text{h}^{-1}$ ] is the dilution rate, and  $q_S$  [ $\text{g}_S \text{g}_X^{-1} \text{h}^{-1}$ ] is the biomass-specific glucose consumption rate. The specific substrate consumption rate can be described by the Herbert-Pirt relation (Equation 5.5), in which  $Y_{X/S}^{\max}$  [ $\text{g g}^{-1}$ ] is the maximum biomass yield on glucose, and  $m_S$  [ $\text{g}_S \text{g}_X^{-1} \text{h}^{-1}$ ] is the maintenance coefficient in gram glucose per gram biomass and hour. Because retentostats were glucose limited and  $C_{S,in} \gg C_S$ , the glucose concentration in the retentostat was assumed to be in a pseudo-steady state such that  $\frac{dC_S}{dt} \approx 0$ .

To run simulations, the model required inputs for  $m_S$  (assumed to be growth-rate independent) and  $Y_{X/S}^{\max}$ , which were extrapolated from a  $q_S$ - $\mu$  relationship from duplicate chemostat experiments performed at 4 different dilution rates between 0.025  $\text{h}^{-1}$  and 0.10  $\text{h}^{-1}$ . In addition, the model required inputs for variables  $V$  [L],  $\varphi_V$  [ $\text{L h}^{-1}$ ],  $C_{S,MC}$  [ $\text{g L}^{-1}$ ],  $C_{S,MR}$  [ $\text{g L}^{-1}$ ], and  $V_S$  [L], and generated time-dependent profiles for biomass accumulation, glucose concentration in the feed, specific glucose consumption rate, and specific growth rate. The final operational conditions

chosen for the retentostat experiments are described above. For instructions on how to perform this analysis in MATLAB including the respective MATLAB codes see Supplementary data of Chapter 4.

**Biomass measurement** | Biomass dry weight concentrations were routinely determined in technical duplicates unless stated otherwise. For pre-steady-state chemostat samples, 5 mL of culture broth were harvested, washed with demineralized water, transferred to a pre-weighed beaker and dried at 105 °C for at least 24 h. Chemostat cultures were considered to be in steady state when, after at least five resident times, biomass concentrations changed by less than 3 % over two consecutive volume changes. Steady-state dry biomass determination was performed using 25 mL of culture broth. To determine dry mass from retentostat phase as well as the preceding chemostat phase, samples were diluted in demineralized water to an approximate cell concentration of 2.5 mg L<sup>-1</sup>. Subsequently, exactly 10 mL of the diluted sample were filtered over pre-dried and pre-weighed membrane filters (pore size 0.45 µm, Pall Life Sciences, USA), washed with demineralized water and dried in a microwave oven for 20 min at 350 W. Biomass determination for calculations of µ<sub>max</sub> from shake-flask cultures for the two strains was based on wet cell weight because flocculation disturbed OD600 measurements. 1 mL of sample was pipetted in a pre-weighed Eppendorf tube and centrifuged at 10,000 × g. The supernatant was carefully removed and the tube weighed again.

**Viability assay** | To measure the viability of retentostat cultures, samples were diluted in PBS to an OD600 of 0.1 and double stained with propidium iodide (PI) stock solution and 5-carboxyfluorescein diacetate acetoxyethyl ester (5-CFDA, AM) stock solution to a final concentration of 2.0 µmol L<sup>-1</sup> and 53.24 µmol L<sup>-1</sup>, respectively (FungaLight 5-CFDA, AM/PI yeast viability kit, Invitrogen, USA). PI is a DNA intercalating fluorescence dye that can only enter cells with compromised cell membranes. Binding of PI to DNA leads to a strong increase in red fluorescence. 5-CFDA, AM is a non-polar and nonfluorescent cell-permeant esterase substrate. Hydrolysis by nonspecific esterases within the cell leads to the generation of polar carboxyfluorescein, a green fluorescent dye, which is no longer cell-permeable. Cells were considered as viable and metabolically active if they were 5-carboxyfluorescein positive and PI negative. Samples were analysed on the Accuri flow cytometer (BD Biosciences, USA).

**Cell size measurement** | Bright field micrographs were converted into 8-bit greyscale images and analyzed with ImageJ. Per reactor and sample point at least 160 cells were measured using the elliptical or the freehand selection tool.

**Regression analysis of biomass accumulation in retentostats** | The maintenance-energy requirements and biomass-specific death rate of *P. pastoris* in aerobic retentostat were estimated from a least-squares regression analysis of data points for the biomass concentration (dry-weight) and the viable biomass concentration over time, using a MATLAB model. From these parameters, the specific growth rate and substrate consumption rates were derived. The curve shape was determined by the solution of the following ordinary differential equations with the smallest sum of square errors:



$$\frac{dC_{X_V}}{dt} = \mu C_{X_V} - k_d C_{X_V} \quad (5.6)$$

$$\frac{dC_{X_d}}{dt} = k_d C_{X_V} \quad (5.7)$$

$$\frac{dC_S}{dt} = \frac{\Phi_V}{V} (C_{S,in} - C_S) - q_S C_X \quad (5.8)$$

In these equations,  $C_{X_V}$  is the viable biomass concentration [ $\text{g L}^{-1}$ ],  $k_d$  is the death rate [ $\text{h}^{-1}$ ] and Equation 5.5 was used to define the specific substrate uptake rate ( $q_S$ ). The model required input for the biomass concentrations measured at different time points, and the following variables:  $V$  [L],  $\varphi_V$  [ $\text{L h}^{-1}$ ],  $C_{S,MC}$  [ $\text{g L}^{-1}$ ],  $C_{S,MR}$  [ $\text{g L}^{-1}$ ],  $V_S$  [L] and  $Y_{X/S}^{\max}$  [ $\text{g g}^{-1}$ ]. A value for  $m_S$  was approximated using parameter estimation. The time-dependent change of  $q_S$  and  $\mu$  during the course of the retentostat followed from the regression analysis. To respect small differences in operational variables per experiment, regression analyses were performed separately on each independent retentostat experiment. For instructions on how to perform this analysis in MATLAB including the respective MATLAB codes see supplemental methods and Supplementary data of Chapter 4..

**HPLC analysis** | For chemostat cultivations the glucose concentration in the feed media was measured with an HPLC set-up (Shimadzu Corporation, Japan) equipped with a Rezex ROA-Organic Acid H + column (300 mm  $\times$  7.8 mm, Phenomenex, USA). A refraction-index detector (RID-10A, Shimadzu Corporation, Japan) was used for quantitation. The column was operated at 60 °C, the flow rate was set at 1 mL  $\text{min}^{-1}$  and 4 mM  $\text{H}_2\text{SO}_4$  served as mobile phase. Before injection, 900  $\mu\text{L}$  sample was mixed with 100  $\mu\text{L}$  of 0.04 M  $\text{H}_2\text{SO}_4$  and filtered through a 0.20  $\mu\text{m}$  RC membrane filter (KC90.1, Roth, Germany). The injection volume was 10  $\mu\text{L}$ .

Determination of the glucose concentration in the mixing vessel, intracellular trehalose contents, and glucose equivalents of intracellular glycogen contents (see below) during retentostat cultivation and the preceding chemostat cultivation was done on an Agilent 1100 HPLC (Agilent Technologies, USA) equipped with an Aminex HPX 87H ion exchange column (BioRad, The Netherlands), operated at 60 °C with 5 mM  $\text{H}_2\text{SO}_4$  as the mobile phase at a flow rate of 0.6 mL  $\text{min}^{-1}$ . Detection was by means of a dual-wavelength absorbance detector (G1314A, Agilent, USA) and a refractive index detector (G1362A, Agilent, USA).

**Calculations on growth rate dependency of  $m_S$  and  $Y_{X/S}^{\max}$**  | To determine how the maintenance energy-substrate requirements and maximum theoretical biomass yield ( $m_S$  and  $Y_{X/S}^{\max}$ ) change with growth rate,  $q_S$  was determined at different  $\mu$  in chemostat and retentostat cultures, and regression analysis on moving windows of four duplicate  $q_S$  values calculated at four different consecutive  $\mu$  values were used to determine  $m_S$  (intercept at y-axis) and  $Y_{X/S}^{\max}$  (reciprocal of the slope). Values for  $\mu$  and  $q_S$  from duplicate chemostat cultures were derived by solving the biomass and substrate mass balances for steady-state conditions respectively. For retentostat cultures, a value for  $\mu$  between two consecutive sampling points was derived by solving

the biomass balance ( $\frac{dC_X}{dt}$ ) between two time points  $t_1$  and  $t_2$  [h] using the corresponding biomass concentrations ( $C_X$ ) [ $\text{g L}^{-1}$ ], resulting in:

$$\mu = \ln \frac{(C_{X2} - C_{X1})}{(t_2 - t_1)} \quad (5.9)$$

The  $q_S$  depends on the amount of limiting substrate glucose (S) [g] consumed in retentostat between certain time points, which follows from integration of Equation 5.2 multiplied by the constant flow rate at which medium is supplied to the bioreactor ( $\phi_V$ ) [ $\text{L h}^{-1}$ ], according to:

$$S_2 - S_1 = \left( \int_{t_1}^{t_2} C_{S,in}(t) \right) \cdot \Phi_V \quad (5.10)$$

The apparent biomass yield on glucose ( $Y_{X/S}$ ) [ $\text{g g}^{-1}$ ] in this period can then be calculated according to:

$$Y_{X/S} = \frac{((C_{X2} - C_{X1}) \cdot V)}{(S_2 - S_1)} \quad (5.11)$$

In this equation,  $V$  [L] represents the bioreactor volume and the glucose entering the bioreactor is assumed to be completely consumed. Accordingly,  $q_S$  can be calculated as:

$$q_S = \frac{\mu}{Y_{X/S}} \quad (5.12)$$

Individual  $q_S$ - $\mu$  plots and corresponding linear regression analyses are shown in Supplementary figure 5.12. Values for  $m_S$  and  $Y_{X/S}^{\max}$  were only derived from  $q_S$ - $\mu$  relationships considered linear ( $R^2 > 0.99$ ).

**Analysis of intracellular glycogen and trehalose content** | Immediately after sampling, 1 mL broth was added to 5 mL of pre-cooled methanol ( $-40$  °C), mixed and centrifuged at  $4,400 \times g$  at  $-19$  °C for 5 min. Cell pellets were washed with 5 mL pre-cooled methanol and stored at  $-80$  °C. For analysis, the pellets were then resuspended and diluted in  $\text{Na}_2\text{CO}_3$  (0.25 M), and further processed as described previously [206]. Trehalose was measured directly by HPLC, whereas glucose released from glycogen was measured by HPLC after overnight incubation of the samples with  $\alpha$ -amylglucosidase (from *Aspergillus niger*, Sigma-Aldrich, Netherlands) at  $57$  °C.

**RNA extraction, microarray hybridization and transcriptome data analysis** | Chemostat and retentostat samples for RNA isolation were immediately added in a 2:1 ratio to a precooled fixing solution (5 % v/v phenol in ethanol absolute) and centrifuged at  $10,000 \times g$  for 1 min. Pellets were stored at  $-80$  °C before further processing. RNA isolation was done using TRI reagent according to the suppliers' instructions (Ambion, USA). RNA integrity and concentration were analyzed

using RNA nano chips (Agilent, USA) and a Nanodrop (Thermo Scientific, USA), respectively. For transcriptome analysis, in-house designed *P. pastoris*-specific oligonucleotide arrays (AMAD-ID: 034821, 8×15K custom arrays, Agilent, USA) were used [107]. Synthesis of cRNA, hybridization as well as scanning was carried out according to the Agilent protocol for 2-color expression arrays. Samples were labeled with Cy3 and Cy5 in triplicates and hybridized against a reference pool generated from cells grown at various culture conditions. For all samples dye swap experiments were carried out.

Normalization steps and statistical analysis of microarray data included background correction with the “normexp” method with an offset of 50 [228], removal of color bias using locally weighted MA-scatterplot smoothing (LOESS) followed by between array normalization using the “Aquantile” method. The p-values associated with the differential expression values were calculated using a linear model fit and an eBayes adjustment (limma R package), subsequently they were adjusted for multiple testing using the method of Benjamini and Hochberg [22] using the BH method of limma R package. For identifying differentially expressed genes, the following criteria were applied: fold change (FC) cut-off of at least  $2 > FC > 1/2$  and adjusted p-value  $< 0.05$ . All steps were done using the R software package <http://www.rproject.org>, and the limma package. Samples taken from the different bioreactor systems were not directly compared to each other, but log<sub>2</sub> fold change (FC) values were calculated in both cases against the  $0.1 \text{ h}^{-1}$  chemostat set point. Transcriptomics data have been deposited at Gene Expression Omnibus with the accession number GSE81070.

**Cluster analysis and Gene Ontology (GO) term enrichment** | Genes that were differentially expressed at least in one comparison (see above) were grouped according to their expression profile by the Genesis software tool [260] employing k-means clustering and Pearson correlation. According to Figure of Merit analysis a k of 2 was determined to be the ideal number of clusters for the dataset. For determination of enriched Gene Ontology (GO) terms in the respective clusters the online Generic GO Term Finder tool <http://go.princeton.edu/cgi-bin/GOTermFinder> and Saccharomyces Genome Database (SGD) annotations were used. The cut off for the corrected p-value (Bonferroni correction) was set to 0.05 and a *P. pastoris* specific background list comprised of all annotated genes and genes with unknown function was provided.

**Determination of residual glucose** | Rapid sampling and quenching with cold steel beads of culture broth was done as described previously [183]. Residual glucose concentrations were measured using the GOPOD D-Glucose Assay (Megazymes, Ireland). The protocol provided by the manufacturer was adapted to a 96-well format. Briefly, 60  $\mu\text{L}$  of sample were mixed with an equal volume of GOPOD reagent. After incubation at 37 °C for 30 min, absorbance at 510 nm was measured with a Tecan plate reader (Switzerland). A standard curve and linear regression was used to calculate residual glucose concentrations. Absorbance to glucose concentration ratios were linear down to  $1 \text{ mg L}^{-1}$  glucose.

**Cell cycle distribution analysis** | For fixation, 1 mL of 70 % ethanol was added dropwise to 20  $\mu\text{L}$  of the cell culture and subsequently stored at -20 °C. To measure cell cycle distribution, an aliquot of 350  $\mu\text{L}$  was centrifuged for 3 min at  $10,000 \times g$  and washed using PBS-Tween20 (0.1 %) employing

the same centrifuge settings. Pellets were resuspended in 1 mL PBS and 10  $\mu\text{L}$  of a 100  $\text{mg mL}^{-1}$  RNAse A (from bovine pancreas, Sigma-Aldrich, USA) solution were added. After incubation for 1 h at 37 °C, samples were pelleted again and washed as described before. Finally, the cell pellets were resuspended in 1 mL PBS and sonicated twice at 85 % for 10 s each (Ultrasonic processor UIS250L & Sonotrode LTS24d10.4L2, Hielscher, Germany). A 150  $\mu\text{L}$  aliquot of the sonicated cell suspension was mixed with 150  $\mu\text{L}$  PI stock solution (4.30  $\mu\text{M}$ ) and analyzed on the Gallios™ flow cytometer (Beckman Coulter, USA).

## Supplementary material Chapter

### Supplementary figures

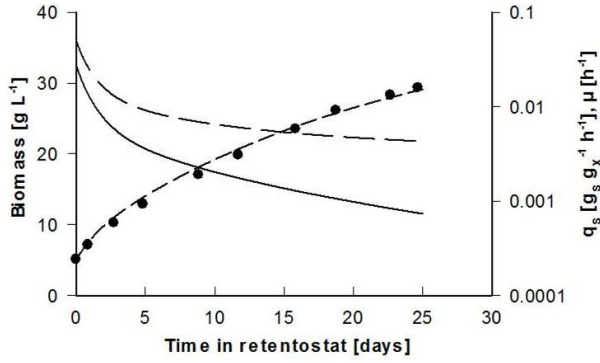


**Figure 5.11:** Example of non-linear regression analysis of viable biomass for one retentostat. Viable biomass (closed circles), non-linear regression of viable biomass (short dashed line) and resulting glucose uptake rate ( $q_s$ , long dashed line) as well as specific growth rate ( $\mu$ , solid line).

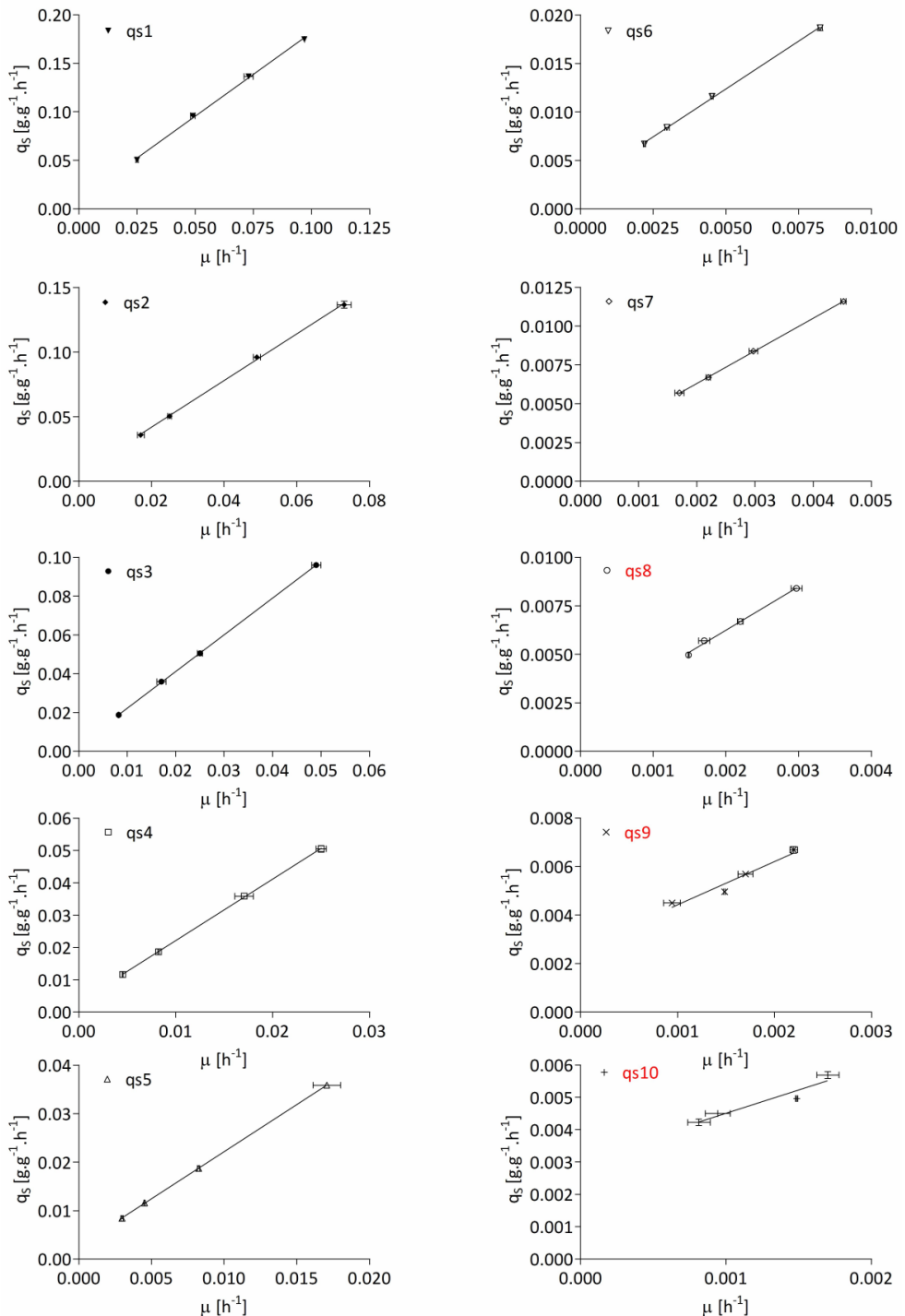


**Figure 5.12:** Regression analysis on overlapping sets of specific growth rate versus glucose uptake rate relations ( $\mu$  -  $q_s$ ) from four data points measured at different consecutive specific growth rates (see Materials and Methods). Values for the maintenance coefficient ( $m_s$ ) and the maximum yield on biomass ( $Y_{X/S}^{\max}$ ) were calculated from plots qs1 - qs7 which resulted in a  $R^2$  of at least 0.99. Linear regression on data represented in plots qs8 - qs10 resulted in  $R^2$  values below 0.99 and were not considered further to assess the growth rate dependency of  $m_s$  and  $Y_{X/S}^{\max}$  as depicted in Figure 5.6 in the manuscript.

## Supplementary tables

**Table 5.3:** Apparent biomass yield ( $Y_{X/S}$ ) and maximum specific growth rate ( $\mu_{\max}$ ) of wild-type *P. pastoris* CBS 7435 (*FLO8*) and an isogenic  $\Delta flo8$  strain.

Strain	$Y_{X/S}^*$ ( $\pm$ SD)	$\mu_{\max}$ ( $\pm$ SD)
CBS 7435 $\Delta flo8$	0.511 $\pm$ 0.0045	0.22 $\pm$ 0.0013
CBS 7435 <i>FLO8</i>	0.534 $\pm$ 0.0030	0.25 $\pm$ 0.0026

**Table 5.4:** Colony-forming units (CFU)\* in percent of total cell concentration during retentostat cultivation.

Days after switch to retentostat mode	CFU for reactor 1 (%)	CFU for reactor 2 (%)
18.8	139 $\pm$ 1.3	106 $\pm$ 8.0
22.7	91 $\pm$ 3.4	92 $\pm$ 4.6
23.7	103 $\pm$ 6.7	85 $\pm$ 5.1

\*CFU was assessed by diluting cells in sterile 0.1 % peptone to approximately  $5 \times 10^7$  cells per mL and sonicated at 8 ampere for 3 seconds (Soniprep 150, Fisher Scientific, USA). The exact cell concentration was determined using a hemocytometer and tenfold dilution series were made (5 to 6 dilutions) in 0.1 % peptone.

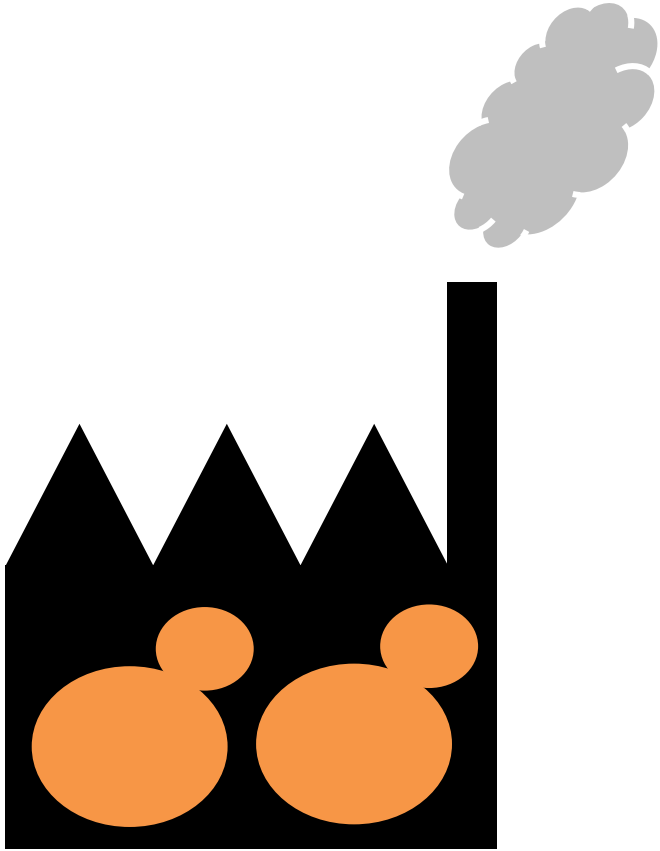
Appropriate aliquots of the final dilutions were plated on YPD plates in at least 2 technical duplicates and incubated at 30 °C for two days before colonies were counted.

## Additional files

The MATLAB codes and instructions on how to use them in order to run the retentostat prediction model and the regression model are equal to the MATLAB codes and instructions described for *S. cerevisiae* in the additional files of Chapter 4, with the following modifications: the strain specific parameters ( $m_S$  and  $Y_{X/S}^{\max}$ ) and operational parameters ( $C_{S,MC}$  and  $C_{S,MR}$ ) are adjusted as described in the Methods section.







## Bibliography

- [1] ABBOTT, D. A., KNIJNENBURG, T. A., DE POORTER, L. M. I., REINDERS, M. J. T., PRONK, J. T., AND VAN MARIS, A. J. A. Generic and specific transcriptional responses to different weak organic acids in anaerobic chemostat cultures of *Saccharomyces cerevisiae*. *FEMS yeast research* 7, 6 (sep 2007), 819–33.
- [2] ABU-ZEID, M. Water and sustainable development: the vision for world water, life and the environment. *Water Policy* 1, 1 (feb 1998), 9–19.
- [3] AERTS, A. M., ZABROCKI, P., GOVAERT, G., MATHYS, J., CARMONA-GUTIERREZ, D., MADEO, F., WINDERICKX, J., CAMMUE, B. P. A., AND THEVISSSEN, K. Mitochondrial dysfunction leads to reduced chronological lifespan and increased apoptosis in yeast. *FEBS Letters* 583, 1 (jan 2009), 113–117.
- [4] AHMAD, M., HIRZ, M., PICHLER, H., AND SCHWAB, H. Protein expression in *Pichia pastoris*: Recent achievements and perspectives for heterologous protein production. *Applied Microbiology and Biotechnology* 98, 12 (2014), 5301–5317.
- [5] ALLEN, C. Isolation of quiescent and nonquiescent cells from yeast stationary-phase cultures. *The Journal of Cell Biology* 174, 1 (jul 2006), 89–100.
- [6] ANDRIANANTOANDRO, E., BASU, S., KARIG, D. K., AND WEISS, R. Synthetic biology: new engineering rules for an emerging discipline. *Molecular Systems Biology* 2 (may 2006).
- [7] ARAGON, A. D., AND RODRIGUEZ, A. L. Characterization of differentiated quiescent and nonquiescent cells in yeast stationary-phase cultures. *Molecular Biology of the Cell* 19, March (2008), 1271–1280.
- [8] ARBIGE, M., AND CHESBRO, W. R. W. R. Very slow growth of *Bacillus polymyxa*: Stringent response and maintenance energy. *Archives of Microbiology* 132, 4 (oct 1982), 338–344.
- [9] ATKINSON, D. E. Energy charge of the adenylate pool as a regulatory parameter. Interaction with feedback modifiers. *Biochemistry* 7, 11 (nov 1968), 4030–4034.
- [10] ATTFIELD, P. V. Stress tolerance: The key to effective strains of industrial baker's yeast. *Nature Biotechnology* 15, 13 (dec 1997), 1351–1357.
- [11] BACHMANN, H., STARRENBURG, M. J. C., MOLENAAR, D., KLEEREBEZEM, M., AND VAN HYLCKAMA Vlieg, J. E. T. Microbial domestication signatures of *Lactococcus lactis* can be reproduced by experimental evolution. *Genome research* 22, 1 (jan 2012), 115–24.
- [12] BAGANZ, F., HAYES, A., MARREN, D., GARDNER, D. C. J., AND OLIVER, S. G. Suitability of replacement markers for functional analysis studies in *Saccharomyces cerevisiae*. *Yeast* 13, 16 (dec 1997), 1563–1573.

- [13] BAKKER, B. M., OVERKAMP, K. M., VAN MARIS, A. J. A., KÖTTER, P., LUTTIK, M. A. H., VAN DIJKEN, J. P., AND PRONK, J. T. Stoichiometry and compartmentation of NADH metabolism in *Saccharomyces cerevisiae*. *FEMS microbiology reviews* 25, 1 (jan 2001), 15–37.
- [14] BALABAN, R. S., NEMOTO, S., AND FINKEL, T. Mitochondria, oxidants, and aging. *Cell* 120, 4 (feb 2005), 483–95.
- [15] BALL, W. J., AND ATKINSON, D. E. Adenylate energy charge in *Saccharomyces cerevisiae* during starvation. *Journal of bacteriology* 121, 3 (mar 1975), 975–82.
- [16] BARROS, M. H., DA CUNHA, F. M., OLIVEIRA, G. A., TAHARA, E. B., AND KOWALTOWSKI, A. J. Yeast as a model to study mitochondrial mechanisms in ageing. *Mechanisms of Ageing and Development* 131, 7-8 (jul 2010), 494–502.
- [17] BARTHELMEBS, L., DIVIES, C., AND CAVIN, J. F. Knockout of the p-coumarate decarboxylase gene from *Lactobacillus plantarum* reveals the existence of two other inducible enzymatic activities involved in phenolic acid metabolism. *Applied and environmental microbiology* 66, 8 (aug 2000), 3368–75.
- [18] BASSO, L. C., BASSO, T. O., AND ROCHA, S. N. Ethanol Production in Brazil : The Industrial Process and Its Impact on Yeast Fermentation. In *Biofuel production recent developments and prospects*, M. dos Santos Bernardes, Ed., vol. 1530. Intech, Rijeka, 2011, pp. 85–100.
- [19] BECKER, J., ARMSTRONG, G., VANDERMERWE, M., LAMBRECHTS, M., VIVIER, M., AND PRETORIUS, I. Metabolic engineering of for the synthesis of the wine-related antioxidant resveratrol. *FEMS Yeast Research* 4, 1 (oct 2003), 79–85.
- [20] BEEKWILDER, J., WOLSWINKEL, R., JONKER, H., HALL, R., DE VOS, C. H. R., AND BOVY, A. Production of Resveratrol in Recombinant Microorganisms. *Applied and Environmental Microbiology* 72, 8 (aug 2006), 5670–5672.
- [21] BELL-LELONG, D. A., CUSUMANO, J. C., MEYER, K., AND CHAPPLE, C. Cinnamate-4-hydroxylase expression in *Arabidopsis*. Regulation in response to development and the environment. *Plant physiology* 113, 3 (1997), 729–38.
- [22] BENJAMINI, J., AND HOCHBERG, Y. Controlling the false discovery rate: a practical and powerful approach to multiple testing. *Journal of the Royal Statistical Society. Series B (Methodological)* 57, 1 (1995), 289–300.
- [23] BENOIT, I., CULLETON, H., ZHOU, M., DIFALCO, M., AGUILAR-OSORIO, G., BATTAGLIA, E., BOUZID, O., BROUWER, C. P. J. M., EL-BUSHARI, H. B. O., COUTINHO, P. M., GRUBEN, B. S., HILDÉN, K. S., HOUBRAKEN, J., BARBOZA, L. A. J., LEVASSEUR, A., MAJOUR, E., MÄKELÄ, M. R., NARANG, H.-M., TREJO-AGUILAR, B., VAN DEN BRINK, J., VANKUYK, P. A., WIEBENGA, A., MCKIE, V., MCCLEARY, B., TSANG, A., HENRISSAT, B., AND DE VRIES, R. P. Closely related fungi employ diverse enzymatic strategies to degrade plant biomass. *Biotechnology for Biofuels* 8, 1 (dec 2015), 107.
- [24] BINAI, N. A., BISSCHOPS, M. M. M., VAN BREUKELLEN, B., MOHAMMED, S., LOEFF, L., PRONK, J. T., HECK, A. J. R., DARAN-LAPUJADE, P., AND SLIJPER, M. Proteome adaptation of *Saccharomyces cerevisiae* to severe calorie restriction in Retentostat cultures. *Journal of proteome research* 13, 8 (3553 2014), 3542.
- [25] BISSCHOPS, M. M. M., VOS, T., MARTINEZ-MORENO, R., DE LA TORRE CORTES, P., PRONK, J. T., AND DARAN-LAPUJADE, P. Oxygen availability strongly affects chronological lifespan and thermotolerance in batch cultures of *Saccharomyces cerevisiae*. *Microbial Cell* 2, 11 (nov 2015), 429–444.
- [26] BISSCHOPS, M. M. M., ZWARTJENS, P., KEUTER, S. G. F., PRONK, J. T., AND DARAN-LAPUJADE, P. To divide or not to divide: a key role of Rim15 in calorie-restricted yeast cultures. *Biochimica et biophysica acta* 1843, 5 (may 2014), 1020–30.
- [27] BOENDER, L. G. M., ALMERING, M. J. H., DIJK, M., VAN MARIS, A. J. A., DE WINDE, J. H., PRONK, J. T., AND DARAN-LAPUJADE, P. Extreme calorie restriction and energy source starvation in *Saccharomyces cerevisiae* represent distinct physiological states. *Biochimica et biophysica acta* 1813, 12 (dec 2011), 2133–44.

- [28] BOENDER, L. G. M., DE HULSTER, E. A. F., VAN MARIS, A. J. A., DARAN-LAPUJADE, P., AND PRONK, J. T. Quantitative physiology of *Saccharomyces cerevisiae* at near-zero specific growth rates. *Applied and environmental microbiology* 75, 17 (sep 2009), 5607–14.
- [29] BOENDER, L. G. M., VAN MARIS, A. J. A., DE HULSTER, E. A. F., ALMERING, M. J. H., VAN DER KLEI, I. J., VEENHUIS, M., DE WINDE, J. H., PRONK, J. T., AND DARAN-LAPUJADE, P. Cellular responses of *Saccharomyces cerevisiae* at near-zero growth rates: transcriptome analysis of anaerobic retentostat cultures. *FEMS yeast research* 11, 8 (dec 2011), 603–20.
- [30] BOER, V. M., CRUTCHFIELD, C. A., BRADLEY, P. H., BOTSTEIN, D., AND RABINOWITZ, J. D. Growth-limiting intracellular metabolites in yeast growing under diverse nutrient limitations. *Molecular biology of the cell* 21, 1 (jan 2010), 198–211.
- [31] BOLES, E., AND HOLLENBERG, C. P. The molecular genetics of hexose transport in yeasts. *FEMS Microbiology Reviews* 21, 1 (1997), 85–111.
- [32] BONAWITZ, N. D., CHATENAY-LAPOINTE, M., PAN, Y., AND SHADEL, G. S. Reduced TOR Signaling Extends Chronological Life Span via Increased Respiration and Upregulation of Mitochondrial Gene Expression. *Cell Metabolism* 5, 4 (apr 2007), 265–277.
- [33] BOTSTEIN, D., AND FINK, G. R. Yeast: An Experimental Organism for 21st Century Biology. *Genetics* 189, 3 (nov 2011), 695–704.
- [34] BOULTON, C., AND BOX, W. *Formation and Disappearance of Diacetyl During Lager Fermentation*. Blackwell Science, 2008, pp. 181–195.
- [35] BOUTTE, C. C., AND CROSSON, S. Bacterial lifestyle shapes stringent response activation. *Trends in microbiology* 21, 4 (apr 2013), 174–80.
- [36] BRAUER, M. J. M. J., HUTTENHOWER, C., AIROLDI, E. M. E. M., ROSENSTEIN, R., MATESE, J. C. J. C., GRESHAM, D., BOER, V. M. V. M., TROYANSKAYA, O. G., AND BOTSTEIN, D. Coordination of growth rate, cell cycle, stress response, and metabolic activity in yeast. *Molecular Biology of the Cell* 19, 1 (2008), 352–367.
- [37] BREITENBACH, M., JAZWINSKI, S., AND LAUN, P. *Aging research in yeast*. Springer Netherlands, Dordrecht, 2012.
- [38] BREITENBACH, M., RINNERHALER, M., HARTL, J., STINCONE, A., VOWINCKEL, J., BREITENBACH-KOLLER, H., AND RALSER, M. Mitochondria in ageing: there is metabolism beyond the ROS. *FEMS Yeast Research* 14, 1 (feb 2014), 198–212.
- [39] BRIDGES, H. R., GRGIC, L., HARBOUR, M. E., AND HIRST, J. The respiratory complexes I from the mitochondria of two *Pichia* species. *Biochemical Journal* 422, 1 (aug 2009), 151–159.
- [40] BROCK, T. D. Microbial growth rates in nature. *Bacteriological reviews* 35, 1 (mar 1971), 39–58.
- [41] BROWN, C. J., TODD, K. M., AND ROSENZWEIG, R. F. Multiple duplications of yeast hexose transport genes in response to selection in a glucose-limited environment. *Molecular biology and evolution* 15, 8 (aug 1998), 931–42.
- [42] BROWN, J. E., AND DAWES, I. W. Regulation of chorismate mutase in *Saccharomyces cerevisiae*. *Molecular & general genetics : MGG* 220, 2 (jan 1990), 283–8.
- [43] BÜCHS, J. Introduction to advantages and problems of shaken cultures. *Biochemical Engineering Journal* 7, 2 (mar 2001), 91–98.
- [44] BURTNER, C. R., MURAKAMI, C. J., OLSEN, B., KENNEDY, B. K., AND KAEBERLEIN, M. A genomic analysis of chronological longevity factors in budding yeast. *Cell Cycle* 10, 9 (may 2011), 1385–1396.
- [45] CANELAS, A. B., RAS, C., TEN PIERICK, A., VAN DAM, J. C., HEIJNEN, J. J., AND VAN GULIK, W. M. Leakage-free rapid quenching technique for yeast metabolomics. *Metabolomics* 4, 3 (sep 2008), 226–239.

- [46] CASPETA, L., CHEN, Y., GHIACI, P., FEIZI, A., BUSKOV, S., HALLSTROM, B. M., PETRANOVIC, D., AND NIELSEN, J. Altered sterol composition renders yeast thermotolerant. *Science* 346, 6205 (oct 2014), 75–78.
- [47] CASTRILLO, J. I., ZEEF, L. A., HOYLE, D. C., ZHANG, N., HAYES, A., GARDNER, D. C. J., CORNELL, M. J., PETTY, J., HAKES, L., WARDLEWORTH, L., RASH, B., BROWN, M., DUNN, W. B., BROADHURST, D., O'DONOGHUE, K., HESTER, S. S., DUNKLEY, T. P. J., HART, S. R., SWAINSTON, N., LI, P., GASKELL, S. J., PATON, N. W., LILLEY, K. S., KELL, D. B., AND OLIVER, S. G. Growth control of the eukaryote cell: a systems biology study in yeast. *Journal of biology* 6, 2 (2007), 4.
- [48] CHAMBEL, A., VIEGAS, C., AND SÁ-CORREIA, I. Effect of cinnamic acid on the growth and on plasma membrane H<sup>+</sup>-ATPase activity of *Saccharomyces cerevisiae*. *International journal of food research* 50 (1999), 173–179.
- [49] CHAO, R., YUAN, Y., AND ZHAO, H. Recent advances in DNA assembly technologies. *FEMS Yeast Research* 15, 1 (2015), 1–9.
- [50] CHAO, Y. Y., AND KEARNS, D. R. Magnetic resonance studies of copper(II) interaction with nucleosides and nucleotides. *Journal of the American Chemical Society* 99, 19 (sep 1977), 6425–34.
- [51] CHEMLER, J. A., YAN, Y., AND KOFFAS, M. A. G. Biosynthesis of isoprenoids, polyunsaturated fatty acids and flavonoids in *Saccharomyces cerevisiae*. *Microbial cell factories* 5 (2006), 20.
- [52] CHEN, Q., DING, Q., AND KELLER, J. N. The stationary phase model of aging in yeast for the study of oxidative stress and age-related neurodegeneration. *Biogerontology* 6, 1 (2005), 1–13.
- [53] CHESBRO, W., EVANS, T., AND EIFERT, R. Very slow growth of *Escherichia coli*. *Journal of Bacteriology* 139, 2 (1979), 625–638.
- [54] CHESTER, V. E. The dissimilation of the carbohydrate reserves of a strain of *Saccharomyces cerevisiae*. *The Biochemical journal* 86 (jan 1963), 153–60.
- [55] CHOI, J.-S., AND LEE, C.-K. Maintenance of cellular ATP level by caloric restriction correlates chronological survival of budding yeast. *Biochemical and Biophysical Research Communications* 439, 1 (sep 2013), 126–131.
- [56] CHRISTIANO, R., NAGARAJ, N., FRÖHLICH, F., AND WALTHER, T. C. Global Proteome Turnover Analyses of the Yeasts *S. cerevisiae* and *S. pombe*. *Cell reports* 9, 5 (dec 2014), 1959–1965.
- [57] COHEN, J. E. Human population: the next half century. *Science (New York, N.Y.)* 302, 5648 (nov 2003), 1172–1175.
- [58] COHEN, S. N., CHANG, A. C. Y., BOYER, H. W., AND HELLING, R. B. Construction of Biologically Functional Bacterial Plasmids In Vitro. *Proceedings of the National Academy of Sciences* 70, 11 (nov 1973), 3240–3244.
- [59] COX, K. H. Cytoplasmic Compartmentation of Gln3 during Nitrogen Catabolite Repression and the Mechanism of Its Nuclear Localization during Carbon Starvation in *Saccharomyces cerevisiae*. *Journal of Biological Chemistry* 277, 40 (sep 2002), 37559–37566.
- [60] CREGG, J. M., BARRINGER, K. J., HESSLER, A. Y., AND MADDEN, K. R. *Pichia pastoris* as a host system for transformations. *Molecular and Cellular Biology* 5, 12 (dec 1985), 3376–3385.
- [61] CROUGHAN, M. S., KONSTANTINOV, K. B., AND COONEY, C. The future of industrial bioprocessing: batch or continuous? *Biotechnology and bioengineering* 112, 4 (apr 2015), 648–51.
- [62] CROWE, J. H. Trehalose as a "chemical chaperone": Fact and fantasy. *Advances in experimental medicine and biology* 594 (2007), 143–158.
- [63] CULLEN, P. J., AND SPRAGUE, G. F. The Regulation of Filamentous Growth in Yeast. *Genetics* 190, 1 (jan 2012), 23–49.
- [64] CURTIS, T., DARAN, J.-M., PRONK, J. T., FREY, J., JANSSON, J. K., ROBBINS-PIANKA, A., KNIGHT, R., SCHNÜRER, A., SMETS, B. F., SMID, E. J., ABEE, T., VICENTE, M., AND ZENGLER, K. Crystal ball - 2013. *Microbial Biotechnology* 6, 1 (jan 2013), 3–16.

- [65] DARAN-LAPUJADE, P., DARAN, J. M., KÖTTER, P., PETIT, T., PIPER, M. D. W., AND PRONK, J. T. Comparative genotyping of the *Saccharomyces cerevisiae* laboratory strains S288C and CEN.PK113-7D using oligonucleotide microarrays. *FEMS yeast research* 4, 3 (dec 2003), 259–69.
- [66] DARAN-LAPUJADE, P., DARAN, J.-M., LUTTIK, M. A. H., ALMERING, M. J. H., PRONK, J. T., AND KÖTTER, P. An atypical PMR2 locus is responsible for hypersensitivity to sodium and lithium cations in the laboratory strain *Saccharomyces cerevisiae* CEN.PK113-7D. *FEMS yeast research* 9, 5 (aug 2009), 789–92.
- [67] DARAN-LAPUJADE, P., JANSSEN, M. L. A., DARAN, J.-M., VAN GULIK, W., DE WINDE, J. H., AND PRONK, J. T. Role of transcriptional regulation in controlling fluxes in central carbon metabolism of *Saccharomyces cerevisiae*: A chemostat culture study. *Journal of Biological Chemistry* 279, 10 (2004), 9125–9138.
- [68] DARAN-LAPUJADE, P., ROSSELL, S., VAN GULIK, W. M., LUTTIK, M. A. H., DE GROOT, M. J. L., SLIJPER, M., HECK, A. J. R., DARAN, J.-M., DE WINDE, J. H., WESTERHOFF, H. V., PRONK, J. T., AND BAKKER, B. M. The fluxes through glycolytic enzymes in *Saccharomyces cerevisiae* are predominantly regulated at posttranscriptional levels. *Proceedings of the National Academy of Sciences of the United States of America* 104, 40 (oct 2007), 15753–8.
- [69] DAVIDSON, G. S., JOE, R. M., AND ROY, S. The proteomics of quiescent and nonquiescent cell differentiation in yeast stationary-phase cultures. *Molecular biology of the cell* (2011).
- [70] DE DEKEN, R. H. The Crabtree effect: a regulatory system in yeast. *Journal of general microbiology* 44, 2 (aug 1966), 149–56.
- [71] DE GROOT, M. J. L., DARAN-LAPUJADE, P., VAN BREUKELLEN, B., KNIJNENBURG, T. A., DE HULSTER, E. A. F., REINDERS, M. J. T., PRONK, J. T., HECK, A. J. R., AND SLIJPER, M. Quantitative proteomics and transcriptomics of anaerobic and aerobic yeast cultures reveals post-transcriptional regulation of key cellular processes. *Microbiology* 153, Pt 11 (nov 2007), 3864–78.
- [72] DE HOLLANDER, J. A. Kinetics of microbial product formation and its consequences for the optimization of fermentation processes. *Antonie van Leeuwenhoek* 63, 3-4 (sep 1993), 375–81.
- [73] DE VIRGILIO, C., HOTTIGER, T., DOMINGUEZ, J., BOLLER, T., AND WIEMKEN, A. The role of trehalose synthesis for the acquisition of thermotolerance in yeast. I. Genetic evidence that trehalose is a thermoprotectant. *European journal of biochemistry / FEBS* 219, 1-2 (1994), 179–186.
- [74] DELIC, M., MATTANOVICH, D., AND GASSER, B. Monitoring intracellular redox conditions in the endoplasmic reticulum of living yeasts. *FEMS microbiology letters* 306, 1 (may 2010), 61–6.
- [75] DELUNA, A., AVENDANO, A., RIEGO, L., AND GONZALEZ, A. NADP-glutamate dehydrogenase isoenzymes of *Saccharomyces cerevisiae*. Purification, kinetic properties, and physiological roles. *The Journal of biological chemistry* 276, 47 (2001), 43775–83.
- [76] DENOTH LIPPUNER, A., JULOU, T., AND BARRAL, Y. Budding yeast as a model organism to study the effects of age. *FEMS Microbiology Reviews* 38, 2 (2014), 300–325.
- [77] DICARLO, J. E., NORVILLE, J. E., MALI, P., RIOS, X., AACH, J., AND CHURCH, G. M. Genome engineering in *Saccharomyces cerevisiae* using CRISPR-Cas systems. *Nucleic acids research* 41, 7 (apr 2013), 4336–43.
- [78] DIDERICH, J. A., SCHEPPER, M., VAN HOEK, P., LUTTIK, M. A. H., VAN DIJKEN, J. P., PRONK, J. T., KLAASSEN, P., BOELEN, H. F., DE MATTOS, M. J., VAN DAM, K., AND KRUCKEBERG, A. L. Glucose uptake kinetics and transcription of *HXT* genes in chemostat cultures of *Saccharomyces cerevisiae*. *The Journal of biological chemistry* 274, 22 (may 1999), 15350–9.
- [79] DUFOURC, E. J. Sterols and membrane dynamics. *Journal of Chemical Biology* 1, 1-4 (nov 2008), 63–77.
- [80] EASTMOND, D. L., AND NELSON, H. C. M. Genome-wide analysis reveals new roles for the activation domains of the *Saccharomyces cerevisiae* heat shock transcription factor (Hsf1) during the transient heat shock response. *The Journal of biological chemistry* 281, 43 (oct 2006), 32909–21.
- [81] EGLI, T. How to live at very low substrate concentration. *Water research* 44, 17 (sep 2010), 4826–37.

- [82] EHLTING, J., BÜTTNER, D., WANG, Q., DOUGLAS, C. J., SOMSSICH, I. E., AND KOMBRINK, E. Three 4-coumarate:coenzyme A ligases in *Arabidopsis thaliana* represent two evolutionarily divergent classes in angiosperms. *The Plant journal : for cell and molecular biology* 19, 1 (1999), 9–20.
- [83] ENGELS, B., DAHM, P., AND JENNEWEIN, S. Metabolic engineering of taxadiene biosynthesis in yeast as a first step towards Taxol (Paclitaxel) production. *Metabolic Engineering* 10, 3-4 (may 2008), 201–206.
- [84] ENTIAN, K.-D., AND KÖTTER, P. 25 Yeast Genetic Strain and Plasmid Collections. 629–666.
- [85] ERCAN, O., BISSCHOPS, M. M. M., OVERKAMP, W., JØRGENSEN, T. R., RAM, A. F., SMID, E. J., PRONK, J. T., KUIPERS, O. P., DARAN-LAPUJADE, P., AND KLEEREBEZEM, M. Physiological and transcriptional responses of different industrial microbes at near-zero specific growth rates. *Applied and environmental microbiology* 81, 17 (jun 2015), 5662–5670.
- [86] ERCAN, O., SMID, E. J., AND KLEEREBEZEM, M. Quantitative physiology of *Lactococcus lactis* at extreme low-growth rates. *Environmental Microbiology* 15, 8 (2013), 2319–2332.
- [87] FABRIZIO, P., AND LONGO, V. D. The chronological life span of *Saccharomyces cerevisiae*. *Aging cell* 2, 2 (apr 2003), 73–81.
- [88] FAIRHEAD, C., LLORENTE, B., DENIS, F., SOLER, M., AND DUJON, B. New vectors for combinatorial deletions in yeast chromosomes and for gap-repair cloning using 'split-marker' recombination. *Yeast (Chichester, England)* 12, 14 (nov 1996), 1439–57.
- [89] FAMILI, I., FORSTER, J., NIELSEN, J., AND PALSSON, B. O. *Saccharomyces cerevisiae* phenotypes can be predicted by using constraint-based analysis of a genome-scale reconstructed metabolic network. *Proceedings of the National Academy of Sciences of the United States of America* 100, 23 (2003), 13134–9.
- [90] FAZIO, A., JEWETT, M. C., DARAN-LAPUJADE, P., MUSTACCHI, R., USAITE, R., PRONK, J. T., WORKMAN, C. T., AND NIELSEN, J. Transcription factor control of growth rate dependent genes in *Saccharomyces cerevisiae*: a three factor design. *BMC genomics* 9 (jan 2008), 341.
- [91] FERENCI, T. Hungry bacteria - definition and properties of a nutritional state. *Environmental Microbiology* 3, 10 (oct 2001), 605–611.
- [92] FICHTNER, L., SCHULZE, F., AND BRAUS, G. H. Differential Flo8p-dependent regulation of *FLO1* and *FLO11* for cell-cell and cell-substrate adherence of *S. cerevisiae* S288c. *Molecular Microbiology* 66, 5 (dec 2007), 1276–1289.
- [93] FRANÇOIS, J., AND PARROU, J. L. J. L. Reserve carbohydrates metabolism in the yeast *Saccharomyces cerevisiae*. *FEMS Microbiology Reviews* 25, 1 (jan 2001), 125–145.
- [94] FREIRE-MORAN, L., ARONSSON, B., MANZ, C., GYSSENS, I. C., SO, A. D., MONNET, D. L., AND CARS, O. Critical shortage of new antibiotics in development against multidrug-resistant bacteria - Time to react is now. *Drug Resistance Updates* 14, 2 (2011), 118–124.
- [95] GALDIERI, L., MEHROTRA, S., YU, S., AND VANCURA, A. Transcriptional Regulation in Yeast during Diauxic Shift and Stationary Phase. *OMICS: A Journal of Integrative Biology* 14, 6 (dec 2010), 629–638.
- [96] GANCEDO, J. M. Yeast carbon catabolite repression. *Microbiology and molecular biology reviews : MMBR* 62, 2 (jun 1998), 334–61.
- [97] GASCH, A. P., SPELLMAN, P. T., KAO, C. M., CARMEL-HAREL, O., EISEN, M. B., STORZ, G., BOTSTEIN, D., AND BROWN, P. O. Genomic Expression Programs in the Response of Yeast Cells to Environmental Changes. *Molecular Biology of the Cell* 11, 12 (dec 2000), 4241–4257.
- [98] GASSER, B., MAURER, M., GACH, J., KUNERT, R., AND MATTANOVICH, D. Engineering of *Pichia pastoris* for improved production of antibody fragments. *Biotechnology and bioengineering* 94, 2 (jun 2006), 353–61.
- [99] GASSER, B., PRIELHOFER, R., MARX, H., MAURER, M., NOCON, J., STEIGER, M., PUXBAUM, V., SAUER, M., AND MATTANOVICH, D. *Pichia pastoris*: protein production host and model organism for biomedical research. *Future microbiology* 8, 2 (feb 2013), 191–208.

- [100] GIBNEY, P. A., LU, C., CAUDY, A. A., HESS, D. C., AND BOTSTEIN, D. Yeast metabolic and signaling genes are required for heat-shock survival and have little overlap with the heat-induced genes. *Proceedings of the National Academy of Sciences* 110, 46 (nov 2013), E4393–E4402.
- [101] GIBSON, B. R., LAWRENCE, S. J., LECLAIRE, J. P. R., POWELL, C. D., AND SMART, K. A. Yeast responses to stresses associated with industrial brewery handling: Figure 1. *FEMS Microbiology Reviews* 31, 5 (sep 2007), 535–569.
- [102] GIBSON, D. G. Synthesis of DNA fragments in yeast by one-step assembly of overlapping oligonucleotides. *Nucleic Acids Research* 37, 20 (nov 2009), 6984–6990.
- [103] GIUSEPPIN, M. L. F., ALMKERK, J. W., HEISTEK, J. C., AND VERRIPS, C. T. A comparison of guar  $\alpha$ -galactosidase production by *Saccharomyces cerevisiae* SU50B and *Hansenula polymorpha* 8/2 in continuous cultures. *Progress in Biotechnology* 9 (1994), 421–424.
- [104] GODDARD, M. R., AND GREIG, D. *Saccharomyces cerevisiae*: a nomadic yeast with no niche? *FEMS Yeast Research* 15, 3 (apr 2015), fov009–fov009.
- [105] GOFFEAU, A., BARRELL, B. G., BUSSEY, H., DAVIS, R. W., DUJON, B., FELDMANN, H., GALIBERT, F., HOHEISEL, J. D., JACQ, C., JOHNSTON, M., LOUIS, E. J., MEWES, H. W., MURAKAMI, Y., PHILIPPSSEN, P., TETTELIN, H., AND OLIVER, S. G. Life with 6000 Genes. *Science* 274, October (1996), 546–567.
- [106] GOFFIN, P., VAN DE BUNT, B., GIOVANE, M., LEVEAU, J. H. J., HÖPPENER-OGAWA, S., TEUSINK, B., AND HUGENHOLTZ, J. Understanding the physiology of *Lactobacillus plantarum* at zero growth. *Molecular systems biology* 6, 413 (2010), 413.
- [107] GRAF, A., GASSER, B., DRAGOSITS, M., SAUER, M., LEPARC, G. G., TÜCHLER, T., KREIL, D. P., AND MATTANOVICH, D. Novel insights into the unfolded protein response using *Pichia pastoris* specific DNA microarrays. *BMC Genomics* 9, 1 (2008), 390.
- [108] GRAY, J. V., PETSKO, G. A., JOHNSTON, G. C., RINGE, D., SINGER, R. A., AND WERNER-WASHBURNE, M. Sleeping Beauty: Quiescence in *Saccharomyces cerevisiae*. *Microbiology and Molecular Biology Reviews* 68, 2 (jun 2004), 187–206.
- [109] GRECO, M. A., HRAB, D. I., MAGNER, W., AND KOSMAN, D. J. Cu,Zn superoxide dismutase and copper deprivation and toxicity in *Saccharomyces cerevisiae*. *Journal of bacteriology* 172, 1 (jan 1990), 317–25.
- [110] GUYOT, S., GERVAIS, P., YOUNG, M., WINCKLER, P., DUMONT, J., AND DAVEY, H. M. Surviving the heat: heterogeneity of response in *Saccharomyces cerevisiae* provides insight into thermal damage to the membrane. *Environmental Microbiology* 17, 8 (aug 2015), 2982–2992.
- [111] HAGMAN, A., AND PIŠKUR, J. A Study on the Fundamental Mechanism and the Evolutionary Driving Forces behind Aerobic Fermentation in Yeast. *PLOS ONE* 10, 1 (jan 2015), e0116942.
- [112] HAGMAN, A., SÄLL, T., COMPAGNO, C., AND PISKUR, J. Yeast 'Make-Accumulate-Consume' Life Strategy Evolved as a Multi-Step Process That Predates the Whole Genome Duplication. *PLoS ONE* 8, 7 (jul 2013), e68734.
- [113] HAMILTON, S. R., DAVIDSON, R. C., SETHURAMAN, N., NETT, J. H., JIANG, Y., RIOS, S., BOBROWICZ, P., STADHEIM, T. A., LI, H., CHOI, B.-K., HOPKINS, D., WISCHNEWSKI, H., ROSER, J., MITCHELL, T., STRAWBRIDGE, R. R., HOOPES, J., WILDT, S., AND GERNGROSS, T. U. Humanization of Yeast to Produce Complex Terminally Sialylated Glycoproteins. *Science* 313, 5792 (sep 2006), 1441–1443.
- [114] HANSEN, E. H., MØLLER, B. L., KOCK, G. R., BÜNNER, C. M., KRISTENSEN, C., JENSEN, O. R., OKKELS, F. T., OLSEN, C. E., MOTAWIA, M. S., AND HANSEN, J. De novo biosynthesis of vanillin in fission yeast (*Schizosaccharomyces pombe*) and baker's yeast (*Saccharomyces cerevisiae*). *Applied and environmental microbiology* 75, 9 (may 2009), 2765–74.
- [115] HARBISON, C. C. T., GORDON, D. B. D., LEE, T. T. I., RINALDI, N. J., MACISAAC, K. D., DANFORD, T. W., HANNETT, N. M., TAGNE, J.-B., REYNOLDS, D. B., YOO, J., JENNINGS, E. G., ZEITLINGER, J., POKHOLOK, D. K., KELLIS, M., ROLFE, P. A., TAKUSAGAWA, K. T., LANDER, E. S., GIFFORD, D. K., FRAENKEL, E., AND



- YOUNG, R. A. Transcriptional regulatory code of a eukaryotic genome. *Nature* 431, 7004 (sep 2004), 99–104.
- [116] HARDJITO, L., GREENFIELD, P. F., AND LEE, P. L. Recombinant protein production via fed-batch culture of the yeast *Saccharomyces cerevisiae*. *Enzyme and Microbial Technology* 15, 2 (feb 1993), 120–126.
- [117] HARTNER, F. S., AND GLIEDER, A. Regulation of methanol utilisation pathway genes in yeasts. *Microbial Cell Factories* 5, 1 (2006), 39.
- [118] HASLBECK, M. Hsp26: a temperature-regulated chaperone. *The EMBO Journal* 18, 23 (dec 1999), 6744–6751.
- [119] HEBLY, M., DE RIDDER, D., DE HULSTER, E. A. F., DE LA TORRE CORTES, P., PRONK, J. T., AND DARAN-LAPUJADE, P. Physiological and Transcriptional Responses of Anaerobic Chemostat Cultures of *Saccharomyces cerevisiae* Subjected to Diurnal Temperature Cycles. *Applied and environmental microbiology* 80, 14 (jul 2014), 4433–49.
- [120] HEIJNEN, J. J. Application of balancing methods in modeling the penicillin fermentation. *Biotechnology and ... XXI*, 1979 (1979), 2175–2201.
- [121] HEIJNEN, J. J. Impact of thermodynamic principles in systems biology. *Advances in biochemical engineering/biotechnology* 121 (2010), 139–62.
- [122] HENSING, M. C. M., ROUWENHORST, R. J., HEIJNEN, J. J., DIJKEN, J. P., AND PRONK, J. T. Physiological and technological aspects of large-scale heterologous-protein production with yeasts. *Antonie van Leeuwenhoek* 67, 3 (1995), 261–279.
- [123] HERBERT, D. The chemical composition of microorganisms as a function of their environment. In *Microbial Reaction to Environment: 11th Symposium of the Society for General Microbiology* (Cambridge, 1961), G. Meynell and H. Gooder, Eds., pp. 391–416.
- [124] HERBERT, D. The continuous culture of bacteria; a theoretical and experimental study. In *Continuous culture of microorganisms, vol. 12*. Society of Chemical Industry, London, 1961, pp. 21–53.
- [125] HEYLAND, J., FU, J., AND BLANK, L. M. Correlation between TCA cycle flux and glucose uptake rate during respiro-fermentative growth of *Saccharomyces cerevisiae*. *Microbiology (Reading, England)* 155, Pt 12 (dec 2009), 3827–37.
- [126] HEYLAND, J., FU, J., BLANK, L. M., AND SCHMID, A. Quantitative physiology of *Pichia pastoris* during glucose-limited high-cell density fed-batch cultivation for recombinant protein production. *Biotechnology and bioengineering* 107, 2 (oct 2010), 357–68.
- [127] HINO, A., MIHARA, K., NAKASHIMA, K., AND TAKANO, H. Trehalose levels and survival ratio of freeze-tolerant versus freeze-sensitive yeasts. *Applied and environmental microbiology* 56, 5 (1990), 1386–1396.
- [128] HONG, K.-K., AND NIELSEN, J. Metabolic engineering of *Saccharomyces cerevisiae*: a key cell factory platform for future biorefineries. *Cellular and molecular life sciences : CMLS* 69, 16 (aug 2012), 2671–90.
- [129] HONG, K.-K. K., HOU, J., SHOAIE, S., NIELSEN, J., AND BORDEL, S. Dynamic 13 C-labeling experiments prove important differences in protein turnover rate between two *Saccharomyces cerevisiae* strains. *FEMS Yeast Research* 12, 7 (nov 2012), 741–747.
- [130] IKEDA, M., AND NAKAGAWA, S. The *Corynebacterium glutamicum* genome: features and impacts on biotechnological processes. *Applied Microbiology and Biotechnology* 62, 2-3 (aug 2003), 99–109.
- [131] JAMIESON, D. J. Oxidative stress responses of the yeast *Saccharomyces cerevisiae*. *Yeast* 14, 16 (1998), 1511–1527.
- [132] JANSEN, M. L. A., DIDERICH, J. A., MASHEGO, M., HASSANE, A., DE WINDE, J. H., DARAN-LAPUJADE, P., AND PRONK, J. T. Prolonged selection in aerobic, glucose-limited chemostat cultures of *Saccharomyces cerevisiae* causes a partial loss of glycolytic capacity. *Microbiology* 151, 5 (may 2005), 1657–1669.

- [133] JAWOREK, D., AND WELSCH, J. Adenosine 5'-diphosphate and adenosine 5'-monophosphate. In *Methods of enzymatic analysis*, H. Bergmeyer, J. Bergmeyer, and M. Graal, Eds. Verlagsgesellschaft mbH, Weinheim, 1985, pp. 365–370.
- [134] JAY, J. M. History of Microorganisms in Food. In *Modern Food Microbiology*. Springer US, Boston, MA, pp. 3–9.
- [135] JIA, H., FAN, Y., FENG, X., AND LI, C. Enhancing stress-resistance for efficient microbial biotransformations by synthetic biology. 1–6.
- [136] JOHANSSON, N., QUEHL, P., NORBECK, J., AND LARSSON, C. Identification of factors for improved ethylene production via the ethylene forming enzyme in chemostat cultures of *Saccharomyces cerevisiae*. *Microbial cell factories* 12, 1 (jan 2013), 89.
- [137] JOHNSON, I. Human insulin from recombinant DNA technology. *Science* 219, 4585 (feb 1983), 632–637.
- [138] JOHNSON, K., KLEEREBEZEM, R., AND VAN LOOSDRECHT, M. C. M. M. Model-based data evaluation of polyhydroxybutyrate producing mixed microbial cultures in aerobic sequencing batch and fed-batch reactors. *Biotechnology and Bioengineering* 104, 1 (sep 2009), 50–67.
- [139] JORGENSEN, T. R., NITSCHKE, B. M., LAMERS, G. E., ARENTSHORST, M., VAN DEN HONDEL, C. A., AND RAM, A. F. Transcriptomic Insights into the Physiology of *Aspergillus niger* Approaching a Specific Growth Rate of Zero. *Applied and Environmental Microbiology* 76, 16 (2010), 5344–5355.
- [140] JULES, M., BELTRAN, G., FRANÇOIS, J., AND PARROU, J.-L. New insights into trehalose metabolism by *Saccharomyces cerevisiae*: NTH2 encodes a functional cytosolic trehalase, and deletion of TPS1 reveals Ath1p-dependent trehalose mobilization. *Applied and Environmental Microbiology* 74, 3 (2008), 605–614.
- [141] KAEBERLEIN, M. Lessons on longevity from budding yeast. *Nature* 464, 7288 (mar 2010), 513–9.
- [142] KARAS, B. J., MOLPARIA, B., JABLANOVIC, J., HERMANN, W. J., LIN, Y.-C., DUPONT, C. L., TAGWERKER, C., YONEMOTO, I. T., NOSKOV, V. N., CHUANG, R.-Y., ALLEN, A. E., GLASS, J. I., HUTCHISON, C. A., SMITH, H. O., VENTER, J. C., AND WEYMAN, P. D. Assembly of eukaryotic algal chromosomes in yeast. *Journal of biological engineering* 7, 1 (2013), 30.
- [143] KATZ, M., DURHUUS, T., SMITS, H., AND FORSTER, J. Production of metabolites, 2011.
- [144] KAVŠČEK, M., STRAŽAR, M., CURK, T., NATTER, K., AND PETROVIČ, U. Yeast as a cell factory: current state and perspectives. *Microbial Cell Factories* 14, 1 (2015), 94.
- [145] KAWALEK, A., AND VAN DER KLEI, I. J. At neutral pH the chronological lifespan of *Hansenula polymorpha* increases upon enhancing the carbon source concentrations. 189–202.
- [146] KAZEMI SERESHT, A., CRUZ, A. L., DE HULSTER, E. A. F., HEBLY, M., PALMQVIST, E. A., VAN GULIK, W. M., DARAN, J.-M., PRONK, J. T., AND OLSSON, L. Long-term adaptation of *Saccharomyces cerevisiae* to the burden of recombinant insulin production. *Biotechnology and bioengineering* 110, 10 (oct 2013), 2749–63.
- [147] KELLY, S. T., SENYO OPONG, W., AND ZYDNEY, A. L. The influence of protein aggregates on the fouling of microfiltration membranes during stirred cell filtration. *Journal of Membrane Science* 80, 1 (jun 1993), 175–187.
- [148] KENG, T. *HAPI* and *ROX1* form a regulatory pathway in the repression of *HEM13* transcription in *Saccharomyces cerevisiae*. *Molecular and Cellular Biology* 12, 6 (jun 1992), 2616–2623.
- [149] KLIENER, P. *The Fleischmann Yeast Family*. Arcada Publishing, Charleston, 2004.
- [150] KNIJNENBURG, T. A., DE WINDE, J. H., DARAN, J.-M., DARAN-LAPUJADE, P., PRONK, J. T., REINDERS, M. J. T., AND WESSELS, L. F. A. Exploiting combinatorial cultivation conditions to infer transcriptional regulation. *BMC genomics* 8 (jan 2007), 25.
- [151] KOCHARIN, K., AND NIELSEN, J. Specific growth rate and substrate dependent polyhydroxybutyrate production in *Saccharomyces cerevisiae*. *AMB Express* 3, 1 (mar 2013), 18.

- [152] KOLEWE, M. E., GAURAV, V., AND ROBERTS, S. C. Pharmaceutically Active Natural Product Synthesis and Supply via Plant Cell Culture Technology. *Molecular Pharmaceutics* 5, 2 (apr 2008), 243–256.
- [153] KOLKMAN, A. Comparative Proteome Analysis of *Saccharomyces cerevisiae* Grown in Chemostat Cultures Limited for Glucose or Ethanol. *Molecular & Cellular Proteomics* 4, 1 (oct 2004), 1–11.
- [154] KOOPMAN, F., BEEKWILDER, J., CRIMI, B., VAN HOUWELINGEN, A., HALL, R. D., BOSCH, D., VAN MARIS, A. J. A., PRONK, J. T., AND DARAN, J.-M. *De novo* production of the flavonoid naringenin in engineered *Saccharomyces cerevisiae*. *Microbial cell factories* 11 (jan 2012), 155.
- [155] KOZAK, B. U., VAN ROSSUM, H. M., BENJAMIN, K. R., WU, L., DARAN, J.-M. G., PRONK, J. T., AND VAN MARIS, A. J. A. Replacement of the *Saccharomyces cerevisiae* acetyl-CoA synthetases by alternative pathways for cytosolic acetyl-CoA synthesis. *Metabolic engineering* 21 (2014), 46–59.
- [156] KREN, A., MAMNUN, Y. M., BAUER, B. E., SCHÜLLER, C., WOLFGER, H., HATZIXANTHIS, K., MOLLAPOUR, M., GREGORI, C., PIPER, P., AND KUCHLER, K. War1p, a novel transcription factor controlling weak acid stress response in yeast. *Molecular and cellular biology* 23, 5 (2003), 1775–85.
- [157] KRESNOWATI, M. T. A. P., VAN WINDEN, W. A., ALMERING, M. J. H., TEN PIERICK, A., RAS, C., KNIJNENBURG, T. A., DARAN-LAPUJADE, P., PRONK, J. T., HEIJNEN, J. J., AND DARAN, J. M. When transcriptome meets metabolome: fast cellular responses of yeast to sudden relief of glucose limitation. *Molecular systems biology* 2 (jan 2006), 49.
- [158] KUIJPERS, N. G. A., CHROUMPI, S., VOS, T., SOLIS-ESCALANTE, D., BOSMAN, L., PRONK, J. T., DARAN, J.-M., AND DARAN-LAPUJADE, P. One-step assembly and targeted integration of multigene constructs assisted by the I-SceI meganuclease in *Saccharomyces cerevisiae*. *FEMS yeast research* 13, 8 (dec 2013), 769–81.
- [159] KURTZMAN, C. P. Biotechnological strains of *Komagataella (Pichia) pastoris* are *Komagataella phaffii* as determined from multigene sequence analysis. *Journal of Industrial Microbiology & Biotechnology* 36, 11 (2009), 1435–1438.
- [160] KUYPER, M., HARTOG, M., TOIRKENS, M. J., ALMERING, M. J. H., WINKLER, A., VAN DIJKEN J P, AND T, P. J. Metabolic engineering of a xylose-isomerase-expressing strain for rapid anaerobic xylose fermentation. *FEMS Yeast Research* 5, 4-5 (feb 2005), 399–409.
- [161] LEADSHAM, J. E., SANDERS, G., GIANNAKI, S., BASTOW, E. L., HUTTON, R., NAEIMI, W. R., BREITENBACH, M., AND GOURLAY, C. W. Loss of Cytochrome c Oxidase Promotes RAS-Dependent ROS Production from the ER Resident NADPH Oxidase, Yno1p, in Yeast. *Cell Metabolism* 18, 2 (aug 2013), 279–286.
- [162] LEE, P., KIM, M. S., PAIK, S.-M., CHOI, S.-H., CHO, B.-R., AND HAHN, J.-S. Rim15-dependent activation of Hsf1 and Msn2/4 transcription factors by direct phosphorylation in *Saccharomyces cerevisiae*. *FEBS letters* 587, 22 (nov 2013), 3648–55.
- [163] LEE, S. S., VIZCARRA, I. A., HUBERTS, D. H. E. W., LEE, L. P., AND HEINEMANN, M. Whole lifespan microscopic observation of budding yeast aging through a microfluidic dissection platform. *Proceedings of the National Academy of Sciences* 109, 13 (mar 2012), 4916–4920.
- [164] LEGRAS, J. L., MERDINOGLU, D., CORNUET, J. M., AND KARST, F. Bread, beer and wine: *Saccharomyces cerevisiae* diversity reflects human history. *Molecular Ecology* 16, 10 (2007), 2091–2102.
- [165] LI, L., MILES, S., MELVILLE, Z., PRASAD, A., BRADLEY, G., AND BREEDEN, L. L. Key events during the transition from rapid growth to quiescence in budding yeast require posttranscriptional regulators. *Molecular biology of the cell* 24, 23 (dec 2013), 3697–709.
- [166] LI, Y., LI, Y., WANG, Y., CHEN, L., YAN, M., CHEN, K., XU, L., AND OUYANG, P. Production of Rebaudioside A from Stevioside Catalyzed by the Engineered *Saccharomyces cerevisiae*. *Applied Biochemistry and Biotechnology* (jan 2016).
- [167] LIN, S.-J., KAEBERLEIN, M., ANDALIS, A. A., STURTZ, L. A., DEFOSSEZ, P.-A., CULOTTA, V. C., FINK, G. R., AND GUARENTE, L. Calorie restriction extends *Saccharomyces cerevisiae* lifespan by increasing respiration. *Nature* 418, 6895 (jul 2002), 344–348.

- [168] LINDQUIST, S., AND KIM, G. Heat-shock protein 104 expression is sufficient for thermotolerance in yeast. *Proceedings of the National Academy of Sciences* 93, 11 (may 1996), 5301–5306.
- [169] LIU, H., STYLES, C. A., AND FINK, G. R. *Saccharomyces cerevisiae* S288C has a mutation in *FLO8*, a gene required for filamentous growth. *Genetics* 144, 3 (1996), 967–978.
- [170] LIU, Z., HOU, J., MARTÍNEZ, J. L., PETRANOVIC, D., AND NIELSEN, J. Correlation of cell growth and heterologous protein production by *Saccharomyces cerevisiae*. *Applied microbiology and biotechnology* 97, 20 (oct 2013), 8955–62.
- [171] LONGO, V. D., AND FABRIZIO, P. Chronological aging in *Saccharomyces cerevisiae*. In *Aging Research in Yeast*. Springer Netherlands, Dordrecht, 2012, pp. 101–121.
- [172] LONGO, V. D., SHADEL, G. S., KAEBERLEIN, M., AND KENNEDY, B. Replicative and Chronological Aging in *Saccharomyces cerevisiae*. *Cell metabolism* 16, 1 (jul 2012), 18–31.
- [173] LOOSER, V., BRUHLMANN, B., BUMBAK, F., STENGER, C., COSTA, M., CAMATTARI, A., FOTIADIS, D., AND KOVAR, K. Cultivation strategies to enhance productivity of *Pichia pastoris*: A review. *Biotechnology advances* 33, 6 Pt 2 (nov 2015), 1177–93.
- [174] LU, C., BRAUER, M. J., AND BOTSTEIN, D. Slow Growth Induces Heat-Shock Resistance in Normal and Respiratory-deficient Yeast. *Molecular Biology of the Cell* 20, 3 (dec 2008), 891–903.
- [175] LUDOVICO, P., AND BURHANS, W. C. Reactive oxygen species, ageing and the hormesis police. *FEMS Yeast Research* 14, 1 (feb 2014), 33–39.
- [176] LUTTIK, M. A. H., VURALHAN, Z., SUIR, E., BRAUS, G. H., PRONK, J. T., AND DARAN, J. M. Alleviation of feedback inhibition in *Saccharomyces cerevisiae* aromatic amino acid biosynthesis: quantification of metabolic impact. *Metabolic engineering* 10, 3-4 (2008), 141–53.
- [177] MAA, Y.-F., AND HSU, C. C. Investigation on fouling mechanisms for recombinant human growth hormone sterile filtration. *Journal of Pharmaceutical Sciences* 87, 7 (jul 1998), 808–812.
- [178] MACCANI, A., LANDES, N., STADLMAYR, G., MARESCH, D., LEITNER, C., MAURER, M., GASSER, B., ERNST, W., KUNERT, R., AND MATTANOVICH, D. *Pichia pastoris* secretes recombinant proteins less efficiently than Chinese hamster ovary cells but allows higher space-time yields for less complex proteins. *Biotechnology Journal* 9, 4 (apr 2014), 526–537.
- [179] MAGOC, T., WOOD, D., AND SALZBERG, S. L. EDGE-pro: Estimated Degree of Gene Expression in Prokaryotic Genomes. *Evolutionary bioinformatics online* 9 (jan 2013), 127–36.
- [180] MANS, R., VAN ROSSUM, H. M., WIJSMAN, M., BACKX, A., KUIJPERS, N. G. A., VAN DEN BROEK, M., DARAN-LAPUJADE, P., PRONK, J. T., VAN MARIS, A. J. A., AND DARAN, J.-M. G. CRISPR/Cas9: a molecular Swiss army knife for simultaneous introduction of multiple genetic modifications in *Saccharomyces cerevisiae*. *FEMS Yeast Research* 15, 2 (mar 2015), fov004–fov004.
- [181] MARTINEZ, M. J. J., ROY, S., ARCHULETTA, A. B., WENTZELL, P. D., ANNA-ARRIOLA, S. S., RODRIGUEZ, A. L., ARAGON, A. D., QUIÑONES, G. A., ALLEN, C., AND WERNER-WASHBURN, M. Genomic analysis of stationary-phase and exit in *Saccharomyces cerevisiae*: gene expression and identification of novel essential genes. *Molecular biology of the cell* 15, 12 (dec 2004), 5295–305.
- [182] MARX, H., SAUER, M., RESINA, D., VAI, M., PORRO, D., VALERO, F., FERRER, P., AND MATTANOVICH, D. Cloning, disruption and protein secretory phenotype of the GAS1 homologue of *Pichia pastoris*. *FEMS microbiology letters* 264, 1 (nov 2006), 40–7.
- [183] MASHEGO, M. R., VAN GULIK, W. M., VINKE, J. L., AND HEIJNEN, J. J. Critical evaluation of sampling techniques for residual glucose determination in carbon-limited chemostat culture of *Saccharomyces cerevisiae*. *Biotechnology and bioengineering* 83, 4 (2003), 395–9.
- [184] MATTANOVICH, D., BRANDUARDI, P., DATO, L., GASSER, B., SAUER, M., AND PORRO, D. Recombinant protein production in yeasts. *Methods in molecular biology (Clifton, N.J.)* 824 (2012), 329–58.

- [185] MATTANOVICH, D., GRAF, A., STADLMANN, J., DRAGOSITS, M., REDL, A., MAURER, M., KLEINHEINZ, M., SAUER, M., ALTMANN, F., AND GASSER, B. Genome, secretome and glucose transport highlight unique features of the protein production host *Pichia pastoris*. *Microbial Cell Factories* 8, 1 (2009), 29.
- [186] MAURER, M., KÜHLEITNER, M., GASSER, B., AND MATTANOVICH, D. Versatile modeling and optimization of fed batch processes for the production of secreted heterologous proteins with *Pichia pastoris*. *Microbial cell factories* 5 (jan 2006), 37.
- [187] MEADEN, P. G., DICKINSON, F. M., MIFSUD, A., TESSIER, W., WESTWATER, J., BUSSEY, H., AND MIDGLEY, M. The *ALD6* gene of *Saccharomyces cerevisiae* encodes a cytosolic, Mg(2+)-activated acetaldehyde dehydrogenase. *Yeast (Chichester, England)* 13, 14 (1997), 1319–27.
- [188] MEI, Y.-Z., LIU, R.-X., WANG, D.-P., WANG, X., AND DAI, C.-C. Biocatalysis and biotransformation of resveratrol in microorganisms. *Biotechnology letters* (sep 2014).
- [189] MENDES, F., SIEUWERTS, S., DE HULSTER, E., ALMERING, M. J. H., LUTTIK, M. A. H., PRONK, J. T., SMID, E. J., BRON, P. A., AND DARAN-LAPUJADE, P. Transcriptome-Based Characterization of Interactions between *Saccharomyces cerevisiae* and *Lactobacillus delbrueckii subsp. bulgaricus* in Lactose-Grown Chemostat Cocultures. *Applied and Environmental Microbiology* 79, 19 (oct 2013), 5949–5961.
- [190] MENDOZA-VEGA, O., SABATIÉ, J., AND BROWN, S. W. Industrial production of heterologous proteins by fed-batch cultures of the yeast *Saccharomyces cerevisiae*. *FEMS microbiology reviews* 15, 4 (dec 1994), 369–410.
- [191] MESQUITA, A., WEINBERGER, M., SILVA, A., SAMPAIO-MARQUES, B., ALMEIDA, B., LEÃO, C., COSTA, V., RODRIGUES, F., BURHANS, W. C., LUDOVICO, P., LEAO, C., COSTA, V., RODRIGUES, F., BURHANS, W. C., AND LUDOVICO, P. Caloric restriction or catalase inactivation extends yeast chronological lifespan by inducing H<sub>2</sub>O<sub>2</sub> and superoxide dismutase activity. *Proceedings of the National Academy of Sciences* 107, 34 (aug 2010), 15123–15128.
- [192] MIRISOLA, M. G., BRAUN, R. J., AND PETRANOVIC, D. Approaches to study yeast cell aging and death. *FEMS yeast research* 14 (oct 2013), 109–118.
- [193] MIZUTANI, M., AND OHTA, D. Two isoforms of NADPH:cytochrome P450 reductase in *Arabidopsis thaliana*. Gene structure, heterologous expression in insect cells, and differential regulation. *Plant physiology* 116, 1 (jan 1998), 357–67.
- [194] MONOD, J. The growth of bacterial cultures. *Annual review of microbiology* 3 (1949), 371–394.
- [195] NAGARAJAN, S., KRUCKEBERG, A. L., SCHMIDT, K. H., KROLL, E., HAMILTON, M., MCINNERNEY, K., SUMMERS, R., TAYLOR, T., AND ROSENZWEIG, F. Uncoupling reproduction from metabolism extends chronological lifespan in yeast. *Proceedings of the National Academy of Sciences* 111, 15 (apr 2014), E1538–E1547.
- [196] NIELSEN, J. Synthetic Biology for Engineering Acetyl Coenzyme A Metabolism in Yeast. *mBio* 5, 6 (dec 2014), e02153–14.
- [197] NIJKAMP, J. F., VAN DEN BROEK, M., DATEMA, E., DE KOK, S., BOSMAN, L., LUTTIK, M. A. H., DARAN-LAPUJADE, P., VONGSANGNAK, W., NIELSEN, J., HEIJNE, W. H., KLAASSEN, P., PADDON, C. J., PLATT, D., KOTTER, P., VAN HAM, R. C., REINDERS, M. J. T., PRONK, J. T., RIDDER, D. D. E., AND DARAN, J.-M. De novo sequencing, assembly and analysis of the genome of the laboratory strain *Saccharomyces cerevisiae* CEN.PK113-7D, a model for modern industrial biotechnology. *Microbial Cell Factories* 11, 1 (2012), 36.
- [198] NOVICK, A., AND SZILARD, L. Description of the chemostat. *Science* 112 (1950), 715–716.
- [199] OCAMPO, A., LIU, J., SCHROEDER, E. A., SHADEL, G. S., AND BARRIENTOS, A. Mitochondrial Respiratory Thresholds Regulate Yeast Chronological Life Span and its Extension by Caloric Restriction. *Cell Metabolism* 16, 1 (jul 2012), 55–67.
- [200] ONISHI, T. Mechanism of electron transport and energy conservation in the site I region of the respiratory chain. *Biochimica et biophysica acta* 301, 2 (dec 1973), 105–28.

- [201] OTERO, J. M., PANAGIOTOU, G., AND OLSSON, L. Fueling Industrial Biotechnology Growth with Bioethanol. In *Biofuels*. Springer Berlin Heidelberg, Berlin, Heidelberg, pp. 1–40.
- [202] OVERKAMP, W., ERCAN, O., HERBER, M., VAN MARIS, A. J. A., KLEEREBEZEM, M., AND KUIPERS, O. P. Physiological and cell morphology adaptation of *Bacillus subtilis* at near-zero specific growth rates: a transcriptome analysis. *Environmental Microbiology* 17, 2 (2015), 346–363.
- [203] PAALMAN, J. W. G., VERWAAL, R., SLOFSTRA, S. H., VERKLEIJ, A. J., BOONSTRA, J., AND VERRIPS, C. T. Trehalose and glycogen accumulation is related to the duration of the G1 phase of *Saccharomyces cerevisiae*. *FEMS Yeast Research* 3, 3 (may 2003), 261–268.
- [204] PADDON, C. J., WESTFALL, P. J., PITERA, D. J., BENJAMIN, K., FISHER, K., MCPHEE, D., LEAVELL, M. D., TAI, A., MAIN, A., ENG, D., POLICHUK, D. R., TEOH, K. H., REED, D. W., TREYNOR, T., LENIHAN, J., FLECK, M., BAJAD, S., DANG, G., DENGROVE, D., DIOLA, D., DORIN, G., ELLENS, K. W., FICKES, S., GALAZZO, J., GAUCHER, S. P., GEISTLINGER, T., HENRY, R., HEPP, M., HORNING, T., IQBAL, T., JIANG, H., KIZER, L., LIEU, B., MELIS, D., MOSS, N., REGENTIN, R., SECREST, S., TSURUTA, H., VAZQUEZ, R., WESTBLADE, L. F., XU, L., YU, M., ZHANG, Y., ZHAO, L., LIEVENSE, J., COVELLO, P. S., KEASLING, J. D., REILING, K. K., RENNINGER, N. S., AND NEWMAN, J. D. High-level semi-synthetic production of the potent antimalarial artemisinin. *Nature* 496, 7446 (apr 2013), 528–32.
- [205] PAREKH, S., VINCI, V. A., AND STROBEL, R. J. Improvement of microbial strains and fermentation processes. *Applied Microbiology and Biotechnology* 54, 3 (sep 2000), 287–301.
- [206] PARROU, J. L., AND FRANÇOIS, J. A Simplified Procedure for a Rapid and Reliable Assay of both Glycogen and Trehalose in Whole Yeast Cells. *Analytical Biochemistry* 248, 1 (may 1997), 186–188.
- [207] PARTOW, S., SIEWERS, V., BJØRN, S., NIELSEN, J., AND MAURY, J. Characterization of different promoters for designing a new expression vector in *Saccharomyces cerevisiae*. *Yeast (Chichester, England)* 27, 11 (nov 2010), 955–64.
- [208] PAULOVÁ, L., HYKA, P., BRANSKÁ, B., MELZUCH, K., AND KOVAR, K. Use of a mixture of glucose and methanol as substrates for the production of recombinant trypsinogen in continuous cultures with *Pichia pastoris* Mut+. *Journal of biotechnology* 157, 1 (jan 2012), 180–8.
- [209] PERRONE, G. G., TAN, S.-X., AND DAWES, I. W. Reactive oxygen species and yeast apoptosis. *Biochimica et Biophysica Acta (BBA) - Molecular Cell Research* 1783, 7 (jul 2008), 1354–1368.
- [210] PÉTER, G., TORNAI-LEHOCZKI, J., AND DLAUCHY, D. *Ogataea populiabae* sp. nov., a yeast species from white poplar. *FEMS yeast research* 9, 6 (sep 2009), 936–41.
- [211] PETITJEAN, M., TESTE, M.-A., FRANÇOIS, J. M., AND PARROU, J.-L. Yeast Tolerance to Various Stresses Relies on the Trehalose-6P Synthase (Tps1) Protein, Not on Trehalose. *Journal of Biological Chemistry* 290, 26 (2015), 16177–16190.
- [212] PETTI, A. A., CRUTCHFIELD, C. A., RABINOWITZ, J. D., AND BOTSTEIN, D. Survival of starving yeast is correlated with oxidative stress response and nonrespiratory mitochondrial function. *Proceedings of the National Academy of Sciences of the United States of America* 108, 45 (nov 2011), E1089–98.
- [213] PHAFF, H. J., AND KNAPP, E. P. The taxonomy of yeasts found in exudates of certain trees and other natural breeding sites of some species of *Drosophila*. *Antonie van Leeuwenhoek* 22, 2 (1956), 117–30.
- [214] PIPER, M. D. W., DARAN-LAPUJADE, P., BRO, C., REGENBERG, B., KNUDSEN, S., NIELSEN, J., AND PRONK, J. T. Reproducibility of Oligonucleotide Microarray Transcriptome Analyses; an interlaboratory comparison using chemostat cultures of *Saccharomyces cerevisiae*. *Journal of Biological Chemistry* 277, 40 (sep 2002), 37001–37008.
- [215] PIPER, P., AND CALDERON, C. O. Weak acid adaptation: the stress response that confers yeasts with resistance to organic acid food preservatives. *Microbiology* 3, 17 (2001), 2635–2642.
- [216] PIPER, P. W., TALREJA, K., PANARETOU, B., B, K., PRAEKELT, U. M., AND M, P. Induction of major heat-shock proteins of *Saccharomyces cerevisiae*, including plasma membrane Hsp30, by ethanol levels above a critical threshold. *Microbiology* 140 (1994), 3031–3038.

- [217] PIRT, S. J. The maintenance energy of bacteria in growing cultures. *Proceedings of the Royal Society of London. Series B, Containing papers of a Biological character. Royal Society (Great Britain)* 163, 991 (oct 1965), 224–31.
- [218] PIRT, S. J. Maintenance energy: a general model for energy-limited and energy-sufficient growth. *Archives of microbiology* 133, 4 (1982), 300–2.
- [219] POSTMA, E., VERDUYN, C., SCHEFFERS, W. A., AND VAN DIJKEN, J. P. Enzymic analysis of the crabtree effect in glucose-limited chemostat cultures of *Saccharomyces cerevisiae*. *Applied and environmental microbiology* 55, 2 (feb 1989), 468–77.
- [220] PRAEKELT, U. M., AND MEACOCK, P. A. *HSP12*, a new small heat shock gene of *Saccharomyces cerevisiae*: Analysis of structure, regulation and function. *MGG Molecular & General Genetics* 223, 1 (aug 1990), 97–106.
- [221] PRIELHOFER, R., CARTWRIGHT, S. P., GRAF, A. B., VALLI, M., BILL, R. M., MATTANOVICH, D., AND GASSER, B. *Pichia pastoris* regulates its gene-specific response to different carbon sources at the transcriptional, rather than the translational, level. *BMC genomics* 16 (2015), 167.
- [222] PRIELHOFER, R., MAURER, M., KLEIN, J., WENGER, J., KIZIAK, C., GASSER, B., AND MATTANOVICH, D. Induction without methanol: novel regulated promoters enable high-level expression in *Pichia pastoris*. *Microbial Cell Factories* 12, 1 (2013), 5.
- [223] RACHIDI, N., MARTINEZ, M.-J., BARRE, P., AND BLONDIN, B. *Saccharomyces cerevisiae* PAU genes are induced by anaerobiosis. *Molecular Microbiology* 35, 6 (jan 2002), 1421–1430.
- [224] REBNEGGER, C., GRAF, A. B., VALLI, M., STEIGER, M. G., GASSER, B., MAURER, M., AND MATTANOVICH, D. In *Pichia pastoris*, growth rate regulates protein synthesis and secretion, mating and stress response. *Biotechnology journal* 9, 4 (apr 2014), 511–25.
- [225] REGENBERG, B., GROTKJAER, T., WINTHER, O., FAUSBØLL, A., AKESSON, M., BRO, C., HANSEN, L. K., BRUNAK, S., AND NIELSEN, J. Growth-rate regulated genes have profound impact on interpretation of transcriptome profiling in *Saccharomyces cerevisiae*. *Genome biology* 7, 11 (jan 2006), R107.
- [226] REICH, M., LIEFELD, T., GOULD, J., LERNER, J., TAMAYO, P., AND MESIROV, J. P. GenePattern 2.0. *Nature genetics* 38, 5 (may 2006), 500–1.
- [227] REIFENBERGER, E., BOLES, E., AND CIRIACY, M. Kinetic Characterization of Individual Hexose Transporters of *Saccharomyces cerevisiae* and their Relation to the Triggering Mechanisms of Glucose Repression. *European Journal of Biochemistry* 245, 2 (apr 1997), 324–333.
- [228] RITCHIE, M. E., SILVER, J., OSHLACK, A., HOLMES, M., DIYAGAMA, D., HOLLOWAY, A., AND SMYTH, G. K. A comparison of background correction methods for two-colour microarrays. *Bioinformatics (Oxford, England)* 23, 20 (oct 2007), 2700–7.
- [229] RITTERSHAUS, E. S. C., BAEK, S.-H., AND SASSETTI, C. M. The Normalcy of Dormancy: Common Themes in Microbial Quiescence. *Cell Host & Microbe* 13, 6 (jun 2013), 643–651.
- [230] ROGERS, P. J., AND STEWART, P. R. Energetic efficiency and maintenance. Energy characteristics of *Saccharomyces cerevisiae* (wild type and petite) and *Candida parapsilosis* grown aerobically and micro-aerobically in continuous culture. *Archives of microbiology* 99, 1 (jan 1974), 25–46.
- [231] ROHDE, A., MORREEL, K., RALPH, J., GOEMINNE, G., HOSTYN, V., RYCKE, R. D., AND KUSHNIR, S. Molecular Phenotyping of the *pal1* and *pal2* Mutants of *Arabidopsis thaliana* Reveals Far-Reaching Consequences on Phenylpropanoid, Amino Acid, and Carbohydrate Metabolism. *The Plant Cell* 16, 10 (2004), 2749–2771.
- [232] ROMAGNOLI, G., LUTTIK, M. A. H., KÖTTER, P., PRONK, J. T., AND DARAN, J.-M. Substrate specificity of thiamine pyrophosphate-dependent 2-oxo-acid decarboxylases in *Saccharomyces cerevisiae*. *Applied and environmental microbiology* 78, 21 (2012), 7538–48.

- [233] ROSEGRANT, M. W., AND CLINE, S. A. Global Food Security : Challenges and Policies. *Science* 302, 5652 (2003), 1917–1919.
- [234] ROSENFELD, E., AND BEAUVOIT, B. Role of the non-respiratory pathways in the utilization of molecular oxygen by *Saccharomyces cerevisiae*. *Yeast* 20, 13 (2003), 1115–1144.
- [235] ROSENFELD, E., AND BEAUVOIT, B. Role of the non-respiratory pathways in the utilization of molecular oxygen by *Saccharomyces cerevisiae*. *Yeast* 20, 13 (oct 2003), 1115–1144.
- [236] RYAZANOV, A. G., AND NEFSKY, B. S. Protein turnover plays a key role in aging. *Mechanisms of Ageing and Development* 123, 2-3 (jan 2002), 207–213.
- [237] SANDER, J. D., AND JOUNG, J. K. CRISPR-Cas systems for editing, regulating and targeting genomes. *Nature Biotechnology* 32, 4 (mar 2014), 347–355.
- [238] SANGER, F., NICKLEN, S., AND COULSON, A. R. DNA sequencing with chain-terminating inhibitors. *Proceedings of the National Academy of Sciences* 74, 12 (dec 1977), 5463–5467.
- [239] SCALCINATI, G., PARTOW, S., SIEWERS, V., SCHALK, M., DAVIET, L., AND NIELSEN, J. Combined metabolic engineering of precursor and co-factor supply to increase  $\alpha$ -santalene production by *Saccharomyces cerevisiae*. *Microbial cell factories* 11, 1 (jan 2012), 117.
- [240] SCHMIDT, F. R. Optimization and scale up of industrial fermentation processes. *Applied microbiology and biotechnology* 68, 4 (sep 2005), 425–35.
- [241] SCHRICKX, J. M., RAEDTS, M. J., STOUTHAMER, A. H., AND VAN VERSEVELD, H. W. Organic acid production by *Aspergillus niger* in recycling culture analyzed by capillary electrophoresis. *Analytical Biochemistry* 231, 1 (1995), 175–81.
- [242] SCHRICKX, J. M., STOUTHAMER, A. H., AND VANVERSEVELD, H. W. Growth-Behavior and Glucoamylase Production by *Aspergillus niger* N402 and a Glucoamylase Overproducing Transformant in Recycling Culture without a Nitrogen-Source. *Applied Microbiology and Biotechnology* 43, 1 (1995), 109–116.
- [243] SHARMA, P. K., AGRAWAL, V., AND ROY, N. Mitochondria-mediated hormetic response in life span extension of calorie-restricted *Saccharomyces cerevisiae*. *AGE* 33, 2 (jun 2011), 143–154.
- [244] SHELDON, J. G., WILLIAMS, S. P., FULTON, A. M., AND BRINDLE, K. M. 31P NMR magnetization transfer study of the control of ATP turnover in *Saccharomyces cerevisiae*. *Proceedings of the National Academy of Sciences of the United States of America* 93, June (1996), 6399–6404.
- [245] SHI, L., SUTTER, B. M., YE, X., AND TU, B. P. Trehalose is a key determinant of the quiescent metabolic state that fuels cell cycle progression upon return to growth. *Molecular biology of the cell* 21, 12 (jun 2010), 1982–90.
- [246] SHI, S., CHEN, Y., SIEWERS, V., AND NIELSEN, J. Improving production of malonyl coenzyme A-derived metabolites by abolishing Snf1-dependent regulation of Acc1. *mBio* 5, 3 (may 2014), e01130–14.
- [247] SILLJE, H. H., TER SCHURE, E. G., ROMMENS, A. J., HULS, P. G., WOLDRINGH, C. L., VERKLEIJ, A. J., BOONSTRA, J., AND VERRIPS, C. T. Effects of different carbon fluxes on g1 phase duration, cyclin expression, and reserve carbohydrate metabolism in *saccharomyces cerevisiae*. *Journal of Bacteriology* 179, 21 (1997), 6560–5.
- [248] SINCLAIR, D. A. Toward a unified theory of caloric restriction and longevity regulation. *Mechanisms of Ageing and Development* 126, 9 SPEC. ISS. (sep 2005), 987–1002.
- [249] SLAVOV, N., AND BOTSTEIN, D. Coupling among growth rate response, metabolic cycle, and cell division cycle in yeast. *Molecular biology of the cell* 22, 12 (jun 2011), 1997–2009.
- [250] SMETS, B., GHILLEBERT, R., DE SNIJDER, P., BINDA, M., SWINNEN, E., DE VIRGILIO, C., AND WINDERICKX, J. *Life in the midst of scarcity: Adaptations to nutrient availability in Saccharomyces cerevisiae*, vol. 56. 2010.



- [251] SMITH, JR, D. L., MCCLURE, J. M., MATECIC, M., AND SMITH, J. S. Calorie restriction extends the chronological lifespan of *Saccharomyces cerevisiae* independently of the Sirtuins. *Aging Cell* 6, 5 (oct 2007), 649–662.
- [252] SMOLIGA, J. M., BAUR, J. A., AND HAUSENBLAS, H. A. Resveratrol and health - A comprehensive review of human clinical trials. *Molecular Nutrition & Food Research* 55, 8 (aug 2011), 1129–1141.
- [253] SOARES, E. V. Flocculation in *Saccharomyces cerevisiae*: a review. *Journal of Applied Microbiology* 110, 1 (jan 2011), 1–18.
- [254] SOETAERT, W., AND VANDAMME, E. The impact of industrial biotechnology. *Biotechnology Journal* 1, 7-8 (2006), 756–769.
- [255] SOHN, S. B., GRAF, A. B., KIM, T. Y., GASSER, B., MAURER, M., FERRER, P., MATTANOVICH, D., AND LEE, S. Y. Genome-scale metabolic model of methylotrophic yeast *Pichia pastoris* and its use for in silico analysis of heterologous protein production. *Biotechnology journal* 5, 7 (jul 2010), 705–15.
- [256] SOLIS-ESCALANTE, D., KUIJPERS, N. G. A., BARRAJON-SIMANCAS, N., VAN DEN BROEK, M., PRONK, J. T., DARAN, J.-M., AND DARAN-LAPUJADE, P. A Minimal Set of Glycolytic Genes Reveals Strong Redundancies in *Saccharomyces cerevisiae* Central Metabolism. *Eukaryotic cell* 14, 8 (aug 2015), 804–16.
- [257] SOLIS-ESCALANTE, D., KUIJPERS, N. G. A., BONGAERTS, N., BOLAT, I., BOSMAN, L., PRONK, J. T., DARAN, J.-M., AND DARAN-LAPUJADE, P. *amdSYM*, a new dominant recyclable marker cassette for *Saccharomyces cerevisiae*. *FEMS Yeast Research* 13, 1 (feb 2013), 126–139.
- [258] SONNLEITNER, B., AND KÄPPELI, O. Growth of *Saccharomyces cerevisiae* is controlled by its limited respiratory capacity: Formulation and verification of a hypothesis. *Biotechnology and Bioengineering* 28, 6 (jun 1986), 927–937.
- [259] STOUTHAMER, A. H. A theoretical study on the amount of ATP required for synthesis of microbial cell material. *Antonie van Leeuwenhoek* 39, 1 (dec 1973), 545–565.
- [260] STURN, A., QUACKENBUSH, J., AND TRAJANOSKI, Z. Genesis: cluster analysis of microarray data. *Bioinformatics (Oxford, England)* 18, 1 (jan 2002), 207–8.
- [261] SUPEK, F., BOŠNJAK, M., ŠKUNCA, N., AND ŠMUC, T. REVIGO Summarizes and Visualizes Long Lists of Gene Ontology Terms. *PLoS ONE* 6, 7 (jul 2011), e21800.
- [262] SWINNEN, E., WANKE, V., ROOSEN, J., SMETS, B., DUBOULOZ, F., PEDRUZZI, I., CAMERONI, E., DE VIRGILIO, C., AND WINDERICKX, J. Rim15 and the crossroads of nutrient signalling pathways in *Saccharomyces cerevisiae*. *Cell Division* 1, 1 (jan 2006), 3.
- [263] TAHARA, E. B., CUNHA, F. M., BASSO, T. O., DELLA BIANCA, B. E., GOMBERT, A. K., AND KOWALTOWSKI, A. J. Calorie Restriction Hysteretically Primes Aging *Saccharomyces cerevisiae* toward More Effective Oxidative Metabolism. *PLoS ONE* 8, 2 (feb 2013), e56388.
- [264] TAI, S. L., BOER, V. M., DARAN-LAPUJADE, P., WALSH, M. C., DE WINDE, J. H., DARAN, J.-M., AND PRONK, J. T. Two-dimensional Transcriptome Analysis in Chemostat Cultures: Combinatorial effects of oxygen availability and macronutrient limitation in *Saccharomyces cerevisiae*. *Journal of Biological Chemistry* 280, 1 (2005), 437–447.
- [265] TÄNNLER, S., DECASPER, S., AND SAUER, U. Maintenance metabolism and carbon fluxes in *Bacillus* species. *Microbial Cell Factories* 7, 1 (2008), 19.
- [266] TAPPE, W., LAVERMAN, A., BOHLAND, M., BRASTER, M., RITTERSHAUS, S., GROENEWEG, J., AND VAN VERSEVELD, H. W. Maintenance energy demand and starvation recovery dynamics of *Nitrosomonas europaea* and *Nitrobacter winogradskyi* cultivated in a retentostat with complete biomass retention. *Applied and environmental microbiology* 65, 6 (jun 1999), 2471–7.
- [267] TER LINDE, J. J. M., LIANG, H., DAVIS, R. W., STEENSMAN, H. Y., VAN DIJKEN, J. P., AND PRONK, J. T. Genome-wide transcriptional analysis of aerobic and anaerobic chemostat cultures of *Saccharomyces cerevisiae*. *Journal of bacteriology* 181, 24 (dec 1999), 7409–13.

- [268] TESTE, M.-A., DUQUENNE, M., FRANÇOIS, J. M., AND PARROU, J.-L. Validation of reference genes for quantitative expression analysis by real-time RT-PCR in *Saccharomyces cerevisiae*. *BMC Molecular Biology* 10, 1 (2009), 99.
- [269] THOMSSON, E., LARSSON, C., ALBERS, E., NILSSON, A., FRANZEN, C. J., AND GUSTAFSSON, L. Carbon Starvation Can Induce Energy Deprivation and Loss of Fermentative Capacity in *Saccharomyces cerevisiae*. *Applied and Environmental Microbiology* 69, 6 (jun 2003), 3251–3257.
- [270] THOMSSON, E., SVENSSON, M., AND LARSSON, C. Rapamycin pre-treatment preserves viability, ATP level and catabolic capacity during carbon starvation of *Saccharomyces cerevisiae*. *Yeast* 22, 8 (jun 2005), 615–623.
- [271] TIJHUIS, L., VAN LOOSDRECHT, M. C., AND HEIJNEN, J. J. A thermodynamically based correlation for maintenance gibbs energy requirements in aerobic and anaerobic chemotrophic growth. *Biotechnology and bioengineering* 42, 4 (1993), 509–19.
- [272] VAN BODEGOM, P. Microbial maintenance: a critical review on its quantification. *Microbial ecology* 53, 4 (may 2007), 513–23.
- [273] VAN DEN BERG, M. A., ALBANG, R., ALBERMANN, K., BADGER, J. H., DARAN, J.-M., M DRIESSEN, A. J., GARCIA-ESTRADA, C., FEDOROVA, N. D., HARRIS, D. M., HEIJNE, W. H. M., JOARDAR, V., W KIEL, J. A. K., KOVALCHUK, A., MARTÍN, J. E., NIERMAN, W. C., NIJLAND, J. G., PRONK, J. T., ROUBOS, J. A., VAN DER KLEI, I. J., VAN PEIJ, N. N. M. E., VEENHUIS, M., VON DÖHREN, H., WAGNER, C., WORTMAN, J., AND BOVENBERG, R. A. L. Genome sequencing and analysis of the filamentous fungus *Penicillium chrysogenum*. *Nature Biotechnology* 26, 10 (oct 2008), 1161–1168.
- [274] VAN DEN BRINK, J., CANELAS, A. B., VAN GULIK, W. M., PRONK, J. T., HEIJNEN, J. J., DE WINDE, J. H., AND DARAN-LAPUJADE, P. Dynamics of Glycolytic Regulation during Adaptation of *Saccharomyces cerevisiae* to Fermentative Metabolism. *Applied and Environmental Microbiology* 74, 18 (2008), 5710–5723.
- [275] VAN DIJKEN, J. P., BAUER, J., BRAMBILLA, L., DUBOC, P., FRANCOIS, J. M., GANCEDO, C., GIUSEPPIN, M., HEIJNEN, J. J., HOARE, M., LANGE, H. C., MADDEN, E. A., NIEDERBERGER, P., NIELSEN, J., PARROU, J. P., PETIT, T., PORRO, D., REUSS, M., N, V. R., RIZZI, M., STEENSMA, H. Y., VERRIPS, C. T., VINDELØV, J., AND PRONK, J. T. An interlaboratory comparison of physiological and genetic properties of four *Saccharomyces cerevisiae* strains. *Enzyme and microbial technology* 26, 9-10 (jun 2000), 706–714.
- [276] VAN DIJKEN, J. P., WEUSTHUIS, R. A., AND PRONK, J. T. Kinetics of growth and sugar consumption in yeasts. *Antonie van Leeuwenhoek* 63, 3-4 (sep 1993), 343–352.
- [277] VAN HOEK, P., DE HULSTER, E., VAN DIJKEN, J. P., AND PRONK, J. T. Fermentative capacity in high-cell-density fed-batch cultures of baker's yeast. *Biotechnology and bioengineering* 68, 5 (jun 2000), 517–23.
- [278] VAN HOEK, P., VAN DIJKEN, J. P., AND PRONK, J. T. Effect of specific growth rate on fermentative capacity of baker's yeast. *Applied and environmental microbiology* 64, 11 (nov 1998), 4226–33.
- [279] VAN HOEK P, VAN DIJKEN J P, AND PRONK, J. T. Regulation of fermentative capacity and levels of glycolytic enzymes in chemostat cultures of *Saccharomyces cerevisiae*. *Enzyme and microbial technology* 26, 9-10 (jun 2000), 724–736.
- [280] VAN LEEWENHOECK, A. Observations, communicated to the publisher by Mr. Antony van Leewenhoek, in a Dutch letter of the 9th of Octob. 1676: Concerning little animals by him observed in rain-well-sea. and snow water; as also in water wherein pepper had lain in. *Philosophical Transactions of the Royal Society of London* 12, 133-142 (jan 1677), 821–831.
- [281] VAN ROERMUND, C. W. T., WATERHAM, H. R., IJLST, L., AND WANDERS, R. J. A. Fatty acid metabolism in *Saccharomyces cerevisiae*. *Cellular and Molecular Life Sciences (CMLS)* 60, 9 (sep 2003), 1838–1851.
- [282] VAN URK, H., MAK, P. R., SCHEFFERS, W. A., AND VAN DIJKEN, J. P. Metabolic responses of *Saccharomyces cerevisiae* CBS 8066 and *Candida utilis* CBS 621 upon transition from glucose limitation to glucose excess. *Yeast (Chichester, England)* 4, 4 (1988), 283–91.

- [283] VAN URK, H., POSTMA, E., SCHEFFERS, W. A., AND VAN DIJKEN, J. P. Glucose transport in crabtree-positive and crabtree-negative yeasts. *Journal of general microbiology* 135, 9 (sep 1989), 2399–406.
- [284] VAN VERSEVELD, H. W., ARBIGE, M., AND CHESBRO, W. R. Continuous culture of bacteria with biomass retention. *Trends in Biotechnology* 2, 1 (jan 1984), 8–12.
- [285] VAN VERSEVELD, H. W., CHESBRO, W. R., BRASTER, M., AND STOUTHAMER, A. H. Eubacteria have 3 growth modes keyed to nutrient flow. Consequences for the concept of maintenance and maximal growth yield. *Archives of microbiology* 137, 2 (feb 1984), 176–84.
- [286] VAN VERSEVELD, H. W., DE HOLLANDER, J. A., FRANKENA, J., BRASTER, M., LEEUWERIK, F. J., AND STOUTHAMER, A. H. Modeling of microbial substrate conversion, growth and product formation in a recycling fermentor. *Antonie van Leeuwenhoek* 52, 4 (jan 1986), 325–42.
- [287] VANROLLEGHEM, P. A., DE JONG-GUBBELS, P., VAN GULIK, W. M., PRONK, J. T., VAN DIJKEN, J. P., AND HEIJNEN, S. Validation of a metabolic network for *Saccharomyces cerevisiae* using mixed substrate studies. *Biotechnology Progress* 12, 4 (1996), 434–448.
- [288] VERDUYN, C., POSTMA, E., SCHEFFERS, W. A., AND VAN DIJKEN, J. P. Energetics of *Saccharomyces cerevisiae* in anaerobic glucose-limited chemostat cultures. *Journal of general microbiology* 136, 3 (mar 1990), 405–412.
- [289] VERDUYN, C., POSTMA, E., SCHEFFERS, W. A., AND VAN DIJKEN, J. P. Physiology of *Saccharomyces cerevisiae* in Anaerobic Glucose-Limited Chemostat Cultures. *Journal of general microbiology* 136, 3 (mar 1990), 395–403.
- [290] VERDUYN, C., POSTMA, E., SCHEFFERS, W. A., AND VAN DIJKEN, J. P. Effect of benzoic acid on metabolic fluxes in yeasts: A continuous-culture study on the regulation of respiration and alcoholic fermentation. *Yeast* 8, 7 (jul 1992), 501–517.
- [291] VERDUYN, C., STOUTHAMER, A. H., SCHEFFERS, W. A., AND VAN DIJKEN, J. P. A theoretical evaluation of growth yields of yeasts. *Antonie van Leeuwenhoek* 59, 1 (jan 1991), 49–63.
- [292] VERGHESE, J., ABRAMS, J., WANG, Y., AND MORANO, K. A. Biology of the Heat Shock Response and Protein Chaperones: Budding Yeast (*Saccharomyces cerevisiae*) as a Model System. *Microbiology and Molecular Biology Reviews* 76, 2 (jun 2012), 115–158.
- [293] VISSER, W., SCHEFFERS, W. A., BATENBURG-VAN DER VEGTE, W. H., AND VAN DIJKEN, J. P. Oxygen requirements of yeasts. *Applied and environmental microbiology* 56, 12 (dec 1990), 3785–92.
- [294] VOGL, T., HARTNER, F. S., AND GLIEDER, A. New opportunities by synthetic biology for biopharmaceutical production in *Pichia pastoris*. *Current Opinion in Biotechnology* 24, 6 (dec 2013), 1094–1101.
- [295] VOS, T., DE LA TORRE CORTÉS, P., VAN GULIK, W. M., PRONK, J. T., AND DARAN-LAPUJADE, P. Growth-rate dependency of de novo resveratrol production in chemostat cultures of an engineered *Saccharomyces cerevisiae* strain. *Microbial cell factories* 14, 1 (jan 2015), 133.
- [296] WALSH, G. Biopharmaceutical benchmarks 2014. *Nature biotechnology* 32, 10 (oct 2014), 992–1000.
- [297] WALTHER, G.-R., POST, E., CONVEY, P., MENZEL, A., PARMESAN, C., BEEBEE, T. J. C., FROMENTIN, J.-M., HOEGH-GULDBERG, O., AND BAIRLEIN, F. Ecological responses to recent climate change. *Nature* 416, 6879 (mar 2002), 389–95.
- [298] WANICHTHANARAK, K., WONGTOSRAD, N., AND PETRANOVIC, D. Genome-wide expression analyses of the stationary phase model of ageing in yeast. *Mechanisms of Ageing and Development* 149 (jul 2015), 65–74.
- [299] WEI, M., FABRIZIO, P., HU, J., GE, H., CHENG, C., LI, L., AND LONGO, V. D. Life Span Extension by Calorie Restriction Depends on Rim15 and Transcription Factors Downstream of Ras/PKA, Tor, and Sch9. *PLoS Genetics* 4, 1 (jan 2008), e13.

- [300] WEIZMANN, C., AND ROSENFELD, B. The activation of the butanol-acetone fermentation of carbohydrates by *Clostridium acetobutylicum* (Weizmann). *The Biochemical journal* 31, 4 (apr 1937), 619–39.
- [301] WERNER-WASHBURNE, M., BRAUN, E., JOHNSTON, G. C., AND SINGER, R. A. Stationary phase in the yeast *Saccharomyces cerevisiae*. *Microbiological reviews* 57, 2 (jun 1993), 383–401.
- [302] WERNER-WASHBURNE, M., STONE, D. E., AND CRAIG, E. A. Complex interactions among members of an essential subfamily of hsp70 genes in *Saccharomyces cerevisiae*. *Molecular and Cellular Biology* 7, 7 (jul 1987), 2568–2577.
- [303] WESTERHEIDE, S. D., AND MORIMOTO, R. I. Heat Shock Response Modulators as Therapeutic Tools for Diseases of Protein Conformation. *Journal of Biological Chemistry* 280, 39 (sep 2005), 33097–33100.
- [304] WILSON, K., AND MCLEOD, B. J. The influence of conditions of growth on the endogenous metabolism of *Saccharomyces cerevisiae*: effect on protein, carbohydrate, sterol and fatty acid content and on viability. *Antonie van Leeuwenhoek* 42, 4 (jan 1976), 397–410.
- [305] WISSELINK, H. W., TOIRKENS, M. J., DEL ROSARIO FRANCO BERRIEL, M., WINKLER, A. A., VAN DIJKEN, J. P., PRONK, J. T., AND VAN MARIS, A. J. A. Engineering of *Saccharomyces cerevisiae* for Efficient Anaerobic Alcoholic Fermentation of L-Arabinose. *Applied and Environmental Microbiology* 73, 15 (aug 2007), 4881–4891.
- [306] WOO, D. K., AND POYTON, R. O. The absence of a mitochondrial genome in rho0 yeast cells extends lifespan independently of retrograde regulation. *Experimental Gerontology* 44, 6-7 (jun 2009), 390–397.
- [307] ZAKRZEWSKA, A., VAN EIKENHORST, G., BURGGRAAFF, J. E. C., VIS, D. J., HOEFSLOOT, H., DELNERI, D., OLIVER, S. G., BRUL, S., AND SMITS, G. J. Genome-wide analysis of yeast stress survival and tolerance acquisition to analyze the central trade-off between growth rate and cellular robustness. *Molecular Biology of the Cell* 22 (2011), 4435–4446.
- [308] ZHANG, N., WU, J., AND OLIVER, S. G. Gis1 is required for transcriptional reprogramming of carbon metabolism and the stress response during transition into stationary phase in yeast. *Microbiology* 155, 5 (2009), 1690–8.
- [309] ZIV, N., BRANDT, N. J., AND GRESHAM, D. The Use of Chemostats in Microbial Systems Biology. *Journal of Visualized Experiments* 80 (2013), e50168.



Summary  
Samenvatting

## Summary

Industrial biotechnology, the application of microorganisms for the production of economically interesting compounds, contributes to developing a (bio-based) circular economy by replacing (petro)chemical processes with ecologically more sustainable processes. The wide range of products that are nowadays produced by microorganisms include bio-fuels, medicine, and nutritional ingredients. Their production is based on the conversion of renewable carbon and energy substrates, such as sugar molecules derived from plant (waste) material.

Microorganisms grow by converting carbon sources and other essential nutrients into biomass. The free energy required for microbial growth and maintenance of cellular homeostasis is derived from catabolizing energy substrate to smaller molecules. These catabolic processes conserve free energy in the form of chemiosmotic potentials across biological membranes or as ATP. Microbial production of anabolic compounds, such as proteins, vitamins, or pharmaceuticals, requires additional carbon source and a net input of ATP to enable the respective metabolic pathways. Because of this demand for carbon and ATP, formation of these compounds competes for energy substrate with growth. The energy required for cellular maintenance, which includes, amongst other processes, protein turnover and homeostasis of chemiosmotic gradients, represents a continuous demand for energy substrate to keep the “microbial cell factories” alive and metabolically active.

The budding yeasts *Saccharomyces cerevisiae* and *Pichia pastoris* are intensively applied microbial production platforms. These yeasts are capable to convert simple sugars into added-value biochemicals, including non-native metabolites and (pharmaceutical) proteins. Their robust phenotypes, their genetic accessibility and simple nutritional requirements are key factors in their popularity in academic and industrial research. The cost effectiveness of yeast-based production of economically interesting compounds is critically determined by the overall productivity, the product titer and, especially in the case of large-volume products, by the product yield on sugar. Theoretically, maximum product yields can be obtained in the absence of growth, when sugars are solely invested in product formation and in meeting maintenance-energy requirements. Since anabolic production pathways are also an integral part of, and depend on, the metabolic machinery that supports growth, the biomass-specific rate of product formation and the pathway capacity for product formation are likely to correlate with the specific growth rate of the host. This coupling of growth and product formation poses a challenge for the production of energy-demanding products at near zero-growth rates.

In addition, obtaining high yields of anabolic products require cells to maximize their ATP yield on energy substrate. When oxygen is available as an electron acceptor, the most efficient mode of sugar catabolism in *S. cerevisiae* and *P. pastoris* is their

complete respiratory dissimilation to carbon dioxide and water. In large-scale fed-batch processes, limited capacities for oxygen transfer and heat exchange require microbes to grow at rates that are far below their maximum specific growth rate. These low growth rates result in relatively low anabolic (production) rates and a relatively large contribution of dissimilatory metabolism to overall sugar metabolism meet maintenance energy requirements. These matters underline the relevance of slow growth studies for understanding and optimizing yeast cell factories, with the ultimate aim to uncouple growth from microbial production of anabolic compounds and to minimize the impact of microbial maintenance energy requirements on industrial bioprocesses.

How specific growth rate impacts anabolic product formation depends on the product of interest, and is difficult to predict. The competition between product formation and growth for substrate and metabolites is dictated by the distribution of nutrients, ATP, and redox cofactors over enzymes in competing metabolic pathways. Because specific growth rate can affect the intracellular abundance of enzymes and metabolites and thereby the yields and rates of product formation, it is important to quantitatively assess the impact of specific growth rate on microbial production. Chemostats are continuous bioreactor cultures in which the specific growth rate can be kept constant by maintaining a fixed dilution rate, and are very suitable to study steady-state microbial physiology at different specific growth rates. In Chapter 2 of this thesis, a series of glucose-limited chemostats operated at different dilution rates were used to investigate the impact of specific growth rate on the production characteristics and physiology of an engineered *S. cerevisiae* strain producing the economically interesting nutraceutical resveratrol. This engineered yeast strain contained a heterologous metabolic pathway encoded by four plant genes. A stoichiometric model based on *S. cerevisiae* central carbon metabolism, extended with the heterologous enzymatic steps, revealed that 13 mol ATP were required to produce 1 mol of resveratrol from glucose, not taking into account regeneration of co-factors. In addition to resveratrol, pathway intermediates were excreted by the engineered strain. In glucose-limited, aerobic chemostat cultures, the specific rate of product formation displayed a strong positive correlation with specific growth rate. Calculations based on the Pirt equation, which describes the distribution of substrate over growth, maintenance and product formation (see Chapter 1), showed that at an industrially relevant, low specific growth rate ( $0.03 \text{ h}^{-1}$ ), the fraction of substrate invested in cellular maintenance (ca 30%) caused a substantial loss of carbon and energy source. A high maintenance energy requirement was also observed for the reference *S. cerevisiae* strain CEN.PK113-7D (which does not produce heterologous compounds) and was attributed to the presence of high copper concentrations in the growth media, which were necessary to induce the transcription of heterologous genes in the production pathway of the engineered strain. Comparing how mRNA levels responded to specific growth rates between the engineered strain and the reference strain showed that genes involved in pathways for precursor supply were differentially expressed. Moreover, this transcriptome analysis



identified a transcriptional response related to higher relative growth rates ( $\mu/\mu_{\max}$ ) and corresponding higher residual glucose levels for the resveratrol producing strain.

In an 'ideal' yeast-based bioprocess, carbon and energy substrates are solely used for product formation and for supplying the cellular energy required for product formation and maintenance. Such an ideal situation implies the absence of growth. Switching metabolism, at will, between growth and product formation represents a formidable challenge for synthetic biologists. Before successful engineering studies in this direction can be contemplated, it is necessary to study and understand the physiology of non-growing yeast cells. Previous studies on non-dividing *S. cerevisiae* were predominantly performed in aerobic stationary-phase cultures and anaerobic retentostat cultures. Stationary phase represents the final phase of a batch culture, during which growth had ceased, generally due to depletion of the carbon and energy source. When *S. cerevisiae* is grown on glucose in aerobic batch cultures, cells enter stationary phase after a phase of respirofermentative glucose metabolism, followed by fully respiratory growth on non-fermentable carbon sources (mostly ethanol) produced during the first phase. However, the low metabolic activity and loss of viability of stationary phase cultures limits their industrial applicability. Alternatively, zero growth can be studied in retentostats. These are nutrient-limited continuous bioreactor systems resembling chemostats, in which fresh medium is continuously supplied and only spent medium is removed while cells are retained inside the bioreactor by means of an effluent port equipped with a filter. At a constant, limiting glucose supply, biomass accumulation in retentostats results in a progressive decrease of the glucose availability per cell, up to the point where cells solely catabolize sugars to provide energy for cellular maintenance and growth is absent. Anaerobic glucose-limited retentostat cultures of *S. cerevisiae* have previously been studied in the Industrial Microbiology section of the Delft University of Technology. Anaerobic conditions facilitated a quantitative analysis of the correlation between growth and formation of ATP, which is stoichiometrically coupled to the formation of ethanol, the main catabolic product in anaerobic yeast cultures. Indeed, near-zero specific growth rates were achieved with metabolically active and viable anaerobic cultures. In these cultures, near-theoretical yields of ethanol on glucose were obtained, as well as an accurate estimation of the maintenance energy requirements. Moreover, the extremely slow growing retentostat cultures exhibited a high tolerance to heat shock. While these previous anaerobic experiments provided important new insights into the near-zero growth physiology of *S. cerevisiae*, many industrial applications of this yeast require fully aerobic conditions to respire glucose and, thus, to maximize ATP yields. Furthermore, oxygen availability might strongly influence the physiology of (non-dividing) *S. cerevisiae*, for example by affecting the mode of glucose metabolism and by the generation of reactive oxygen species (ROS) and induction of oxidative stress responses. The impact of oxygen on non-dividing *S. cerevisiae* in stationary phase batch cultures and in retentostat cultures is addressed in Chapters 3 and 4 of this thesis, respectively.

In Chapter 3, the transcriptome and physiology of *S. cerevisiae* batch cultures grown in the presence or complete absence of oxygen in tightly controlled bioreactors were analyzed and compared. Special attention was paid to survival and robustness during stationary phase. The chronological lifespan (e.g. survival) of anaerobic stationary phase cultures was almost two-fold lower than that of aerobic stationary phase cultures. An even more pronounced difference was found for the heat-shock tolerance of aerobic and anaerobic cultures. While aerobic cultures were more resistant to heat-shock than anaerobic cultures, genes encoding heat-shock proteins or genes otherwise involved in thermotolerance did not display higher expression levels in aerobic stationary phase cultures. The transcriptional reprogramming of aerobic cultures mostly occurred during the respiratory, post-diauxic growth phase preceding stationary phase. Conversely, in anaerobic cultures, which are devoid of a post-diauxic growth phase, this reprogramming occurred at the end of the exponential growth phase on glucose, but was much less pronounced than in the aerobic cultures. Measurements of intracellular ATP, ADP and AMP levels revealed a much stronger decrease of the energy charge upon entry into stationary phase in anaerobic cultures than in aerobic cultures, even though anaerobic cultures displayed higher glycogen levels. The apparent limitation in energetic flexibility of anaerobic cultures entering stationary phase possibly affects protein synthesis even more than transcription, resulting in lower heat-shock tolerance and shorter chronological lifespan than observed in aerobic stationary phase cultures. Earlier studies on anaerobic retentostat cultures did not involve an abrupt depletion of the carbon and energy source, but rather a smooth decrease in glucose availability and a concomitant decrease in specific growth rate. Such a less abrupt decrease of the specific growth rate, which to a lesser extent also occurs in aerobic cultures during the slow post-diauxic growth phase, correlated with increased resistance towards heat stress and starvation. The research in Chapter 3 therefore identified cellular energetic status as a key factor in the acquisition of longevity and robustness during transition of *S. cerevisiae* into a stationary growth phase triggered by energy source depletion.

Since yeast-based production of anabolic compounds has an inherent requirement for the high ATP yields characteristic of respiratory metabolism, aerobic retentostat cultivation was implemented as a tool to study non-dividing, metabolically active and fully respiring yeast cultures. Chapter 4 covers the operational design of aerobic retentostats and a first physiological characterization of fully respiring *S. cerevisiae* under near-zero growth conditions. Retentostat cultures offer the unique possibility to estimate maintenance-energy requirements at near zero growth. These estimates are more accurate than those derived from traditional methods, which are based on extrapolation of data from a range of chemostat cultures operated at relatively fast growth rates. This study showed that the energy requirement for cellular maintenance of respiring *S. cerevisiae* retentostat cultures was ca. 30% lower than observed in anaerobic retentostat cultures. These data can serve as benchmarks to compare how substrate expenditure

for cellular maintenance differs between microorganisms and culture conditions and to calculate its impact on bioprocess economics. Aerobic retentostat cultures displayed an unprecedented heat-shock tolerance at near-zero growth rates, indicating that a smooth transition from exponential growth to zero growth in aerobic cultures provides an optimal conditioning for heat-shock tolerance in this yeast. Concomitantly, expression of stress-responsive genes was upregulated during retentostat cultivation, while genes related to biosynthesis displayed decreasing mRNA levels with decreasing growth rate. These transcriptional changes corresponded well with observations from anaerobic retentostat cultures. While, as expected, *in vivo* catabolic rates at near-zero growth rates were low and approximated the cellular maintenance requirements, off-line measurements of the fermentative capacity (i.e. rate of ethanolic fermentation in a nutrient-rich and anaerobic environment) of retentostat cultures showed that their catabolic capacity remained high. These observations provide a solid basis to further develop *S. cerevisiae* into a non-dividing, metabolically active cell factory that can produce economically interesting compounds in the absence of excess biomass formation.

The successful implementation of aerobic retentostats led to a fruitful collaboration with colleagues from the University of Natural Resources and Life Sciences in Vienna, Austria. This study, described in Chapter 5, explores the physiology of the widely applied industrial yeast *Pichia pastoris* at near-zero growth rates. A knock-out of an ortholog of the *S. cerevisiae* transcription-factor encoding *FLO8* gene abolished surface attachment of the yeast cells and eliminated clogging of the retentostat filter probe. With the *flo8Δ* strain, it was possible to achieve full biomass retention in the retentostats for prolonged periods of time. Contrary to *S. cerevisiae*, *P. pastoris* showed a remarkable decrease in energy expenditure on endogenous maintenance processes at near-zero growth rates, while maintaining a culture viability close to 100% during 25 days of retentostat cultivation. *P. pastoris* displayed ca. three-fold lower substrate requirements for maintenance than observed in *S. cerevisiae* retentostat cultures and directed the 'saved' carbon and energy source to anabolism, as revealed by higher than predicted biomass accumulation in retentostat. Retentostat cultures of *P. pastoris* exhibited an accumulation of the storage carbohydrates glycogen and trehalose, transcriptional derepression of genes involved in alternative energy substrate metabolism and increased expression of stress-related genes. These observations suggest that *P. pastoris* adapts its physiology to anticipate potential modifications in its environment such as the complete depletion of energy sources or the sudden access of (non)preferred energy substrates. Physiological characteristics of such a 'be prepared' strategy (a term coined by the Swiss microbial ecologist Thomas Egli) were observed in retentostat cultures of *S. cerevisiae* as well as in those of other industrially relevant microorganisms. The high viability and low cellular maintenance requirements of *P. pastoris* as compared to *S. cerevisiae* at extremely slow growth rates, combined with its intrinsically favorable respiratory energetics are attractive properties for industrial production of proteins and other anabolic compounds.

An obvious next step in studying zero growth physiology of industrially relevant microorganisms is to research the impact on anabolic product formation. Extrapolating the strong positive correlation between growth and production observed for an engineered resveratrol-producing yeast strain at a range of relatively fast growth rates (Chapter 2) suggested that anabolic product formation at zero-growth is very limited. However, only a quantitative experimental assessment could give the true production kinetics at near-zero growth rates and provide leads for strain or process engineering to boost production. Researchers at the Delft University of Technology are continuing their efforts on the zero-growth line of research by studying the physiology of engineered yeast strains producing anabolic products in retentostat cultures. This thesis illustrates that retentostats are a powerful tool to gain more insight into the diversity and molecular basis of energetic requirements and cellular robustness of industrially applied cell factories at extremely low growth rates. Moreover, this cultivation system provides an excellent platform to evaluate metabolic engineering strategies aimed at uncoupling anabolic product formation from microbial growth and, thereby, contributes to the development of a bio-based, circular economy.

## Samenvatting

Industriële biotechnologie, de toepassing van microorganismen voor de productie van economisch interessante producten, draagt bij aan ontwikkeling van een ('bio-based') circulaire economie. Hierbij is het streven om petrochemische processen te vervangen door ecologisch duurzamere alternatieven. Biobrandstoffen, medicijnen en voedingsingrediënten zijn slechts enkele van de producten die tegenwoordig geproduceerd worden met behulp van microorganismen. Microbiële productieprocessen zijn gebaseerd op conversie van hernieuwbare koolstof- en energiesubstraten zoals suikermoleculen uit plantaardige materialen, waaronder reststromen van de landbouw.

Microorganismen groeien door koolstofbronnen en andere essentiële voedingsstoffen om te zetten in biomassa. De vrije energie die nodig is voor microbiële groei en voor het onderhouden van cellulaire homeostase wordt beschikbaar gemaakt door dissimilatie: de omzetting van energiesubstraat tot kleinere moleculen. Bij de dissimilatie van energiesubstraten wordt vrije energie geconserveerd in de vorm van chemisch-osmotische potentialen over biologische membranen of als ATP. Microbiële productie van assimilatoire producten, zoals eiwitten, vitaminen en medicijnen, vereist precursormoleculen die uit de stofwisseling afkomstig zijn en, bovendien, een netto input van vrije energie. Door deze vraag naar koolstof en energie competeert de vorming van zulke assimilatoire producten met groei van het organisme, zowel voor vrije energie als voor precursormoleculen. Cellulaire onderhoudsprocessen, zoals het recyclen van beschadigde eiwitten en het handhaven van chemisch-osmotische gradiënten over membranen, leiden tot een aanvullende en constante vraag naar energiesubstraat om de 'microbiële celfabrieken' metabool actief en in leven te houden.

De knopvormende gisten *Saccharomyces cerevisiae* en *Pichia pastoris* zijn veelgebruikte microbiële productiesystemen. Deze gisten kunnen simpele suikers omzetten in waardevolle biochemicalïen, zoals heterologe metabolieten en (farmacologische) eiwitten. Het robuuste fenotype, de genetische toegankelijkheid en simpele voedingsbehoeften van deze gisten dragen bij aan hun populariteit in het academisch en industrieel onderzoek. De kosteneffectiviteit van met gist geproduceerde, economisch interessante producten wordt bepaald door de productiviteit, de producttiter en, in het bijzonder voor bulkproducten, de productopbrengst op substraat. Theoretisch gezien kunnen maximale productopbrengsten alleen gehaald worden in de afwezigheid van groei, wanneer suikers uitsluitend worden geïnvesteerd in productvorming en energieconservering voor celonderhoud. Omdat assimilatoire productieroutes afhankelijk zijn en een integraal onderdeel vormen van de stofwisseling die groei bewerkstelligt, is het niet verrassend dat de biomassa-specifieke snelheid van productvorming invloed heeft op de specifieke groeisnelheid van het producerende micro-organisme. Deze koppeling van groei en productvorming vormt een uitdaging voor de productie van energie-eisende producten bij (bijna) nulgroei.

Voor hoge opbrengsten van assimilatoire producten is daarnaast van belang dat cellen hun ATP- opbrengst op het energiesubstraat maximaliseren. Wanneer zuurstof beschikbaar is als elektronacceptor, is complete respiratoire dissimilatie van suikers tot koolstofdioxide en water de meest efficiënte modus van suikermetabolisme in *S. cerevisiae* en *P. pastoris*. In fed-batchprocessen op grote schaal leiden de beperkte zuurstof- en warmteoverdrachtscapaciteit van industriële reactoren ertoe dat microben groeien met snelheden die ver beneden hun maximale groeisnelheid liggen. Deze lage groeisnelheden resulteren in relatief lage assimilatoire stofwisselingsnelheden. Bovendien wordt een relatief groot deel van de beschikbare suiker via ademhaling verbrand om te voldoen aan de energiebehoefte voor celonderhoud. Een beter begrip van de fysiologie van gisten bij extreem lage groeisnelheden is noodzakelijk voor verdere optimalisatie van gistcelfabrieken, met als uiteindelijk doelen het ontkoppelen van groei en microbiële productie van assimilatoire productvorming en de minimalisatie van de impact van energiebehoefte voor celonderhoud op industriële bio-processen.

Hoe specifieke groeisnelheid anabole productvorming precies beïnvloedt, hangt af van het product en is moeilijk te voorspellen. De competitie tussen productvorming en groei voor substraat en metabolieten wordt bepaald door de verdeling van nutriënten, ATP en redox-cofactoren over enzymen in competerende stofwisselingsroutes. Omdat specifieke groeisnelheid de intracellulaire concentraties van enzymen en metabolieten, en daarmee de opbrengst en snelheden van productvorming kan beïnvloeden, is het belangrijk om de impact van de specifieke groeisnelheid op microbiële productvorming kwantitatief te analyseren. Chemostaten zijn continue kweeksystemen waarin de specifieke groeisnelheid van een microbiële cultuur gecontroleerd kan worden door toepassing van een constante verdunningsnelheid. Chemostaten zijn daarom in het bijzonder geschikt om steady-state microbiële fysiologie en productvorming bij verschillende groeisnelheden te bestuderen.

In Hoofdstuk 2 van dit proefschrift werd een reeks glucose-gelimiteerde chemostaten, gekweekt bij verschillende verdunningsnelheden, ingezet om de impact van groeisnelheid op een genetisch gemodificeerde *S. cerevisiae*-stam te onderzoeken. Deze gist produceerde de economisch interessante “neutraceutical” resveratrol, en bevatte daarvoor een heterologe stofwisselingsroute, gecodeerd door vier in het gistgenoom ingebrachte plantengenen. Een stoichiometrisch model gebaseerd op het centraal metabolisme van *S. cerevisiae*, uitgebreid met de toegevoegde heterologe enzymatische reacties, liet zien dat voor productie van 1 mol resveratrol uit glucose 13 mol ATP nodig is (waarbij regeneratie van cofactoren buiten beschouwing gelaten is). Naast resveratrol werden ook intermediären uit de stofwisselingsroute voor resveratrolvorming uitgescheiden. In glucose-gelimiteerde aërobe chemostaatcultures vertoonde de specifieke productvormingsnelheid een sterke positieve correlatie met de specifieke groeisnelheid. Berekeningen gebaseerd op de Pirt-vergelijking, die beschrijft hoe substraat wordt verdeeld over groei, celonderhoud en productvorming (zie Hoofdstuk

1), lieten zien dat bij een industrieel relevante, lage specifieke groeisnelheid ( $0,03 \text{ h}^{-1}$ ) de fractie van het substraat die werd geïnvesteerd in celonderhoud (ca. 30%) een substantiële “drain” van koolstof- en energiesubstraat vertegenwoordigde. Deze hoge energiebehoefte voor celonderhoud werd, onder dezelfde condities, ook gevonden voor de niet-producerende referentiestam *S. cerevisiae* CEN.PK113-7D. Deze verrassende waarneming werd toegeschreven aan de hoge concentratie koper in het kweekmedium, die noodzakelijk was voor inductie van transcriptie van de heterologe genen in de productvormingsroute van de genetisch gemodificeerde stam. Een vergelijking van mRNA-niveaus in de genetisch gemodificeerde stam en de referentiestam, gekweekt bij verschillende groeisnelheden, liet zien dat genen betrokken bij de stofwisselingsroutes voor precursortoevoer verschillend tot expressie kwamen. Deze transcriptoomanalyse suggereerde dat de hogere relatieve groeisnelheid ( $\mu/\mu_{\max}$ ) van de producerende stam en de daaraan gekoppelde hogere residuele suikerconcentraties in de chemostaatcultures, in belangrijke mate bijdroegen aan de waargenomen verschillen.

In een ‘ideaal’ gist-gebaseerd bioproces worden koolstof- en energiesubstraat uitsluitend gebruikt voor productvorming en voorziening in de energiebehoefte voor productvorming en celonderhoud. Zo'n ideaal scenario impliceert dat groei afwezig is. Het naar believen schakelen van metabolisme tussen groei en productvorming vertegenwoordigt een enorme uitdaging voor synthetisch biologen. Voordat succesvolle “engineering”-studies om dit doel te verwezenlijken kunnen worden overwogen, is het noodzakelijk om de fysiologie van niet-groeiende gistcultures te bestuderen en doorgronden. Niet-delende *S. cerevisiae* is tot nu toe voornamelijk bestudeerd in aërobe stationaire-fase batchcultures en in anaërobe retentostaatcultures. De stationaire fase, de laatste fase van een batchcultuur waarin groei is gestopt, treedt in de meeste batchcultures die in het laboratorium gekweekt worden, in door depletie van de koolstof- en energiebron. Wanneer *S. cerevisiae* wordt gekweekt op glucose in aërobe batchcultures, betreden cellen de stationaire fase na een eerste fase van respirofermentatief glucosemetabolisme, gevolgd door volledige respiratoire groei op de niet-fermenteerbare koolstofbronnen (voornamelijk ethanol) die zijn geproduceerd in de eerste fase. Echter, de lage stofwisselingsactiviteit en het verlies van vitaliteit van stationaire-fasecultures beperkt hun industriële toepasbaarheid. Als alternatief kan nulgroei worden bestudeerd in retentostaten. Deze nutriënt-gelimiteerde continue bioreactorsystemen lijken op chemostaten, en net als in chemostaten wordt continue vers medium toegevoegd. Echter, in retentostaten wordt alleen gebruikt medium verwijderd, terwijl de cellen (biomassa) in de bioreactor blijven doordat de effluentleiding voorzien is van een filter. Bij een constante, gelimiteerde glucosetoevoer zal hierdoor biomassa in de retentostaat ophopen. Deze ophoping resulteert in een progressieve daling van de glucosebeschikbaarheid per tijdeenheid per cel, tot op het punt waarop de cellen de suikers nog uitsluitend gebruiken om in de energiebehoefte voor celonderhoud te voorzien en er dus geen groei meer optreedt. Anaërobe, glucose-gelimiteerde

retentostaatcultures van *S. cerevisiae* zijn al eerder bestudeerd in de Sectie Industriële Microbiologie van de Technische Universiteit Delft. Gebruik van anaërobe condities maakte het eenvoudig om kwantitatief te analyseren hoe groei was gecorreleerd aan ATP-vorming. Immers, in anaërobe gistcultures is zijn productie van ethanol, het belangrijkste dissimilatieproduct onder anaërobe omstandigheden, en ATP-productie stoichiometrisch gekoppeld.

Het lukte inderdaad om anaërobe retentostaatcultures te kweken bij extreem lage groeisnelheden ( $< 0,001$  uur<sup>-1</sup>), waarbij cellen in de cultures levensvatbaar en metabool actief bleven. In deze cultures werd de theoretisch maximale opbrengst van ethanol op glucose (2 mol ethanol per mol glucose) benaderd en kon een zeer precieze schatting van de daadwerkelijke energiebehoefte voor celonderhoud gemaakt worden. Bovendien hadden de langzaam groeiende retentostaatcultures een hoge hittebestendigheid. Deze eerdere, anaërobe experimenten leverden belangrijke nieuwe inzichten in de fysiologie van *S. cerevisiae* bij (bijna) nulgroei. Veel industriële toepassingen van deze gist vereisen echter volledig aërobe condities om glucose te kunnen verademen en, op die manier, ATP-opbrengsten te maximaliseren. De beschikbaarheid van zuurstof kan de fysiologie van (niet-delende) *S. cerevisiae* cultures op verschillende manieren beïnvloeden, bijvoorbeeld door veranderingen in het glucosemetabolisme of door vorming van zuurstofradicalen en inductie van een oxidatieve stressrespons. De impact van zuurstof op niet-delende *S. cerevisiae* batchcultures die in stationaire fase verkeren en in retentostaatcultures was het onderwerp van hoofdstukken 3 en 4 van dit proefschrift.

In hoofdstuk 3 werden het transcriptoom en de fysiologie vergeleken van batchcultures van *S. cerevisiae* die werden gekweekt in strikt gecontroleerde bioreactoren, ofwel in de aanwezigheid, ofwel in de complete afwezigheid van zuurstof. Hierbij werd in het bijzonder aandacht besteed aan overleving en stressbestendigheid gedurende de stationaire fase. De chronologische levensduur van anaërobe stationaire-fasecultures was bijna twee keer lager dan die van aërobe stationaire-fasecultures. De verschillen in de hittetolerantie van aërobe en anaërobe cultures waren zelfs nog groter. Terwijl aërobe cultures in de stationaire fase duidelijk meer hittebestendig bleken dan anaërobe cultures, toonden de genen die coderen voor 'heat-shock' eiwitten en andere genen betrokken bij hittetolerantie geen hogere expressiewaarden in de aërobe cultures. In zowel aërobe als anaërobe cultures veranderde het transcriptome gedurende de verschillende groeifasen. De transcriptionele herprogrammering van aërobe cultures speelde zich voornamelijk af tijdens de respiratoire, post-diauxische groeifase voorafgaande aan de stationaire fase. In anaërobe cultures, waarin geen post-diauxische fase optrad omdat groei op ethanol niet mogelijk is in afwezigheid van zuurstof, trad deze herprogrammering op aan het einde van de exponentiële groeifase op glucose. Echter, deze herprogrammering in anaërobe condities was veel minder uitgesproken dan in aërobe cultures. Metingen van intracellulaire ATP-, ADP- en AMP-concentraties toonden aan dat, tijdens de transitie naar stationaire fase, een veel sterkere daling van de 'energy charge' optrad in anaërobe



cultures dan in aërobe cultures. Dit verschil trad op ondanks het feit dat anaërobe cultures hogere gehalten van het reservemateriaal glycogeen hadden. De ogenschijnlijke limitatie in energetische flexibiliteit van anaërobe batchcultures tijdens de transitie naar stationaire fase heeft mogelijk een nog sterkere invloed op translatie dan op transcriptie. Dit kan resulteren in een lagere hittetolerantie en een kortere chronologische levensduur dan in aërobe stationaire-fasecultures.

Eerdere studies met anaërobe retentostaatcultures leidden, in tegenstelling tot de situatie in anaërobe batchcultures, niet tot een abrupte depletie van de koolstof- en energiebron. In plaats hiervan zorgde het gebruik van retentostaten voor een geleidelijke afname van de glucose- beschikbaarheid, gekoppeld aan een even geleidelijke afname van de specifieke groeisnelheid. Deze geleidelijke transitie vertoont parallellen de langzame groei in de post-diauxische groeifase van aërobe batchcultures, die cellen de tijd verschaft om zich 'voor te bereiden' op een situatie van nulgroei. Inderdaad vertoonden ook anaërobe retentostaatcultures een sterke toename in hitte- en starvatietolerantie. Het onderzoek in Hoofdstuk 3 toonde aan dat de cellulaire energiestatus een belangrijke factor is voor het verwerven van een lange levensduur en een robuust fenotype tijdens de overgang, veroorzaakt door uitputting van de energiebron, van snelgroeïende *S. cerevisiae*-cultures naar stationaire fase.

Op gist gebaseerde productie van assimilatoire producten vereist een hoge ATP-opbrengst in de dissimilatie. Dit vereist dat suiker wordt gedissimileerd via ademhaling. Om volledig respirerende gistcultures met een actieve stofwisseling te kunnen bestuderen bij nulgroei, werden aërobe retentostaatcultures opgezet. Hoofdstuk 4 beschrijft het operationele ontwerp van aërobe retentostaten en de eerste fysiologische karakterisering van volledige respiratoire *S. cerevisiae*-cultures onder condities waarbij nulgroei wordt benaderd. Retentostaatcultures bieden de unieke mogelijkheid om de energiebehoefte voor celonderhoud te schatten bij zeer langzame groeisnelheden. Deze schattingen zijn veel accurater dan bij gebruik van traditionele methoden, die zijn gebaseerd op extrapolatie van data van een serie chemostaatcultures uitgevoerd bij verschillende, relatief hoge groeisnelheden. In Hoofdstuk 4 wordt aangetoond dat de energiebehoefte (mATP) voor celonderhoud van respirerende *S. cerevisiae*-retentostaatcultures ca. 30% lager is dan in anaërobe retentostaatcultures. Deze data kunnen worden gebruikt als benchmark om te vergelijken hoe substraatverbruik voor celonderhoud verschilt tussen organismen en groeicondities. Bovendien kan deze nauwkeurige schatting van de kosten van celonderhoud in *S. cerevisiae* worden gebruikt bij ontwerp en optimalisatie van fed-batchprocessen in de industrie.

*S. cerevisiae*-cellen gekweekt bij extreem lage groeisnelheden in aërobe retentostaatcultures, vertoonden een ongeëvenaarde hittebestendigheid. Dit geeft aan dat een geleidelijke overgang van exponentiële groei naar nulgroei in aërobe retentostaatcultures de gistcellen optimaal conditioneert voor hittetolerantie. Expressie van verschillende stress-

responsieve genen nam toe gedurende retentostaatcultivatie, terwijl genen gerelateerd aan biosynthese bij afnemende groeisnelheid juist dalende mRNA-gehalten lieten zien. Deze transcriptionele veranderingen corresponderden met eerdere waarnemingen aan anaërobe retentostaatcultures. Zoals verwacht waren bij nulgroei de *in vivo* dissimilatoire omzettingssnelheden laag en benaderden deze de substraatbehoefte voor celonderhoud. Desondanks toonden metingen van de fermentatieve capaciteit (de snelheid van alcoholische fermentatie bij toevoeging van overmaat suiker aan anaërobe celsuspensies) van gistcellen uit retentostaatcultures aan dat de disssimilatiecapaciteit ook bij nulgroei hoog bleef. Deze waarnemingen vormen een solide basis om *S. cerevisiae* verder te ontwikkelen als een niet-delende celfabriek met een actief metabolisme, die economisch interessante producten kan produceren in afwezigheid van biomassavorming.

De succesvolle implementatie van aërobe retentostaten leidde tot een vruchtbare samenwerking met collega's van de Universität für Bodenkultur in Wenen, Oostenrijk. Het resultaat van deze samenwerking is beschreven in Hoofdstuk 5. Dit hoofdstuk beschrijft een verkenning van de fysiologie van de breed toegepaste industriële gist *Pichia pastoris* bij extreem lage groeisnelheden. Deletie van een gen dat ortholoog is aan *S. cerevisiae* *FLO8*, dat codeert voor een transcriptiefactor, elimineerde oppervlaktehechting van gistcellen aan bioreactoronderdelen, en voorkwam tevens verstopping van de retentostaatfilter. De *flo8* $\Delta$  stam maakte het mogelijk om volledige celretentie te realiseren in de retentostaten en deze gedurende een aantal weken te kweken. In tegenstelling tot *S. cerevisiae* toonde *P. pastoris* een opmerkelijke afname in energieverbruik voor celonderhoud bij (bijna) nulgroei, terwijl de levensvatbaarheid van de cultuur zelfs na 25 dagen extreem trage groei in de retentostaat op bijna 100% bleef. De substraatbehoefte voor celonderhoud bij nulgroei was drie keer lager in *P. pastoris* dan in vergelijkbare retentostaatcultures van *S. cerevisiae*. De hiermee 'gespaarde' koolstof- en energiebron wist *P. pastoris* te gebruiken voor assimilatie, hetgeen resulteerde in een hogere biomassa-ophoging dan vooraf werd gemodelleerd. Retentostaatcultures van *P. pastoris* vertoonden intracellulaire ophoping van de reservekoolhydraten glycogeen en trehalose, transcriptionele de-repressie van genen betrokken bij metabolisme van alternatieve energiesubstraten en een verhoogde expressie van stress-gerelateerde genen. Deze observaties suggereren dat *P. pastoris* zijn fysiologie aanpast om te kunnen anticiperen op potentiële veranderingen in zijn omgeving, zoals depletie van energiebronnen, of plotselinge overmaat aan alternatieve energiesubstraten. Fysiologische karakteristieken van een dergelijke 'be prepared'-strategie (een term bedacht door de Zwitserse microbiële ecoloog Thomas Egli) werden ook waargenomen in retentostaatcultures van *S. cerevisiae* en andere industrieel relevante microorganismen. De hoge vitaliteit en lage energiebehoefte voor celonderhoud in *P. pastoris*, gecombineerd met de intrinsiek voordelige respiratoire energetica van deze gist, zijn aantrekkelijke eigenschappen voor industriële productie van eiwitten of en andere assimilatoire producten.

Een logische volgende stap in het bestuderen van nulgroei-fysiologie van industrieel

relevante micro-organismen is onderzoek naar de impact van nulgroei op assimilatoire productvorming. Extrapolatie van de sterke positieve correlatie tussen groei en productiviteit die werd waargenomen in een genetisch gemodificeerde, resveratrol-producerende giststam (Hoofdstuk 2) suggereerde dat assimilatoire productvorming bij nulgroei zeer beperkt is. Een kwantitatieve experimentele analyse van productvorming in niet-groeiende cultures is echter de enige manier om de werkelijke productiekinetiek bij nulgroei te beschrijven. Zulk onderzoek zou belangrijke aanwijzingen kunnen opleveren voor optimalisatie van giststammen of bio-processen. Dit proefschrift illustreert dat de retentostaat een krachtig instrument is om meer inzicht te krijgen in de robuustheid, fysiologie en energetica van industriële micro-organismen bij zeer lage groeisnelheden. Bovendien is dit kweekstelsel een uitstekend platform om 'metabolic engineering' strategieën voor ontkoppeling van assimilatoire productvorming en microbiële groei te evalueren, en draagt het daarmee bij aan de ontwikkeling van een 'bio-based', circulaire economie. Voortbouwend op het in dit proefschrift beschreven onderzoek, zetten onderzoekers aan de Technische Universiteit Delft hun inspanningen voort om productvorming bij nulgroei te begrijpen en verbeteren, daarbij intensief gebruik makend van retentostaatcultures en van genetisch gemodificeerde giststammen die assimilatoire producten maken.

## Acknowledgements

This thesis has been made possible thanks to the work and support of many. First, I would like to extend my gratitude to my promoter Jack Pronk and my co-promoter Pascale Daran-Lapujade. Thank you both for welcoming me in the group and guiding and teaching me how to do science. Thank you for seeing something in me during my master end-project and allowing me to explore the field of biotechnology and develop myself further during my PhD at IMB.

Pascale, I look back at five really nice years of working together and am grateful for everything you taught me, your open attitude, all the pleasant chats, your critical thinking, and your touch of perfectionism that often helped me out. In addition to the research we performed, I keep fond memories of teaching Metabolic Reprogramming together with you in the Life Science & Technology Master curriculum. Thank you!

Jack, you are an inspiring researcher and teacher and I am happy and grateful to have had the pleasure of working in your group. Many thanks for your everlasting (scientific) enthusiasm, your open-door policy, your personal interests in me, our scientific discussions, your positivism, trust, and steering during critical moments in my PhD.

To everyone at IMB and BT that I had the pleasure to meet and work with I extend my appreciation. I will not attempt to put everyone's name here, but would like to thank all my (ex-) colleagues for all the help you have given me in one way or another, and for greatly enhancing the pleasure of going to the lab every day, even when experiments failed or when facing other challenges. Keep up the nice atmosphere!

Next, I would like to thank a number of people (in random order) who have particularly contributed to my time as a PhD student. Niels, thank you for showing me the fun in science. Big chance I wouldn't have considered doing a PhD if it wasn't for the nice work we did together. Pilar, I still remember advising Jack and Pascale to hire you during your interview at IMB. Without a doubt the best thing I did during my PhD. Thank you for your tremendous efforts on the arrays, the lovely chats we had, your joy, great personality, and for being my paranymph. Ton and Erik, your expertise has been pivotal to every chapter in this thesis, thank you. Marcel, thanks for the games of darts. Also thanks to all the students I had the pleasure to work with. Carmen, Sophie, Dorotka, Rinke, Pauline and Xavier, it was a privilege to supervise you in your bachelor and master projects. Xavier, thank you for your excellent contribution to the aerobic retentostat work which resulted in a nice joint publication. I am happy, and a bit proud as well, that you are continuing the zero-growth work together with Pascale. Also, thank you for being my paranymph. Markus, thank you for involving me in the stationary phase work. I have learned a lot and much enjoyed working with you. All those overnight experiments were soon forgotten seeing our nice publication being 'most viewed' for months. Thanks to co-authors Walter, Rubén, Alexandra and Minoska for contributing to this thesis. In addition, I would like to thank all members of the RoBoYeast team. In particular many thanks to Prof. Ralf Takors

for coordinating the RoBoYeast project. Although unforeseen events lead to a premature termination of the project, I look back at a nice collaboration in the first year of my PhD.

Corinna, without your efforts Chapter 5 of this thesis would have never been there. Thank you for deciding to perform part of your research in Delft, for your dedication and persistence when facing multiple hurdles in the project, and just for being a great person. I really enjoyed our collaboration, and especially all the fun we had in the lab and whilst writing the manuscript. I would like to extend my gratitude to Prof. Diethard Mattanovich as well, for fuelling this nice collaboration and welcoming me in his lab during my visit to Vienna.

M'n vrienden hebben ook een belangrijke bijdrage geleverd. Ik wil jullie allemaal bedanken voor de hoognodige afleiding, relativering, en gezelligheid gedurende de afgelopen jaren! Boys, de LW houden we erin. Danki mi ruman.

Mijn familie heeft me altijd gemotiveerd om er vol voor te gaan tijdens m'n studies en banen, bedankt voor het goede voorbeeld. Lieve mam en pap, heel erg bedankt voor jullie onvoorwaardelijke steun. Mam, dankjewel voor alle duwtjes in de rug.

Susanne, jij laat me dagelijks realiseren wat echt belangrijk is in het leven. Ik had dit niet zonder jou willen doen, en zie uit naar onze toekomst samen. Ik hou van je.

## *Curriculum Vitae*

Tim Vos was born on July 6, 1987 in Bobeldijk, the Netherlands. After receiving his VWO diploma at the Copernicus in Hoorn in 2005, he embarked on an academic study in Life Science and Technology, offered as a joint programme organized by the Delft University of Technology and Leiden University. Tim concluded his BSc studies with a research project at the Immunology and Infectious Diseases Section of the Leiden University Medical Centre, which focused on immune modulatory effects of small peptides on human macrophages. In 2008, he enrolled in the two-year MSc programme Life Science and Technology. During his MSc studies, Tim joined the TU Delft team that participated in the 2009 International Genetically Engineered Machine (iGEM) competition of 2009 which was awarded the “Best Information Processing project” award. In 2010, he interrupted his studies for 6 months to work in Japan, as a researcher in a joint project of the Rathenau Institute in The Hague and the Netherlands Office for Science and Technology at the Netherlands Embassy in Tokyo. This project focused on monitoring and reporting current developments and prospects of synthetic biology research in Japan by discussing locally with scientific leaders in academia and industry. After this international experience, Tim started his MSc research project in the Industrial Microbiology group at TU Delft, led by Jack Pronk. During this project, he investigated novel synthetic biology tools for accelerating and intensifying genetic engineering of baker’s yeast, under the supervision of Pascale Daran-Lapujade and Niels Kuijpers. After receiving his MSc degree in October 2011, he started his PhD in Jack Pronk’s group, under supervision of Pascale Daran-Lapujade. This project, which involved close collaboration with Pilar de la Torre Cortes, Mark Bisschops, Corinna Rebnegger and Xavier Hakkaart, ultimately resulted in this thesis. Since March 2016, Tim is employed as a policy officer at the Netherlands Organisation for Scientific Research (NWO) in The Hague, The Netherlands.

## List of publications

1. Rebnegger C\*, **Vos T\***, Graf AB, Valli M, Pronk JT, Daran-Lapujade P, Mattanovich D, *Pichia pastoris* exhibits a high viability and low maintenance-energy requirement at near-zero specific growth rates, *Applied and Environmental Microbiology*, 2016, **82**:4570-4583 \* Joint first authorship
2. **Vos T**, Hakkaart XDV, de Hulster EAF, van Maris AJA, Pronk JT, Daran-Lapujade P, Maintenance-energy requirements and robustness of *Saccharomyces cerevisiae* during aerobic cultivation at near-zero specific growth rates, *Microbial Cell Factories*, 2016, **15**:111.
3. **Vos T**, de la Torre Cortes P, van Gulik WM, Pronk JT, Daran-Lapujade P, Growth-rate dependency of de novo resveratrol production in chemostat cultures of an engineered *Saccharomyces cerevisiae* strain, *Microbial Cell Factories*, 2015, **14**:131
4. Bisschops MMM\*, **Vos T\***, Martinez-Moreno R, de la Torre Cortes P, Pronk JT, Daran-Lapujade P, Oxygen availability strongly affects chronological lifespan and thermotolerance in batch cultures of *Saccharomyces cerevisiae*, *Microbial Cell*, 2015, **2**:429-444. \* Joint first authorship
5. Kuijpers NG, Chroumpi S, **Vos T**, Solis-Escalante D, Bosman L, Pronk JT, Daran J-M, Daran-Lapujade P: One-step assembly and targeted integration of multigene constructs assisted by the I-SceI meganuclease in *Saccharomyces cerevisiae*. *FEMS Yeast Research*, 2013, **13**:769-781.
6. Van der Does AM, Beekhuizen H, Ravensbergen B, **Vos T**, Ottenhoff THM, van Dissel JT, Drijfhout JW, Hiemstra PS, Nibbering PH: LL-37 directs macrophage differentiation toward macrophages with a proinflammatory signature. *Journal of Immunology*, 2010, **185**:1442-1449.



